

FINAL REPORT SYSTEM DESIGN OF THE PIONEER VENUS SPACECRAFT

VOLUME 3 SYSTEMS ANALYSIS

By
J. N. FISHER
ET AL.

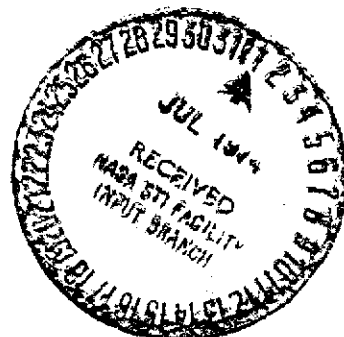
July 1973



Prepared Under
Contract No. [REDACTED] NAS 2-7250

By
HUGHES AIRCRAFT COMPANY
EL SEGUNDO, CALIFORNIA

For
AMES RESEARCH CENTER
NATIONAL AERONAUTICS AND
SPACE ADMINISTRATION



(NASA-CR-137490) SYSTEM DESIGN OF THE
PIONEER VENUS SPACECRAFT. VOLUME 3:
SYSTEMS ANALYSIS Final Report (Hughes
Aircraft Co.) 223 p HC \$14.25 CSCL 22B
G3/31 Unclas 41558
N74-27373

PREFACE

The Hughes Aircraft Company Pioneer Venus final report is based on study task reports prepared during performance of the "System Design Study of the Pioneer Spacecraft." These task reports were forwarded to Ames Research Center as they were completed during the nine months study phase. The significant results from these task reports, along with study results developed after task report publication dates, are reviewed in this final report to provide complete study documentation. Wherever appropriate, the task reports are cited by referencing a task number and Hughes report reference number. The task reports can be made available to the reader specifically interested in the details omitted in the final report for the sake of brevity.

This Pioneer Venus Study final report describes the following baseline configurations:

- "Thor/Delta Spacecraft Baseline" is the baseline presented at the midterm review on 26 February 1973.
- "Atlas/Centaur Spacecraft Baseline" is the baseline resulting from studies conducted since the midterm, but prior to receipt of the NASA execution phase RFP, and subsequent to decisions to launch both the multiprobe and orbiter missions in 1978 and use the Atlas/Centaur launch vehicle.
- "Atlas/Centaur Spacecraft Midterm Baseline" is the baseline presented at the 26 February 1973 review and is only used in the launch vehicle utilization trade study.

The use of the International System of Units (SI) followed by other units in parentheses implies that the principal measurements or calculations were made in units other than SI. The use of SI units alone implies that the principal measurements or calculations were made in SI units. All conversion factors were obtained or derived from NASA SP-7012 (1969).

The Hughes Aircraft Company final report consists of the following documents:

Volume 1 - Executive Summary - provides a summary of the major issues and decisions reached during the course of the study. A brief description of the Pioneer Venus Atlas/Centaur baseline spacecraft and probes is also presented.

Volume 2 - Science - reviews science requirements, documents the science-peculiar trade studies and describes the Hughes approach for science implementation.

Volume 3 - Systems Analysis - documents the mission, systems, operations, ground systems, and reliability analysis conducted on the Thor/Delta baseline design.

Volume 4 - Probe Bus and Orbiter Spacecraft Vehicle Studies - presents the configuration, structure, thermal control and cabling studies for the probe bus and orbiter. Thor/Delta and Atlas/Centaur baseline descriptions are also presented.

Volume 5 - Probe Vehicle Studies - presents configuration, aerodynamic and structure studies for the large and small probes pressure vessel modules and deceleration modules. Pressure vessel module thermal control and science integration are discussed. Deceleration module heat shield, parachute and separation/despin are presented. Thor/Delta and Atlas/Centaur baseline descriptions are provided.

Volume 6 - Power Subsystem Studies

Volume 7 - Communication Subsystem Studies

Volume 8 - Command/Data Handling Subsystems Studies

Volume 9 - Altitude Control/Mechanisms Subsystem Studies

Volume 10 - Propulsion/Orbit Insertion Subsystem Studies

Volumes 6 through 10 - discuss the respective subsystems for the probe bus, probes, and orbiter. Each volume presents the subsystem requirements, trade and design studies, Thor/Delta baseline descriptions, and Atlas/Centaur baseline descriptions.

Volume 11 - Launch Vehicle Utilization - provides the comparison between the Pioneer Venus spacecraft system for the two launch vehicles, Thor/Delta and Atlas/Centaur. Cost analysis data is presented also.

Volume 12 - International Cooperation - documents Hughes suggested alternatives to implement a cooperative effort with ESRO for the orbiter mission. Recommendations were formulated prior to the deletion of international cooperation.

Volume 13 - Preliminary Development Plans - provides the development and program management plans.

Volume 14 - Test Planning Trades - documents studies conducted to determine the desirable testing approach for the Thor/Delta spacecraft system. Final Atlas/Centaur test plans are presented in Volume 13.

Volume 15 - Hughes IR&D Documentation - provides Hughes internal documents generated on independent research and development money which relates to some aspects of the Pioneer Venus program. These documents are referenced within the final report and are provided for ready access by the reader.

Data Book - presents the latest Atlas/Centaur Baseline design in an informal tabular and sketch format. The informal approach is used to provide the customer with the most current design with the final report.

CONTENTS

| | Page |
|---|------|
| 1. SUMMARY | 1-1 |
| 2. INTRODUCTION | 2-1 |
| 3. MISSION ANALYSIS | 3-1 |
| 3.1 Multiprobe Mission - Summary | 3-1 |
| Transit Trajectory Analysis - Summary | 3-2 |
| Probe and Orbiter Midcourse ΔV Requirements | 3-15 |
| Nominal Probe Targeting | 3-19 |
| Probe Targeting Dispersions | 3-34 |
| 3.2 Orbiter Mission - Summary | 3-36 |
| Orbiter Transit Trajectory Analysis - Summary | 3-37 |
| Nominal Orbital Elements - Summary | 3-51 |
| Orbiter Transit Trajectory Selection - Summary | 3-76 |
| 3.3 References | 3-92 |
| 4. MISSION OPERATIONS AND GROUND SYSTEMS | 4-1 |
| 4.1 Major Impact on Spacecraft Design | 4-2 |
| 4.2 Spacecraft Launch Operations | 4-4 |
| Countdown | 4-4 |
| Boost Phase | 4-5 |
| Post Injection | 4-5 |
| 4.3 Multiprobe Mission Operations | 4-7 |
| Constraints | 4-7 |
| Conclusions | 4-13 |
| 4.4 Orbiter Mission Operations | 4-17 |
| Constraints | 4-17 |
| Mission Description | 4-19 |
| Sequences | 4-19 |
| Conclusion | 4-23 |
| 4.5 Ground Data System Interfaces | 4-27 |
| Tracking, Command and Telemetry | 4-27 |
| DSN Predetection Recording Plan | 4-27 |
| Telemetry Data Recovery | 4-33 |
| Software | 4-43 |
| References | 4-49 |

PRECEDING PAGE BLANK NOT FILMED

| | | |
|-----|--------------------------------------|------|
| 5. | SYSTEM TRADE STUDIES | 5-1 |
| 5.1 | Summary | 5-1 |
| 5.2 | Background | 5-2 |
| 5.3 | Spin Axis Orientation Trade Study | 5-3 |
| | Spin Axis Perpendicular to Ecliptic | 5-5 |
| | Spin Axis Directed to Earth | 5-5 |
| | Spacecraft Configuration | 5-10 |
| 5.4 | Bus Antenna Trades | 5-15 |
| | Mission Requirements | 5-15 |
| | Probe Bus Antenna Selection | 5-16 |
| | Orbiter Antenna Selection | 5-19 |
| 5.5 | Communication System Design Trades | 5-25 |
| | Small Probe Modulation Selection | 5-25 |
| | Probe Coding Selection | 5-27 |
| | Probe Doppler Tracking | 5-31 |
| | Predetection Recording | 5-31 |
| | Large Probe Frequency Selection | 5-33 |
| | Orbiter Doppler Tracking | 5-37 |
| | Link Analysis | 5-37 |
| 5.6 | Probe Descent Trades | 5-41 |
| | Parachute Selection | 5-41 |
| | Jettison Altitude | 5-41 |
| | Sensitivity to the Atmospheric Model | 5-43 |
| 5.7 | Reduced Science Payload | 5-46 |
| | Large Probe | 5-46 |
| | Small Probe | 5-46 |
| 5.8 | Conclusions | 5-47 |
| | References | 5-50 |
| 6. | RELIABILITY | 6-1 |
| 6.1 | Overview | 6-1 |
| | General Assumptions | 6-1 |
| 6.2 | Orbiter Mission | 6-3 |
| 6.3 | Probe Bus Spacecraft Mission | 6-4 |
| | Probe Bus Mission | 6-5 |
| | Large Probe Mission | 6-7 |
| | Small Probe Mission | 6-9 |
| | APPENDIX A. SEQUENCING PROBE ENTRY | A-1 |

1. SUMMARY

Mission, operations, and system tradeoffs were particularly significant in designing the spacecraft to satisfy the science requirements and to meet the Thor/Delta payload capability constraints. Mission trades included transit trajectory, launch windows, midcourse maneuvers, probe targeting, and orbit parameters. Operations trades included scheduling, development of sequences, launch operations, probe entry timing, orbit insertion timing, and ground processing. System trades included bus spin axis orientation, bus antenna design, communication parameters, and probe descent profiles. Table 1-1 summarizes the major mission and system analysis decisions. All trade documented in this volume are for the Thor/Delta launch vehicle. Corresponding Atlas/Centaur data is briefly reviewed in the data book. Final Atlas/Centaur mission and system data will be provided in the Hughes execution phase proposal.

Type I and type II trajectories were considered for both multiprobe and orbiter missions. A type I trajectory was selected for the multiprobe mission because the launch energy requirements were much less than for type II. For the orbiter mission, the payload weight in orbit was about the same for either type, and both trajectories were analyzed in detail. The type II trajectory was selected since it offered the best science coverage and in particular the number of daylight periapsis passages before crossing the terminator was maximized.

Launch dates were selected for both missions to provide maximum payload weight. The period from 6 January to 15 January 1977 was selected as the minimum energy 10 day launch window for the multiprobe mission. A launch energy versus injection energy trade was made for the orbiter and the period from 25 May to 10 June 1978 was selected as the 10 day launch window providing maximum payload weight in orbit.

A 99 percent Monte Carlo analysis defined the midcourse maneuvers required to provide the desired impact points and a fixed arrival date. Early maneuvers involved reorientation for axial thrust to save fuel weight. Later maneuvers employed thrust vectoring for minimum operational complexity.

Probe and bus target points were selected to provide the desired science return with a minimum weight and cost system design. In particular, the large probe was targeted at the equator 25 deg on the dayside of the

TABLE 1-1. MISSION AND SYSTEM DECISION RATIONALE

| Design Feature | Rationale |
|--|---|
| MULTIPROBE MISSION | |
| Type I Trajectory | Maximum payload mass |
| Launch Date 6 January to 15 January 1977 | Minimum energy 10 day launch window |
| Midcourse maneuver at L + 5, +20, +50, E-30 days | Correct target dispersions and provide fixed arrival date (fixed arrival geometry); axial thrust used for first two maneuvers to minimize fuel requirement; thrust vectoring used otherwise for operational simplicity. |
| Large probe targeted at equator 25 deg from terminator | Best communication angle that guarantees science requirement of descent ≥ 20 deg from terminator |
| Small probes targeted 60 deg from sub-earth point | Maximum spacing of entry locations consistent with adequate communication performance (actual targeting consistent with maximum latitude spacing while providing entry angles less than -20 deg) |
| Bus targeted for minimum entry angle of -20 deg and earth angle of 2.5 deg with 0.0 deg angle of attack | Time between 160 and 130 km altitude maximized with guaranteed survival to 130 km plus minimum earth communication angle for best science sampling (zero angle of attack) |
| Bus retarded for 1-1/2 hours | Provide a known trajectory reference for DLBI experiment |
| Simultaneous probe entry | Minimum weight approach (but requires predetection recording) |
| ORBITER MISSION | |
| Type II Trajectory | Best science coverage; provides sufficient daylight viewing at mission start |

TABLE 1-1 (continued)

| Design Feature | Rationale |
|--|--|
| ORBITER MISSION (continued) | |
| Launch Date 25 May to 10 June 1978 | Maximum payload weight in orbit. |
| Midcourse maneuver at L+5, +20, +50, E-20 days | Same as multiprobe mission |
| 150 km altitude of periapsis | Minimum safe altitude |
| 24 hour period | Simple ground operations |
| Polar orbit | Best science coverage |
| 26°N periapsis | Mid-latitude for best science coverage; 26°N provides small spacecraft and operational advantage compared to 50°S (System easily modified for either south or north) |
| MISSION OPERATIONS AND GROUND SYSTEMS | |
| 7 day probe release sequence | Provide adequate time to perform necessary maneuvers and tests |
| Fixed probe entry date and time | Provides guaranteed ground station overlap |
| Predetection recording | Most reliable means of acquiring data from four simultaneous vehicles |
| Storage of periapsis data during all orbits | Ground operation simplicity and minimum real time data rate requirement |
| Command verification | Fault isolation and reliability |
| SYSTEM TRADE STUDIES | |
| Spin axis oriented perpendicular to ecliptic plane | Best orbiter science coverage and spacecraft mechanization simplicity |
| Mechanically despun orbiter HGA | Development status, ease of integrating rf occultation experiment |

TABLE 1-1 (continued)

| Design Feature | Rationale |
|---|---|
| SYSTEM TRADE STUDIES (continued) | |
| Bicone horn for probe bus cruise | Minimum weight |
| Medium gain horn for probe bus entry | Minimum weight |
| PCM/PSK/PM coherent signaling | Available flight hardware |
| Sequential decoding | DSN compatibility |
| Two-way doppler tracking on large probe/one-way doppler tracking on small probe | Science requirements |
| 3.5m diameter large probe parachute jettisoned at 55 km altitude | Minimum system weight consistent with required science return |

terminator to guarantee the required 20 deg spacing, but minimize communication angle. Small probes were targeted 60 deg from the subearth point to provide maximum spacing consistent with a practical common antenna design. The bus was targeted at a shallow entry angle of -12 deg and at a location where the earth angle would be minimal for zero angle of attack. The shallow entry angle provided maximum sampling from 160 to 130 km altitude with guaranteed survival to 130 km. Zero angle of attack provided the best science sampling and the small earth angle accommodated a high rate of data return.

Orbital parameters were determined to provide the best science coverage with an operationally simple design. A polar orbit was selected to provide complete planet hemispherical coverage during the course of the Venusian year. A 24 hour period was selected to provide straightforward phasing of ground operation. The periapsis altitude was placed at 150 km since this was the minimum safe altitude where aerodynamic effects could easily be corrected. Finally a 26 deg N periapsis point was selected to cover the most planet area.

Detailed mission sequences were established to identify critical areas and provide phasing of critical operation. The probe release sequence was identified as particularly significant. A 7 day period was provided to accommodate the three changes in spin rate, three spin axis orientation, one velocity change, two probe releases, and two probe tests. The orbit insertion sequence was identified as similarly critical although a thermal constraint imposed by solar interreflection at the non-nominal attitude limited the available time to about 2 hours.

Ground system simplicity was emphasized in determining scheduling and modes of data return. All systems were designed for compatibility with the multiprobe mission Deep Space Set. Format lengths were minimized and identification was provided for ease in ground processing. Provision was made for command verification to provide fault isolation and reliability. Predetection recording was favored to provide reliable recovery of probe encounter data where four vehicles would be transmitting simultaneously and high doppler rates and frequency uncertainty might make real time reception difficult.

Early selection of the spacecraft spin axis orientation was critical because of the direct dependence of the system design. The spin axis was selected perpendicular to the ecliptic based on science requirements and spacecraft mechanization simplicity.

The bus antennas were chosen for the lowest system mass, availability of flight proven hardware, and in the case of orbiter accommodation of the RF occultation experiment. A mechanically despun parabolic reflector was selected over an electronically despun antenna for the orbiter. A biconic horn was selected for probe bus communication during cruise and a medium gain horn for the much higher data rates required at entry.

Tradeoffs of doppler tracking, modulation and coding were performed to optimize the system's communication performance. Although for the large and small probes Viterbi decoding and for the small probes non-coherent signalling (MFSK) were demonstrated to be theoretically superior, practical considerations including DSN capability and availability of spacecraft hardware resulted in selection of coherent signalling (PCM/PSK/PM) and sequential decoding. Two-way doppler was selected for the large probe and one-way for the small probe based on science rather than communications performance considerations. In addition, orbiter doppler tracking was analyzed to determine the ability of the Spacecraft receiver to track the expected doppler rates on the uplink signal.

The probe descent profile was treated as a system tradeoff involving the interaction of transmitter, battery, structure, thermal insulation, and parachute parameters. By varying these parameters the system mass was minimized consistent with the desired science return. It was shown that in general smaller parachute diameters and higher jettison altitudes were favored. A 3.5 m diameter (D_0) parachute with a jettison altitude of 55 km was selected.

A reliability analysis was undertaken to demonstrate the adequacy of the system design. The probability of achieving complete multiprobe mission success was 0.8718. The comparable orbiter mission success probability was only 0.7907 because of the low reliability of the data storage system. Redundant data storage was not provided since failure would only result in a reduced capability and not total failure. A redundant storage unit would have increased the reliability to 0.9283.

2. INTRODUCTION

This volume presents the mission and system trades that were undertaken to achieve a minimum cost and weight spacecraft design. The results presented are based primarily on a set of referenced trade study reports.

Mission studies are presented in Section 3. Mission analysis of the multiprobe mission is presented in Section 3.1. The rationale for selecting the transit trajectory, launch dates, midcourse maneuvers, and probe and bus targeting is presented. The orbiter mission analysis is presented in Section 3.2. Transit trajectories, launch dates, midcourse maneuvers, and orbital parameters are described.

Operations are discussed in Section 4. Section 4.2 considers spacecraft launch operations. Special features such as ground station visibility, boom deployment, and reorientation maneuvers are considered. Multiprobe mission operations are discussed in Section 4.3, including a detailed sequence from launch through probe release and bus entry. Orbiter mission operations are discussed in Section 4.4. Orbit insertion and periapsis data storage are highlighted. The ground data system is discussed in Section 4.5. Interfaces with the DSN are considered, including command, telemetry, and ground data processing.

System trade studies are presented in Section 5. Section 5.3 considers alternate orientations of the spin axis perpendicular or parallel to the ecliptic plane. Section 5.4 discusses trades of the probe bus and orbiter antenna complements. In particular, electronic and mechanical despun antennas are compared. Communication system design trades are covered in Section 5.5. In particular probe modulation, coding, doppler tracking predetection recording, and link analysis are considered. Probe descent trades are discussed in Section 5.6. Special emphasis is placed on minimizing large probe system weight by varying the parachute parameters. The sensitivity of the probe design to the atmospheric model is summarized in Section 5.6. Finally, analysis of a reduced science payload as a means of meeting the Thor/Delta weight constraints while maintaining an adequate weight margin, is presented in Section 5.7.

In Section 6 a system summary reliability analysis is presented.

3. MISSION ANALYSIS

3.1 MULTIPROBE MISSION - SUMMARY

The 1977 multiprobe mission is launched from Cape Kennedy and flies a Type I transit trajectory, arriving at Venus on May 17 at 1300 GMT. Ten daily launch periods of 10 minutes each running from January 6 to January 15 provide a maximum spacecraft mass capability of 384.1 kg using the Thor/Delta launch vehicle. The use of a fixed arrival date imposes essentially no performance penalty and somewhat simplifies considerations associated with probe targeting, communications, and mission operations. Transit times thus vary from 131.3 to 122.3 days over the launch periods with a maximum injection C_3 of 7.614 (km/sec)^2 . The approach asymptote velocity also varies slightly over the launch window with a maximum V_∞ of 4.404 km/sec.

A Monte Carlo error analysis was used to compute ΔV requirements arising from errors in launch vehicle injection, orbit determination, and execution of prior midcourse maneuvers. Total requirement for the Thor/Delta multiprobe mission (99 percent value) is 76.6 m/sec.

Probe target points were selected to be consistent with science, subsystem, and communication constraints. The large probe enters with zero angle of attack at a point 25 deg from the terminator on the ecliptic.

The small probes were targeted so as to obtain as large a separation distance between them while maintaining an acceptable earth communication angle. The nominal locations were chosen to each have a 60 deg communication angle during vertical descent. Additionally, one probe has been targeted for the maximum declination in latitude. Great flexibility exists in placement of the probes and it should be emphasized that changing science or communication requirements can be accommodated by adjustment of the nominal probe target locations.

The bus enters with zero angle of attack and has been targeted for minimum entry angle (consistent with dispersions) to obtain maximum science sampling return. The specific bus target point is defined for the minimum earth communication angle.

Transit Trajectory Analysis - Summary

This section describes the tradeoffs which have been performed in trajectory analysis and defines detailed trajectory parameters for the 1977 multiprobe mission. The baseline launch window provides a maximum spacecraft mass capability of 384.1 kg using the Thor/Delta launch vehicle.

Introduction

Purpose. The trajectory analysis began with an approximate analysis for preliminary performance evaluation and concluded with a detailed simulation of trajectories for final preflight targeting. In general terms these analyses have two broad functional objectives, performance evaluation and guidance analysis. Performance evaluation includes the activities leading to the maximization of payload (subject to appropriate mission constraints) and the selection of the nominal launch conditions (which may require a compromise between maximum payload and other mission features). Guidance analysis includes those activities leading to the specification of spacecraft control commands (including launch requirements, midcourse correction, and so forth). The primary purpose of this section is performance evaluation; guidance considerations have been included only to the extent that they affect the performance evaluation (or conversely to provide confidence that no aspect of a more detailed consideration will produce a noticeable affect on performance tradeoffs). A conservative approach has been adopted to ensure that this objective has been met. The consideration of effects which obviously do not have a significant impact on performance provides a very high confidence that the tradeoffs presented herein are valid.

Computer Programs. Although results from conic (planet point mass) trajectory programs were considered to isolate the regions of interest, detailed trajectory optimization and selection was performed with a conic/integrating/conic trajectory program. The spacecraft is assumed to be boosted from a 185 km altitude circular parking orbit to a selected earth escape hyperbola. Initial conditions for the integration are computed in geocentric coordinates at that point on the earth sphere of influence (e.g., 100 earth radii), intersected by the spacecraft's escape hyperbola. These initial conditions are transformed into heliocentric parameters for integration. The components of forces due to planetary gravitation and solar pressure are computed and summed. The integration is a fixed step size Runge-Kutta technique.

At Venus the position and velocity as a result of the integration is compared to conditions necessary for the required Venus approach hyperbola at a desired sphere of influence. Compatibility of these conditions is obtained by selection of the appropriate parameters for the earth escape hyperbola; this convergence is automated in the program. Since the heliocentric trajectory is integrated, the optimum spheres of influence will be smaller than those values customarily used with patch conic techniques. Moreover, testing has shown that (as expected) results are insensitive to the selection of the sphere of influence. The program computes launch azimuth, parking orbit time, coast time, etc., for the selected trajectory.

Lunar gravitational effects are not explicitly computed but the baseline trajectories considered herein do not pass within 50 earth radii of the moon. Lunar gravity perturbations are therefore less than 10 m/sec (i. e. , much less than the perturbations produced by the launch vehicle injection errors.) Detailed targeting equations will explicitly include lunar effects; the performance impact of these effects is much less than 1 kg of spacecraft mass.

Launch Geometry Considerations. Three geometrical properties that strongly influence the ascent trajectory are launch site location (assumed to be at Cape Kennedy), the outward radial direction, and launch azimuth.

The outward radial direction has the strongest influence on the ascent trajectory. For the interplanetary trajectories, the outward radial direction is defined to be the direction of the outgoing asymptote of the escape hyperbola. The approximation of a hyperbolic conic section near the Earth (less than 100 Earth radii) for interplanetary trajectories is adequate for conceptualization and preliminary analysis. The outward radial direction will be represented by a unit vector S . By specifying the launch date and flight time of the mission, the outward radial S as well as the energy (C_3) of the near-Earth conic become known quantities. This follows from the fact that the four defining quantities of a lunar or interplanetary trajectory are launch date, right ascension and declination of the outward radial, and the energy C_3 . Other sets of quantities may be used to define a trajectory; however, this set of four is minimal and most convenient. Assume the overall mission is specified, then S and energy C_3 are constants of the problem. Thus, it follows that the final criterion for ascent trajectory design is simply that it satisfy the four parameters. At least two requirements immediately become apparent: 1) thrust must be applied until the required energy is achieved, and 2) the trajectory plane must contain the outward radial S .

The effect of launch azimuth on the geometry is that it determines the inclination of the trajectory plane relative to the equatorial plane. When launch azimuth is varied, the trajectory plane is rotated about a line joining the Earth's center and the launch site. However, the trajectory plane must contain the outward radial S . Thus, the trajectory plane must contain both the launcher at launch time and the vector S . If launch time is prespecified, the launch azimuth must be chosen such that the trajectory plane contain S . On the other hand, if the launch azimuth is fixed, launch must occur at the proper time. If the declination of the outward radial S is greater than the launch site latitude, a range of launch azimuths (symmetrical about due east) exist at which it is not possible to fire from that site. If the outward radial declination is less than or equal to the launch site latitude, it is possible to fire at all launch azimuths within range-safety limits.

It is evident that there is a strong relationship between launch time and launch azimuth. An example of plots of launch azimuth versus launch time for two declinations of the outward radial are shown in Figure 3-1. Maximum performance is obtained by launching as near due east (90 deg) as possible (to make maximum use of earth rotation velocity). This leads to two maximum performance launches each day (in Figure 3-1 both Venus launch azimuths are 90 deg; the Mars launch azimuths are about 68 and

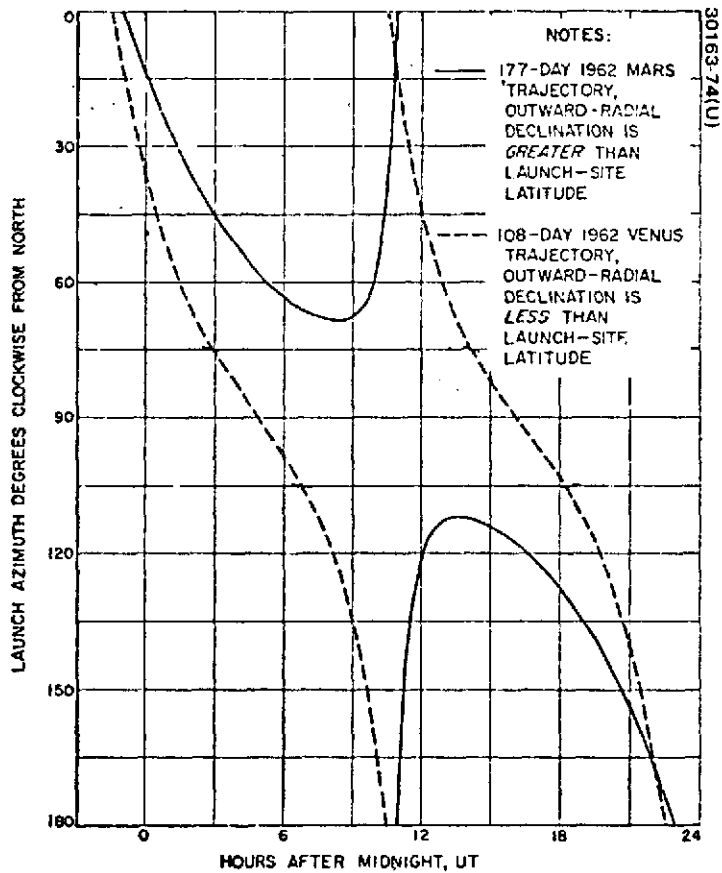


FIGURE 3-1. EXAMPLE OF LAUNCH AZIMUTH VERSUS LAUNCH TIME

112 deg). The coast time required in parking orbit depends on the outward radial S; coast time can vary from a minimum of 0 (direct ascent) to a practical maximum of about one orbit period (90 min).

Assumptions. The maximum available spacecraft launch azimuth (from Cape Kennedy) is assumed to be 108 deg (Reference 1). Trajectory dynamics and avoidance of excessive performance penalties limit available launch time to two relatively short periods each day: only one of these opportunities will be used each day for a variety of spacecraft design and mission operations considerations. Ten daily launch periods of 10 min each have been assumed for both the multiprobe and orbiter mission (Reference 2). Launch experience with the Thor/Delta launch vehicle indicates that these values may be conservative. Thor/Delta launch booster performance capability was taken from the Thor/Delta Launch Vehicle Planning Guide. The performance assumed (90 deg launch azimuth) is given in Table 3-1. Trajectory computations were, of course, performed using Julian dates with calendar dates computed after the fact; JD 2443500.5 = 0000GMT on 23 December 1977.

TABLE 3-1. ASSUMED THOR/DELTA PERFORMANCE CAPABILITY
(Due East Launch)

| C ₃ (km/sec) ² | Injected Mass, * | |
|--------------------------------------|------------------|---------|
| | kg | (lb) |
| 0. | 480.8 | (1060.) |
| 6. | 419.6 | (925.) |
| 8. | 402.3 | (887.) |
| 10. | 385.6 | (850.) |
| 12. | 392.6 | (814.) |
| 14. | 353.3 | (779.) |
| 16. | 338.4 | (746.) |
| 18. | 323.9 | (714.) |
| 20. | 310.7 | (685.) |
| 22. | 297.6 | (656.) |
| 24. | 284.9 | (628.) |
| 26. | 272.6 | (601.) |

*Includes adapter and launch booster telemetry kit of 21.5 kg (47.5 lb).

Multiprobe Mission Trajectories

Type I Versus Type II. A preliminary investigation of the 1976/77 Venus launch opportunity was performed with a conic (no planetary masses) trajectory program. Data were obtained to show the variation of launch energy (C_3) required as a function of launch date for a spread of constant arrival dates. Both Type I (heliocentric transfer angle less than 180 deg), and Type II (heliocentric transfer angle greater than 180 deg) were investigated. This preliminary analysis demonstrated that the launch energy requirements were much less for the Type I trajectory than for the Type II trajectory (Figure 3-2), leading to a strong preference for use of a Type I trajectory for the multiprobe mission from performance considerations. Subsequent examination indicated that the only advantages of the Type II interplanetary trajectory for the 1976 multiprobe mission are:

- 1) A reduction of about 15 deg in large probe communication angle to earth during descent
- 2) A reduction of entry velocity to about 10.9 km/sec from 11.2 km/sec for the Type I trajectory

The spacecraft and subsystem design simplifications permitted by these improvements are very modest in comparison to the performance effect previously mentioned (approximately 45 kg of injected mass). Therefore, all subsequent analysis for the 1976/77 multiprobe mission was performed for Type I trajectories.

Preliminary Analysis. The multiprobe mission has been constrained not only by the launch window considerations but by the desire to hold constant arrival date throughout the launch window. This constraint imposes much less than 1 kg of performance penalty and somewhat simplifies considerations associated with probe targeting, communications, and mission operations.

While not as accurate as an integrating program, the simplicity of the conic program permits parametric data to be compiled quite economically, and a display of these data is convenient to illustrate the concepts which are implemented more precisely with the more costly and detailed trajectories. For example, the contour plot shown in Figure 3-3 (taken from Reference 3) illustrates a sample launch window placed at the peak of the contour. The optimum solution is that placement of the window which provides maximum/minimum spacecraft mass (smallest C_3) throughout the 10 day window. In actuality the problem is a bit more complicated because the launch time is restricted by trajectory dynamics such as azimuth and range safety and the arrival time by the desire to observe the science return from a single ground station. For the purposes of this study, the use of the Goldstone Ground Station has been assumed which leads to a desired arrival time of 1300 GMT for the arrival dates of interest. This discretization of launch and arrival times could be indicated on Figure 3-3, but would serve no practical purpose because the timing errors associated with neglecting the planetary masses are larger than the discretization effects.

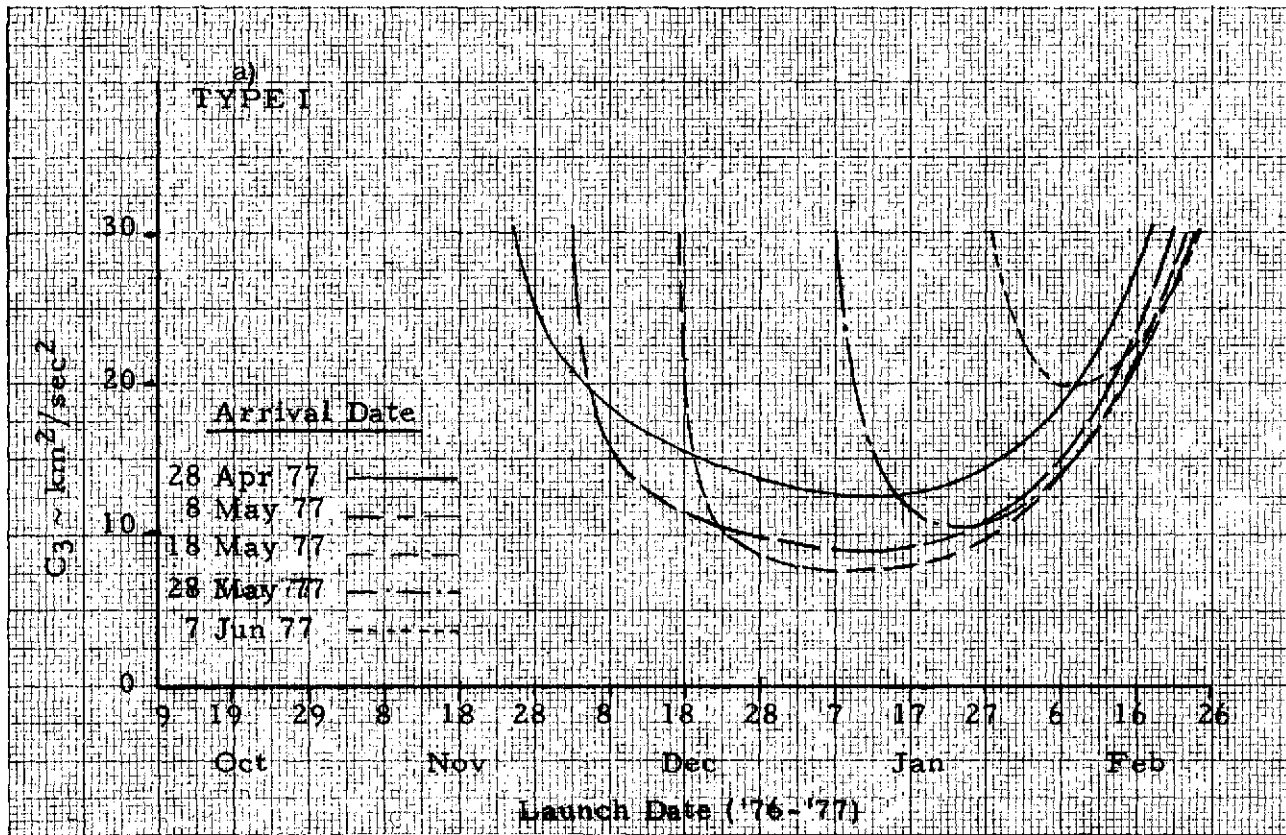
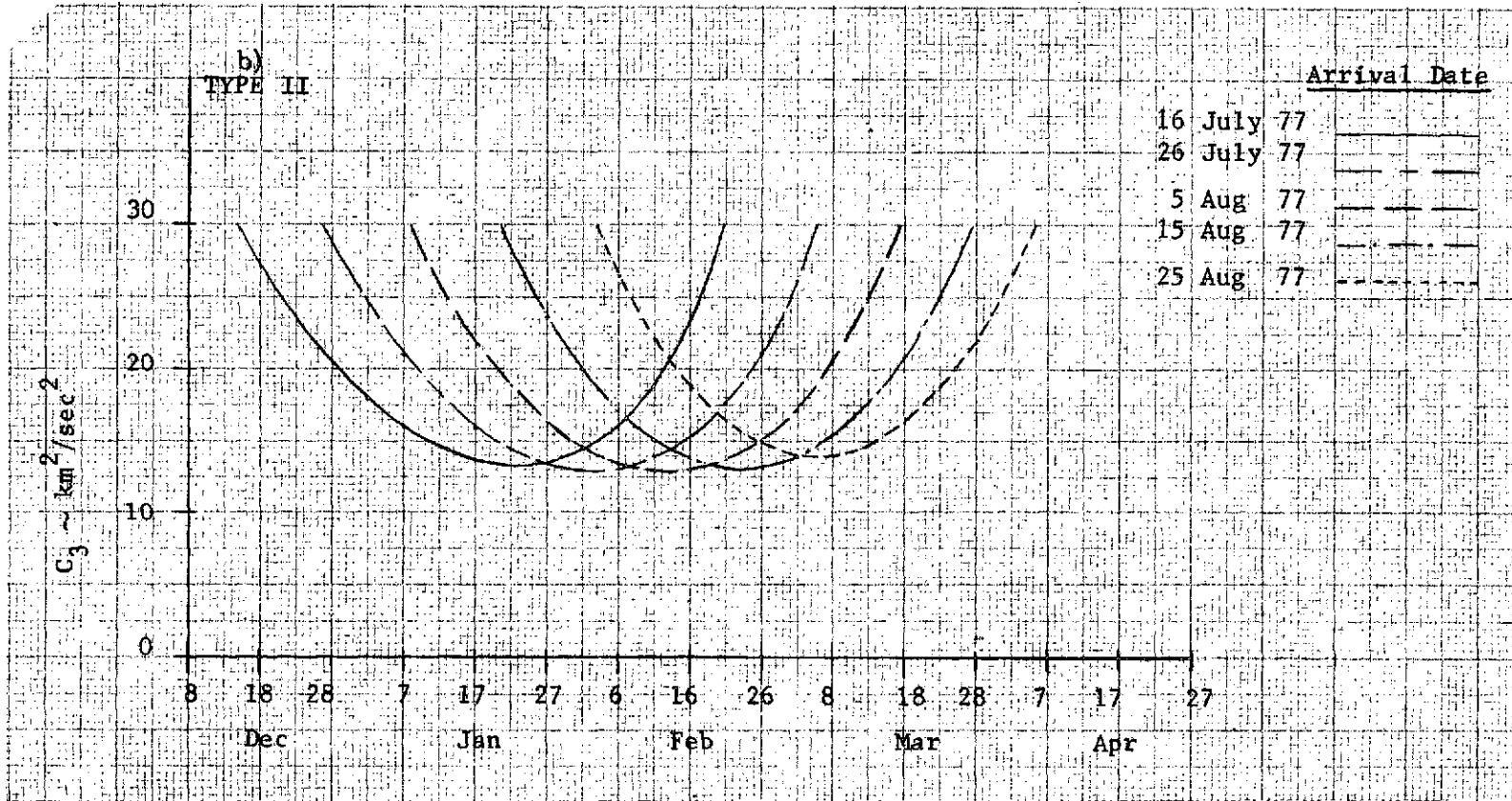
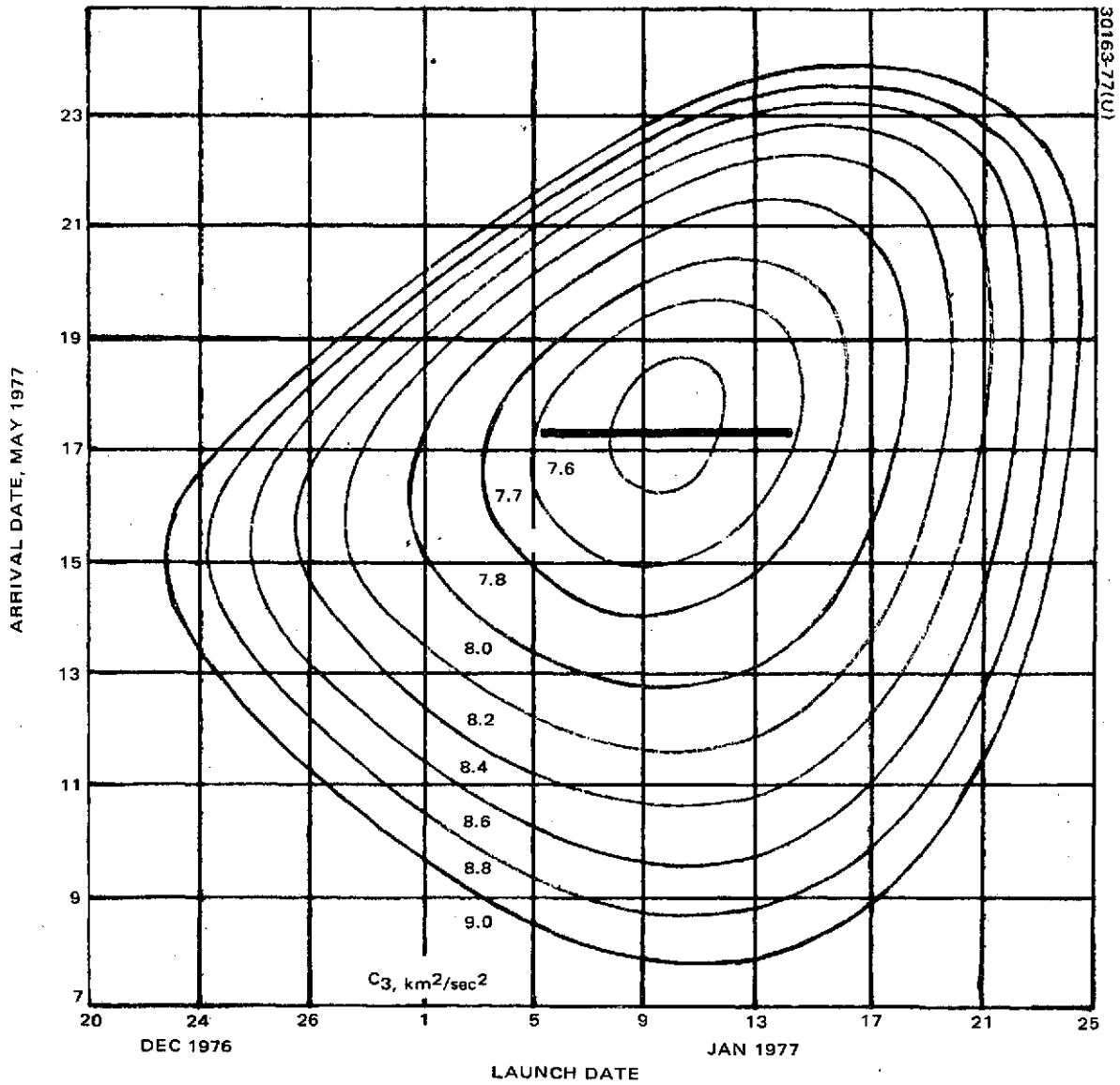


FIGURE 3-2. ENERGY (C_3) AS FUNCTION OF LAUNCH DATE AND ARRIVAL DATE FOR 1976-77 LAUNCH OPPORTUNITY TO VENUS



30163-76(U)

FIGURE 3-2 (continued). ENERGY (C_3) AS FUNCTION OF LAUNCH DATE AND ARRIVAL DATE FOR 2976-77 LAUNCH OPPORTUNITY TO VENUS



30163-77(U)

FIGURE 3-3. REPRESENTATIVE LAUNCH DATE/ARRIVAL DATE/LAUNCH ENERGY CONTOUR MAP WITH MINIMUM ENERGY 10 DAY LAUNCH WINDOW

TABLE 3-2. 1977 PROBE NOMINAL LAUNCH WINDOW

| Launch Date, Month/Day/GMT | Arrival Date, Month/Day/GMT | Parking Orbit Coast Time, Min | Thor/Delta Final Burns | | Solar Aspect Angle, deg | Flight Time, days | C ₃ , (km/sec) ² | Launch Azimuth, deg | Approach Asymptote | | |
|-------------------------------|--------------------------------|-------------------------------------|---------------------------|-----------|-------------------------------|-------------------------|---|---------------------------|-----------------------|------------------------------|--|
| | | | Latitude | Longitude | | | | | V _∞ km/sec | Ecliptic Latitude, deg | Ecliptic Longitude From Sun, deg |
| | May/17/1300 | | | | | | | 90.0 | | | |
| 1/6/0546 | May/17/1300 | 23.1 | -13.2 | 28.8 | 36.3 | 131.3 | 7.614 | 90.0 | 4.404 | -37.0 | 134.9 |
| 1/7/0537 | May/17/1300 | 23.2 | -13.3 | 29.2 | 34.7 | 130.3 | 7.561 | 90.0 | 4.398 | -36.6 | 135.3 |
| 1/8/0529 | May/17/1300 | 23.2 | -13.4 | 29.4 | 33.0 | 129.3 | 7.520 | 90.0 | 4.394 | -36.2 | 135.6 |
| 1/9/0521 | May/17/1300 | 23.2 | -13.5 | 29.6 | 31.4 | 128.3 | 7.490 | 90.0 | 4.391 | -35.9 | 135.9 |
| 1/10/0514 | May/17/1300 | 23.3 | -13.5 | 29.7 | 29.7 | 127.3 | 7.473 | 90.0 | 4.389 | -35.5 | 136.2 |
| 1/11/0506 | May/17/1300 | 23.3 | -13.6 | 29.8 | 28.1 | 126.3 | 7.467 | 90.0 | 4.388 | -35.2 | 136.4 |
| 1/12/0459 | May/17/1300 | 23.3 | -13.6 | 29.8 | 26.4 | 125.3 | 7.474 | 90.0 | 4.388 | -34.9 | 136.7 |
| 1/13/0452 | May/17/1300 | 23.3 | -13.6 | 29.8 | 24.7 | 124.3 | 7.494 | 90.0 | 4.388 | -34.6 | 136.9 |
| 1/14/0445 | May/17/1300 | 23.3 | -13.6 | 29.8 | 23.0 | 123.3 | 7.528 | 90.0 | 4.389 | -34.3 | 137.2 |
| 1/15/0438 | May/17/1300 | 23.3 | -13.5 | 29.7 | 21.4 | 122.3 | 7.575 | 90.0 | 4.391 | -34.1 | 137.4 |

Nominal Launch Conditions. The optimization was performed with the integrating trajectory program. The ten selected launch opportunities are given in Table 3-2 (values are given at the start of each daily window; launch azimuth increase throughout the daily window is about 1 deg with correspondingly small variations in the other variables). The launch times are compatible with trajectory dynamics and the arrival time is 1300 GMT on 17 May 1977 for all trajectories. There are small variations in the arrival asymptote throughout the launch window. These variations are well within the bounds necessary to permit the probe and bus target sites to be held fixed throughout the window (the selected strategy). The trajectories given in Table 3-2 and the performance data of Table 3-1 produce the launch capability given in Table 3-3. The baseline value of the spacecraft mass is derived from the minimum value of launch booster capability and is 384.1 kg. The maximum spacecraft mass is insensitive to the number of days required in the launch window (as expected from the illustrative contours of Figure 3-3).

Transit Geometry. The probe spacecraft is acquired (10 deg elevation angle) by the Canberra (Australia) Tracking Station approximately 15 min after Thor Delta separation and can be tracked continuously from this time. The tracking range and transit trajectory geometry are given in Figures 3-4 and 3-5, respectively.

TABLE 3-3. 1977 MULTIPROBE MISSION
(Thor/Delta)

| Launch Date, January | Launch Booster Capability - kg (lb) * | |
|-------------------------|--|---------|
| 6 | 405.6 | (894.3) |
| 7 | 406.1 | (895.3) |
| 8 | 406.5 | (896.1) |
| 9 | 406.7 | (896.7) |
| 10 | 406.9 | (897.0) |
| 11 | 406.9 | (897.1) |
| 12 | 406.9 | (897.0) |
| 13 | 406.7 | (896.6) |
| 14 | 406.4 | (896.0) |
| 15 | 406.0 | (895.1) |

* Includes adapter and launch booster telemetry kit of 21.5 kg (47.5 lb)
Baseline spacecraft mass = 384.1 kg (846.8 lb)

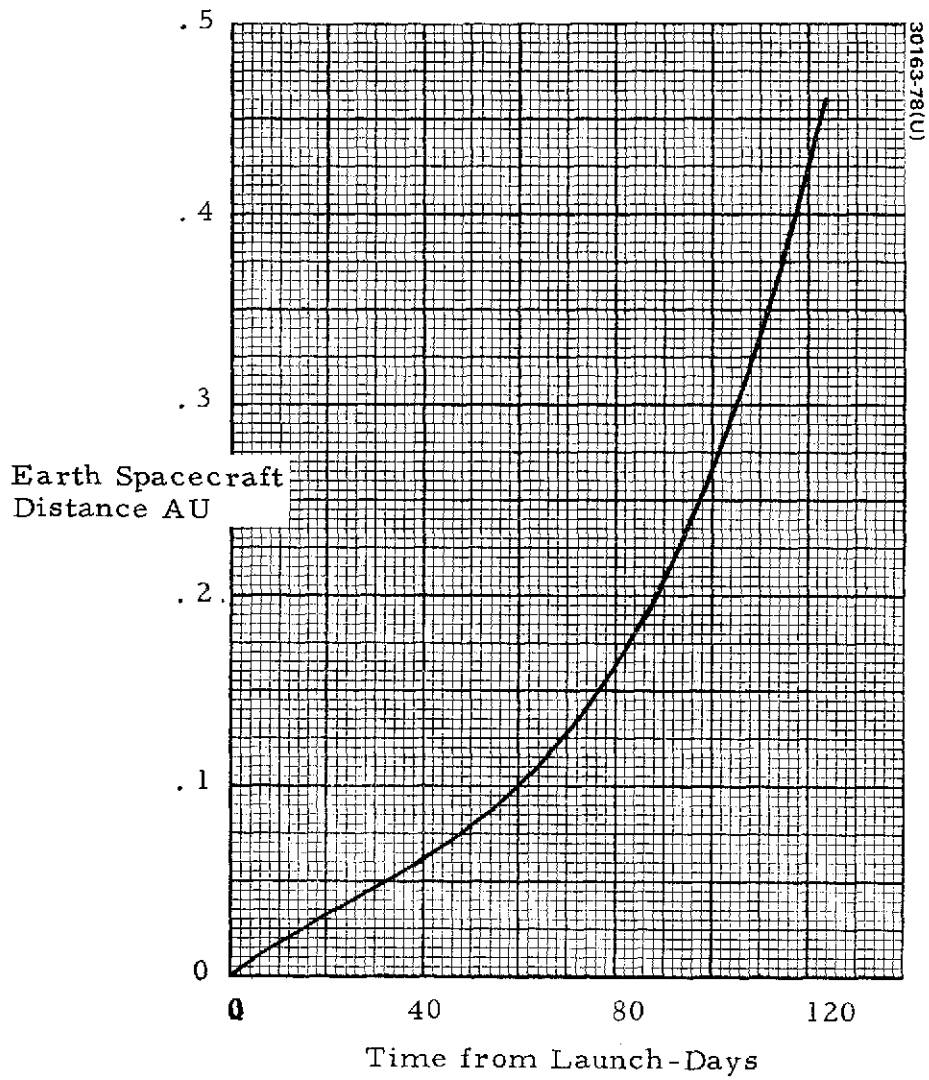


FIGURE 3-4. 1977 MULTIPROBE MISSION TYPE I TRANSIT
TRAJECTORY COMMUNICATION DISTANCE

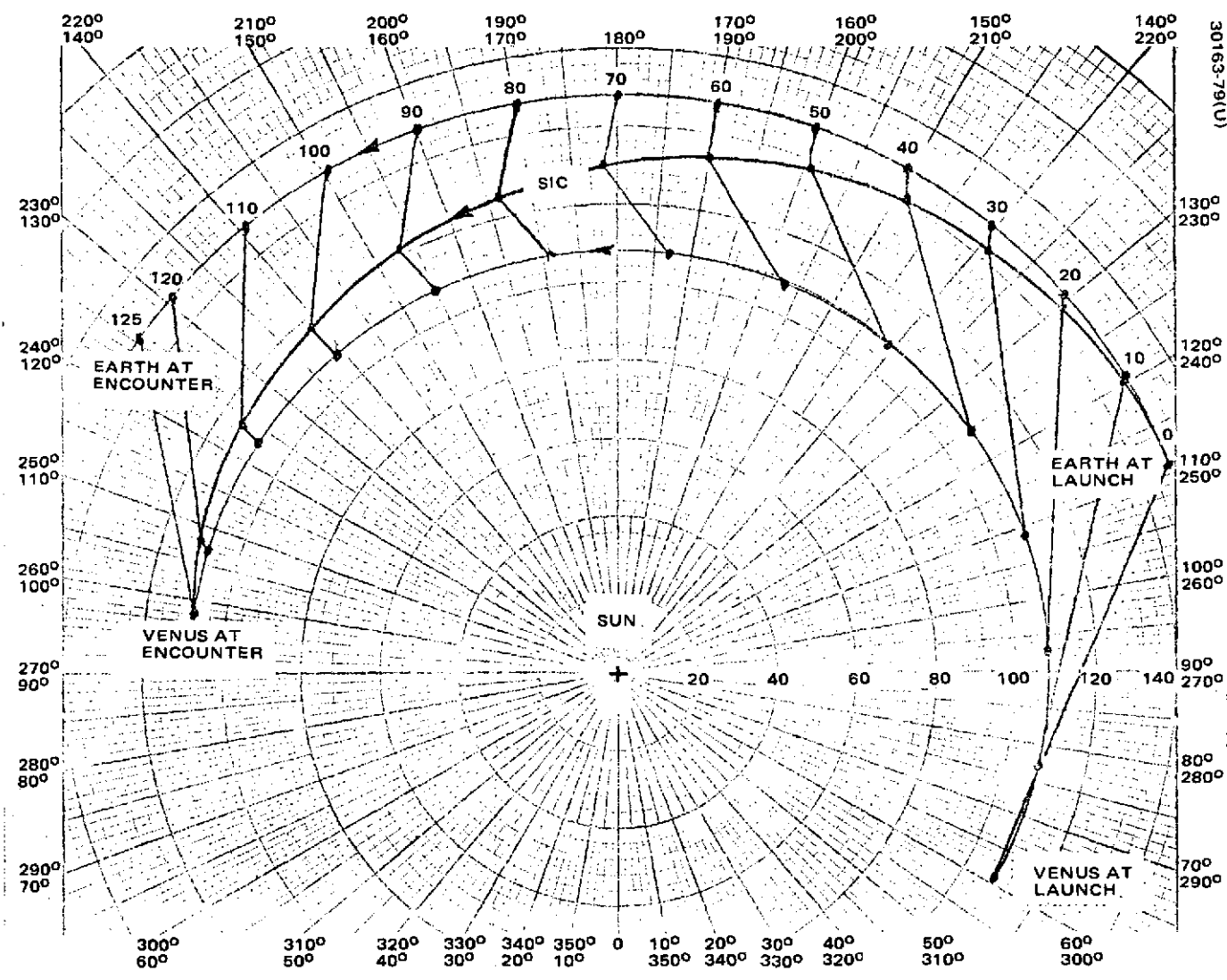


FIGURE 3-5. MULTIPROBE MISSION TRANSIT GEOMETRY

30163-80(U)

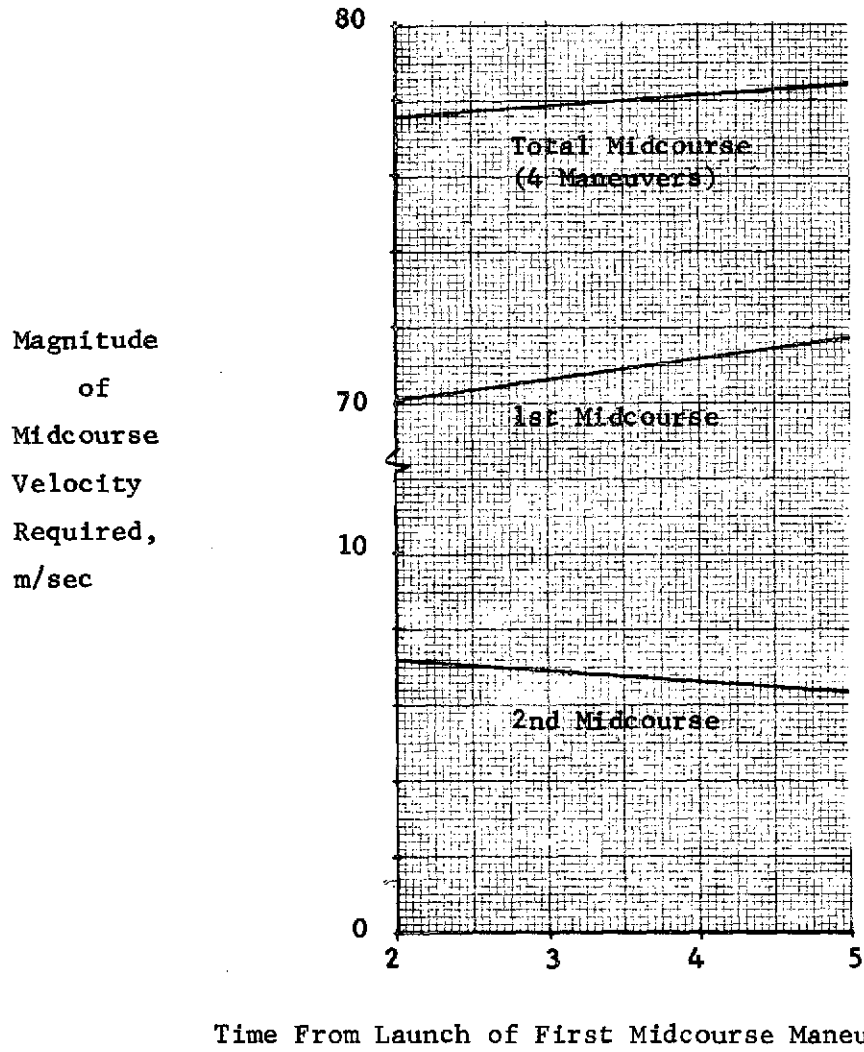


FIGURE 3-6. MIDCOURSE REQUIREMENT VARIATION WITH TIME OF FIRST MANEUVER - THOR/DELTA TYPE II ORBITER

Probe and Orbiter Midcourse ΔV Requirements

The ΔV requirements for both multiprobe and orbiter missions are presented here. Trajectories utilized for the orbiter missions are discussed in subsection 3. 2.

A Monte Carlo analysis was used to compute ΔV requirements arising from errors in launch vehicle injection, orbit determination, and execution of prior midcourse maneuvers. Total requirements for the Thor/Delta missions (99 percent values) are 76.6 m/sec for the probe mission and for the Type I and Type II orbiter missions 80.5 and 78.4 m/sec, respectively.

Midcourse ΔV Error Sources

Maneuver Times. Midcourse maneuvers are required during the transit to Venus to correct launch vehicle injection errors. The maneuver strategy is to correct time of flight as well as miss at Venus to ensure constant relative Earth-Venus-spacecraft geometry at encounter. The first midcourse maneuver should be performed as soon as practical after launch, and a conservative value of 5 days was utilized for the time of the first midcourse correction. This maneuver is by far the largest and is due almost exclusively to the injection errors from the launch vehicle. Figure 3-6 indicates the lack of sensitivity of the total ΔV required to the time of first midcourse maneuver.

The second midcourse maneuver is nominally scheduled 20 days after launch to allow time for precise orbit determination (the magnitude is not sensitive to execution time). The primary contributor to the second midcourse maneuver is the error caused by the execution of the first maneuver. Additional small midcourse maneuvers are required to correct for orbit determination uncertainty as well as execution errors. For purposes of this study, the third midcourse maneuver is scheduled for 50 days after launch; it may be required when injection errors are large in order to ensure that the maneuvers at arrival at Venus (and the resulting execution errors) will be extremely small. Since probe reorientation and targeting commences at 20 days before encounter, the final maneuver for the multiprobe mission takes place 30 days prior to encounter. This 10 day margin leaves sufficient time for postmaneuver orbit determination by the DSN. The fourth maneuver on the orbiter mission is nominally placed at 20 days prior to orbit insertion.

Injection Errors. Injection uncertainties for the Thor/Delta were supplied by ARC (Reference 4) for the multiprobe and both Types I and II orbiter missions. A more complete definition of the V-Y coordinate system and injection locations were supplied in Reference 5. This information permitted transformation of the injection covariances into the tangent plane cartesian coordinate system utilized in the Hughes computer program used for midcourse maneuver determination (TOPCON).

DSN Orbit Determination Errors. Orbit determination accuracy bounds using DSN tracking are given in Reference 6, for both the multiprobe and orbiter missions. Sources of error included not only station errors

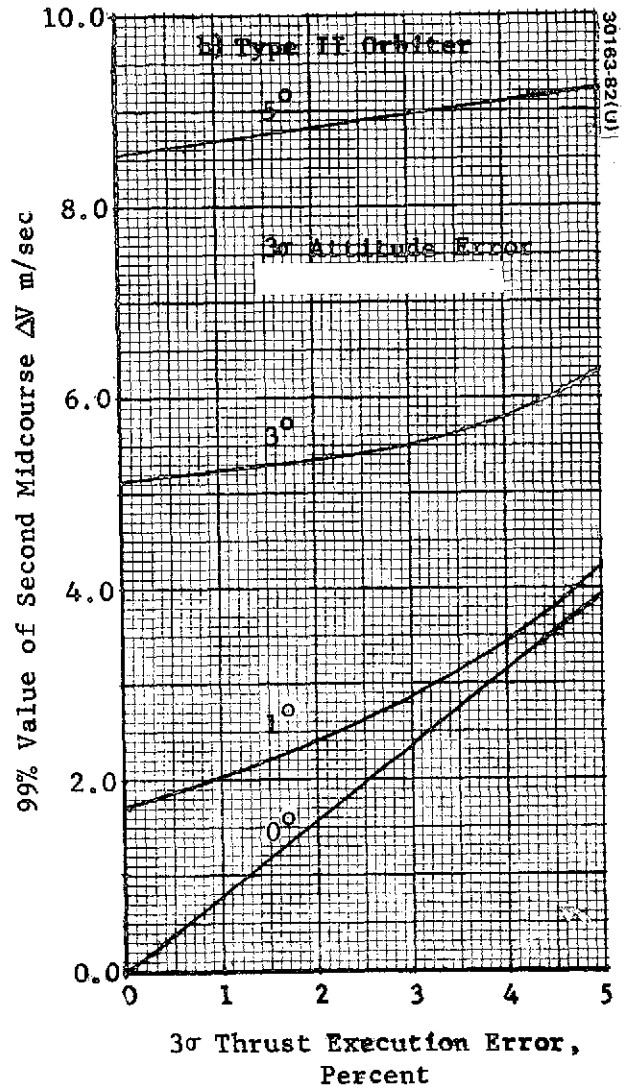
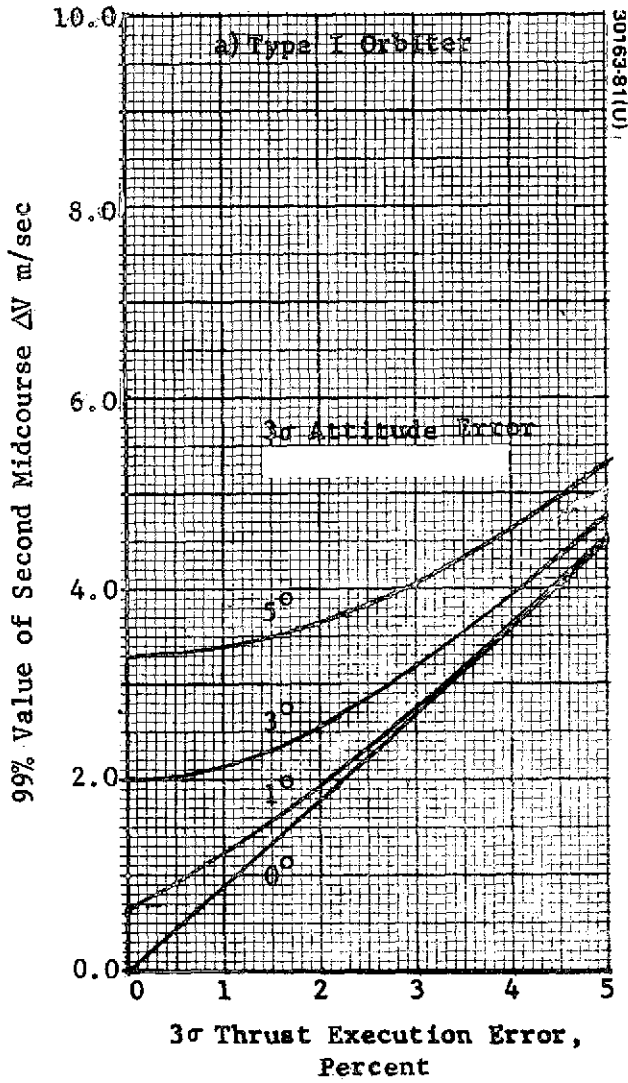


FIGURE 3-7. EFFECT OF MIDCOURSE CORRECTION EXECUTION ERRORS ON SECOND MANEUVER - THOR/DELTA

but stochastic uncertainties in acceleration due to solar radiation, propellant leakage, and mass uncertainty for Venus. The bulk of the ephemeris error in the B plane is due to unmodeled forces and has semimajor and semiminor axes less than 360 and 210 km (3σ), respectively. These position errors have a negligible effect upon the midcourse ΔV requirements.

Previous analysis (Reference 7) has shown that the velocity errors associated with the expected DSN ephemeris errors are about 0.03 m/sec (3σ). The velocity error distribution is nearly spherical and is a very minor contributor to the error ellipse, but for the sake of completeness these DSN errors were included in the derivation of midcourse ΔV requirements.

Maneuver Errors. Due to the nongaussian nature of midcourse errors, a Monte Carlo trajectory simulation (sample size = 10,000) was used to assess total midcourse ΔV requirements. Samples of ΔV having the distribution given by this covariance are generated. For each sample generated, an execution error is computed from a maneuver error model; the resulting error is propagated to the second maneuver. In a similar manner, this execution error of the second midcourse is propagated to the next midcourse, etc. The execution errors are in thrust attitude and thrust impulse magnitude (due to variations in specific impulse and flow rate).

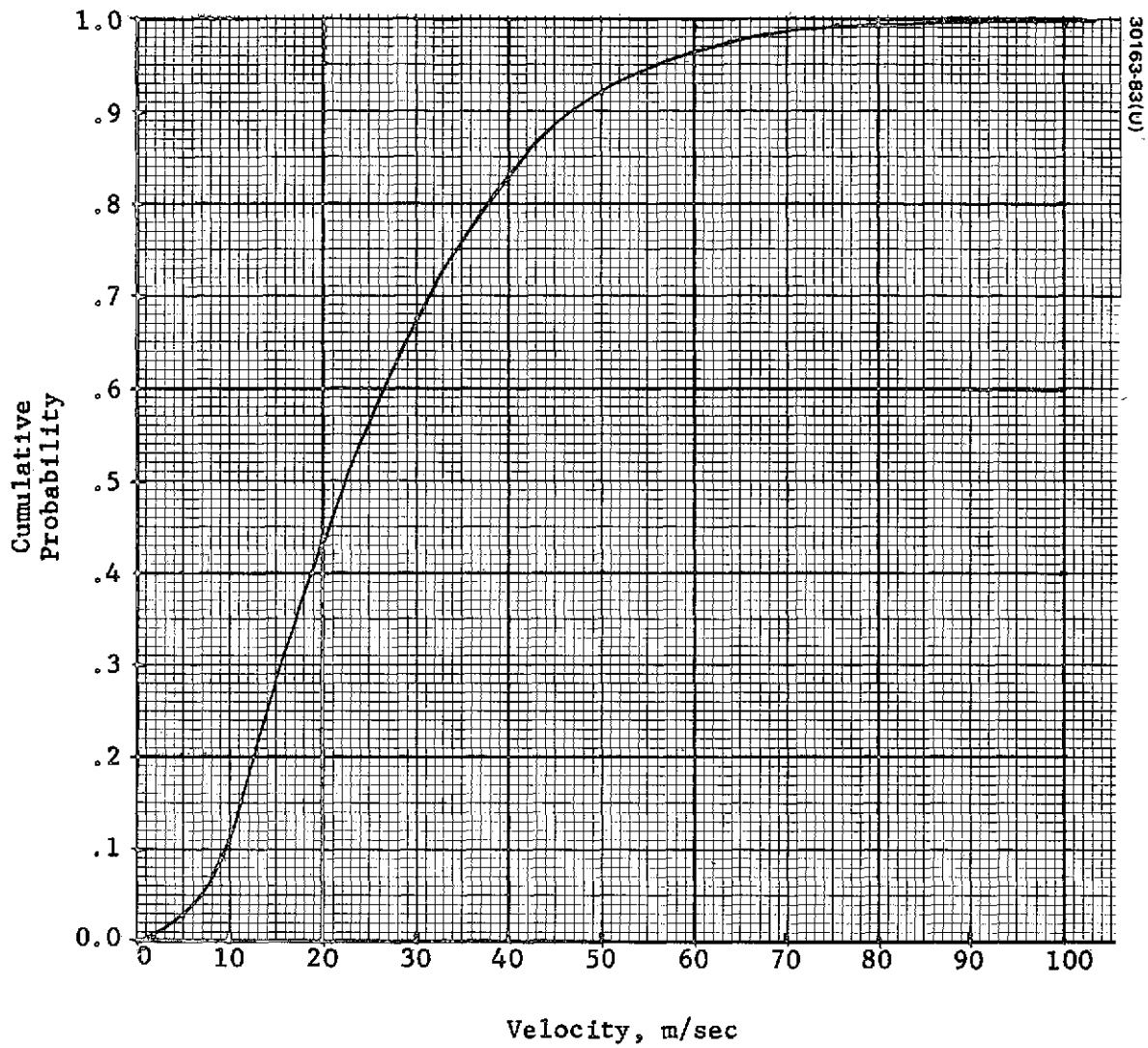
The thrust attitude error is specified relative to ΔV in terms of errors in cone angle (assumed normally distributed) and clock angle (assumed uniformly distributed). The thrust error is computed as a gaussian percentage error of the maneuver magnitude.

The effect of execution errors on the required midcourse correction is shown in Figure 3-7. The magnitude of the first maneuver is obviously independent of execution errors and subsequent maneuvers are small so only the second maneuver is plotted for both Types I and II orbiter missions. The results of 0 percent thrust execution error show the much greater sensitivity of Type II trajectories to attitude errors (approximately linear at 1.7 versus 0.65 m/sec per deg). The 0 deg attitude error curves show that the effect of thrust execution errors is linear and about 10 percent larger on the Type I trajectory.

The curves for the Type I trajectory indicate that thrust magnitude errors of a realistic size (4 to 5 percent) dominate statistically; reducing the thrust attitude error from 3 to 1 deg (3σ) leads to only about 0.3 m/sec reduction in the second midcourse correction. For the Type II trajectories the effect of attitude error is more significant (but still smaller than thrust magnitude errors).

Midcourse ΔV Requirements (Multiprobe and Orbiter Missions)

Execution errors of 5 percent in thrust magnitude and 3 deg in attitude (3σ) were used to derive the midcourse velocity requirements assuming 99 percent probability of success (Table 3-4). The distribution is not gaussian (Figure 3-8), since the ΔV is much less than the 99 percent value. Thus, for a typical mission, a significant mass of propellant will be unused after completion of the midcourse maneuvers.



30163-83(U)

FIGURE 3-8. FIRST MIDCOURSE CORRECTION ERROR DISTRIBUTION FOR MULTIPROBE MISSION - THOR/DELTA

The error remaining after all midcourse maneuvers is a combination of execution errors and orbit determination errors. The magnitude of the last midcourse maneuver is driven to be small so that the resultant execution error is statistically small compared with orbit determination errors.

The magnitude of the total midcourse velocity for the Thor/Delta launch vehicle is about the same for the multiprobe and orbiter missions (Table 3-4). The ΔV required for the first midcourse is most sensitive to errors in the magnitude of the injection velocity vector. But the relative effectiveness of a particular error in velocity magnitude decreases as C_3 increases. Thus, as seen in Table 3-4, the higher injection velocity uncertainty for the Type II orbiter mission is more than offset by the greater C_3 (Table 3-4).

Nominal Probe Targeting

Nominal probe and bus impact sites and parameters have been selected to accomplish scientific objectives while satisfying entry and communication constraints. This section contains nominal probe and bus entry sites, the relative entry times of the probes and bus, ΔV requirements necessary to perform all targeting maneuvers, and bus entry aerodynamic force and heat loads.

TABLE 3-4. MIDCOURSE VELOCITY REQUIREMENTS
(99 PERCENT), m/sec

| Time From Launch, days | Thor/Delta | | |
|------------------------|------------|----------------|-----------------|
| | Multiprobe | Type I Orbiter | Type II Orbiter |
| 5 | 71.9 | 75.1 | 71.7 |
| 20 | 4.2 | 4.8 | 6.3 |
| 50 | 0.4 | 0.5 | 0.3 |
| T_4^* | 0.1 | 0.1 | 0.1 |
| Total | 76.6 m/sec | 80.5 m/sec | 78.4 m/sec |

* T_4 = 30 days prior to encounter for multiprobe mission.
= 20 days prior to encounter for orbiter mission.

Targeting Rationale and Requirements

Large Probe. The large probe is constrained to enter on the day side of Venus in the region of the equator but not closer than 20 deg to the terminator (Reference 8). A nominal vertical descent condition 25 deg from the terminator has been selected to ensure satisfaction of this constraint in the presence of dispersions. The large probe must maintain an acceptable communication angle after release and should enter with a small angle of attack.

Small Probes. All three small probes have the same nominal spin axis orientation because they are spun off simultaneously; therefore, all have the same sun and earth communication angles from probe release to entry. The nominal spin axis is oriented along the velocity vector at small probe release.

Reference 8 indicates that the small probes should be separated by at least 30 deg in latitude and 90 deg in longitude. Day or night entry is acceptable for any or all small probes; entry angles less than -20 deg are preferred. Maximum communication gain occurs (for the baseline design) when vertical descent is at a 60 deg angle from the sub-Earth point. A wider nominal separation would complicate the communication problem and the nominal 60 deg separation more than satisfies the constraints of Reference 8.

Bus. The bus should be targeted to result in maximum time of passage between altitudes of 160 to 130 km, with guaranteed sampling at 130 km; targeting for either the light or dark side is acceptable. The bus should enter at a small angle of attack with an acceptable Earth communication angle. The bus should also be delayed by 1.5 h for experimental Doppler/DLBI to provide a reference, with no unknown velocity components, while probe measurements are being taken.

Nominal Sequence of Events

The encounter phase of the multiprobe mission commences at 20 days before entry into the Venus atmosphere. At this time, the spin axis is precessed to align the large probe for a zero angle of attack entry. After despin to a relatively low spin rate, the large probe is separated with a small separation velocity (release mechanism induced) on the order of 0.6 m/sec. The bus is then spun up to 71.2 rpm and the spin axis precessed for small probe targeting (5.7 m/sec normal to the spin axis) and separation (equivalent $\Delta V = 5.6$ m/sec.) After small probe separation, the bus may be reoriented to obtain a better sun angle for power considerations. The bus then coasts for 2 days to permit orbit determination (and to thereby obtain improved estimates of small probe trajectories). At 18 days before entry, the bus spin axis is precessed to the orientation required to permit targeting and retardation of the bus with one firing of the axial jet; and this maneuver is implemented. A bus trajectory correction will be performed 10 days before entry is necessary. The final bus maneuver is reorientation for entry with zero angle of attack.

Nominal Probe Target Locations and Parameters

Figure 3-9 shows the geometry used to specify the probe-sun angle and probe-Earth communication angle. The time varying nature of these angles is depicted in Figure 3-10 with the identification of four regions (not drawn to scale) in which sun and earth communication angles may be specified. Though the inertial spin axis orientation at probe release and just prior to entry are the same, the relative motion of Sun-Earth-Venus alter the relative orientation angles. The transition region between entry and vertical descent lasts only a few seconds and thus the angles are ignored in this region. Relative planetary motion is negligible from entry to vertical descent; the angle changes reflect the changed spin axis orientation.

The nominal probe and bus orientation are those which exist in the middle of the launch window. The orientation of the asymptote varies by less than 2 deg from this nominal throughout the launch window; the entry angles or communication angles from probe release to entry therefore vary by not more than this amount. The probe and bus impact point are held fixed throughout the window; vertical descent conditions are therefore also fixed. Variation of the asymptote over the launch window in addition to loci of constant entry angle and communication angle are depicted in Figure 3-11. The nominal probe and bus target locations are depicted in Figure 3-12.

Large Probe. Large probe entry at 25 deg from the terminator defines the vertical descent conditions in Table 3-5. Table 3-6 gives orientation angles at release and just prior to entry for the condition of zero angle of attack for the large probe. The conditions given are compatible with subsystem constraints.

Small Probes. The small probe targeting problem was to obtain as large as possible separation distance between probes while maintaining an acceptable communication angle (probe-earth angle). Two parameters are required to satisfy this condition; a third parameter (defining a rotation around the spin axis) is necessary to determine the specific impact points. A special purpose computer program was developed to target the small probes.

It should be emphasized that the nominal small probe target locations are not limited to those depicted in Figure 3-12. The three probes may be targeted to have any desired speed in latitude and longitude. For example, one probe could be targeted for the antisolar point, while a second probe is targeted for the maximum declination (provided communication constraints were relaxed).

Vertical descent conditions obtained for the small probes are depicted in Figure 3-12 and listed in Table 3-5. These locations easily satisfy all Reference 8 constraints. Additionally, since the earth subpoint is at 112.7 deg from the subpolar point, the first probe has been targeted for the maximum declination in latitude (consistent with a 60 deg communication constraint).

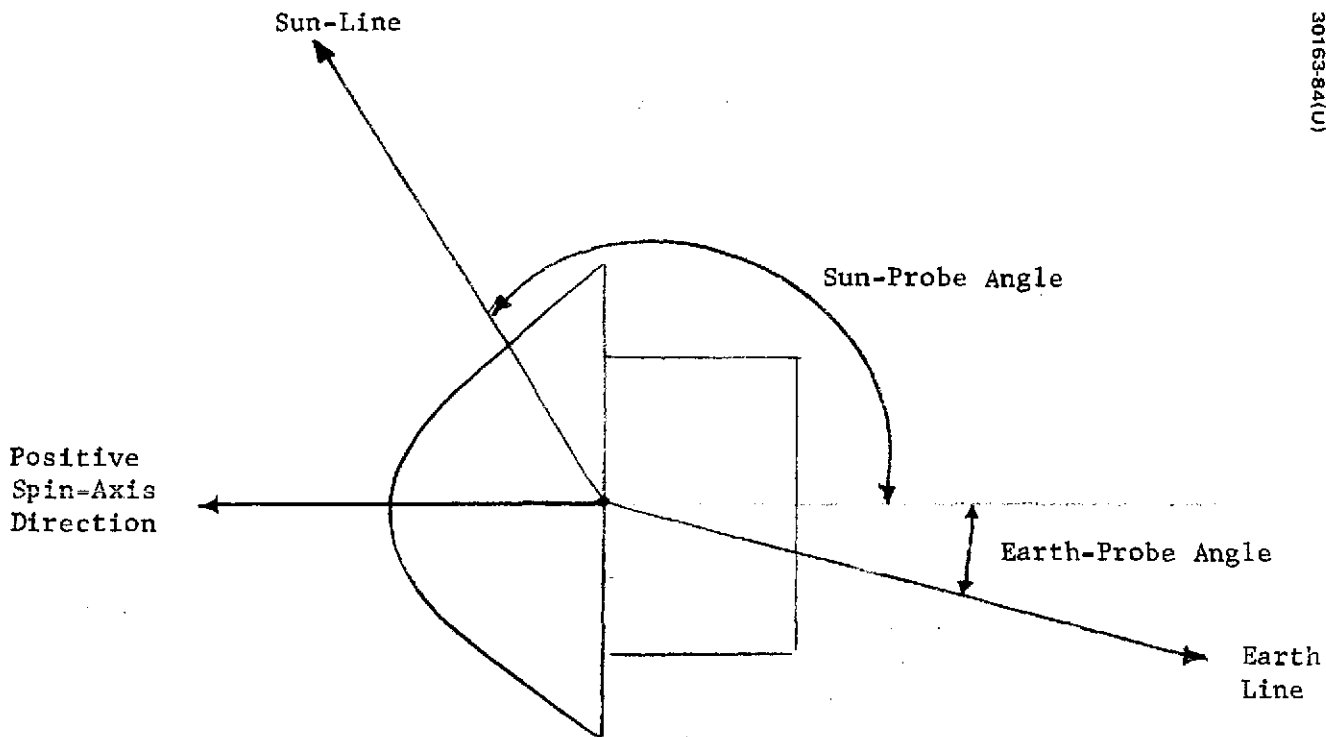


FIGURE 3-9. PROBE-SUN ANGLE AND PROBE-EARTH COMMUNICATION ANGLE

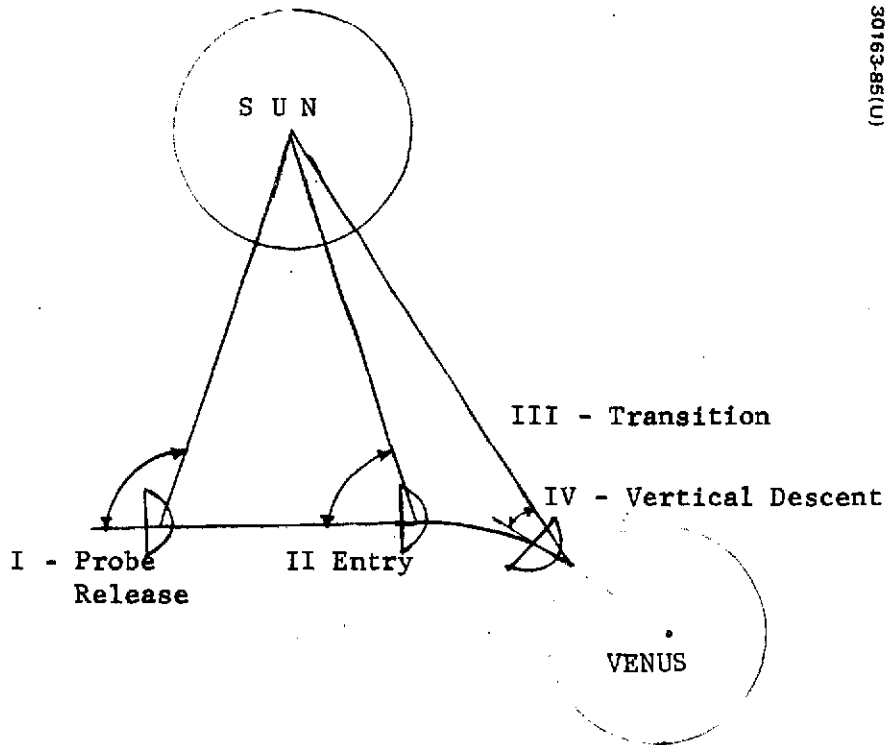
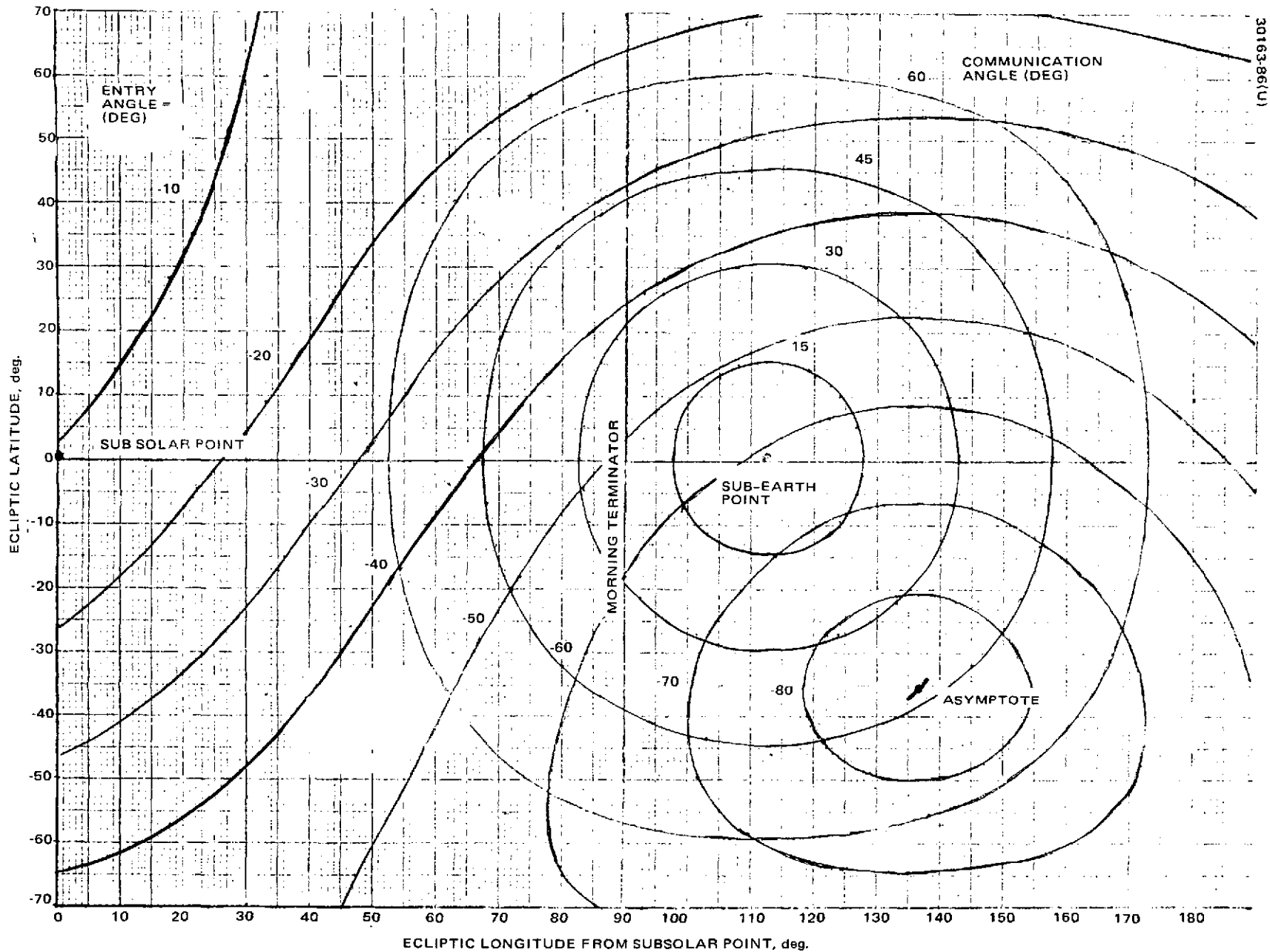


FIGURE 3-10. TIME VARYING GEOMETRY



30163-86(U)

FIGURE 3-11. LOCI OF CONSTANT COMMUNICATION AND ENTRY ANGLES (MIDPOINT OF LAUNCH WINDOW)

3-24

30163-87(U)

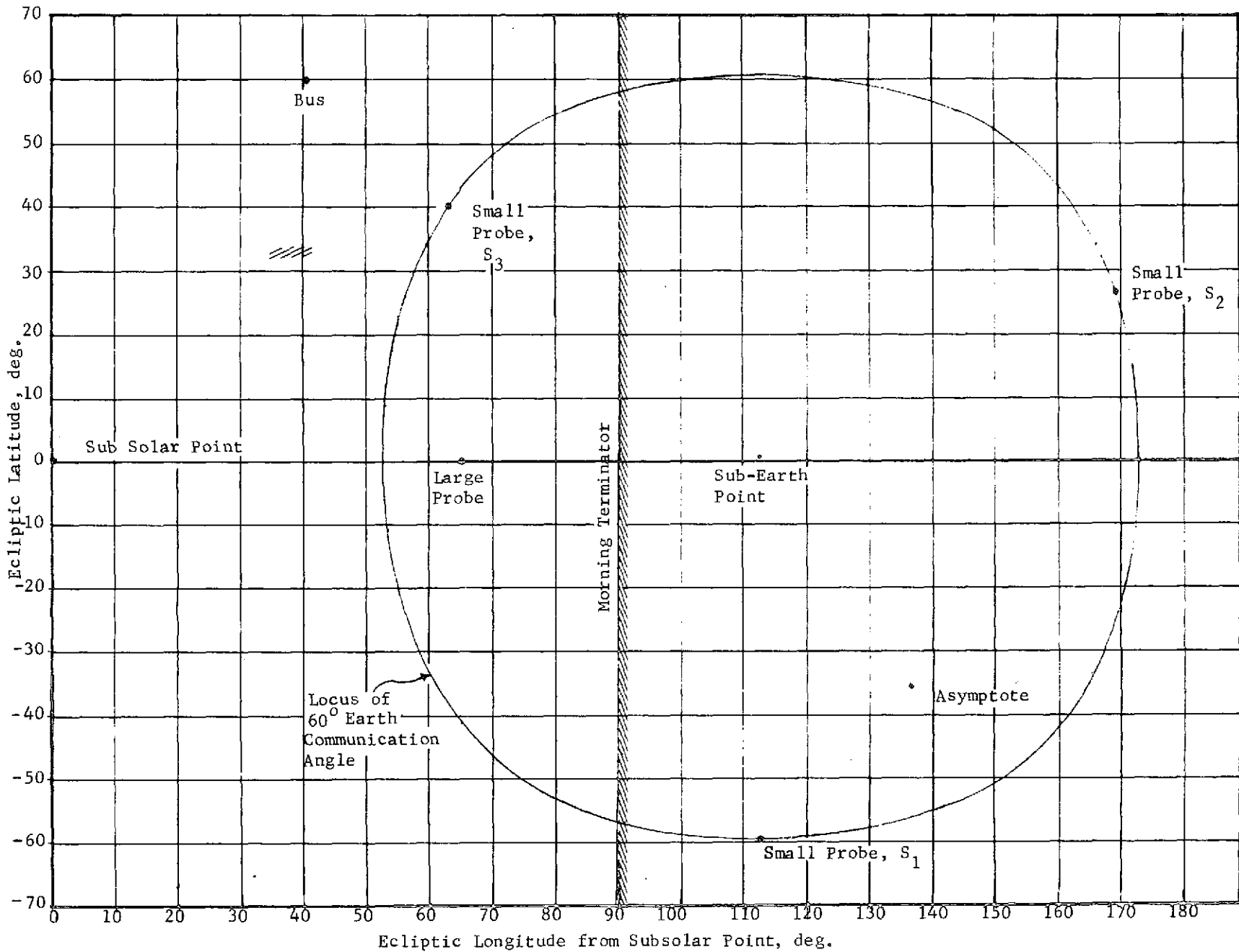


FIGURE 3-12. PROBE TARGETING GEOMETRY, 17 MAY 1977 - COMMUNICATION ANGLE = 60 deg

TABLE 3-5. VERTICAL DESCENT CONDITIONS

| Probe | Impact Latitude, deg | Impact Longitude deg | Probe Sun Angle, deg | Probe Earth Angle, deg |
|-------|----------------------|----------------------|----------------------|------------------------|
| S1 | -59.5 | 112.7 | 101.1 | 60.0 |
| S2 | 26.5 | 169.0 | 151.6 | 60.0 |
| S3 | 40.2 | 62.9 | 69.5 | 60.0 |
| L | 0.0 | 65.0 | 65.0 | 47.7 |
| Bus | 59.7* | 40.2* | -- | -- |

*Impact defined at 70 km altitude.

TABLE 3-6. NOMINAL ORIENTATION OF LARGE PROBE

| Angle | Release, deg | Prior to Entry, deg |
|-----------------|--------------|---------------------|
| Sun angle | 134.8 | 107.9 |
| Earth angle | 28.6 | 28.2 |
| Angle of attack | -- | 0.0 |
| Entry angle | -- | -39.8 |

TABLE 3-7. NOMINAL ORIENTATION OF SMALL PROBES

| Angle | Probe Release, deg | Prior to Entry, deg |
|-------------------|--------------------|---------------------|
| Sun angle | 143.1 | 126.2 |
| Earth angle | 46.0 | 41.7 |
| Angles of attack: | | |
| S_1 | -- | 8.7 |
| S_2 | -- | 21.2 |
| S_3 | -- | 31.8 |
| Entry angles: | | |
| S_1 | -- | -70.4 |
| S_2 | -- | -43.2 |
| S_3 | -- | -23.3 |

TABLE 3-8. NOMINAL ORIENTATION OF BUS PRIOR TO ENTRY

| | |
|-----------------|-------|
| Sun angle | 113.9 |
| Earth angle | 2.5 |
| Angle of attack | 0.0 |
| Entry angle | -12.0 |

The sun and earth communication angles are listed in Table 3-5 during vertical descent and in Table 3-7 for entry and probe release. The assumed orientation of spin axis along the velocity vector at probe release results in the entry angles of attack and entry angles given in Table 3-7. The conditions given are compatible with subsystem constraints.

Bus. The bus target point location is shown in Table 3-5. A dispersion of 300 km in the lateral position of the incoming asymptote was taken as the resultant of the errors in ephemeris estimation from deep space tracking and targeting. Thus, the constraints of maximum sampling time and guaranteed sampling at 130 km along with the dispersion in retargeting from the incoming asymptote define the locus of target points which is a circle centered about the asymptote. The spatial angle of the target point locus around the asymptote (λ_i), is 123 deg (Figure 3-13). The bus target point is then specifically defined for the minimum earth communication angle. This angle occurs when the incoming asymptote, earth subpoint, bus entry point lie in the same plane. The sun and earth communication angles just prior to entry are shown in Table 3-8 for the zero angle of attack constraint on bus entry.

The penalty incurred by moving the bus entry point for a fixed zero angle of attack is an increased communication angle. Figure 3-14 shows the locus of bus target points for minimum entry angle consistent with the above constraints. Corresponding to each point on this locus is another point on the locus defining communication angle when the bus is constrained to enter with zero angle of attack. The great circle distance between the earth subpoint and the antenna orientation is the communication angle. Thus, the penalty paid for moving to a nighttime entry (point A) or entry closest to the pole (point B) are communication angles of greater than 20 deg. The nominal bus target point, as indicated above, is selected to give the minimum communication angle. This angle is computed as the angular distance between the nominal bus antenna orientation and the earth subpoint and has a value of 2.5 deg.

Relative Entry Times and ΔV Requirements. Table 3-9 presents the entry times of the probes and bus. All times are relative to the entry time of the large probe. The bus has been retarded by 1.5 h.

Included in Table 3-9 are the ΔV requirements to perform the targeting maneuvers. Since all small probes are spun off at the same time, only one maneuver is listed for the small probe targeting. Also, the large probe targeting is assumed accomplished by the midcourse maneuvers since (in the nominal sequence of events listed above), the large probe is released first. Finally, the targeting ΔV requirements for the bus at 18 days prior to entry is the resultant of the lateral displacement (6.5 m/sec) and the retardation (15.6 m/sec).

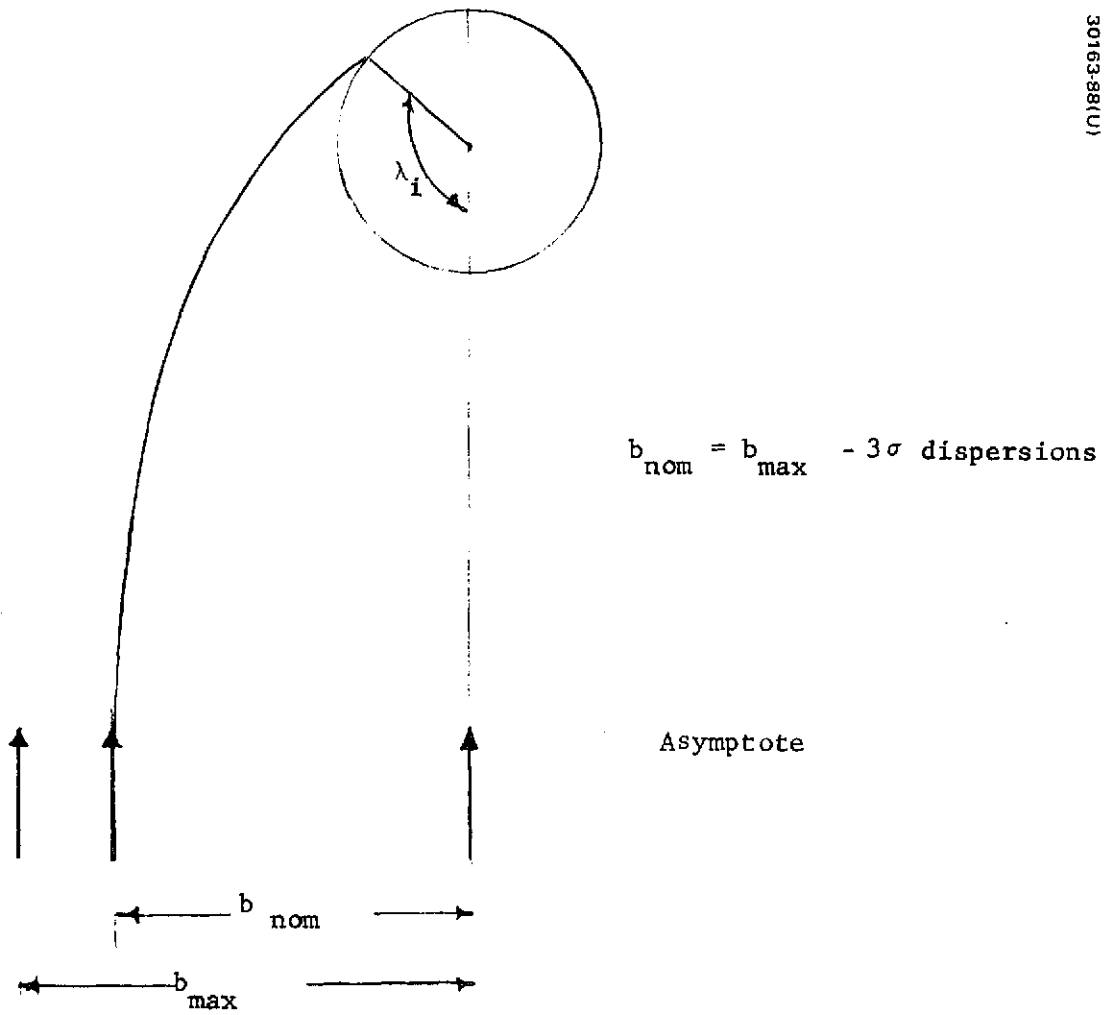
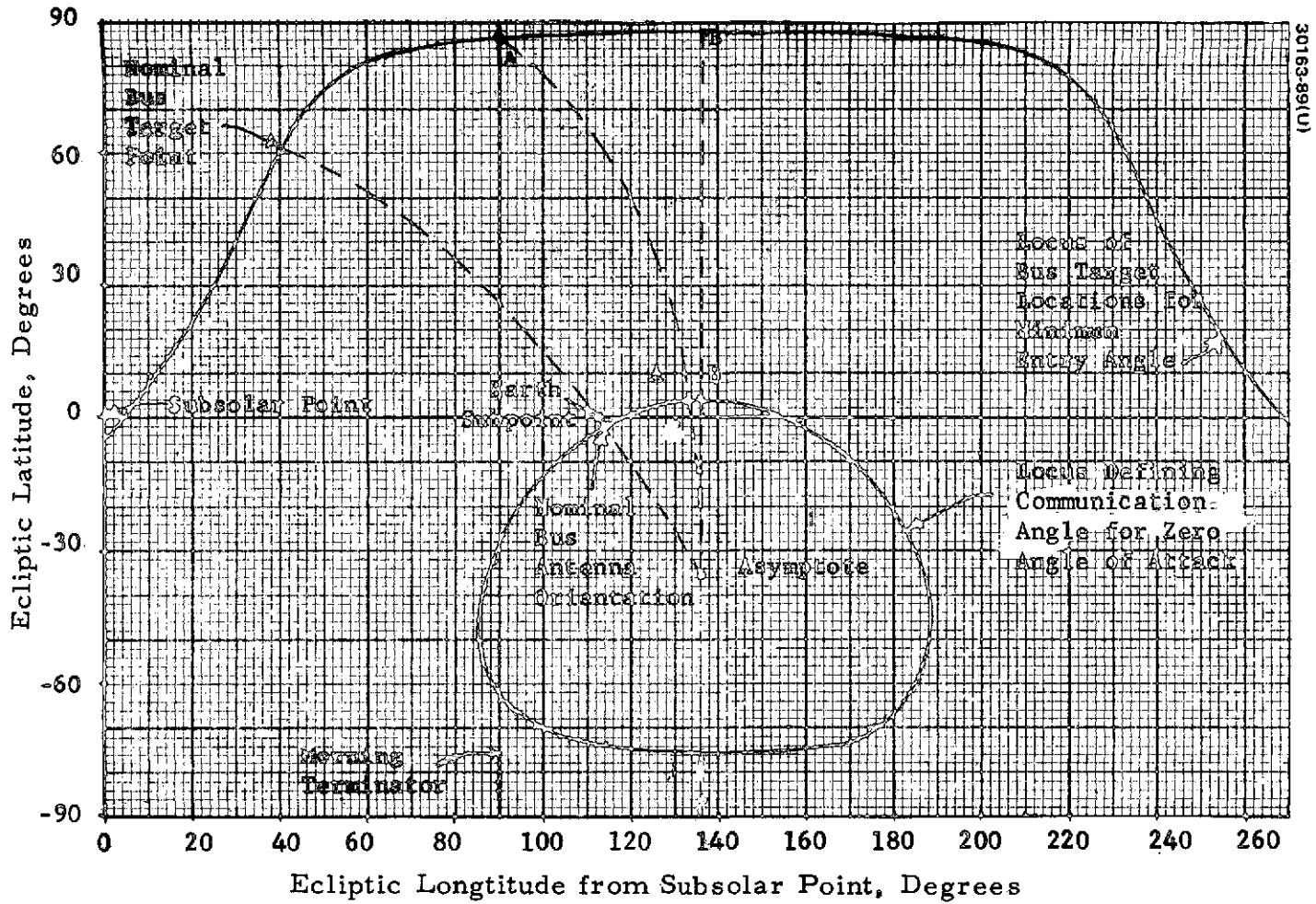


FIGURE 3-13. BUS TARGETING GEOMETRY



30163-89(U)

FIGURE 3-14. COMMUNICATION ANGLE VARIATION WITH BUS ENTRY LOCATION

TABLE 3-9. RELATIVE ENTRY TIMES
AND ΔV REQUIREMENTS

| Probe | Entry Time, min | Bus Targeting, m/sec |
|----------------|--------------------|-------------------------|
| S ₁ | -9.4 | } 5.7 |
| S ₂ | -0.7 | |
| S ₃ | 6.6 | |
| L | 0 | 0 |
| Bus | 90.0 | 16.9 |

Bus Entry Timing, Aerodynamic Force, and Heat Loads. The bus is targeted to obtain maximum sampling time (from 160 to 130 km) with guaranteed sampling at 130 km. Figure 3-15a illustrates altitude time history of the bus entry phase; the scale is expanded in Figure 3-15b for the end of the bus entry phase.

The spacecraft will fail due to thermal effects on entry. The critical failure mode is burnoff of the insulation on the front of the spacecraft and then heating of the spacecraft control electronics. The integral of the heating indicator is the factor which will determine when failure will occur. Preliminary analysis indicates that the value of the integral of the heating indicator at which failure will occur is at approximately 12,600 J/m² or at about 117 km for the Model I atmosphere of Reference 9 (Figure 3-16). The velocity change due to aerodynamic effects to this point is approximately 7 m/sec; the spacecraft reorientation due to torques potentially arising from this drag force is too small (< 3 deg) to interfere with bus communication. A factor which could affect bus communications is blackout due to ionization. This is expected to occur after an aerodynamic deceleration of 0.5 g, or at an altitude about 115 km with the Model I atmosphere. Thus, thermal failure should occur prior to communication blackout.

It should be emphasized that approximations utilized in the above analysis should have little effect upon the general conclusions because of the very steep nature of the curve in Figure 3-16. Even if the maximum allowable quantities were to change by a factor of two, the change in the minimum sampling altitude would be small. The minimum geometric sampling altitude is a function of the atmospheric model, but the density at which events occur will be less sensitive to this variation.

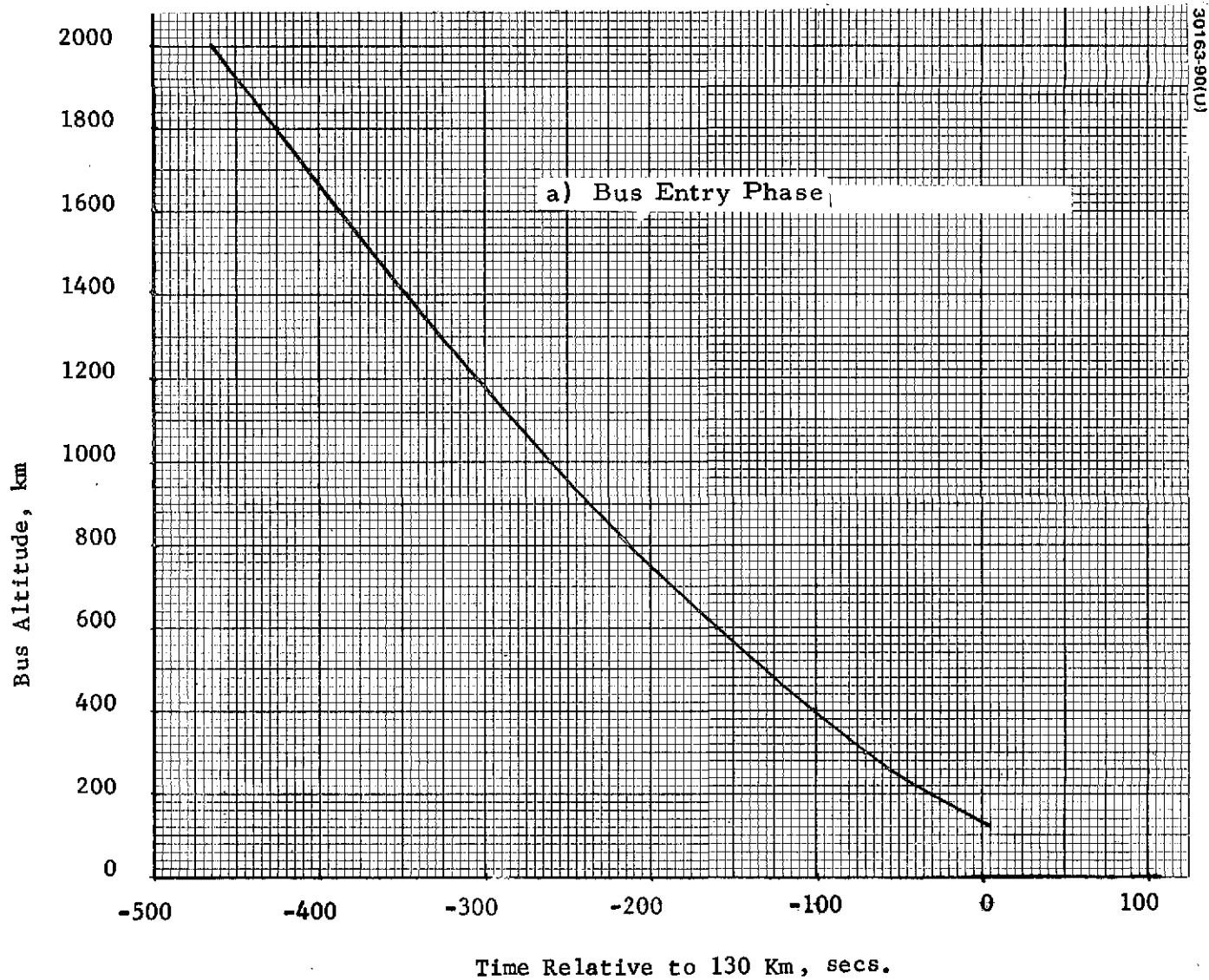


FIGURE 3-15. BUS ALTITUDE-TIME HISTORY

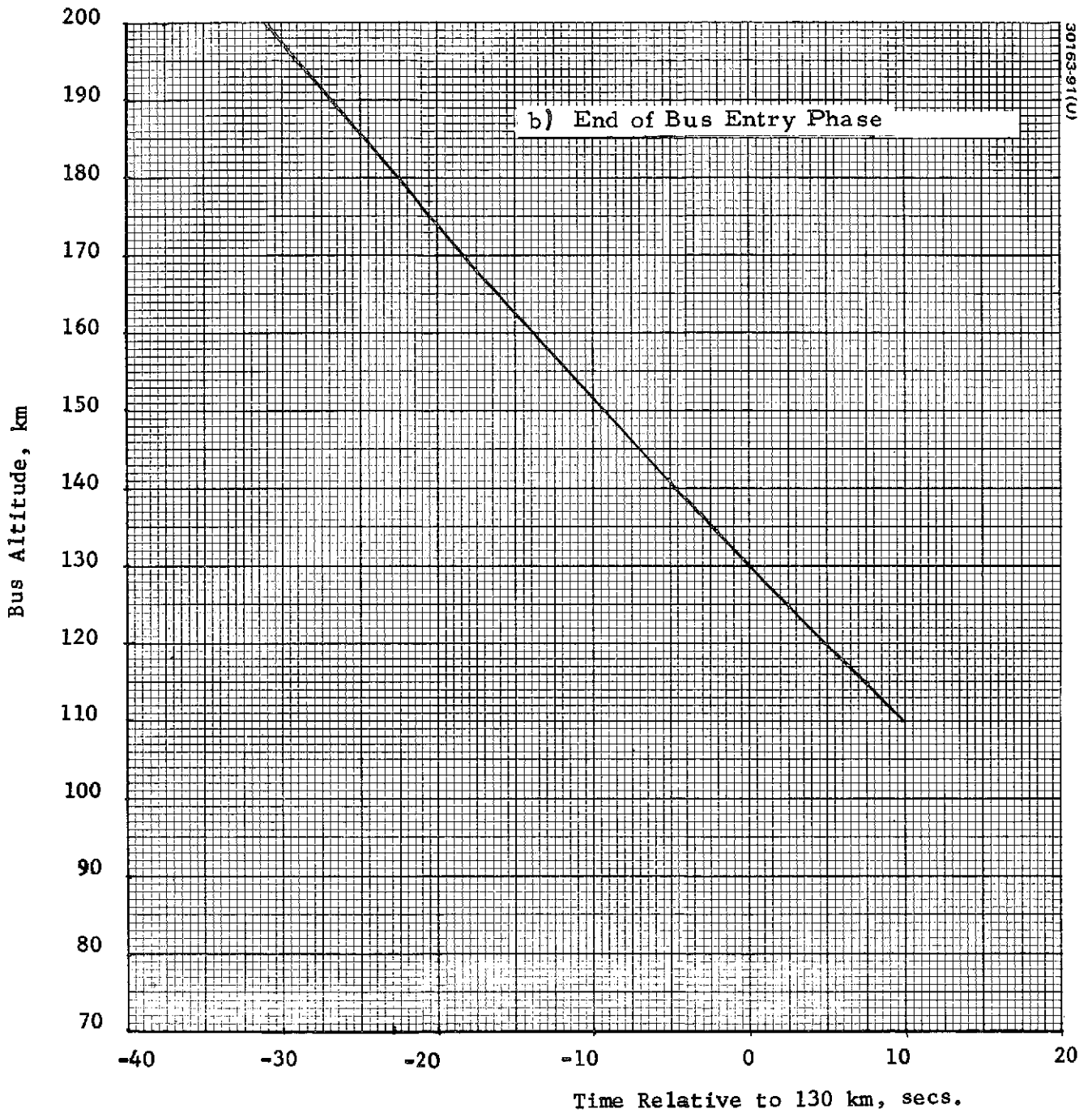


FIGURE 3-15(continued). BUS ALTITUDE-TIME HISTORY

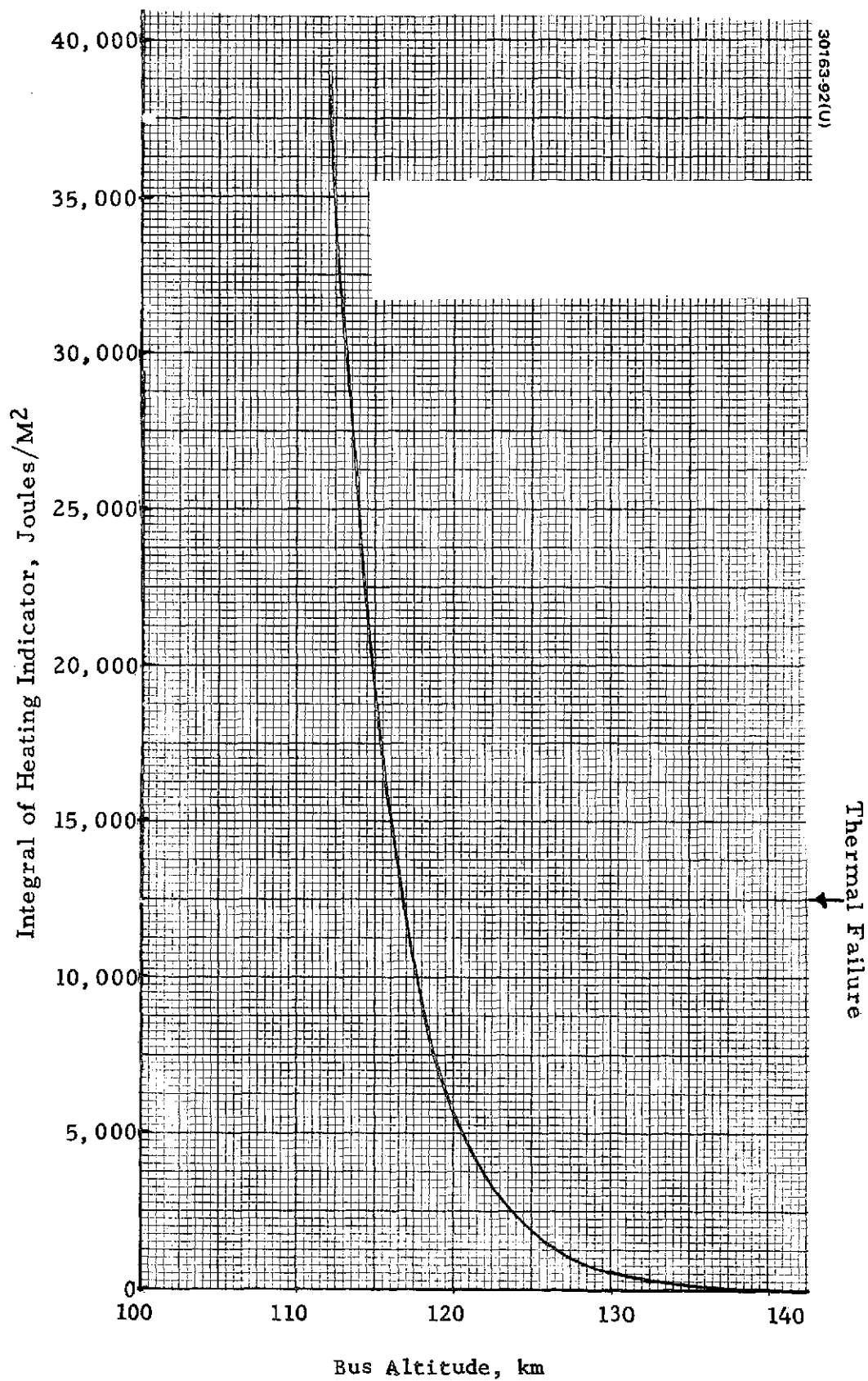


FIGURE 3-16. CHANGE OF INTEGRAL OF HEATING INDICATOR WITH ALTITUDE - MODEL I ATMOSPHERE

Probe Targeting Dispersions

The error sources that affect the impact locations of the probes may be separated into exoatmospheric and endoatmospheric effects. The exoatmospheric effects are due to orbit determination errors, targeting maneuver errors, and separation errors. Endoatmospheric dispersion causes are further separable into entry trajectory errors, probe characteristics, and atmospheric characteristics.

The proper combination of the error sources which effect the probe impact points is complicated by nongaussian statistics, nonlinear effects, and the fact that the error sources act in different directions. Fortunately the systems implications can be evaluated by reference to the major error sources. The following discussion bounds the major error sources.

Table 3-10 presents estimates of the maximum probe impact error sources due to exoatmospheric effects. The dominating error source for the large probe and bus is orbit determination errors (Reference 6). The shallow entry angles (especially for the bus) cause these orbit determination errors to project to fairly sizable dispersions on the surface of Venus (one great circle degree equals 105.59 km). Note that the bus has been targeted to guarantee sampling in the presence of dispersions so that sizable orbit determination error has no further system implications.

The small probe dispersions have been computed for the probe with the shallowest entry angle. As seen in Table 3-10 targeting maneuvers are also significant but these may be known more accurately due to postmaneuver tracking. The separation errors are broken down still further in Table 3-11, but though these error sources can be diminished by systems modifications they are still small with respect to the orbit determination and targeting maneuver errors.

Table 3-12 presents the dispersion estimate due to endoatmospheric effects. The dominant error source is due to the atmospheric wind characteristics. These values were obtained by integrating the Venera 8 upper bound wind curve for the large and small probe descent profiles (assuming the probe follows the wind) to obtain an estimate of the maximum lateral motion (Reference 10). The endoatmospheric effects outlined in Table 3-12 are also seen to be statistically small with the exoatmospheric error sources of Table 3-10.

TABLE 3-10. ESTIMATE OF MAXIMUM PROBE IMPACT ERRORS
DUE TO EXOATMOSPHERIC EFFECTS

| | Large Probe, km | Small Probe, km | Bus, km |
|---------------------|-----------------|-----------------|---------|
| Orbit determination | 250. | 450. | 1051 |
| Targeting maneuvers | <90. | 350. | 100 |
| Separation | <20. | <130. | -- |

TABLE 3-11. ESTIMATE OF MAXIMUM SMALL PROBE IMPACT ERRORS DUE TO SEPARATION ERRORS

| | <u>Impact Error, km</u> |
|------------------------|-------------------------|
| Event timing | 80.0 |
| Spin speed uncertainty | 20.0 |
| rpm | |
| Despin Reference | 40.0 |
| Separation dynamics | < 100.0 |

TABLE 3-12. ESTIMATE OF MAXIMUM PROBE IMPACT ERRORS DUE TO ENDOATMOSPHERIC EFFECTS

| Error Source | Large Probe, km | Small Probe, km |
|---|-----------------|-----------------|
| Entry trajectory errors | <30 | <30 |
| Probe characteristics (ballistic coefficients) | <10 | <10 |
| Atmospheric characteristics | | |
| Density profile | <50 | <50 |
| Winds | <107 | <124 |

3.2 ORBITER MISSION - SUMMARY

The 1978 orbiter mission is launch from Cape Kennedy and flies a Type II transit trajectory arriving at Venus on December 2 at 1800 GMT. Ten daily launch periods of 10 min each running from May 25 to June 3, provide a maximum spacecraft mass capability of 292.9 kg using the Thor/Delta launch vehicle. Transit times vary from 192.0 to 183.0 over the launch periods with a maximum injection C_3 of $19.445 \text{ (km/sec)}^2$. The velocity of the approach asymptote also varies slightly over the launch window with a maximum V_∞ of 3.715 km/sec and was designed to be held as nearly constant as possible without interfering with other trajectory design constraints.

The location of the orbiter periapsis point after injection from the Type II transit trajectory was selected at 26°N (midpoint of launch opportunity). Transit trajectory considerations actually yield two viable alternatives: Type I and Type II, with a range of periapsis locations from north to south depending upon orbiter inclination. Before any selection of transit trajectory can be made it was necessary to analyze those factors affecting the choice. These factors include midcourse ΔV requirements, Venus orbit characteristics, and selection of the orbital elements of the Venus spacecraft.

A Monte Carlo error analysis was used to compute ΔV requirements arising from errors in launch vehicle injection, orbit determination, and execution of prior midcourse maneuvers. Total requirement for the Thor/Delta orbiter missions are 80.5 m/sec for Type I and 78.4 m/sec for Type II.

Periapsis altitude was selected to have a nominal value of 150 km. Science considerations prefer the minimum altitude (consistent with safe operations) for the atmospheric sampling experiments and the choice of 150 km is independent of transit trajectory considerations. Similarly, a 24 h orbital period, selected as the baseline, is not affected by the choice of Type I or Type II transits.

Both the Venus oriented and velocity oriented experiments prefer high inclinations; and all other things being equal, science coverage is optimized for a 90 deg inclination. This choice of inclination is shown to be insensitive to the transit trajectory and it results in the limitation of trajectories to a set of four; a north and south periapsis location for both Type I and Type II. The fact that the Type I south periapsis location is in the polar region eliminates it from further considerations and the choice of periapsis latitude now narrows down to 9°N Type I, 26°N Type II, and 50°N Type II. After examining the tradeoffs between spacecraft/operations and science return in detail the 26°N , Type II periapsis was chosen as the baseline.

Orbiter Transit Trajectory Analysis - Summary

This section describes the tradeoffs which have been performed in trajectory analysis and defines detailed trajectory parameters for the 1978 orbiter mission. The baseline launch windows provide a maximum spacecraft mass capability of 292.9 kg using the Thor/Delta launch vehicle.

Introduction

The philosophy of the trajectory analysis used in the orbiter mission performance evaluation is similar to that of the multiprobe mission discussed in subsection 3.1. Choice of mission launch dates and parameters was primarily accomplished through the utilization of the two computer programs discussed in subsection 3.1, and the launch vehicle considerations (launch azimuth limits, daily launch windows, performance capability, etc.) also are presented in subsection 3.1.

1978 Orbiter Trajectories

Trajectory Constraints. The analysis of orbiter trajectories is considerably more complicated than that required for probe trajectories. The launch window and discretization considerations which have been previously discussed are applicable for the orbiter mission, and the performance optimization also depends not only on the launch energy (C_3) but upon the hyperbolic excess approach velocity at Venus (V_∞). If the orbit insertion motor utilized a liquid propellant, the propellant tank could in principle be appropriately loaded during each day of the launch window to provide retro-propulsion expendables compatible with the approach velocity for that trajectory. However, other spacecraft/mission objectives have led to the selection of a solid propellant orbit insertion motor for the baseline configuration. This suggests that the approach velocity at Venus be held as nearly constant as possible without interfering with other trajectory design constraints. These effects and science coverage considerations not yet introduced indicate that the launch opportunities which are ultimately selected as best satisfying mission objectives will be only loosely related to the unconstrained point optimum.

A Venus orbit inclined 90 deg to the ecliptic has been selected to maximize science return.

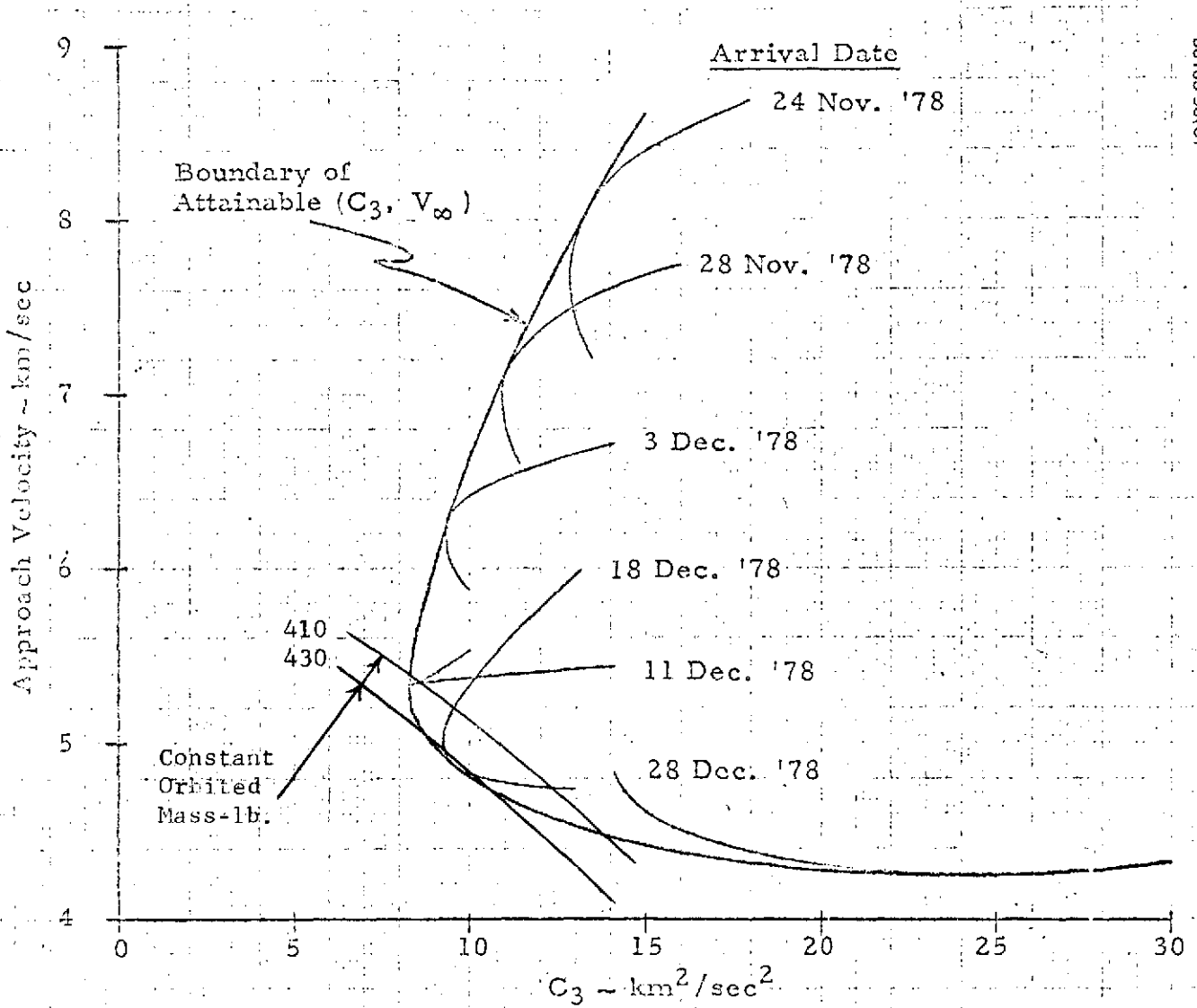
Type I versus Type II. Both Type I and Type II trajectories are contenders for the 1978 orbiter mission. Compared to the Type I trajectory, the Type II trajectory has a higher C_3 and a lower V_∞ ; for the Thor/Delta launch, the differences are such as to produce a nearly identical useful orbited mass. Analysis of the science coverage obtained with the orbits achieved as a result of the two alternatives is discussed below and shows that the Type II trajectory has a significant advantage at constant useful orbited mass (some tradeoff between orbited mass and science coverage is possible). The detailed rationale for selection of the Type II trajectory as the baseline is presented below. Detailed data is presented for both Type I and Type II in the following sections as an aid to transit trajectory selection.

Preliminary Analysis. The spacecraft mass in Venus orbit is maximized by achieving an optimum balance between launch energy and orbit insertion ΔV . As with the probe trajectory, the readily obtainable results from a conic interplanetary trajectory are useful for illustrative and conceptual purposes and for determination of the general region of interest, although not for detailed trajectory selection. The point optimum (1 day launch window) may be determined as shown in Figure 3-17 for the Type I trajectory. Values of approach velocity (V_{∞}) and launch energy (C_3) are obtained by varying the launch date for representative fixed arrival dates. The envelope of these curves define a boundary of attainable C_3 and V_{∞} ; optimum launch energy (C_3) are obtained by varying the launch date for representative fixed arrival dates. The envelope of these curves define a boundary of attainable C_3 and V_{∞} ; optimum launch conditions represent a point on this boundary. Lines of constant orbited mass are shown for the baseline initial orbit and an SVM-2 orbit insertion motor, off-loaded as necessary (selection of optimum interplanetary trajectories is insensitive to these parameters). The curves indicate that the optimum trajectories will have an arrival date near 18 December with $C_3 \approx 9.5 \text{ km}^2/\text{sec}^2$ and $V_{\infty} \approx 4.9 \text{ km/sec}$.

The dependence of useful orbital mass on both C_3 and V_{∞} together with the previously mentioned complexities associated with the launch window precludes a simple general representation of the performance optimum for a multiday launch window (as was possible with the simpler probe trajectories). Conceptually, the optimization procedure is to find the minimum/maximum values of C_3 for selected constant values of V_{∞} , and then find orbited mass (a function of C_3 and V_{∞}) for these cases. The value of V_{∞} which maximizes orbited mass defines the launch window which provides maximum performance. In practice, the selection of an alternative independent variable (e. g., first day of the window) will permit the same optimization process to be implemented more accurately and efficiently when discretization effects are considered.

Curves of C_3 and V_{∞} are shown for launch and arrival dates in the region of interest in Figure 3-18.

Note that the launch azimuth limit constrains the allowable Type II trajectories but is not a factor for the Type I trajectories (or the probe trajectories previously discussed). A representative line of constant approach velocity is illustrated in each figure (at approximately the condition selected for the final trajectories). In analogy to the probe analysis (and for the same reason) discretization of launch and arrival times has been ignored. However, it will also be noted that the effects of the discretization will be much more significant than in the case of the probe analysis; no matter where these discretizations occur some variation from the idealization of a constant V_{∞} throughout the launch window must be accepted. Constraints thus far imposed require a variation in arrival dates throughout the launch window for the Type I trajectory.



30163-93(U)

FIGURE 3-17. APPROACH VELOCITY AT VENUS AS FUNCTION OF ENERGY (C_3) AND ARRIVAL DATE FOR 1978 LAUNCH

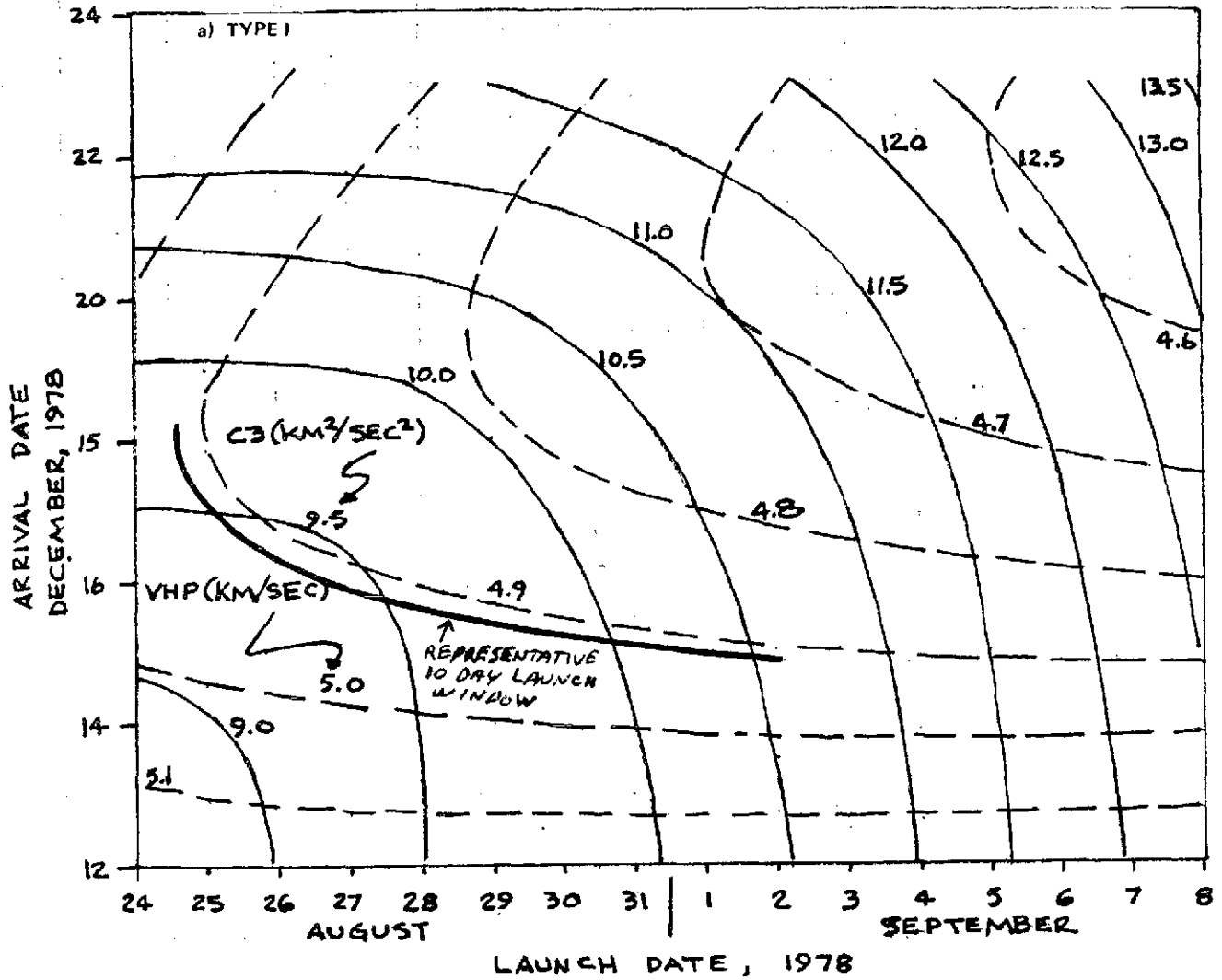


FIGURE 3-18. REPRESENTATIVE EARTH-VENUS TRAJECTORIES

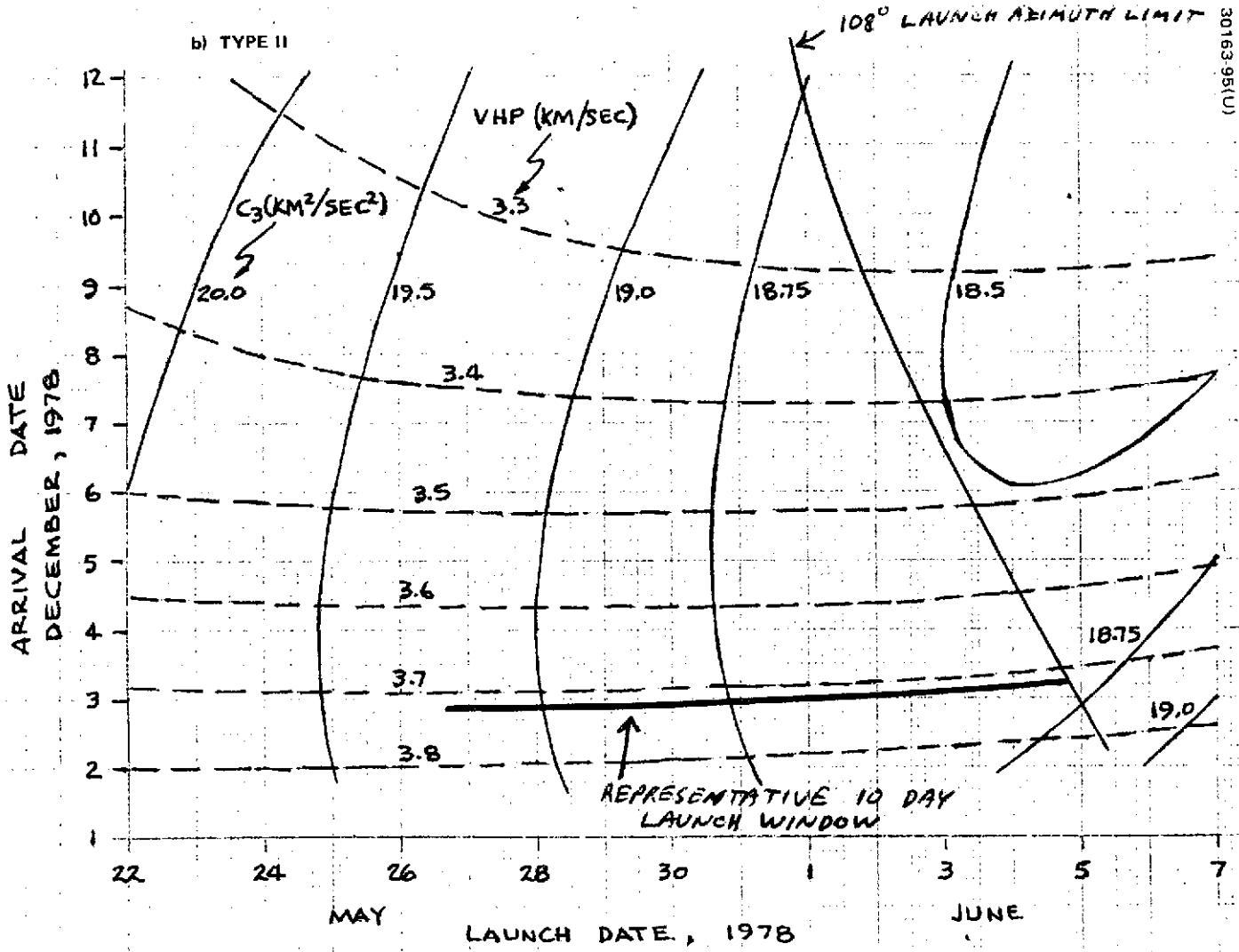


FIGURE 3-18(continued). REPRESENTATIVE EARTH-VENUS TRAJECTORIES

Trajectory Optimization. Trajectory comparisons performed with the integrating trajectory program for the Type I 1978 orbiter mission are shown in Figure 3-19. The performance shown is that obtainable with ten daily launch periods of 10 minutes each. The independent variable is the date of the start of the launch window. For simplicity, continuous curves have been drawn neglecting the effects of discretization. Variations in science coverage obtainable are related to the initial values of periapsis latitude and longitude. As indicated in Figure 3-19, these are quite constant throughout the spread of launch windows of interest and are therefore not a factor in the selection of the desired set of launch opportunities. The initial orbital mass is optimized by starting the launch window on about 19 August. This requires an orbit insertion motor with approximately 154.2 kg of expendables. For the interrelated reasons of cost, confidence, and reliability, it is very desirable to use an existing retro-motor design. Selection of candidate motors in this weight classification is quite limited, the most suitable candidate being the Aerojet General Corporation Model SVM-2 with a maximum loading of 159 kg of propellant at a specific impulse of 287 sec (this specific impulse was used in the data generation). Use of this motor, together with the use of about 3 kg of ACS hydrazine in the retro-propulsion maneuver, represents a reduction in initial orbit mass of about 2 kg with respect to that obtainable with an ideal motor (use of more hydrazine during retro-propulsion does not improve performance). The cost/reliability considerations previously mentioned have led to the decision to utilize the SVM-2 motor for the Type I orbiter mission.

Trajectory analysis similar to that performed above for the Type I trajectory has been performed for the Type II trajectory for the 1978 orbiter and is presented in Figure 3-20. As was the case with the Type I trajectories, the initial value of the periapsis latitude is insensitive to the date of the start of the launch window and this is then not a factor in the selection of the desired set of launch opportunities. However, the initial value of the periapsis longitude from the subsolar point is quite sensitive to the selection of launch opportunity. Science objectives will be best satisfied by having the initial periapsis longitude considerably removed from the terminator; it will be noted that this can be achieved at the expense of a decrease in initial orbited mass. If the final spacecraft orbited mass were known exactly, a baseline selection could readily be made, but in the actual situation a selection between these two conflicting objectives actually reduces to a selection of desired spacecraft performance pad. For the purposes of this study, the baseline selection provides a performance pad approximately equal to that available with the Type I trajectory as defined above. This is a reasonable selection if both Type I and Type II trajectories are deemed viable alternatives for the mission since it permits the most realistic comparison of the science coverage capability obtainable with these two alternatives. This selection corresponds to starting the launch window approximately 2 days later than that date which would provide maximum performance, and represents reduction in orbited mass below the optimum of approximately 4.6 kg.

Nominal Launch Conditions. Detailed launch opportunities have been defined based on the considerations outlined above. These are defined in Tables 3-13 and 3-14 for the Type I and Type II orbiter missions (values are

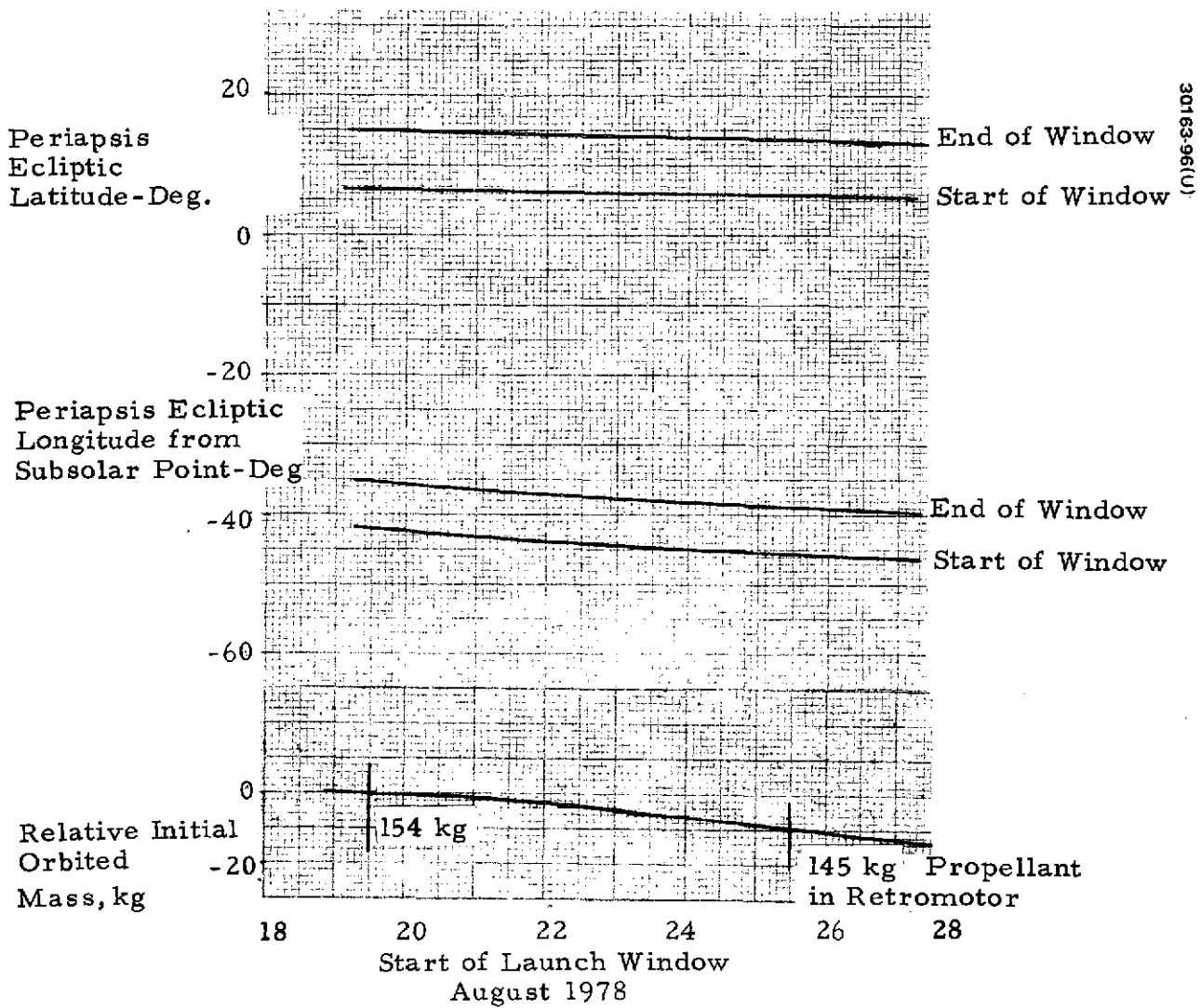


FIGURE 3-19. 1978 ORBITER TYPE I TRAJECTORY - 10 DAILY LAUNCH PERIODS OF 10 MIN

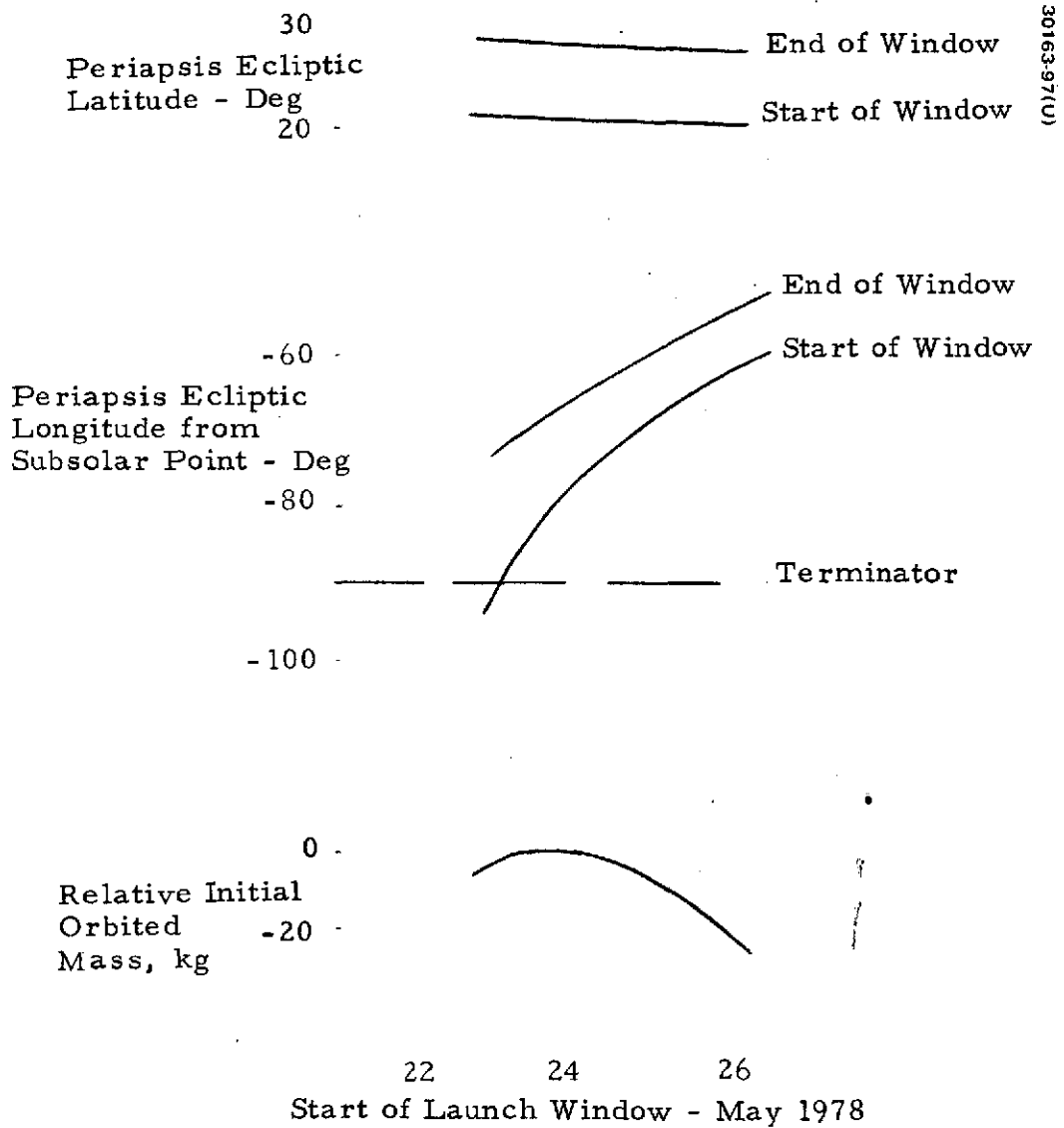


FIGURE 3-20. 1978 ORBITER TYPE II TRAJECTORY - 10 DAILY LAUNCH PERIODS OF 10 MIN (LAUNCH AZIMUTH LIMIT = 108 deg)

TABLE 3-13. 1978 ORBITER NOMINAL LAUNCH WINDOW FOR TYPE I TRAJECTORY

| Launch Date, Month/Day/GMT | Arrival Date Month/Day/GMT | Parking Orbit Coast Time, min | Thor/Delta Final Burns | | Solar Aspect Angle, deg | Flight Time, days | C ₃ (km/sec) ² | Launch Azimuth, deg | Approach Asymptote V _∞ , km/sec | Venus Orbit Periapsis Location | |
|-------------------------------|-------------------------------|-------------------------------------|---------------------------|-----------|-------------------------------|-------------------------|---|---------------------------|--|-----------------------------------|--|
| | | | Latitude | Longitude | | | | | | Ecliptic Latitude, deg | Ecliptic Longitude From Sun, deg |
| August | | | | | | | | | | | |
| /24/0139 | Dec/17/1800 | 32.5 | -26.0 | 71.8 | 10.6 | 115.7 | 9.486 | 90.0 | 4.916 | 4.2 | 314.3 |
| /25/0204 | Dec/16/1800 | 30.5 | -24.0 | 62.7 | 8.2 | 113.7 | 9.334 | 90.0 | 4.906 | 6.5 | 316.6 |
| /26/0202 | Dec/16/1800 | 30.2 | -23.7 | 61.3 | 6.8 | 112.7 | 9.438 | 90.0 | 4.887 | 6.9 | 316.7 |
| /27/0201 | Dec/16/1800 | 29.9 | -23.4 | 59.9 | 5.4 | 111.7 | 9.562 | 90.0 | 4.869 | 7.3 | 316.8 |
| /28/0219 | Dec/15/1800 | 28.4 | -21.5 | 53.0 | 3.5 | 109.7 | 9.569 | 90.0 | 4.895 | 9.6 | 319.0 |
| /29/0216 | Dec/15/1800 | 28.2 | -21.3 | 52.1 | 2.2 | 108.7 | 9.750 | 90.0 | 4.883 | 10.0 | 319.0 |
| /30/0213 | Dec/15/1800 | 28.1 | -21.0 | 51.2 | 0.9 | 107.7 | 9.950 | 90.0 | 4.872 | 10.3 | 319.1 |
| 131/0211 | Dec/15/1800 | 27.9 | -20.8 | 50.4 | 0.4 | 106.7 | 10.176 | 90.0 | 4.862 | 10.7 | 319.1 |
| September | | | | | | | | | | | |
| /01/0208 | Dec/15/1800 | 27.8 | -20.6 | 49.6 | 1.6 | 105.7 | 10.425 | 90.0 | 4.852 | 11.0 | 319.1 |
| /02/0220 | Dec/14/1800 | 26.7 | -19.1 | 44.7 | 3.1 | 103.7 | 10.631 | 90.0 | 4.914 | 13.3 | 321.2 |

TABLE 3-14. 1978 ORBITER NOMINAL LAUNCH FOR TYPE II TRAJECTORY

| Launch Date, Month/Day/GMT | Arrival Date Month/Day/GMT | Parking Orbit Coast Time, min | Thor/Delta Final Burns | | Solar Aspect Angle, deg | Flight Time, days | C ₃ (km/sec) ² | Launch Azimuth deg | Approach Asymptote V _∞ , km/sec | Venus Orbit Periapsis Location | |
|-------------------------------|-------------------------------|-------------------------------------|---------------------------|-----------|-------------------------------|-------------------------|---|--------------------------|--|-----------------------------------|--|
| | | | Latitude | Longitude | | | | | | Ecliptic Latitude, deg | Ecliptic Longitude From Sun, deg |
| May | | | | | | | | | | | |
| /25/1707 | 12/02/1800 | 83.7 | 28.2 | -88.7 | 77.0 | 192.0 | 19.445 | 90.0 | 3.695 | 21.1 | 297.3 |
| /26/1656 | 12/02/1800 | 84.2 | 28.1 | -86.5 | 77.5 | 191.0 | 19.303 | 90.0 | 3.697 | 21.8 | 298.2 |
| /27/1644 | 12/02/1800 | 84.9 | 27.8 | -84.1 | 78.1 | 190.0 | 19.170 | 90.0 | 3.698 | 22.6 | 299.2 |
| /28/1630 | 12/02/1800 | 85.6 | 27.5 | -81.3 | 78.7 | 189.0 | 19.048 | 90.0 | 3.700 | 23.5 | 300.1 |
| /29/1614 | 12/02/1800 | 86.5 | 27.0 | -78.1 | 79.5 | 188.0 | 18.938 | 90.0 | 3.701 | 24.5 | 301.0 |
| /30/1554 | 12/02/1800 | 87.6 | 26.1 | -74.2 | 80.5 | 187.0 | 18.841 | 90.0 | 3.703 | 25.5 | 301.9 |
| /31/1528 | 12/02/1800 | 89.3 | 24.6 | -68.8 | 81.9 | 186.0 | 18.761 | 90.0 | 3.705 | 26.7 | 302.7 |
| June | | | | | | | | | | | |
| /01/1525 | 12/02/1800 | 89.9 | 21.6 | -70.0 | 83.8 | 185.0 | 18.701 | 95.0 | 3.708 | 28.0 | 303.7 |
| /02/1606 | 12/02/1800 | 85.7 | 22.3 | -80.2 | 84.2 | 184.0 | 18.663 | 100.8 | 3.709 | 29.4 | 304.7 |
| /03/1632 | 12/02/1800 | 86.0 | 23.6 | -84.3 | 84.3 | 183.0 | 18.685 | 105.0 | 3.715 | 31.1 | 305.5 |

given at the start of each daily window; launch azimuth increase throughout the daily window is about 1 deg with correspondingly small variations in the other variables). For the Type II mission, there are two potentially interesting periapsis locations, one in the northern and one in the southern hemisphere. The northern hemisphere location has been selected as the baseline and the table corresponds to this alternative. A similar table for trajectories utilizing the south periapsis would be almost identical (e. g., launch times 4 min later).

Note that there is a considerable variation in initial location of periapsis latitude and longitude obtained from the trajectories throughout the launch window. This variation is undesirable for science coverage purposes, because in general science prefers hemispheric coverage to coverage over the equatorial region which is perhaps redundant. Shortening the window to improve science coverage would have little effect on useful orbited mass; the orbited mass capability at the end of the 10 day window is about 2 kg above the baseline (injected mass capability is reduced by about 2 kg by launching at 105 deg).

The maximum total launch vehicle mission time from liftoff to second stage separation is about 99 min on the baseline mission. Although this exceeds the specification limit (90 min) experiments in recent Thor/Delta flights have demonstrated a 110 min capability. Therefore this mission time appears to present no technical problem. If the specification limit is maintained, it will be necessary to move the launch window earlier in time to avoid declinations greater than 27 deg; thereby permitting a short coast time solution throughout the 10 day launch window. This would reduce orbited mass by 2 kg, and degrade science coverage because the resultant periapsis latitude and longitude become less favorable (by about 4 deg each).

Orbiter Spacecraft Mass. The computation and representation of orbited spacecraft mass is more complicated than is the case for probe trajectories because of statistical considerations for the midcourse and orbit deboost maneuvers. The retro-propulsion motor has a fixed mass of expendables, but has a statistical variation in the impulse delivered by the expulsion mass (note that V_{∞} varies throughout the window, with a resulting change in desired impulse). Additional dispersions exist due to errors in targeting and spacecraft orientation during retrofire; there is also a substantial variation in the propellant required for midcourse correction. In the absence of corrections with the ACS, these stochastic effects would lead to a spacecraft orbit after retro-fire which would deviate grossly from the desired baseline orbit. The problem is then to select the amount of retro-motor expendables and an operational procedure for the ACS to maximize performance in the presence of the statistical variations.

The important objective of maximization of orbited mass suggests that propulsion sizing and utilization be optimized for conditions when performance is most critical (minimum). The mass of the retro-propulsion expendables will therefore be chosen to be that exactly required when launching at the injection limit (minimum launch mass) of the launch window with a maximum

TABLE 3-15. 1978 ORBITER SPACECRAFT MASS KG

| | Type I North Periapsis, kg | Type II North Periapsis, kg | Type II South Periapsis, kg |
|--|-------------------------------|--------------------------------|--------------------------------|
| Launch booster capability | 380.4 | 314.4 | 314.6 |
| Adapter and telemetry kit | <u>21.5</u> | <u>21.5</u> | <u>21.5</u> |
| Total spacecraft | 358.8 | 292.9 | 293.1 |
| Expendables prior to retro-fire | 15.3 | 12.7 | 12.7 |
| Orbit insertion expendables (ΔV km/sec) | (1.546) | (1.070) | (1.072) |
| Retro-motor | 142.9 | 88.7 | 88.9 |
| Hydrazine | <u>2.7</u> | -- | -- |
| Initial orbit mass | 197.9 | 191.5 | 191.5 |
| Expendables | 9.7 | 11.6 | 15.5 |
| Propulsion system pressurant | <u>0.1</u> | <u>0.1</u> | <u>0.1</u> |
| Dry orbited mass | 188.1 | 179.8 | 175.9 |
| Orbit insertion motor case | <u>19.1</u> | <u>11.1</u> | <u>11.1</u> |
| Useful orbit mass | 169.0 | 168.7 | 164.8 |

midcourse (developed in subsection 3.) requirements; this will be defined as the baseline case. Additional discussion of dispersions and on-orbit velocity requirements is contained below.

For the baseline case, the orbit resulting from retro-propulsion will differ from that desired only by statistical variations in targeting and execution; hydrazine propellant is provided for these corrections as well as for other on-orbit operations. Any propellant not required because of less than maximum midcourse corrections will increase the spacecraft mass prior to retro-fire and will tend to make the expendables in the orbit insertion motor inadequate to attain the desired orbit. However, part of this hydrazine (about 40 percent) can be used to deboost the remainder with the result that the hydrazine available after the desired orbit is attained will always be equal to or greater than that on the baseline mission. A typical mission will have a significant amount of excess hydrazine, and will include an ACS deboost maneuver during the retromotor firing periapsis. Initial trim to the desired orbit is conceptually identical to the baseline case.

The baseline mass statements as defined above are given in Table 3-15 for the Type I trajectory and two alternatives for the Type II trajectory. A 24 h orbit is assumed; this selection is discussed below. Note that although the two Type II interplanetary trajectories are nearly identical, the on-orbit propellant requirement differs due to differing orbital perturbations.

Transit Geometry. The baseline orbiter spacecraft is acquired (10 deg elevation angle) by the Johannesburg (South Africa) Tracking Station approximately 15 min after Thor/Delta separation and can be tracked continuously from this time. The tracking range and transit trajectory geometry are given in Figures 3-21 and 3-22, respectively.

Orbiter Midcourse ΔV Requirements - Summary

The basic midcourse ΔV requirement for the orbiter mission has already been discussed in subsection 3.1. That discussion assumed a worst case 99 percent dispersion in order to obtain a baseline midcourse requirement. The following paragraphs present alternatives for the case of less than 99 percent dispersions.

The allocation of orbiter ΔV capability is statistical and depends strongly upon the midcourse error ΔV correction. Estimates of baseline orbiter ΔV requirements are listed in Table 3-16 (as given in subsection 3.1). The Type II north periapsis (the study baseline) will be used in the subsequent discussion on strategy alternatives.

The baseline midcourse ΔV strategy is to size hydrazine and retromotor expendables to the 99 percent midcourse (i. e., the probability that midcourse ΔV requirements will exceed the baseline is 0.01). If the midcourse ΔV is less than the baseline, more hydrazine will be available for on-orbit operations. The mass breakdown for this allocation is given in the first two columns of Table 3-17. If the midcourse ΔV is greater than the baseline, the mission will have a shorter than nominal orbital lifetime.

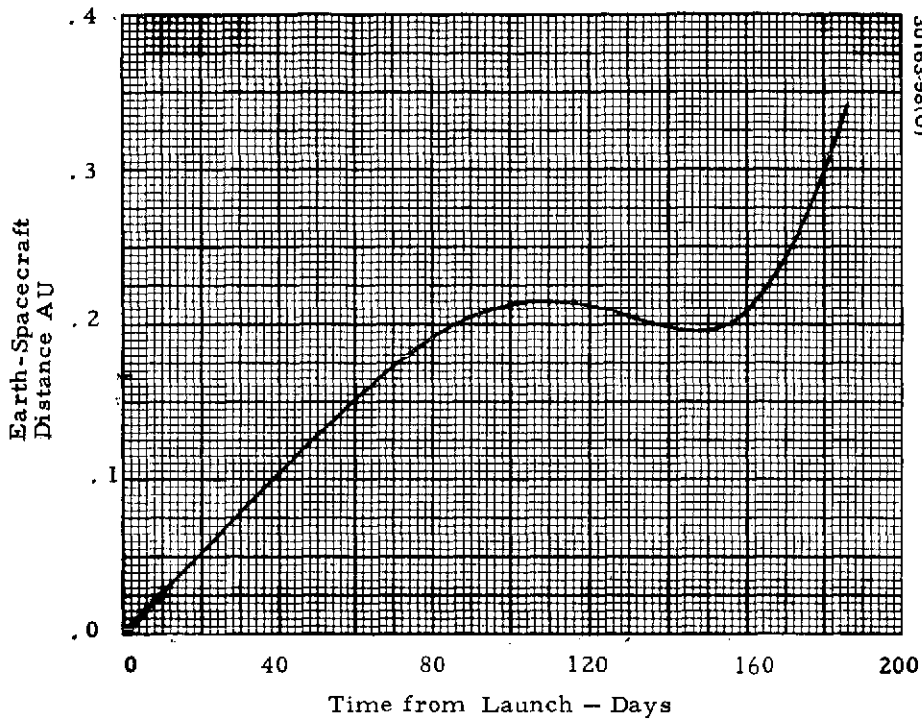


FIGURE 3-21. 1978 ORBITER MISSION TRANSIT TRAJECTORY COMMUNICATION DISTANCE

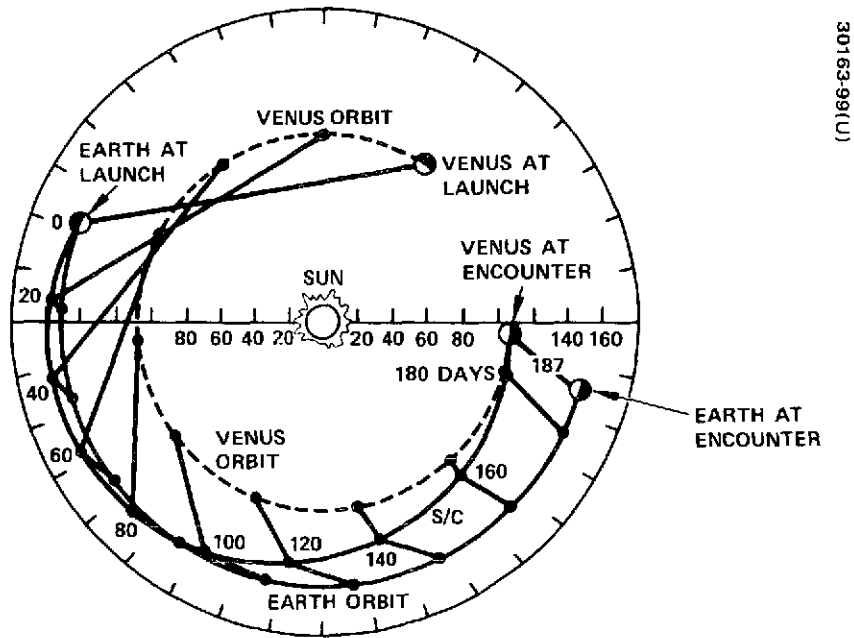


FIGURE 3-22. ORBITER TRANSIT GEOMETRY

TABLE 3-16. ORBITER VELOCITY REQUIREMENTS

| Effect | Type I North Periapsis, m/sec | Type II North Periapsis, m/sec | Type II South Periapsis, m/sec |
|--|--|---|---|
| Correct initial orbit to 24 Hr period with 200 km periapsis altitude | 30 | 26 | 26 |
| Change periapsis by 200 km (at constant orbit period) | 13 | 13 | 13 |
| Atmospheric drag compensation (weekly corrections to minimum altitude) | 25 | 25 | 37 |
| Solar perturbations and period control | <u>30</u> | <u>63</u> | <u>98</u> |
| In-orbit total | 98 | 127 | 174 |

Selection of a strategy which sizes hydrazine and retro-motor expendables to the 90 percent midcourse is an option. This option would increase useful orbited mass by 2.1 kg (Table 3-17) at a cost in an orbit ΔV capability. When the actual midcourse is 90 percent or less, this cost is in the excess hydrazine (above the baseline) which is available for on orbit maneuvers, a penalty which is perfectly acceptable. However, for midcourse errors above 90 percent reduction in on orbit ΔV capability is incurred (e.g., the last column of Table 3-17); this penalty can be significant.

The tradeoff here is one of degraded science return versus spacecraft mass; in the example given a mass of 2.1 kg for a reduction in the time available for science return. This degradation is present for all cases, but for about 9 percent of all cases science return is reduced from values above to values below whatever baseline is selected (e.g., Table 3-16). Figure 3-23 shows this tradeoff in general.

Nominal Orbital Elements - Summary

The baseline orbit characteristics chosen for the Pioneer Venus spacecraft include a minimum (150 km) altitude of periapsis with a 24 h period. The orbit inclination and the spacecraft spin axis are 90 deg to the ecliptic. The above baseline orbit characteristics are independent of whether a Type I or Type II trajectory is flown. Choice of a Type II

TABLE 3-17. 1978 ORBITER SPACECRAFT MASS (KG) - TYPE II NORTH PERIAPSIS

| Planned Midcourse, percent | 99 | 99 | 99 | 99 | 99 |
|---------------------------------|-------------|----------------|-------------|----------------|-------------|
| Actual Midcourse, percent | 99 | <99 | 99 | <99 | 99 |
| Launch booster capability | 314.4 | 314.4 | 314.4 | 314.4 | 314.4 |
| Adapter and telemetry kit | 21.5 | 21.5 | 21.5 | 21.5 | 21.5 |
| Total spacecraft | 292.9 | 292.9 | 292.9 | 292.9 | 292.9 |
| Expendables prior to retro-fire | 12.7 | <12.7 | 9.4 | <9.4 | 12.7 |
| Orbit insertion expendables | | | | | |
| Retro-motor | 88.7 | 88.7 | 89.8 | 89.8 | 89.8 |
| Hydrazine | <u>0.0</u> | <u>>0.0</u> | <u>0.0</u> | <u>>0.0</u> | <u>0.0</u> |
| Initial orbit mass | 191.5 | >191.5 | 193.7 | >193.7 | 190.4 |
| Expendables | 11.6* | >11.6 | 11.7* | >11.7 | 8.4** |
| Propulsion system pressurant | <u>0.1</u> | <u>0.1</u> | <u>0.1</u> | <u>0.1</u> | <u>0.1</u> |
| Dry orbited mass | 179.8 | 179.8 | 181.9 | 181.9 | 181.9 |
| Orbit insertion motor case | <u>11.1</u> | <u>11.1</u> | <u>11.1</u> | <u>11.1</u> | <u>11.1</u> |
| Useful orbit mass | 168.7 | 168.7 | 170.8 | 170.8 | 170.8 |

* Required for baseline ΔV budget.

** 4.0 to 5.9 kg for ΔV after initial orbit trim 8.9 kg for baseline ΔV budget).

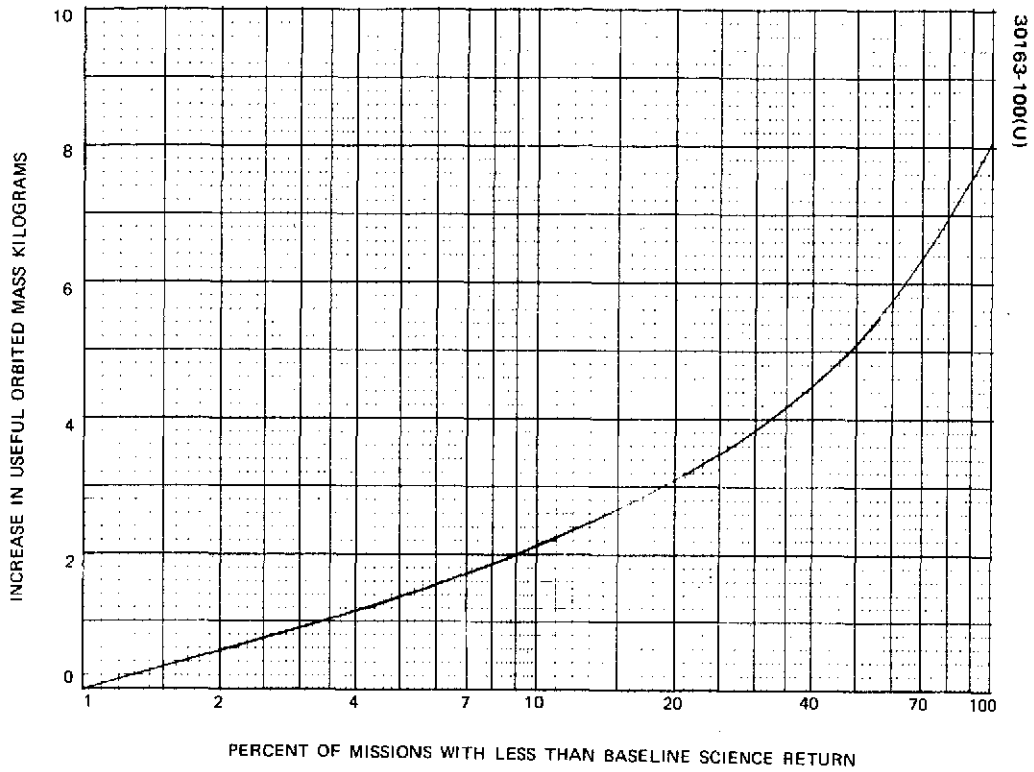


FIGURE 3-23. SPACECRAFT MASS/SCIENCE RETURN TRADEOFF

trajectory as the baseline places the nominal periapsis latitude (midpoint of launch window) at 26° N with the ecliptic longitude at 58 deg from the sub-solar point.

Venus Orbit Characteristics

Before any meaningful selection of orbital elements can be made, it is important to understand how the factors acting to perturb the orbit are a function of the elements. The factors are: uncompensated atmospheric drag; deviation of Venusian gravity from an inverse square gravitational field (oblateness) and third body effects (sun).

Atmospheric Drag Perturbations. Atmospheric drag has the direct effect of lowering the orbital period by decreasing apoapsis (and inclination) at constant periapsis altitude. The magnitude of the drag perturbation depends upon the periapsis altitude and the atmosphere. Thus, selection of a nominal periapsis altitude determines the amount of ΔV which must be put back into the orbit by the attitude control system (ACS) in order to maintain a selected orbital period. As shown below, the ΔV is limited by thermal considerations to relatively very small values (less than 1 m/sec per orbit).

Atmospheric drag indirectly affects periapsis altitude by coupling semimajor axis and eccentricity changes with other effects (such as solar gravity and oblateness). This secondary effect is kept small by the near continuous compensation for atmospheric drag deceleration.

Oblateness Perturbations. Deviation of the Venusian gravitational field from an inverse square will be due to oblateness of the planet (J_2) and other gravitational anomalies. Oblateness has no direct secular effects on semimajor axis and eccentricity. As illustrated in Figure 3-24, periodic effects during an orbit are irrelevant; since periapsis altitude is of interest only in the neighborhood of periapsis, computations of periapsis altitude during other parts of the orbit is not of interest. With these considerations and the fact that the upper bound for the oblateness is small (Reference 11), it may be concluded that this effect of oblateness is negligible for the Venus orbiter. No information is available on other gravitational anomalies (this is an objective of the orbiter mission).

Solar Perturbations. Perturbations due to solar gravity change the orbit eccentricity with only a second order effect on the semimajor axis. Thus, solar gravity changes the periapsis altitude but does not significantly vary the orbital period. During the mission, uncontrolled variations in the inclination, periapsis latitude, and inertial periapsis longitude are each below 1 deg. The uncontrolled variation in orbit period is less than 10 sec (without drag), and periapsis altitude less than 1 km due to maneuver execution errors.

The third body effect of the sun thus becomes the only significant contributor to periapsis altitude variations. Two methods were used to analyze the influence of solar gravity. The first was an approximate analysis which allowed high speed parametric studies for various combinations of orbital elements. These results were then utilized for preliminary analysis of the orbital elements perturbations. An integrating computer program was used to verify the approximate analysis and to obtain the exact periapsis time history variation for specific orbits of interest.

The frequency of periodic components of the solar perturbation allows their conceptual separation. Long period effects (Reference 12) are essentially linear over the lifetime of the orbiter, while medium period perturbations are approximately sinusoidal with a 1/2 Venusian year period. Short period effects occur at spacecraft orbital period and are small. They are also not relevant as discussed above in Figure 3-24.

Figure 3-25 presents a comparison of the uncompensated change in periapsis altitude for three periapsis latitudes of interest. Variation of periapsis altitude can be shown analytically to be monotonic for 90 deg inclinations and the relative phase of the curves are determined by the relative difference in Sun-Venus-orbiter geometry at mission start. The sign of the periapsis variation is due to whether the orbiter is moving toward (positive) or away (negative) from the ecliptic at periapsis. The solar gravity phenomena is caused by the difference in attractive force between Sun-Venus and Sun-orbiter. Choice of direction of motion is dictated by injection from the transit trajectory and will be towards the ecliptic for both north and south periapsis locations for the Pioneer Venus orbiter. The periapsis altitude will therefore increase as shown in Figure 3-25.

Figure 3-26 depicts the relative average periapsis altitude variation over the 225 day mission lifetime as a function of inclination and argument of periapsis. These analytically derived results may be somewhat misleading when dealing with average values since inclinations other than 90 deg cause the periapsis altitude to decrease during those parts of the mission when the orbit approaches the perpendicular to the Venus-sun line. Figure 3-27 compares the monotonic 90 deg inclination to the 70 deg case. Though the average periapsis altitude change has decreased by about 12 percent at the mission termination, the fact that the 70 deg case is not monotonic must be accounted for in any fuel budget analysis. Values for various high inclinations in Figure 3-28 indicate that the absolute value of the ΔV needed to correct solar perturbations increases as the inclination decreases from 90 deg. Also included in Figure 3-28 are the ΔV variations with orbital period.

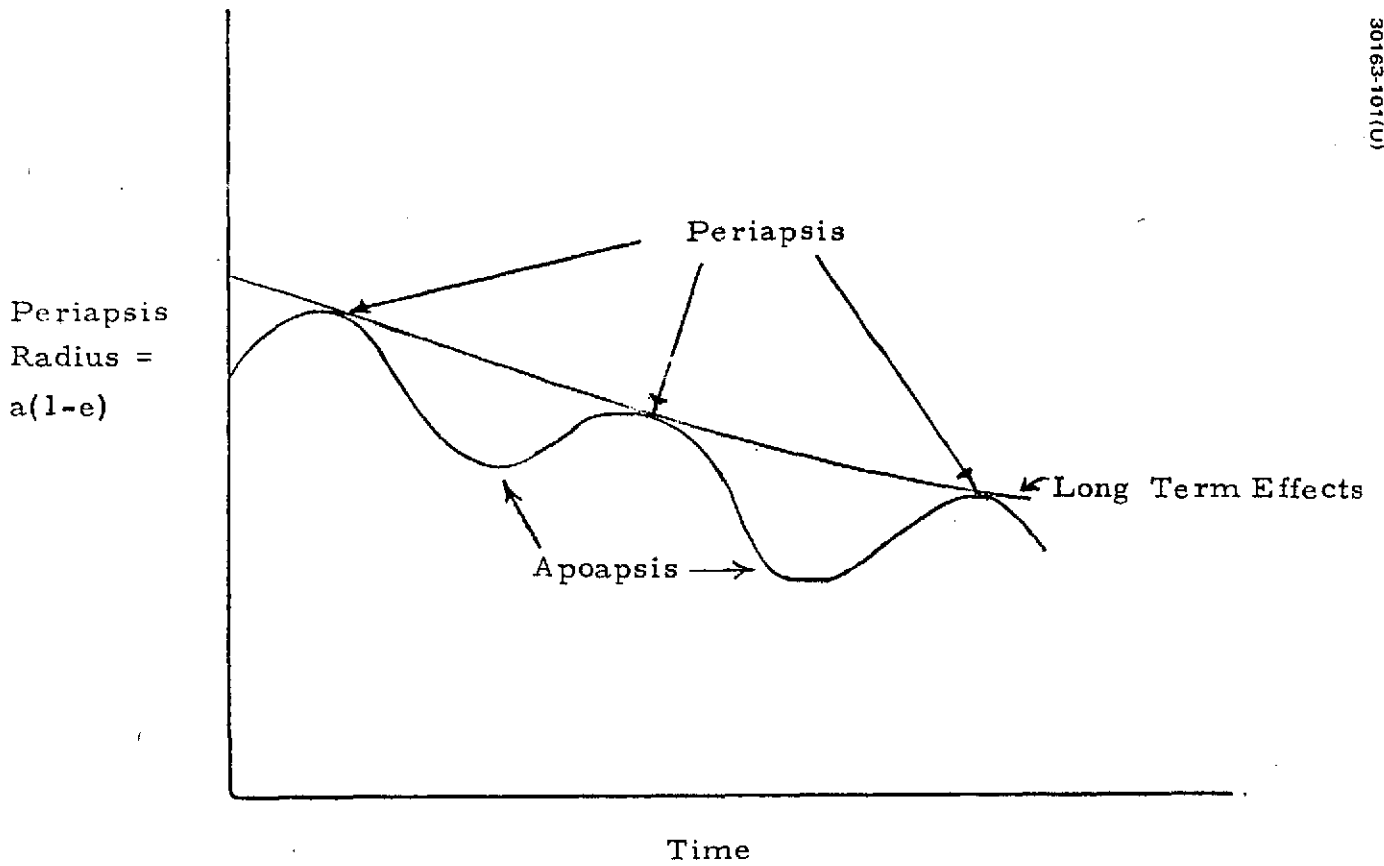


FIGURE 3-24. IRRELEVANCE OF EFFECTS ON PERIAPSIS ALTITUDE DURING ORBITAL PERIOD

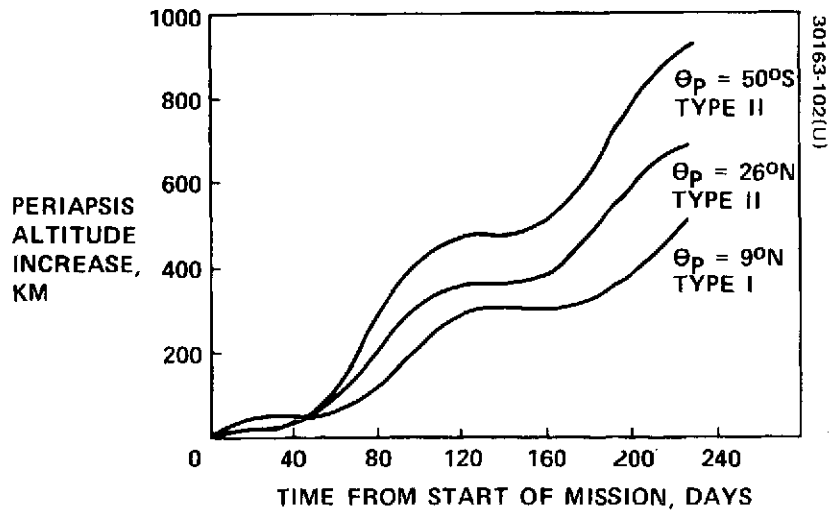


FIGURE 3-25. UNCOMPENSATED PERIAPSIS ALTITUDE INCREASE - MIDPOINT OF LAUNCH WINDOW

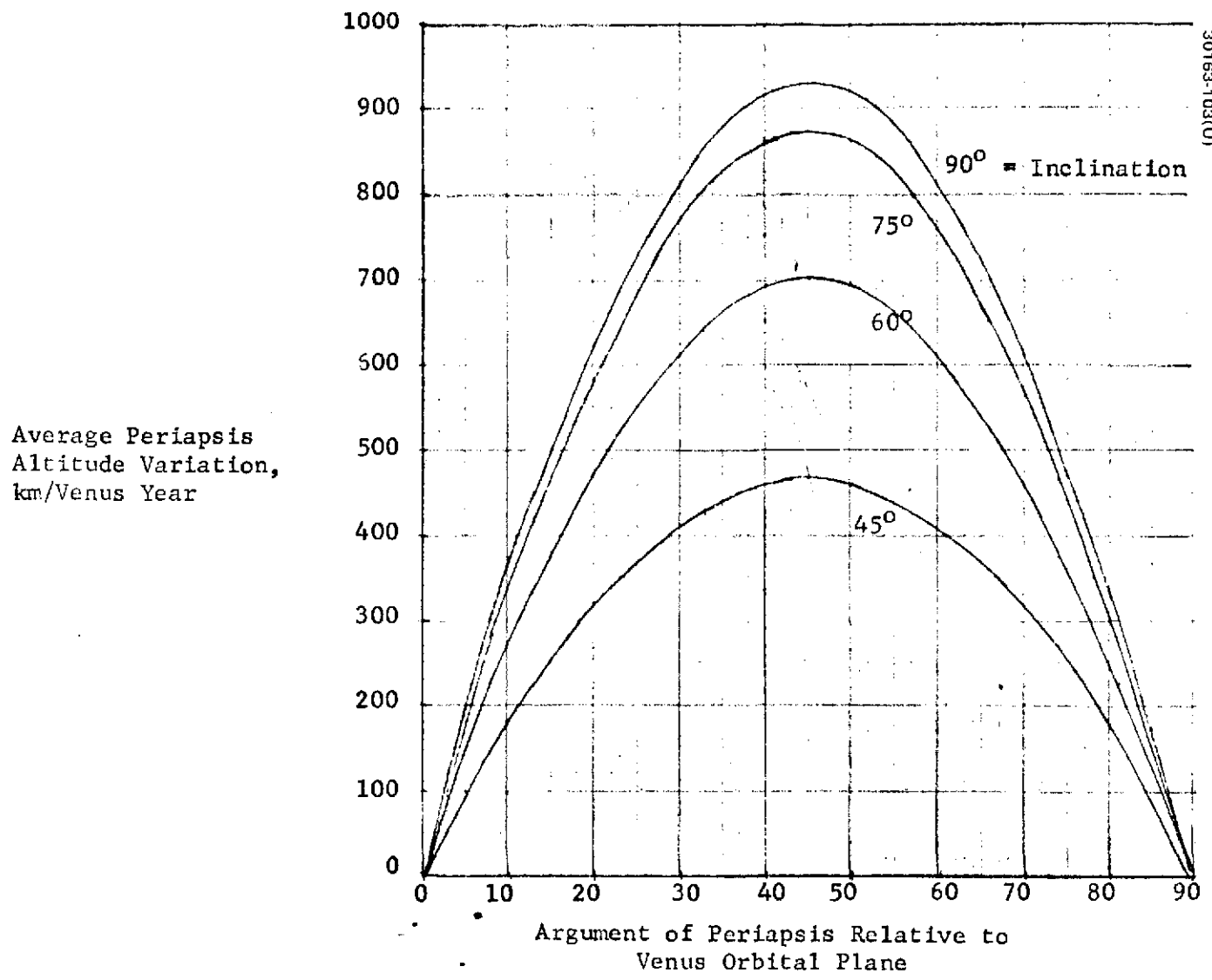


FIGURE 3-26. AVERAGE SOLAR PERTURBATION EFFECT OVER ORBITER LIFETIME

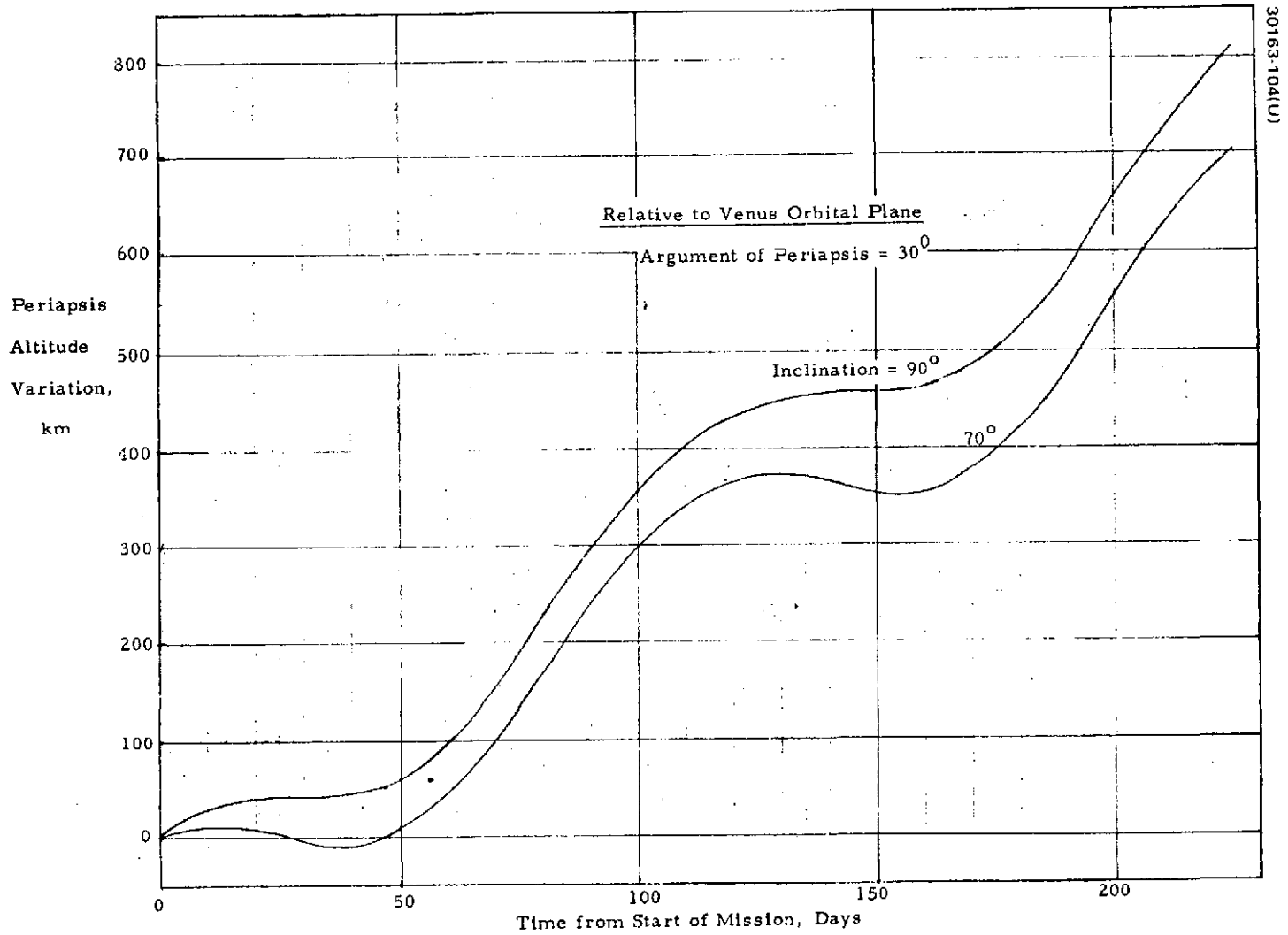
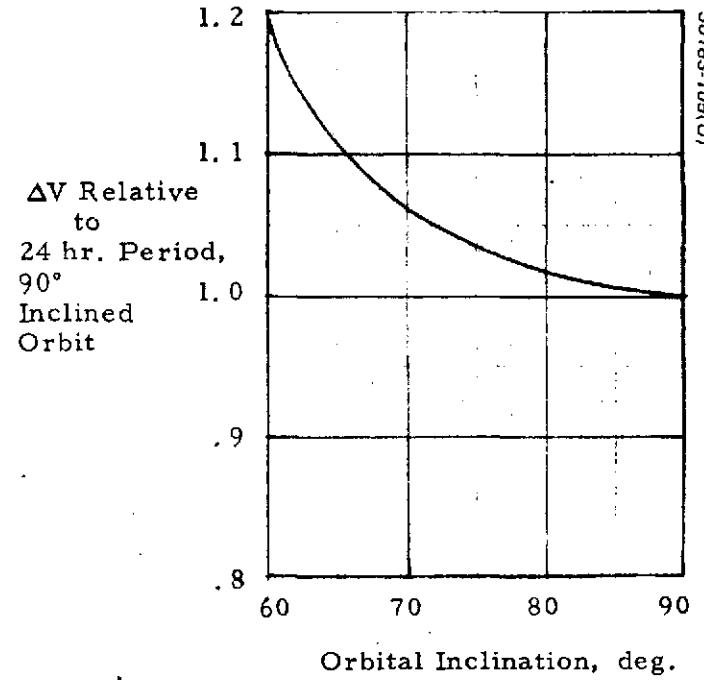
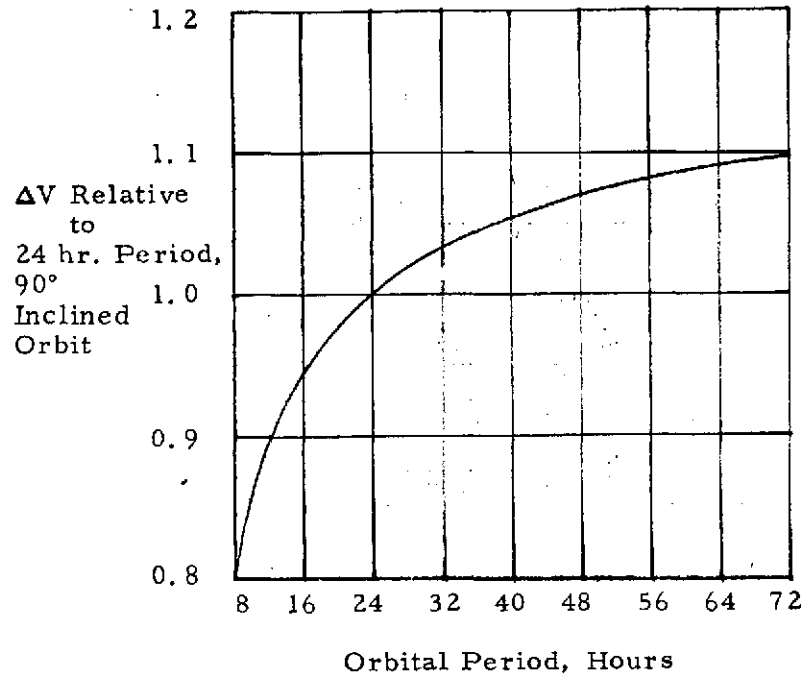


FIGURE 3-27. PERIAPSIS ALTITUDE VARIATION WITH INCLINATION

3-59



30163-105(U)

FIGURE 3-28. SOLAR PERTURBATION ΔV REQUIREMENTS RELATIVE TO 24 HOUR PERIOD, 90 DEG INCLINED ORBIT

Venus Orbit Selection

Periapsis Altitude. The preference for selection of periapsis altitude can be divided up into the areas of science coverage, and spacecraft operational considerations. Additionally, science coverage can be separated by experiment type, i. e., those experiments which point toward Venus; experiments associated with the velocity vector; and the other remaining experiments (e. g., sun-oriented).

For the periapsis altitude both the Venus pointed experiments and the velocity pointed experiments prefer low altitudes. The radar altimeter, for example appears to be limited to the region below 1000 km. More importantly, the function of the velocity pointed experiments is to sample the atmosphere. Quite obviously, these experiments require a periapsis altitude as low as possible to maximize the science return. Thus, every effort should be exerted to minimize periapsis altitude subject to aerodynamic limits on spacecraft operation and the operational necessity of frequent drag corrections of the orbital period. The geometric altitude at the aerodynamic limit is obviously a function of the atmospheric model. Placement of the periapsis altitude at the aerodynamic limit will be assumed for purposes of orbit and spacecraft design; an estimate of this altitude will then be made for use in other system trades.

As seen in Table 3-18 (most probable atmosphere of Reference 13) the dropoff of the baseline atmospheric density between 140 and 200 km is about a factor of 40. Thus, selecting the periapsis altitude entails a determination of the minimum possible altitude consistent with aerodynamic constraints. Aerodynamic heating limits for the orbiter are estimated to be an instantaneous value of the heating indicator ($1/2 PV^3$) of $41.3 \text{ J/m}^2 \text{ sec}$ and an integrated value of this indicator of 7850 J/m^2 . Figures 3-29 and 3-30 present plots of the variation of these aerodynamic heating indicators with altitude. Two different atmospheric models are graphed. The Model I (baseline) atmosphere, and the Model IV atmosphere (the densest model of Reference 12). Each curve also shown the heating indicator limit and the limit with a factor of 4 margin of safety. On Figure 3-29, periapsis altitudes of 145 km for the baseline and 154 km for the worst case correspond to the instantaneous conservative (factor 4) aerodynamic limits. Similarly, values of 136 and 154 km hold for the integrated, factor of 4 safety, heating limits (Figure 3-30). The minimum altitude due to heating is therefore about 150 km for assumed atmosphere models; this value will be used as the study baseline.

The drag velocity which must be put back into the system in order to maintain the orbital period is given in Figure 3-31. Also shown is the maximum ΔV corresponding to a factor of 4 heating limit. The value of 0.2 m/sec for the baseline atmosphere corresponds to a 61.9 sec decrease in a 24 h orbital period.

The choice of minimum periapsis altitude is also affected by the aerodynamic torque acting to precess the spin axis of the orbiter. Figure 3-32 indicates that this precession becomes significant even before the thermal limit of the orbiter is reached. Since this torque can be modeled, the spin

TABLE 3-18. 1972 VENUS ATMOSPHERE (MODEL I)*
(Most Probable Molecular Mass and Mean Solar Activity)

| Altitude (km) | Temperature (K) | Pressure (mb) | Density (g/cm ³) | Speed of Sound (m/s) | Molecular Mass (g/g-mole) | Density Scale Height (km) | Number Density (per cm ³) | Mean Free Path (m) | Viscosity (kg/m·s) |
|---------------|-----------------|---------------|------------------------------|----------------------|---------------------------|---------------------------|---------------------------------------|--------------------|--------------------|
| -4 | 798.1 | 1.20+05 | 7.89-02 | 426. | 43.531 | 20.52 | 1.09+21 | 1.33-09 | 3.33-05 |
| 0** | 767.5 | 9.49+04 | 6.47-02 | 418. | 43.531 | 19.79 | 8.95+20 | 1.62-09 | 3.24-05 |
| 4 | 736.5 | 7.41+04 | 5.27-02 | 410. | 43.531 | 19.06 | 7.29+20 | 1.99-09 | 3.15-05 |
| 8 | 705.2 | 5.73+04 | 4.25-02 | 402. | 43.531 | 18.32 | 5.88+20 | 2.46-09 | 3.06-05 |
| 12 | 673.4 | 4.38+04 | 3.40-02 | 393. | 43.531 | 17.57 | 4.71+20 | 3.07-09 | 2.96-05 |
| 16 | 641.2 | 3.30+04 | 2.70-02 | 384. | 43.531 | 16.81 | 3.73+20 | 3.88-09 | 2.85-05 |
| 20 | 608.5 | 2.46+04 | 2.11-02 | 375. | 43.531 | 16.03 | 2.93+20 | 4.95-09 | 2.74-05 |
| 24 | 575.3 | 1.80+04 | 1.64-02 | 365. | 43.531 | 15.24 | 2.27+20 | 6.39-09 | 2.62-05 |
| 28 | 541.4 | 1.29+04 | 1.25-02 | 355. | 43.531 | 14.43 | 1.73+20 | 8.36-09 | 2.51-05 |
| 32 | 506.8 | 9.10+03 | 9.40-03 | 345. | 43.531 | 13.59 | 1.30+20 | 1.11-08 | 2.39-05 |
| 36 | 471.4 | 6.25+03 | 6.91-03 | 334. | 43.531 | 12.74 | 9.61+19 | 1.51-08 | 2.25-05 |
| 40 | 433.0 | 4.16+03 | 5.03-03 | 321. | 43.531 | 11.82 | 6.97+19 | 2.08-08 | 2.09-05 |
| 44 | 397.6 | 2.67+03 | 3.52-03 | 308. | 43.531 | 10.51 | 4.87+19 | 2.97-08 | 1.95-05 |
| 48 | 371.4 | 1.66+03 | 2.34-03 | 299. | 43.531 | 9.19 | 3.23+19 | 4.47-08 | 1.82-05 |
| 52 | 336.8 | 9.91+02 | 1.54-03 | 286. | 43.531 | 9.36 | 2.13+19 | 6.79-08 | 1.65-05 |
| 56 | 299.6 | 5.57+02 | 9.74-04 | 271. | 43.531 | 7.99 | 1.35+19 | 1.07-07 | 1.49-05 |
| 60 | 267.6 | 2.93+02 | 5.72-04 | 258. | 43.531 | 7.12 | 7.92+18 | 1.83-07 | 1.33-05 |
| 64 | 246.2 | 1.44+02 | 3.06-04 | 249. | 43.531 | 6.13 | 4.24+18 | 3.42-07 | 1.23-05 |
| 68 | 231.9 | 6.71+01 | 1.51-04 | 242. | 43.531 | 5.47 | 2.10+18 | 6.91-07 | 1.16-05 |
| 72 | 217.0 | 2.99+01 | 7.22-05 | 235. | 43.531 | 5.30 | 9.99+17 | 1.45-06 | 1.10-05 |
| 76 | 200.4 | 1.25+01 | 3.27-05 | 227. | 43.531 | 4.76 | 4.53+17 | 3.20-06 | 1.03-05 |
| 80 | 187.9 | 1.92+00 | 1.37-05 | 211. | 43.531 | 4.46 | 1.90+17 | 7.63-06 | .94-05 |
| 84 | 180.1 | 1.84+00 | 5.35-06 | 203. | 43.531 | 4.16 | 7.40+16 | 1.95-05 | .89-05 |
| 88 | 175.2 | 6.65-01 | 1.99-06 | 199. | 43.531 | 3.97 | 2.75+16 | 5.27-05 | .86-05 |
| 92 | 171.4 | 2.35-01 | 7.16-07 | 195. | 43.531 | 3.88 | 9.91+15 | 1.46-04 | .83-05 |
| 96 | 168.3 | 8.11-02 | 2.52-07 | 193. | 43.531 | 3.77 | 3.49+15 | 4.15-04 | .81-05 |
| 100 | 166.5 | 2.77-02 | 8.70-08 | 191. | 43.531 | 3.74 | 1.20+15 | 1.20-03 | .80-05 |
| 110 | 171.0 | 1.86-03 | 5.70-09 | 195. | 43.531 | 3.70 | 7.88+13 | 1.84-02 | .83-05 |
| 120 | 203.9 | 1.59-04 | 4.10-10 | 229. | 43.531 | 4.09 | 5.67+12 | 2.55-01 | 1.04-05 |
| 130*** | 214.0 | 1.91-05 | 4.67-11 | 234. | 43.531 | 4.75 | 6.46+11 | 2.24+00 | 1.09-05 |
| 140 | 268.0 | 3.01-06 | 5.81-12 | 261. | 42.963 | 5.39 | 8.15+10 | 1.79+01 | 1.33-05 |
| 150 | 378.4 | 7.79-07 | 1.04-12 | 308. | 42.015 | 6.92 | 1.49+10 | 9.76+01 | 1.85-05 |
| 160 | 502.4 | 2.98-07 | 2.91-13 | 355. | 40.818 | 9.09 | 4.29+09 | 3.39+02 | 2.37-05 |
| 170 | 591.0 | 1.41-07 | 1.13-13 | 390. | 39.404 | 11.62 | 1.73+09 | 8.40+02 | 2.67-05 |
| 180 | 641.4 | 7.51-08 | 5.32-14 | 414. | 37.732 | 13.93 | 8.49+08 | 1.71+03 | 2.84-05 |
| 190 | 674.9 | 4.28-08 | 2.73-14 | 435. | 35.781 | 15.66 | 4.60+08 | 3.16+03 | 2.96-05 |
| 200 | 691.5 | 2.58-08 | 1.50-14 | 455. | 33.576 | 17.31 | 2.70+08 | 5.39+03 | 3.01-05 |
| 210 | 700.8 | 1.62-08 | 8.66-15 | 475. | 31.179 | 18.70 | 1.67+08 | 8.70+03 | 3.04-05 |
| 220 | 705.5 | 1.06-08 | 5.18-15 | 496. | 28.700 | 20.14 | 1.09+08 | 1.34+04 | 3.06-05 |
| 230 | 707.8 | 7.20-09 | 3.21-15 | 520. | 26.266 | 21.71 | 7.37+07 | 1.97+04 | 3.06-05 |
| 240 | 709.0 | 5.07-09 | 2.06-15 | 544. | 23.994 | 23.49 | 5.18+07 | 2.81+04 | 3.07-05 |
| 250 | 709.4 | 3.69-09 | 1.37-15 | 569. | 21.963 | 25.54 | 3.76+07 | 3.87+04 | 3.07-05 |
| 260 | 709.4 | 2.75-09 | 9.43-16 | 593. | 20.207 | 27.80 | 2.81+07 | 5.18+04 | 3.07-05 |
| 270 | 709.4 | 2.10-09 | 6.68-16 | 616. | 18.719 | 30.21 | 2.15+07 | 6.77+04 | 3.07-05 |
| 280 | 709.4 | 1.64-09 | 4.86-16 | 638. | 17.467 | 32.69 | 1.68+07 | 8.68+04 | 3.07-05 |
| 290 | 709.4 | 1.30-09 | 3.62-16 | 658. | 16.409 | 35.15 | 1.33+07 | 1.10+05 | 3.07-05 |
| 300 | 709.4 | 1.05-09 | 2.75-16 | 677. | 15.499 | 37.52 | 1.07+07 | 1.36+05 | 3.07-05 |
| 310 | 709.5 | 8.51-10 | 2.12-16 | 696. | 14.699 | 39.74 | 8.69+06 | 1.67+05 | 3.07-05 |
| 320 | 709.5 | 7.01-10 | 1.66-16 | 713. | 13.976 | 41.80 | 7.15+06 | 2.03+05 | 3.07-05 |
| 330 | 709.5 | 5.82-10 | 1.31-16 | 731. | 13.306 | 43.71 | 5.95+06 | 2.45+05 | 3.07-05 |
| 340 | 709.5 | 4.89-10 | 1.05-16 | 749. | 12.672 | 45.51 | 4.99+06 | 2.92+05 | 3.07-05 |
| 350 | 709.5 | 4.14-10 | 8.46-17 | 768. | 12.063 | 47.24 | 4.22+06 | 3.44+05 | 3.07-05 |

*A one- or two-digit number (preceded by a plus or minus sign) following an entry indicates the power of ten by which that entry should be multiplied.

**Corresponds to planetary radius of 6050 km.

***Density is 1.44×10^{-11} g/cm³ at the turbopause (lower boundary of upper atmosphere).

Reproduced from
best available copy. 

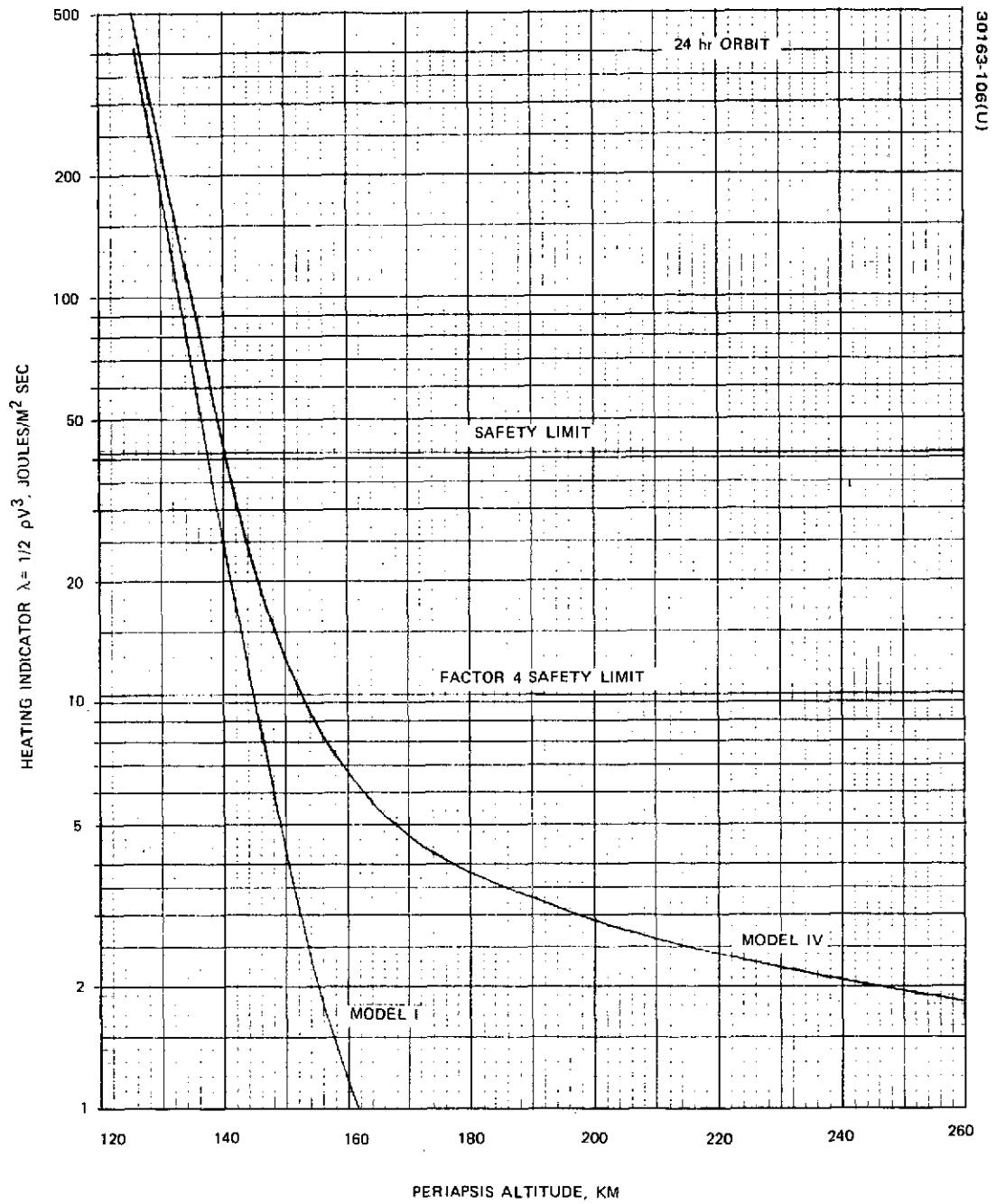


FIGURE 3-29. INSTANTANEOUS HEATING LIMIT - 24 HOUR ORBIT

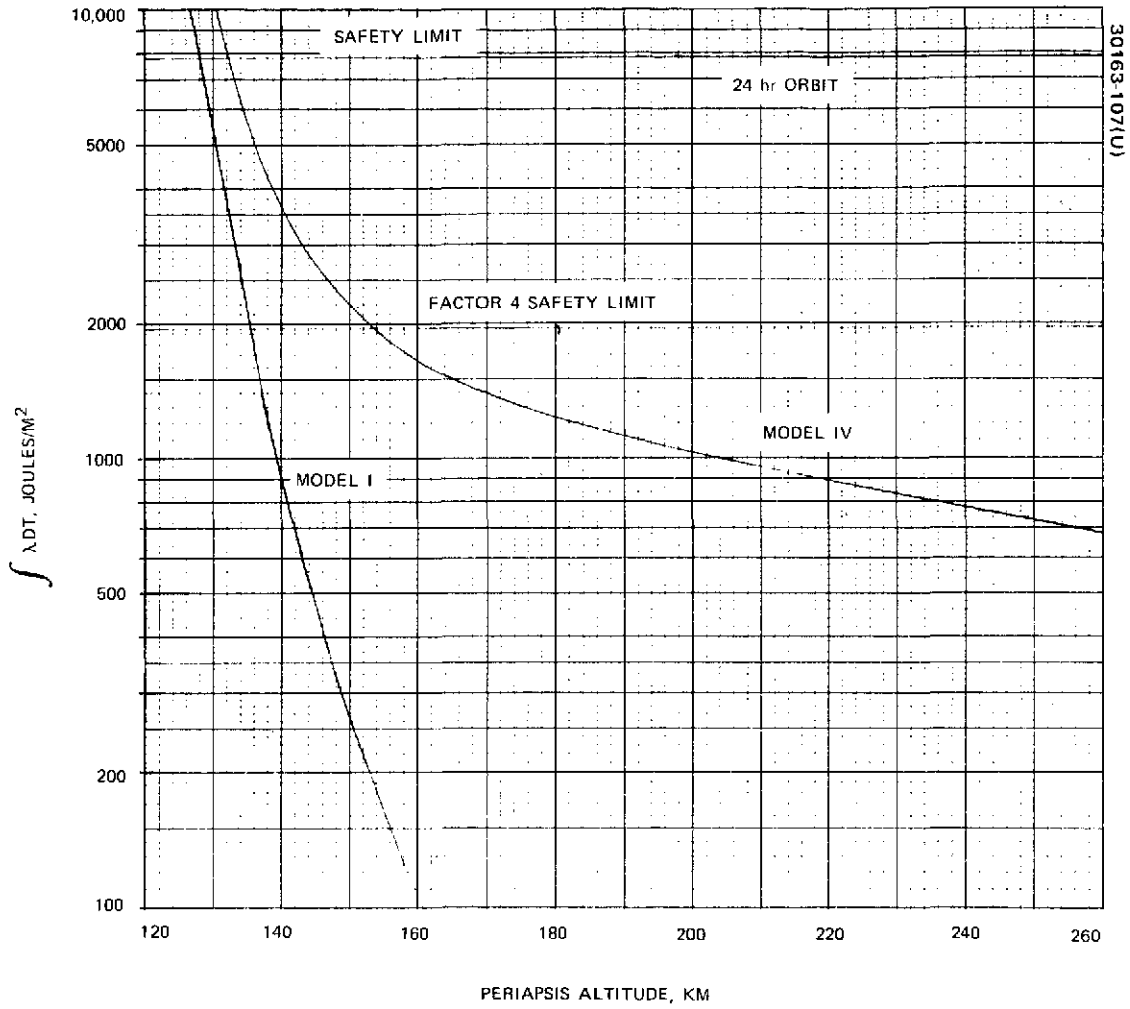


FIGURE 3-30. INTEGRATED HEATING LIMIT

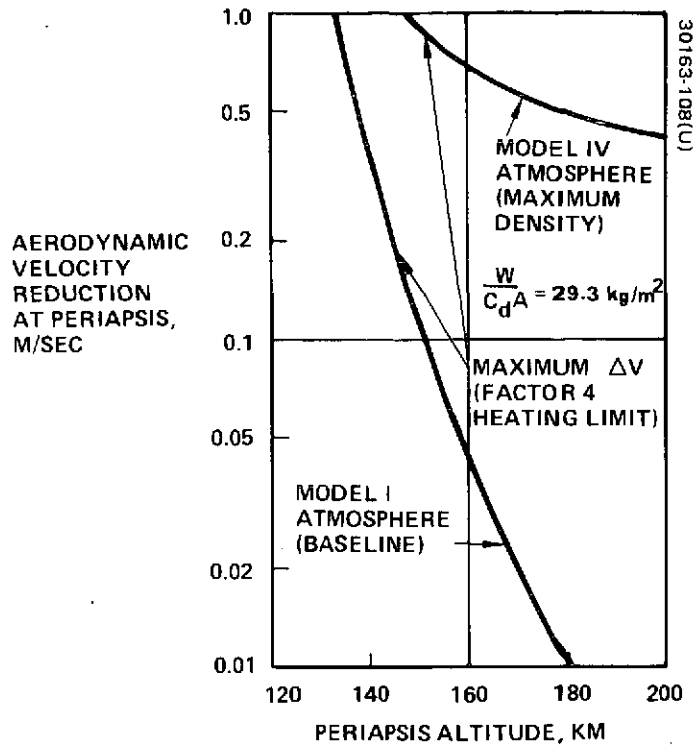


FIGURE 3-31. DRAG EFFECT ON 24 HOUR ORBIT

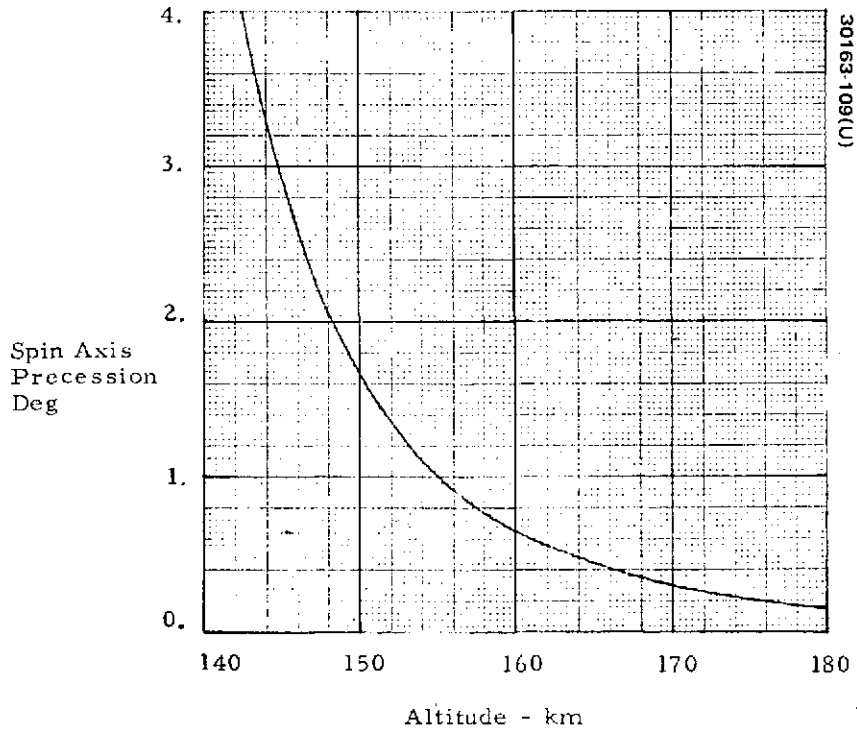


FIGURE 3-32. ESTIMATE OF AERODYNAMIC TORQUE (BASELINE ORBIT - MODEL I ATMOSPHERE)

axis precession does not represent an attitude error. Because the modeling error is about an order of magnitude less than the precession, aerodynamic torque is assumed less limiting than heating.

Another factor which might affect choice of periapsis altitude is its variation due to solar perturbations. As mentioned above for high inclinations, these perturbations tend to raise periapsis altitude throughout most of the mission so the orbiter will not be driven below a safe altitude. The solar perturbations are predictable so for low inclinations, when periapsis altitude decreases, the orbiter would be started from a safe altitude higher than its nominal.

The periapsis altitude during the mission depends upon the actual Venus atmosphere. The minimum safe altitude is desired; this minimum appears to be about 150 km for the atmosphere models of Reference 13. The aerodynamic drag limit of 0.2 m/sec per orbit for the baseline atmosphere is too small for significant shaping (e.g., circularization) but can be compensated for with a practical mass of hydrazine.

Orbit Period. The Pioneer Venus orbiter achieves its science coverage, in longitude, by rotation of the planet beneath the spacecraft between periapsis passages. Total longitudinal coverage is thus a function of mission duration and not orbital period. A mission duration equal to the rotational period of Venus (about 240 days) will yield complete longitudinal coverage regardless of orbiter period.

The major items pacing selection of the orbital period are spacecraft and operational. Spacecraft mass is maximized by a loose capture (minimum retro-propellant) from the transit trajectory resulting in a large orbital period. On the other hand a large orbital period results in longer eclipse times and the need for larger batteries to maintain the spacecraft during eclipse. Solar perturbations also increase with orbital period. Operationally, a spacecraft orbital period which is an integral number of days is to be preferred since this requires only a single ground station for communication purposes. Science prefers short orbital periods with more periapsis passes, but spacecraft and operational considerations dominate choice of orbital period.

The performance tradeoff with orbit period is depicted in Figure 3-33 relative to a 24 h orbiter period (including solar perturbation variation with orbital period). The curve of relative useful orbited mass versus orbital period is a function of the amount of propellant which must be expended in order to achieve the capture around Venus. The definition of useful orbited mass used elsewhere (spacecraft dry mass less the retro-motor case mass) does not consider allocation of this mass between subsystem and is shown in Figure 3-33 are "without battery change." Actually the increased eclipse times associated with longer orbital periods require increased battery mass since these eclipse times size the battery requirements. The curve "including battery change" is thus more representative of the performance/orbital period tradeoff.

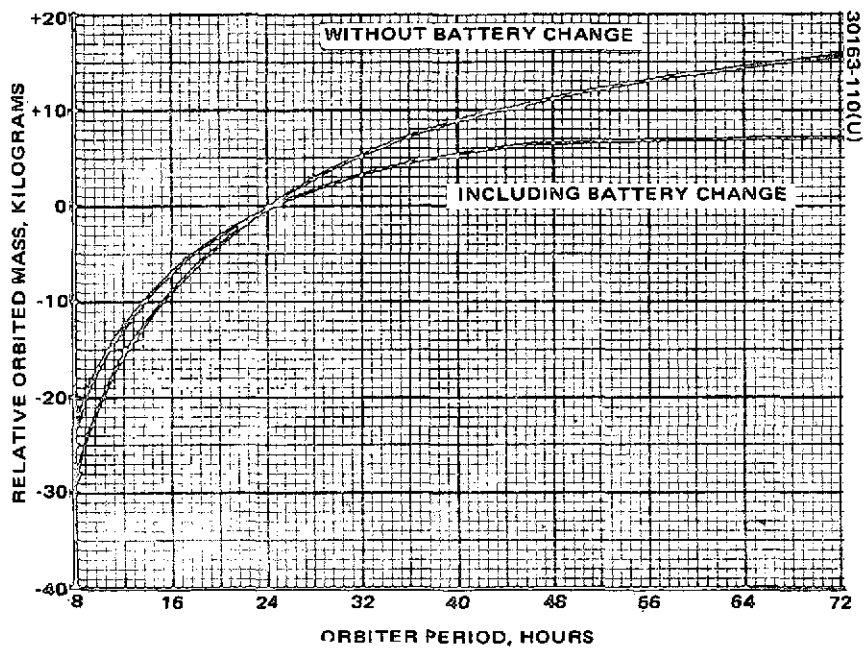


FIGURE 3-33. PERFORMANCE/ORBIT PERIOD TRADEOFF

Certain values of the orbital period suggest themselves because of the operational requirement for the fewest number of ground stations. Thus a 24 h period is preferable to 22 or 28 h periods.

Orbital periods such as 48 or 72 h have only a few pounds of improved performance with the penalty of decreased science performance when compared to the 24 h period. On the other hand, a 12 h orbital period increases science return but at a large cost in useful orbital mass as well as the necessity for having more than one ground station for periapsis science coverage, and as such is considered a less desirable alternative. Thus, choice of the 24 h orbital period appears most satisfactory from a performance/operations viewpoint.

Inclination. Both the Venus-oriented and velocity-pointed experiments prefer high inclinations; and all other things being equal science coverage is optimized for a 90 deg inclination. Inclinations other than 90 deg have some times been suggested on the basis that the location of initial periapsis longitude can be improved. This tradeoff is most conveniently treated during the science coverage tradeoffs. A 90 deg inclination will be assumed for the following discussion; this choice is shown to be best, as discussed later.

Periapsis Latitude and Longitude. Venus-pointed experiments prefer periapsis latitude to be in the midlatitude regime (Reference 8). From a spacecraft point of view, low periapsis latitudes are preferred (for 90 deg inclinations) since this would minimize the effect of solar perturbations upon the orbiter and result in a smaller fuel budget requirement.

From an operational outlook, it is preferred that the orbit not be occulted initially, but since this cannot be satisfied it is not considered in selection of the initial periapsis longitude. Venus-pointed experiments have a major preference for not having the initial periapsis longitude too near the terminator.

The selection of periapsis latitude and longitude is constrained by their dependence upon the transit trajectory. A Type II transit trajectory is chosen as the baseline. The selection of the baseline transit trajectory and the 90 deg orbiter inclination completely determines the periapsis location. This location varies over the launch window as seen in Table 3-19. The nominal periapsis location (defined at the midpoint of the launch window) then becomes 26 deg north ecliptic latitude at about 58 deg ecliptic longitude from the subsolar point (corresponding to 20 days to the terminator).

Baseline Venus Orbit

Occultations and Eclipses. The separation of eclipses and occultations into short and long duration events is convenient. Short duration events occur near periapsis and have a relatively long season while long duration events occur near apoapsis and have a correspondingly short season.

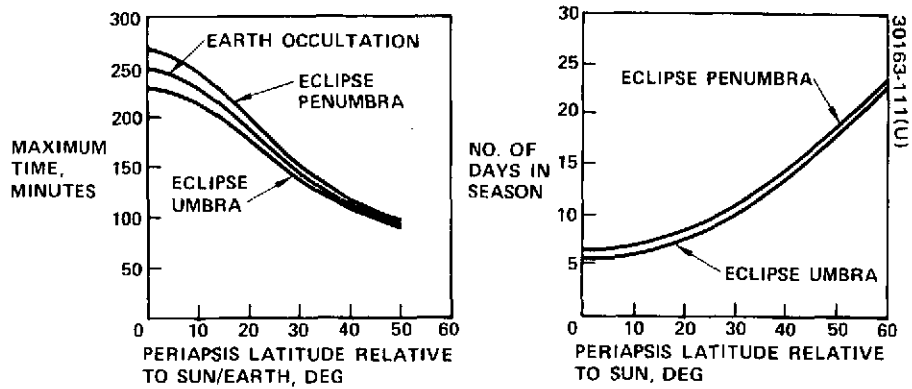


FIGURE 3-34. LONG DURATION ECLIPSES AND OCCULTATIONS

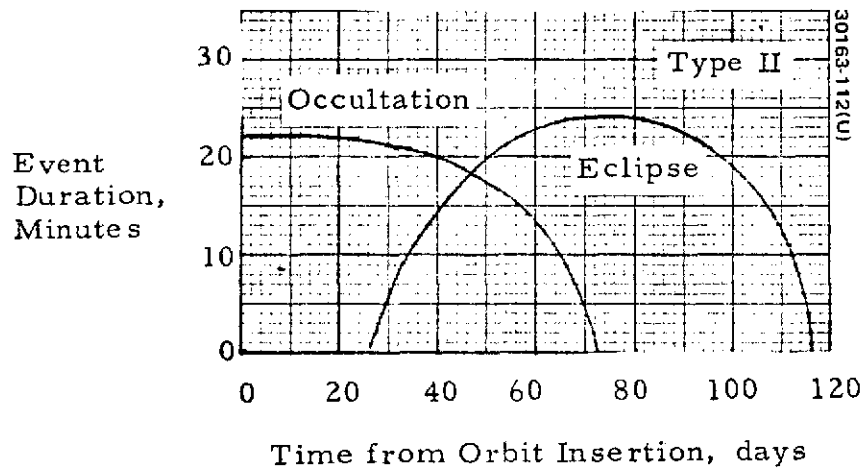


FIGURE 3-35. SHORT DURATION ECLIPSES AND OCCULTATIONS

TABLE 3-19. 1978 ORBITER NOMINAL LAUNCH FOR
Type II Trajectory

| Launch Date, Month/day/ GMT | Arrival Date, Month/day/ GMT | Venus orbit Periapsis Location | |
|-----------------------------------|------------------------------------|-----------------------------------|------------------------------------|
| | | Ecliptic Latitude, Deg | Ecliptic Long, from Sun, deg |
| May/25/1707 | Dec/02/1800 | 21.1 | 297.3 |
| May/25/1656 | Dec/02/1800 | 21.8 | 298.2 |
| May/27/1644 | Dec/02/1800 | 22.6 | 299.2 |
| May/28/1630 | Dec/02/1800 | 23.5 | 300.1 |
| May/29/1614 | Dec/02/1800 | 24.5 | 301.0 |
| May/30/1554 | Dec/02/1800 | 25.5 | 301.9 |
| May/31/1528 | Dec/02/1800 | 26.7 | 302.7 |
| June/01/1525 | Dec/02/1800 | 28.0 | 303.7 |
| June/02/1606 | Dec/02/1800 | 29.4 | 304.7 |
| June/03/1632 | Dec/02/1800 | 31.1 | 305.5 |

Figure 3-34 shows the long duration events as a function of periapsis latitude relative to the occulting body. This figure plots the maximum time of each event. Specific time histories of the events for the baseline mission are shown in Table 3-20 for the midpoint of the launch window. These times vary over the launch window due to changes in periapsis location. As seen in Table 3-21 worst case for the baseline mission occurs at the beginning of the launch window. Short duration eclipses and occultations for the baseline mission are shown in Figure 3-35.

Orbit Perturbations. Figure 3-36 presents the solar perturbation effect as a function of periapsis latitude. As seen previously for the 90 deg inclination, the change of periapsis altitude with time is a monotonic function which is approximately the sum of linear and sinusoidal terms. Figure 3-36 compares the average rate of change.

The effects of solar perturbations on the baseline orbit are shown in Figures 3-37 and 3-38. These curves were generated using the Hughes ENCOUNTER computer program which integrates the exact 3-body equations of motion. Figure 3-37 shows the small variations in inclination, ascending node, and argument of periapsis over the mission duration. Figure 3-38 shows the uncorrected variation of periapsis altitude.

TABLE 3-20. BASELINE MISSION LONG DURATION
ECLIPSES AND OCCULTATIONS
(MIDPOINT OF LAUNCH WINDOW)

| Time From Insertion, days | Occultation, min | Umbra, min | Penumbra, min |
|------------------------------|---------------------|---------------|------------------|
| 157 | 18 | | |
| 158 | 93 | | |
| 159 | 124 | | |
| 160 | 144 | | |
| 161 | 157 | | |
| 162 | 163 | | |
| 163 | 164 | | |
| 164 | 160 | | |
| 165 | 151 | | |
| 166 | 134 | | |
| 167 | 108 | | |
| 168 | 61 | | |
| 183 | | - | 63 |
| 184 | | 112 | 125 |
| 185 | | 134 | 155 |
| 186 | | 153 | 172 |
| 187 | | 159 | 178 |
| 188 | | 156 | 175 |
| 189 | | 142 | 169 |
| 190 | | 112 | 137 |
| 191 | | 45 | 91 |

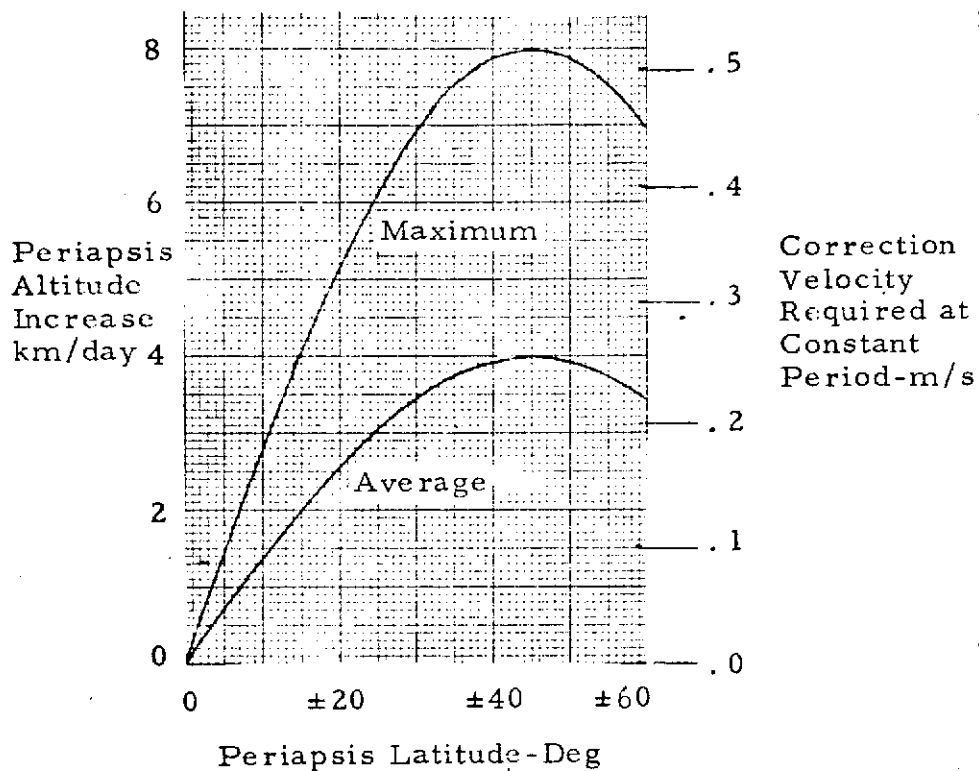


FIGURE 3-36. SOLAR PERTURBATION EFFECT

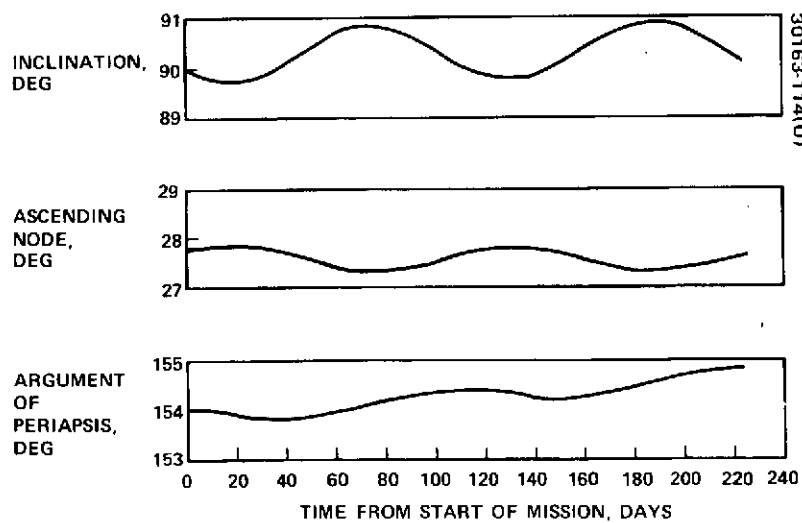


FIGURE 3-37. ORBIT ELEMENT VARIATION DUE TO SOLAR PERTURBATIONS ON BASELINE ORBIT

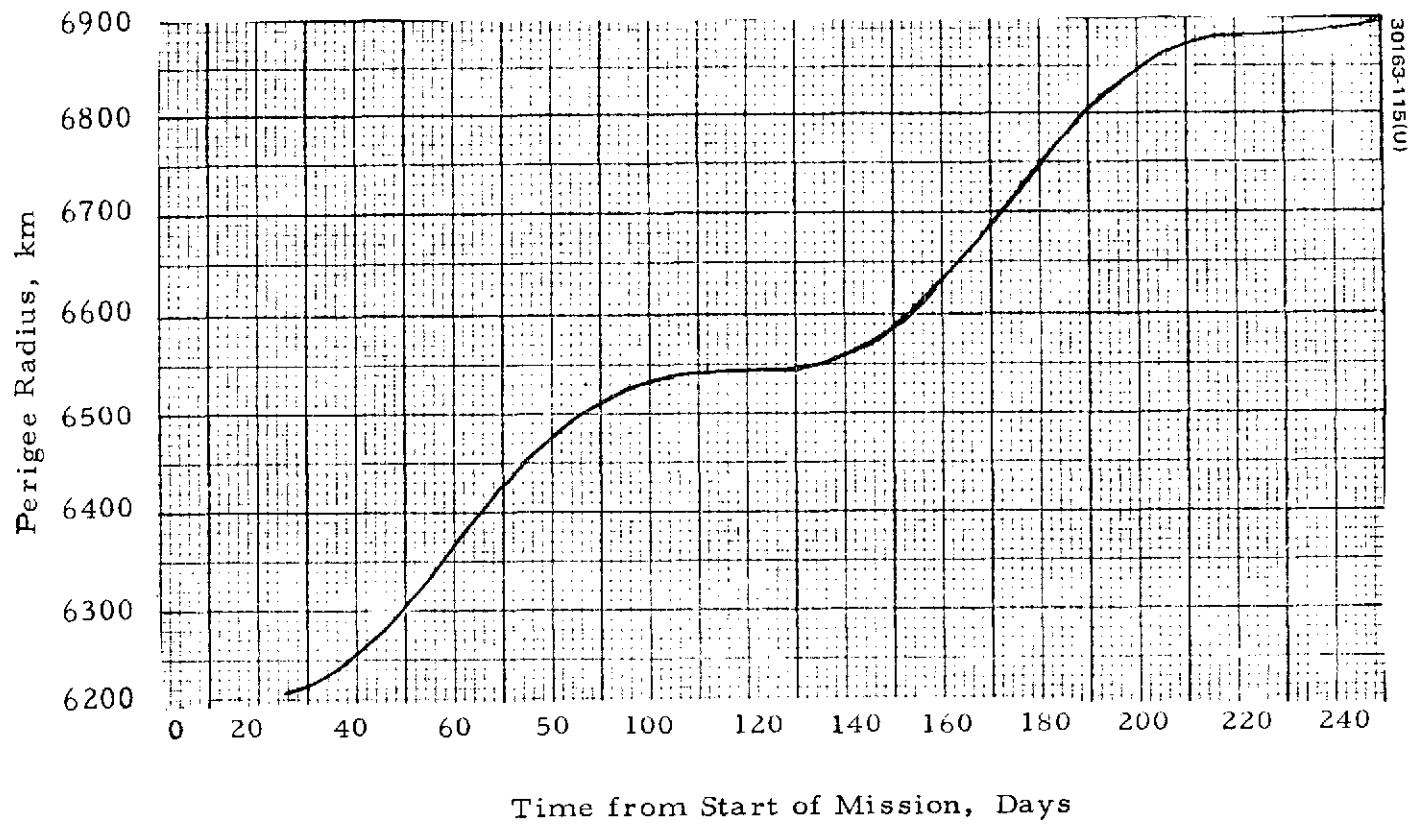


FIGURE 3-38. PERIAPSIS RADIUS VARIATION SOLAR PERTURBATIONS ON BASELINE ORBIT

TABLE 3-21. BASELINE MISSION MAXIMUM ECLIPSE VARIATION OVER LAUNCH WINDOW

| | Umbra, min | Penumbra, min |
|-------------------------|---------------|------------------|
| Launch window beginning | 178 | 201 |
| Launch window midpoint | 159 | 178 |
| Launch window end | 140 | 155 |

Drag perturbations have the effect of lowering orbital period by decreasing apoapsis altitude. The maximum effect of aerodynamic drag for the baseline atmosphere is to require 0.2 m/sec per orbit at the minimum altitude (corresponding to a 61.9 sec maximum decrease in the 24 orbital period).

Attitude Control System Utilization. The choice of a procedure to perform control maneuvers depends on the orientation of the spacecraft spin axis. There are two basic alternatives for the choice of spin axis orientation. These are the normal to the ecliptic which requires a despun antenna and an earth-pointed orientation which can utilize a fixed antenna. A more detailed explanation of these alternatives is given later. The baseline choice is the spin axis normal to the ecliptic.

The periapsis altitude and the orbital period will be controlled by the attitude control system maneuvers. Variations in the other parameters (inclination, periapsis, latitude and longitude) were shown above to be less than 1 deg and these parameters are not controlled. Due to execution errors, the total uncontrolled variations in orbital period and periapsis altitude will be 10 sec and 1 km, respectively.

Proper control of periapsis altitude and orbital period minimizes the required ΔV with the least possible operational difficulty (e. g., loss of earth lock), and without interfering with science data taking. These factors may also be expressed as a preference for using only the axial thrusters (rather than the less efficient radial thrusters) and a preference for not changing the attitude (to maintain communication lock).

A theoretical estimate of ΔV for compensation of solar and drag perturbations for the entire mission may be obtained by considering Hohmann type transfers using the axial thrusters. These periapsis and apoapsis maneuvers are shown in Figure 3-39 as a function of periapsis latitude. The curves include no attitude reorientation to perform the maneuvers and thus they represent a good (but unrealizable) standard of comparison.

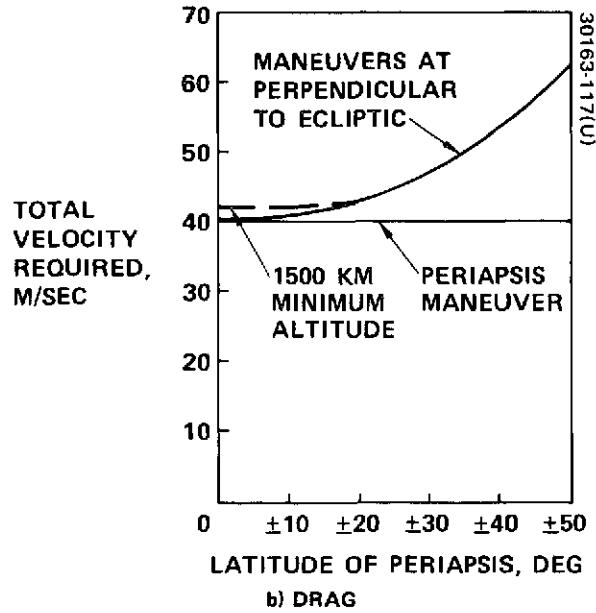
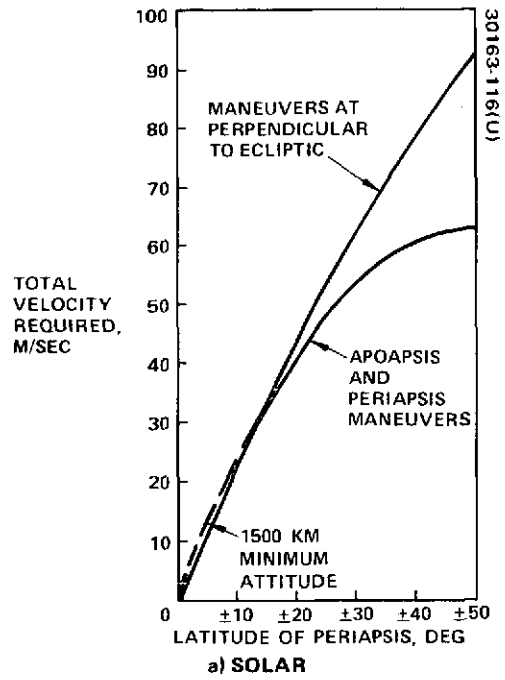


FIGURE 3-39. VELOCITY REQUIRED FOR COMPENSATION OF PERTURBATIONS

Several factors were analyzed in order to achieve a practical system of corrective maneuvers. With the baseline spin axis normal to ecliptic, ACS maneuvers will occur as illustrated in Figure 3-40. After the spacecraft passes periapsis and apoapsis, the spin axis and velocity vector become coincident. At this time, the more efficient axial thrusters are fired with no attitude reorientation. Figure 3-39 depicts the penalty for these maneuvers at perpendicular to the ecliptic by comparison to the standard of apoapsis and periapsis maneuvers. A further restriction of keeping the minimum maneuver altitude above 1500 km (by delaying firing past the point defined above) also will ensure the jet firings occur after the primary periapsis science data have been taken. The system depicted in Figure 3-40 thus achieves the desired criteria for control of periapsis altitude and orbit period with the exception of minimization of ΔV mass. But, as seen in Figure 3-39, the ΔV penalty is only about 10 m/sec for the entire mission (baseline of 26 deg periapsis latitude) when compared to the unrealizable standard (which does not include fuel for attitude reorientation). Obviously, the ACS system of maneuvers illustrated in Figure 3-40 represents a practical system and has been chosen as the baseline.

The next subject which must be addressed is the frequency of correction of the orbit perturbations. The ΔV required for solar perturbations is not a function of the maneuver frequency strategy, but drag corrections do depend on the time between maneuvers. For example, infrequent maneuvers allow the periapsis altitude to increase markedly from the 150 km nominal (Figure 3-38). The higher periapsis altitude results in less drag and a corresponding smaller ΔV required to correct orbital period (and a reduced science return from the velocity pointed instruments).

As discussed above, there is a desire for tightness of control of periapsis altitude (science) and orbital period (communication); operations are somewhat simplified by infrequent maneuvers. The system does not constrain the maneuver frequency; 1 week has been chosen for the baseline. The periapsis altitude and orbit period time histories with corrective maneuvers of solar and drag perturbations at 7 day intervals are shown in Figures 3-41 and 3-42. The altitude is corrected to 150 km (assumed to be the minimum) every 7 days throughout the mission. At times, the solar perturbations cause a weekly increase of over 40 km in the periapsis altitude with a resulting decrease in drag perturbations due to the drop in atmospheric density. At times when the effect of solar perturbations is low, the drag perturbations are high, since the orbiter stays close to the minimum periapsis altitude (Figure 3-42). Figure 3-42 shows the period variations necessary to maintain a single ground station due to the relative Sun-Earth-Venus motion. The nature of the drag perturbation is to take energy out of the orbit and thus always lower the period by decreasing the apoapsis. This monotonic behavior then suggests an overcorrection of the period to decrease the difference between the actual and desired orbital periods. The maximum deviation from constant viewing geometry (for weekly corrections) is 5 min; well within the requirement for communications.

Initial Orbit Dispersions and Orbit Trim. Table 3-22 lists the magnitude and source of the dispersions to be expected in the initial orbit around Venus. Only the periapsis altitude and orbit period will be corrected by orbit trim maneuvers. They will be trimmed in a manner that ensures periapsis occurs at the desired GMT. As seen in the plot of insertion ΔV versus periapsis altitude (Figure 3-43) it is desirable to have the minimum altitude consistent with dispersions. The pessimistic dispersions of 150 km in Reference 6 result in a 350 km initial periapsis altitude.

Table 3-23 describes the orbit trim maneuvers and their effect on periapsis altitude, apoapsis altitude, and period. After estimating the initial orbit dispersions the first maneuver (near periapsis) compensates for the orbit period dispersion in the first orbit. This maneuver is selected to trim the orbit to drift to the desired periapsis GMT (at up to 0.1 h/day) for best communications. The second maneuver (near apoapsis) trims the periapsis altitude to 200 km. Subsequent maneuvers refine the orbital elements to the degree permitted by orbit determination accuracy. Reduction of periapsis altitude for science purposes may be implemented as desired.

Orbiter Velocity Requirements. Velocity requirements for the three missions of interest are given in Table 3-16. Includes in the table are: corrective maneuvers for the initial dispersions on orbit injection, an arbitrary fuel allowance for 200 km of periapsis change at constant orbital period, atmospheric drag compensation, and solar perturbation compensation. Midcourse ΔV is discussed in Subsection 3.1.

Nominal Orbit Parameters. The orbiter time variation as a function of true anomaly is given in Figure 3-44a. Since the orbiter spends most of its time in the region of apoapsis (due to the high eccentricity) the scale is expanded in the near periapsis region in Figure 3-44b.

These curves may be used in conjunction with the plots of orbiter altitude, velocity magnitude, angle of attack, and flight path angle given in Figures 3-45, 3-46 and 3-47 in order to yield orbit parameter time variations.

Orbiter Transit Trajectory Selection - Summary

This section describes the tradeoffs which have been performed to select the baseline transit trajectory type and the orbiter periapsis location (north and south). The Type II north periapsis has been chosen as a result of spacecraft/operations and science return considerations.

Introduction. The considerations influencing selection of the interplanetary transit trajectory fall into two broad categories; those involving the spacecraft and operations and those involving science coverage. In general, the impact of spacecraft considerations can be expressed in terms of useful orbited mass; it happens that neither spacecraft cost or mission operations are materially affected by the choice among the reasonable alternatives for the interplanetary transit trajectory. The performance tradeoff for Thor/Delta launch spacecraft during 1978 launch opportunity is unusual in

- Spin Axis Normal to Ecliptic
- Use Axial Thrusters Only
- 1500 km Minimum Altitude

30163-118(U)

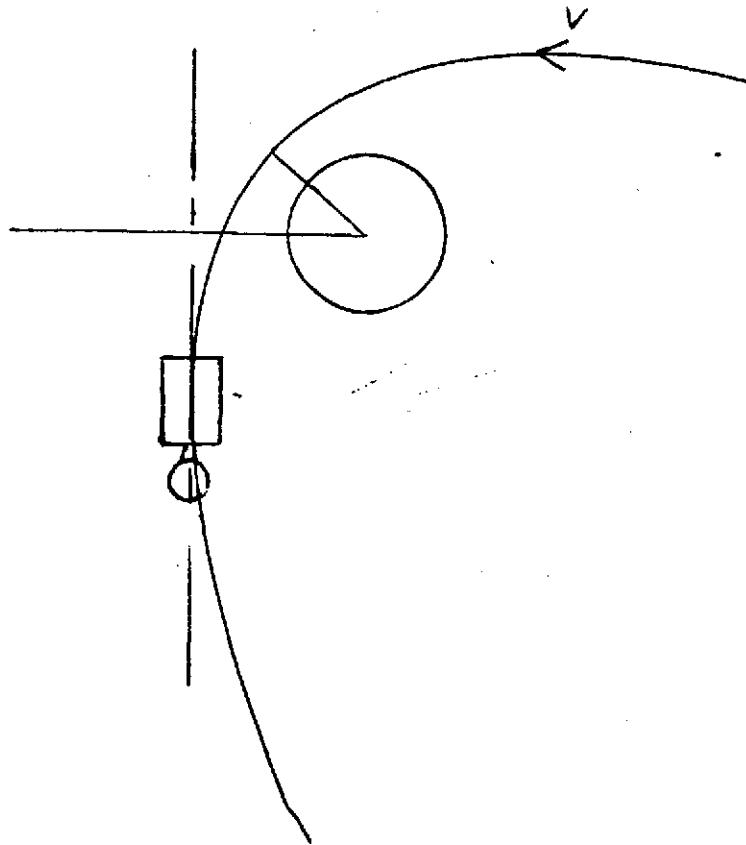


FIGURE 3-40. ACS UTILIZATION

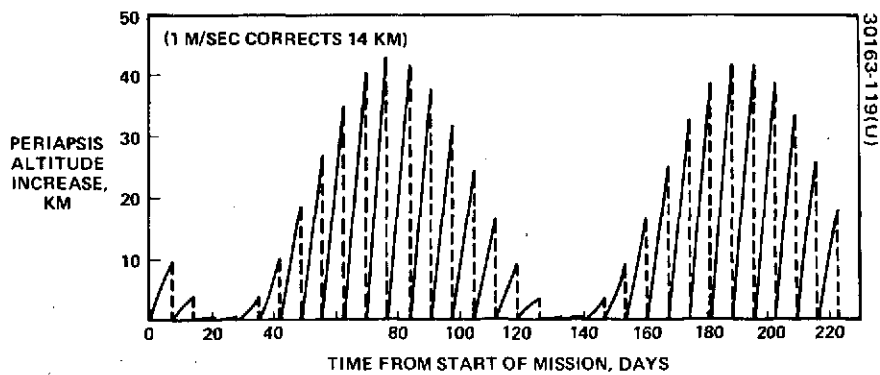


FIGURE 3-41. PERIAPSIS ALTITUDE VARIATION DUE TO SOLAR PERTURBATIONS ON BASELINE ORBIT WITH CORRECTIVE MANEUVERS EVERY 7 DAYS

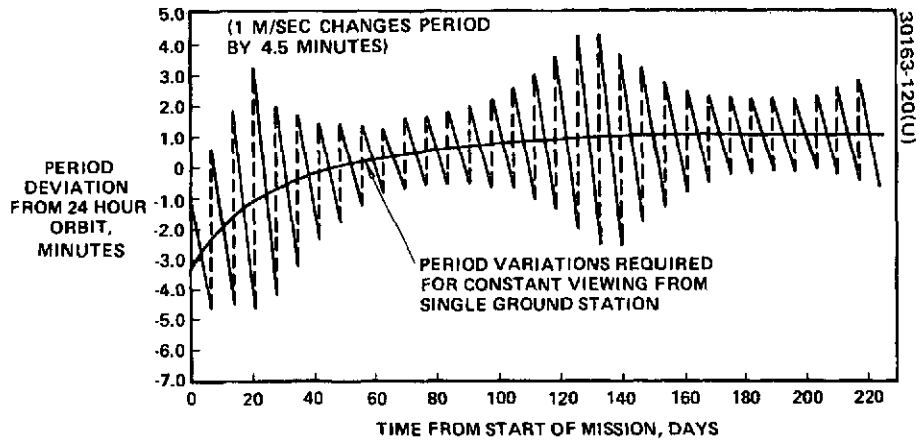


FIGURE 3-42. ORBITAL PERIOD VARIATION DUE TO DRAG PERTURBATIONS ON BASELINE ORBIT WITH CORRECTIVE MANEUVERS EVERY 7 DAYS

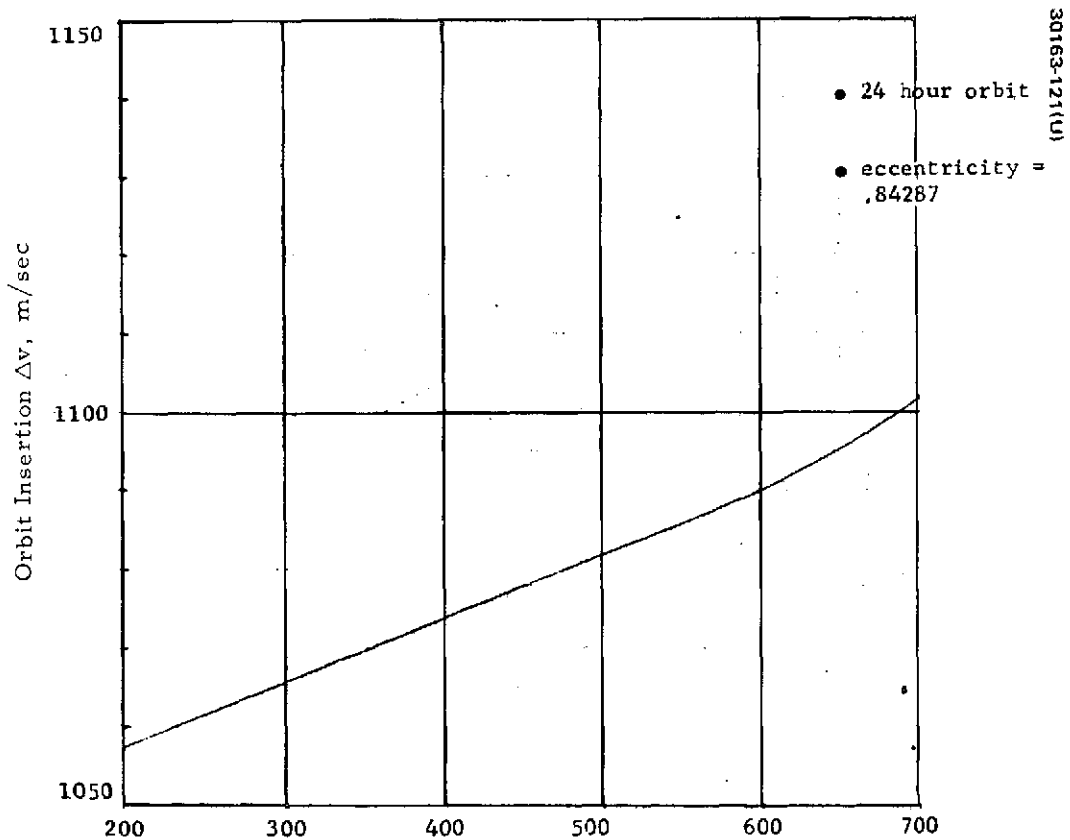


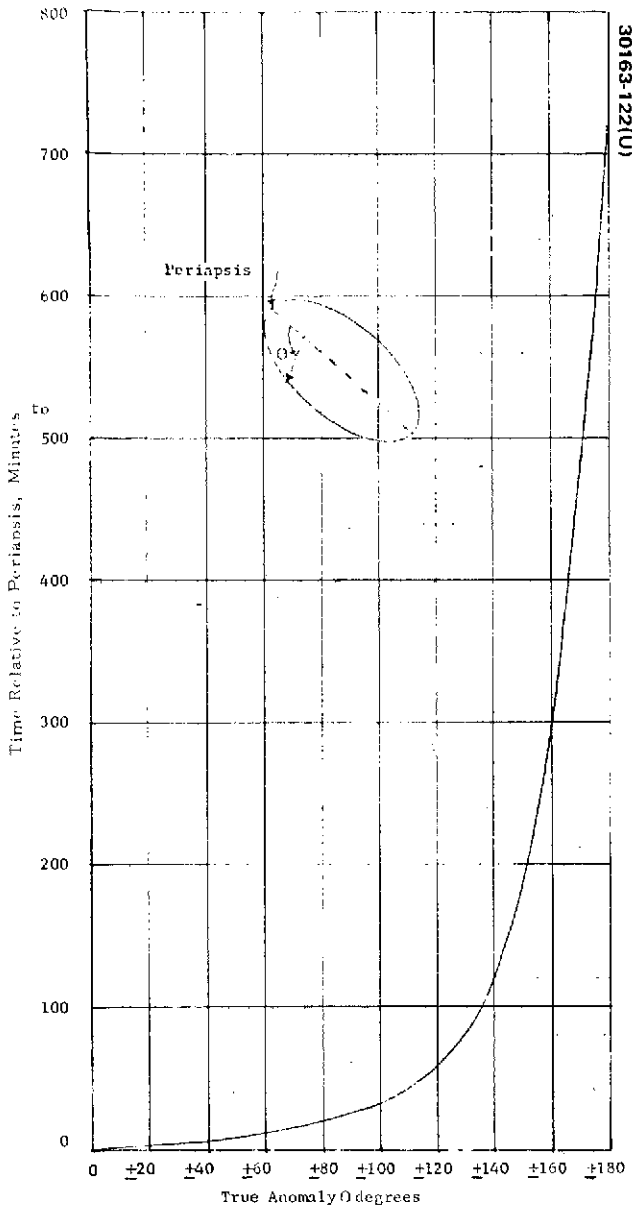
FIGURE 3-43. VARIATION OF ORBIT INSERTION Δv WITH PERIAPSIS ALTITUDE

TABLE 3-22. ORBIT INSERTION DISPERSIONS

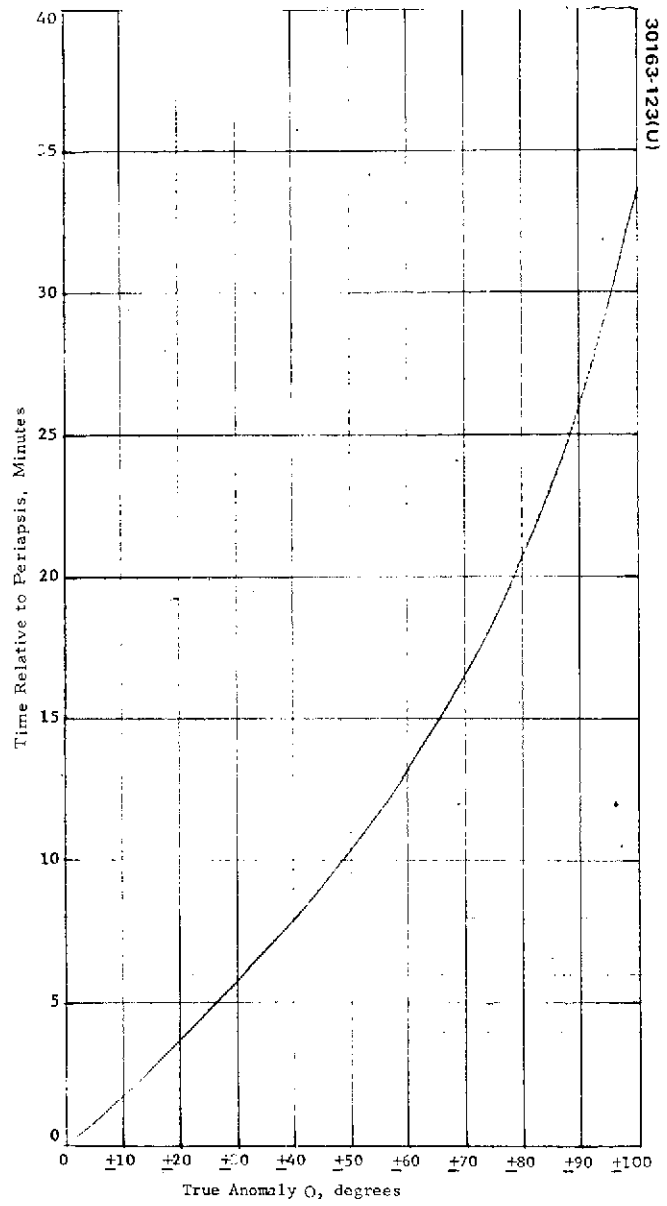
| Dispersion Source | Periapsis Altitude, km | Period, h | Inclination, deg | PERIAPSIS | |
|-------------------|------------------------|-----------|------------------|---------------|----------------|
| | | | | Latitude, deg | Longitude, deg |
| Impulse | -- | 0.9 | -- | 0.1 | -- |
| Altitude | 1. | 0.1 | 0.1 | 0.1 | 0.1 |
| Timing | 1. | 0.1 | -- | 0.1 | -- |
| OD in plane | 100. | 0.6 | -- | 0.3 | -- |
| OD out of plane | -- | -- | 1.0 | -- | 1.0 |
| RSS | 100. | 1.1 | 1.0 | 0.3 | 1.0 |

TABLE 3-23. ALTITUDE VARIATIONS DURING ORBIT TRIM

| Variation | Time From Retro-fire, days | | | | | | | |
|------------------------|--------------------------------|---------------------------|--|---------------------------|---------------------|---------------------------|--|---------------------------------|
| | 0 to 1 | | 1 to 1.5 | | 1.5 to 3 | | 3 to 12 | |
| | Nominal | 3 σ Dispersions | Nominal | 3 σ Dispersions | Nominal | 3 σ Dispersions | Nominal | 3 σ Dispersions |
| Periapsis altitude, km | 350 | 150 | 350 | 150 | 200 | 3 | As Desired | Orbit determination accuracy |
| Apoapsis altitude, km | 66,610 | 2,100 | 66,610 \pm 100 | 40 | 66,610 \pm 100 | 40 | 66,610 \pm 100 | Orbit determination accuracy |
| Period, h | 24.0 | 1.1 | 24.0 \pm 0.1 | 0.02 | 24.0 \pm 0.1 | 0.02 | 24.0 \pm 0.1 | Orbit determination accuracy |
| Orbit trim maneuver | Orbit insertion dispersions | | Compensate for orbit period dispersion in first orbit (trim orbit to drift to desired periapsis GMT) | | Trim periapsis | | Drift to desired periapsis GMT, atmosphere testing by lowering periapsis | |



a) Apoapsis



b) Near Periapsis Region

FIGURE 3-44. ORBITER TIME VARIATION AS FUNCTION OF TRUE ANOMALY

CEP

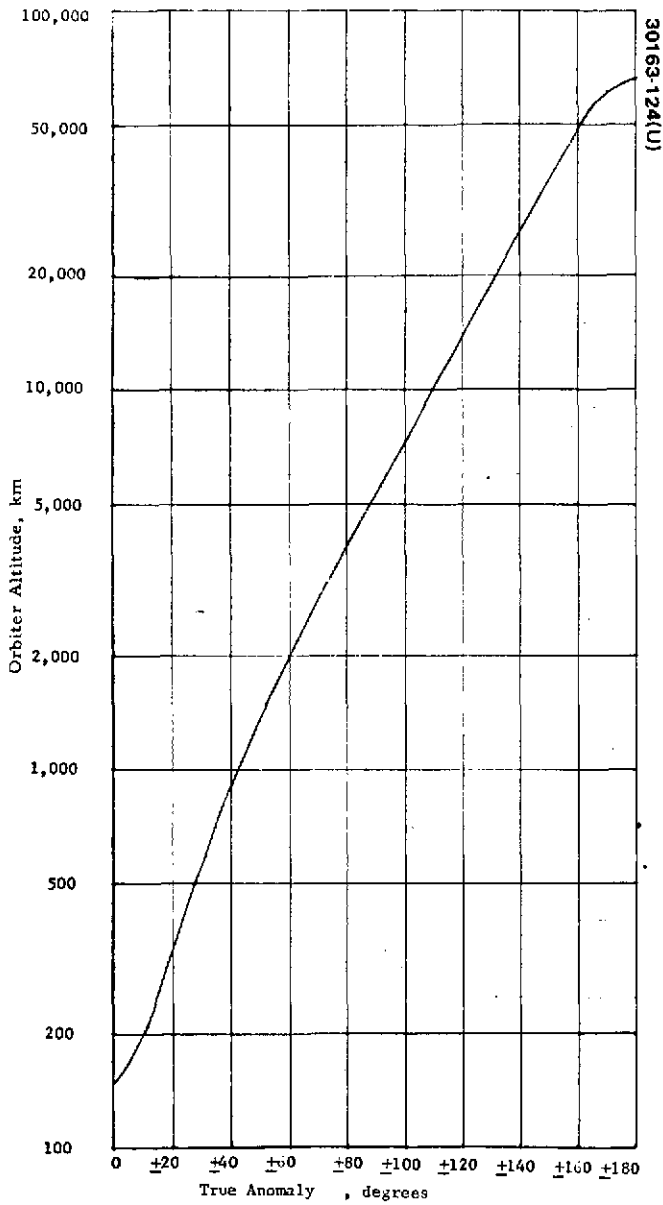


FIGURE 3-45. BASELINE ORBIT ALTITUDE VERSUS TRUE ANOMALY

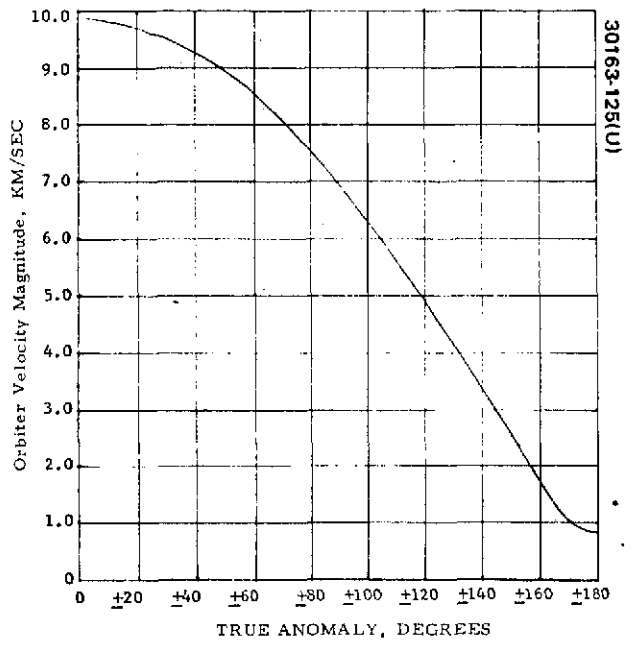


FIGURE 3-46. BASELINE ORBIT VELOCITY VERSUS TRUE ANOMALY

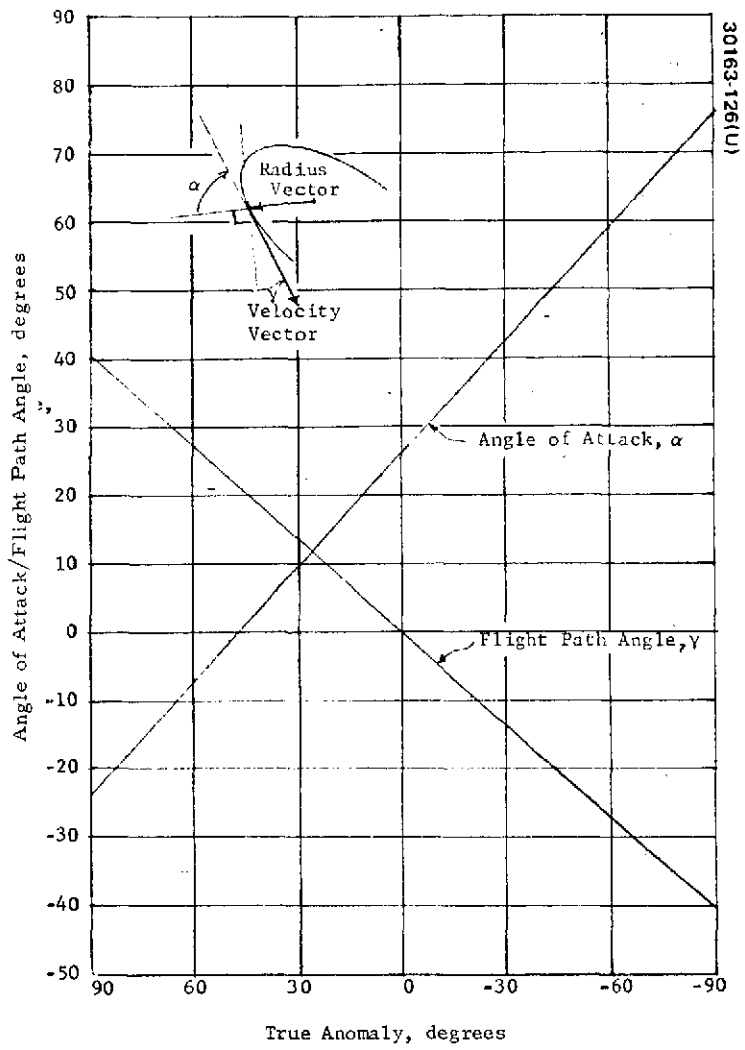


FIGURE 3-47. NEAR PERIAPSIS ANGLE OF ATTACK AND FLIGHT PATH ANGLE FOR BASELINE ORBIT

that the useful spacecraft mass is nearly equal for the Type I and Type II interplanetary transit trajectories. Science considerations, therefore, play a determining role in the transit trajectory selection (science is always a primary consideration).

Assumptions and Alternatives. The spacecraft Venus orbit is presumed to have a 24 h period, a 150 km periapsis altitude, and a 90 deg inclination to the ecliptic. These characteristics of the baseline orbit were derived previously; the desirability of the 90 deg inclination for science coverage is discussed herein. The spacecraft spin axis is normal to the ecliptic plane with a despun earth pointing antenna. Either a Type I or Type II interplanetary transit trajectory can be utilized and the periapsis of the spacecraft orbiter on Venus can be in either the northern or southern hemisphere. The options that are available from the selected transit trajectories are tabulated in Table 3-24. The variations in ecliptic latitude and initial ecliptic longitude are due to variations in the transit trajectory throughout the 10 day launch window. The Type I trajectory with the south periapsis has the periapsis near the pole; since this alternative is extremely undesirable from the standpoint of science coverage, only the other three options will be considered viable. The transit trajectory selection was discussed previously. The characteristics of the selected launch windows (north periapsis options) are summarized above in Tables 3-10 and 3-11.

Spacecraft/Operations Consideration Summary. Velocity requirements after orbit insertion were discussed previously and are summarized in Table 3-16. The ACS propellant required to implement these maneuvers is included in the spacecraft mass statement (Table 3-12).

Spacecraft and operational considerations are summarized in Table 3-25. The long duration eclipses are important because they size the spacecraft battery with 1 h of eclipse increasing spacecraft battery requirements by about 2 kg.

The transit trajectory time for the Type I trajectory is somewhat shorter than for the Type II trajectory, which is favorable for spacecraft reliability. However, the difference is too small a portion of the total mission duration to have a significant impact. The launch dates for the Type II trajectories are about 3 months earlier than for the Type I trajectories (Tables 3-10 and 3-11); program scheduling must be implemented accordingly.

There are more stars of sufficient brightness available to the star sensor in the southern hemisphere than in the northern hemisphere, and therefore periapsis locations in the northern hemisphere are somewhat more desirable than those in the southern hemisphere. This is also not a major consideration as the mission can be accomplished in either case.

The maximum heliocentric radius during the transit trajectory is greater for the Type II trajectory. This reduction in solar energy sizes the solar panel and represents an additional mass of about 1 kg for the Type II trajectories.

TABLE 3-24. POSSIBLE PERIAPSIS LOCATIONS

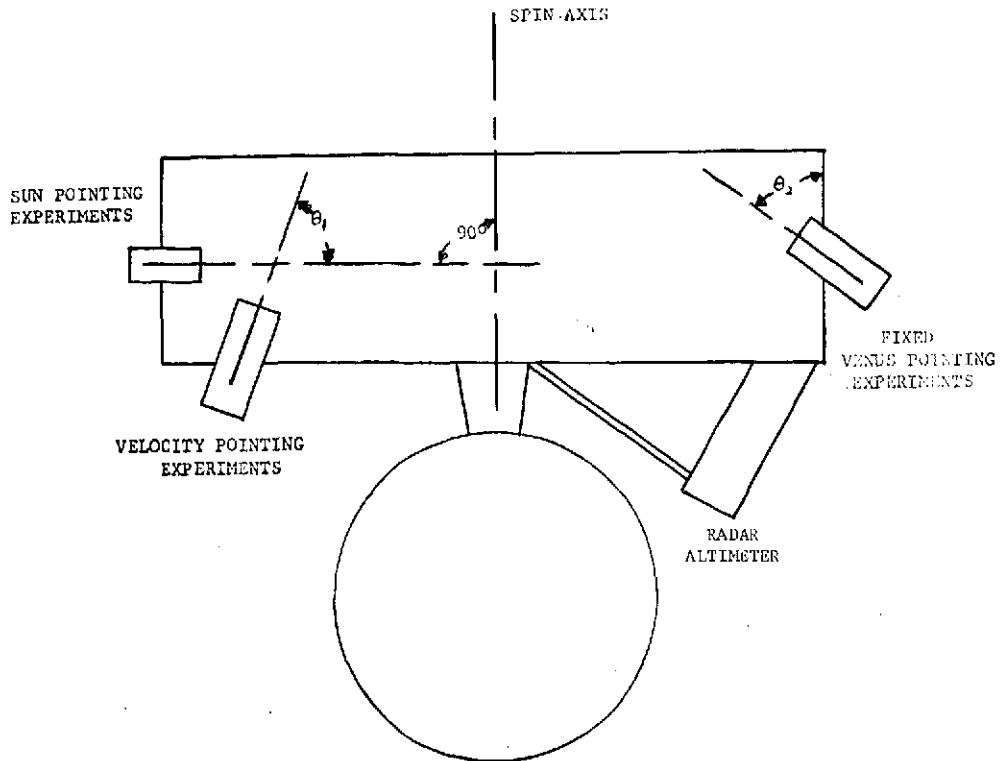
| Trajectory | Ecliptic Latitude, deg | Ecliptic Longitude From Subsolar Point, deg |
|------------|------------------------|---|
| Type I | 4° to 13° N | -46 to -39 |
| | 90° to 81° S | -46 to -39 |
| Type II | 21° to 31° N | -63 to -54 |
| | 55° to 45° S | -63 to -54 |

The useful spacecraft mass is defined herein as the dry mass of the spacecraft less the mass of the retro meter case. The useful spacecraft mass shown in Table 3-25 must be adjusted by the required difference in battery mass (due to maximum eclipse duration variations), and solar panel mass (due to differences in maximum heliocentric radius) to determine impact on science mass capability. The performance capability of all three alternatives are nearly equal with the Type II north periapsis having a slight advantage.

Science Considerations

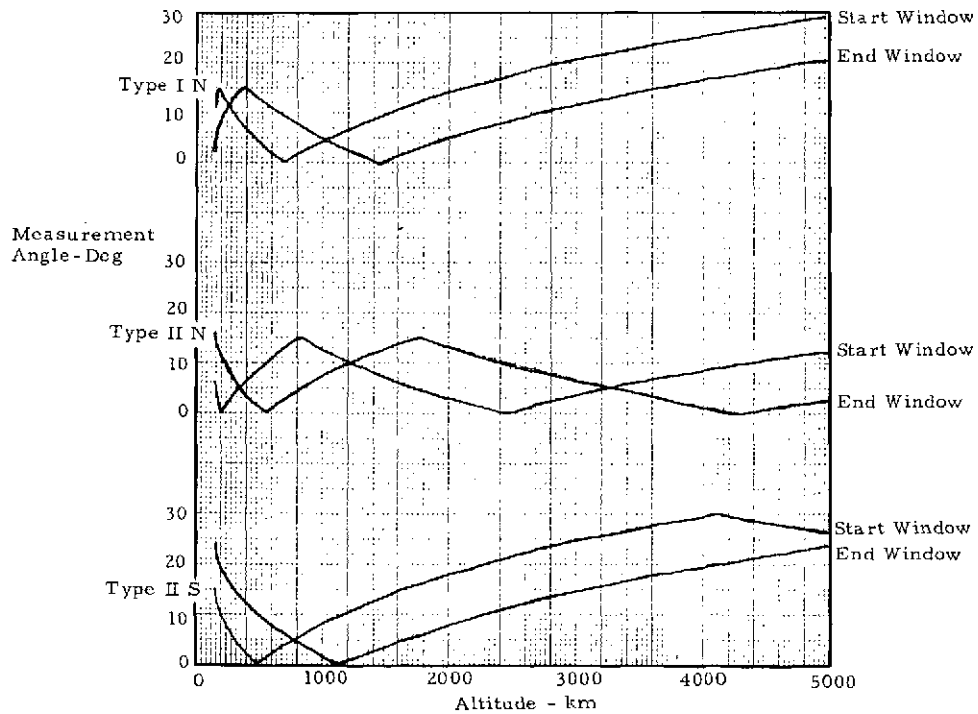
Experiments and Experiment Deployment. Experiments which are inherently insensitive to periapsis location are given in Table 3-26. In essence these experiments either have no pointing requirements, or pointing requirements which are easily or automatically satisfied independent of orbit geometry with respect to the planet.

There are two experiments (the neutral mass spectrometer and the ion mass spectrometer) which are required to point in the direction of the spacecraft velocity vector (within ± 30 deg) at sometime during the spacecraft spin. Coverage obtained from these experiments does depend upon their deployment and periapsis latitude (but not on initial periapsis longitude). There are two planet pointed experiments; the S band radar altimeter is continuously oriented (electronically or mechanically) to provide altitude measurements, and the IR radiometer which makes measurements along the boresight fixed to the rotating spacecraft.



30163-127(U)

FIGURE 3-48. SCIENCE DEPLOYMENT



30163-128(U)

FIGURE 3-49. VELOCITY POINTED EXPERIMENT COVERAGE

TABLE 3-25. SPACECRAFT/OPERATIONS
CONSIDERATIONS SUMMARY

| | Type I North | Type II North | Type II South |
|-----------------------------|-----------------|------------------|------------------|
| Maximum eclipse duration | ~4 h | ~3 h | ~2 h |
| Transit trajectory time | ~110 days | ~190 days | ~190 days |
| Star availability | Better | Better | Satisfactory |
| Maximum heliocentric radius | 1.01 AU | 1.07 AU | 1.07 AU |
| Useful spacecraft mass | 169.2 kg | 168.7 kg | 164.9 kg |

TABLE 3-26. EXPERIMENTS INHERENTLY INSENSITIVE
TO PERIAPSIS LOCATION

| Experiment | Pointing Requirement |
|----------------------------|----------------------------|
| Magnetometer | Any orientation |
| Electron temperature probe | Not in spacecraft wake |
| UV spectrometer | Scans planet limb |
| S band occultation | Uses communication antenna |
| Solar wind probe | Scans sun |

The instruments are mounted as shown in Figure 3-48. Pointing requirements for the sun-pointed experiment are automatically satisfied because the spin axis is held normal to the ecliptic plane. The angles θ_1 and θ_2 are optimized for each of the alternatives in periapsis location.

Science Coverage. The coverage obtained with the velocity pointed experiments is shown in Figure 3-49 for each of the transit trajectory alternatives. An optimum experiment orientation was selected for each of the transit trajectories; the coverage obtained varies throughout the launch window as the periapsis latitude varies. Note that in all cases the maximum

measurement angle is not greater than the limiting value of 30 deg, indicating that satisfactory velocity pointing experiment coverage can be obtained for any of the transit trajectory alternatives when the orbit inclination is 90 deg to the ecliptic. The measurement angles are increased as orbit inclination is decreased; the smaller measurement angles obtained with the Type II north transit trajectory would permit orbit inclination to be reduced to about 70 deg without loss of coverage (for the other trajectory alternatives an inclination reduction leads to loss of coverage). The tradeoffs in the altimetry coverage will be used to represent all planet pointed coverage because the coverage tradeoffs obtained with the altimeter and with an optimally pointed fixed instrument (e.g., the IR radiometer) are essentially identical.

Science coverage considerations include not only periapsis latitude but also the initial value of periapsis longitude. The initial value of periapsis longitude is important because it represents the number of days of sunlit measurements before the spacecraft orbit passes the terminator (this movement with respect to the terminator is due to the rotation of Venus around the sun). Periapsis longitude variation throughout the mission is shown in Figure 3-50 for both Type I and Type II trajectories (north and south periapsis trajectories are the same). Variation and coverage with either trajectory time depends upon what day during the launch window the spacecraft is launched. The Type I trajectories reach the terminator from 28 to 32 days after orbit insertion versus 17 to 23 days for the Type II trajectories. Either of these alternatives appears satisfactory and the initial value of periapsis longitude is therefore not a determining factor in transit trajectory selection.

The coverage obtained with the altimeter is shown in Figure 3-51 (for a 90 deg inclination orbit a true anomaly variation is equivalent to a latitude variation). If the maximum altimetry range is 1000 km, then the maximum latitude coverage band is about 84 deg. Since the slope of the curve is quite steep at this point even a small increase in latitude coverage requires a considerable improvement in instrument performance. It, therefore, appears likely that complete coverage of a single hemisphere during a single mission is unlikely even if an optimum periapsis location could be obtained.

The actual altimeter coverage obtained is shown in Figure 3-52 for the three transit trajectory alternatives. For the Type I trajectory there is complete coverage of the equatorial region, but very limited coverage of the higher latitude even if the spacecraft is launched at the end of the launch window. This science coverage is considered undesirable. The Type II north periapsis trajectory provides complete coverage in the equatorial and middle latitude regions at the expense of leaving a relatively small polar cap unmapped. The Type II south trajectories provide a periapsis which gives coverage at the high latitudes but no coverage at the equator, or even in the equatorial region at the start of the mission. The area of the planet's surface which is mapped is obviously much less for the Type II south trajectory than for either of the other two alternatives. Although there will be mapping coverage in the equatorial region from earth based tracking in the time frame of this mission, this tracking relative to that obtained from mapping with the orbiter may be less accurate. In any case equatorial mapping coverage can be considered a reasonable mission feature.

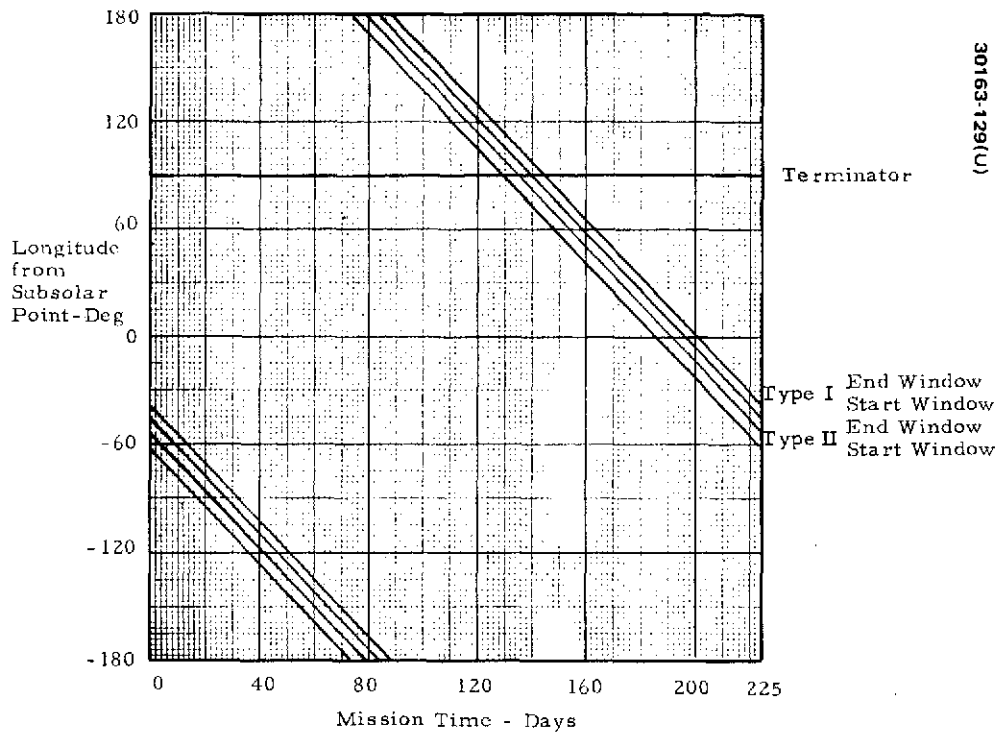


FIGURE 3-50. PERIAPSIS LONGITUDE VARIATION

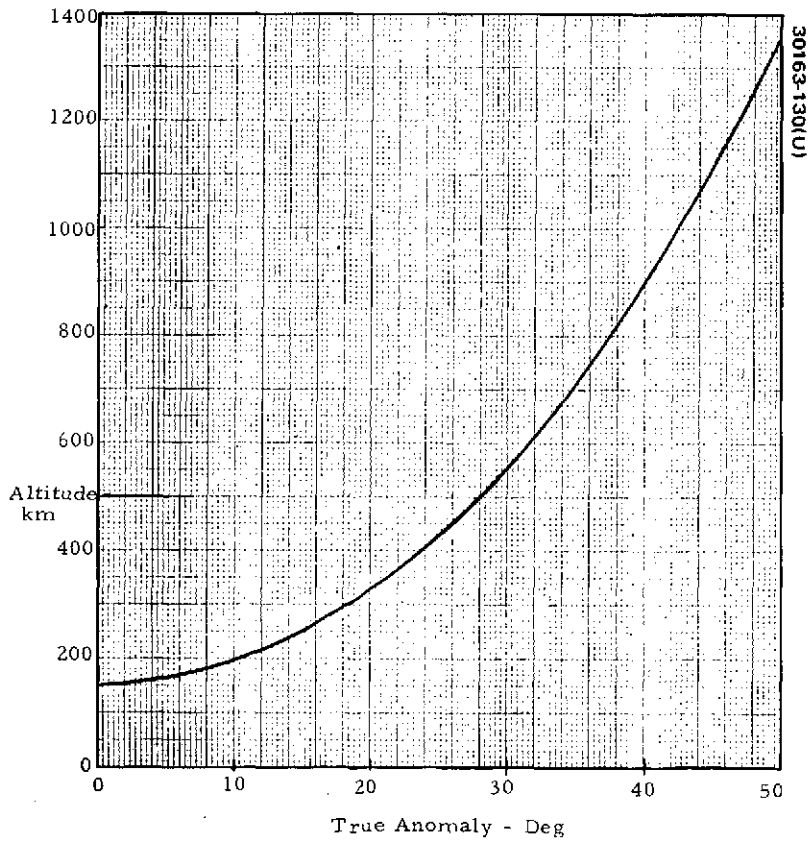


FIGURE 3-51. ALTIMETRY LATITUDE COVERAGE

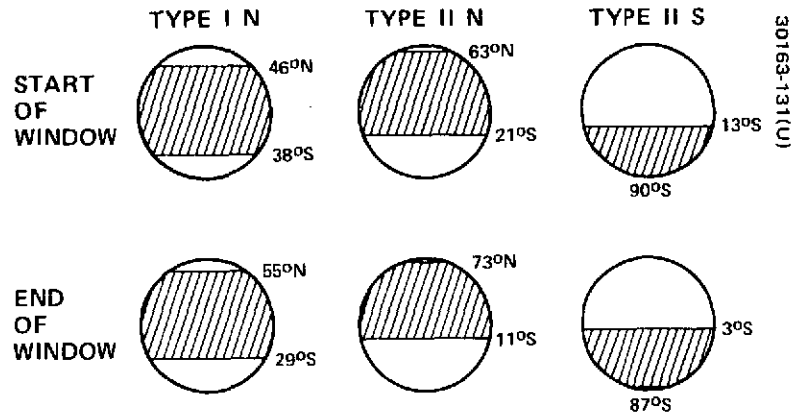


FIGURE 3-52. ALTIMETRY COVERAGE AT ≤ 1000 KM ALTITUDE

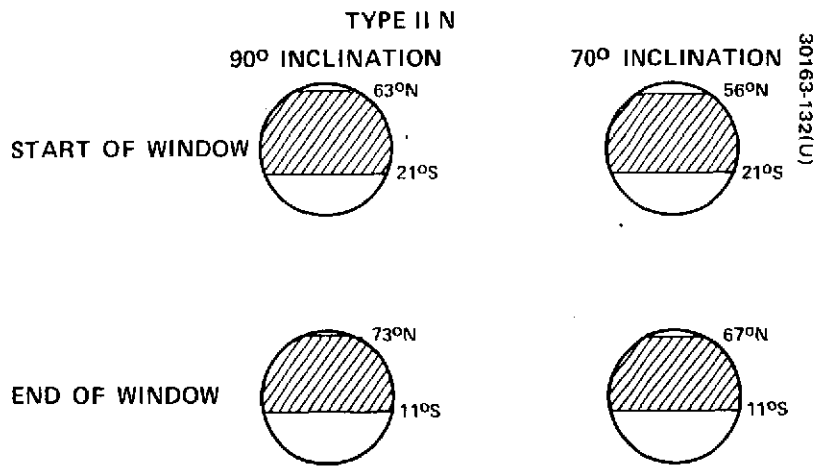


FIGURE 3-53. ALTIMETRY COVERAGE AT ≤ 1000 KM ALTITUDE FOR TYPE II NORTH TRAJECTORY

The judgment that the coverage obtained from the Type I trajectory is inferior to the other two alternatives is probably not controversial, whereas the selection of the north or south periapsis for the Type II trajectory is more subjective. This study assumes that the coverage obtained with the Type II north trajectory is at least as desirable as that obtained with the Type II south, and this alternative has been selected as the baseline.

The effect of orbit inclination on latitude coverage is to decrease the maximum latitude covered. The degradation in latitude coverage for a 70 deg inclination is shown in Figure 3-53 for the Type II north trajectory. Since the maximum latitude covered can never be greater than the orbiting inclination, a 70 deg orbit on the Type II south trajectory would decrease high latitude coverage to 70 deg. This alternative is even less desirable than a 70 deg inclination on the Type II north trajectory because selection of the Type II south trajectories implies a sacrifice of equatorial coverage to obtain high latitude coverage. The only potential advantage of a 70 deg angle inclination orbit is that the latitude of periapsis can be moved about 7 to 8 days further from the terminator than for the 90 deg inclination, but this is not a significant consideration because the periapsis location with respect to the terminator is satisfactory. It may also be noted that both velocity pointed instrument measurement angle and orbit maintenance propellant requirements (due to spin axis/orbit geometry considerations) are degraded as the orbit inclination deviates from 90 degrees. Since orbit inclinations other than 90 deg have considerable disadvantages the selection for the baseline orbit is a 90 deg inclination.

Conclusions

Spacecraft and operational considerations provide a small advantage to the Type II north transit trajectory in comparison to the other alternatives. The spacecraft orbit at Venus which is obtained utilizing a Type I transit trajectory has science coverage which is inferior to that obtained utilizing the Type II transit trajectory. A case can be made that the science coverage obtained with the Type II north periapsis is at least equal to that obtained with the south periapsis. For these reasons, the Type II north periapsis has been selected as the baseline for the purposes of this study. It should be noted, however, that spacecraft modifications required to utilize the south periapsis as the baseline are very minor. The same retrorocket can be used and the hydrazine tankage provided on the baseline is adequate for use with the south periapsis alternative. The only spacecraft design change required is a small variation on the mounting angles of the velocity point and planet pointed science experiments. This reorientation is not difficult.

3.3 REFERENCES

- 1) J. N. Fisher, "Launch Vehicle Data," Telecon to NASA Ames, Jack Dyer, December 8, 1972.
- 2) J. N. Fisher, "Pioneer Venus Mission Analysis," Telecon to NASA Ames, Jacy Dyer, October 18, 1972.
- 3) NASA Ames, "Pioneer Venus Document PV-1002.00 A Baseline System Design," July 24, 1972.
- 4) Ames letter, "Contract NAS 2-7250; Additional Delta 2914 Injection Covariances for 90 rpm Spin Rate," ASD: 244-9/22-277, November 3 1972.
- 5) Ames letter, "Contract NAS 2-7250; Coordinate Definitions and Injection Locations for Delta 2914 Injection Covariance Matrices," ASD: 244-9/32-016, January 31 1973.
- 6) Ames letter, "NAS 2-7250; Orbit Determination Accuracy for Pioneer Venus Estimated by Jet Propulsion Laboratory (JPL)," ASD: 244-9/32-027, February 16 1973.
- 7) System Design Study of the Pioneer Venus Spacecraft, Volumes I and II, Hughes Aircraft Company, HS-507-106, May 1972.
- 8) Pioneer Venus, report of a Study by the Science Steering Group, June 1972.
- 9) Models of Venus Atmosphere (1972), NASA SP-8011, September 1972.
- 10) L. J. Nolte, "Venera Wind Measurements/Probe Response," HS507-0476, March 30 1973.
- 11) "The Long-Term Motion of Artificial Planetary Satellites," (NASA-Cr 109498), McDonnell Douglas Astronautics Co., 1969.
- 12) M. L. Lidov, "On the Approximated Analysis of the Orbit Evolution of Artificial Satellites," from Dynamics of Satellites; IUTAM Symposium Paris 1962, Ed. M. Roy, Academic Press, 1963.
- 13) "Models of the Venus Atmosphere, (NASA-SP-8011), September 1972.

4. MISSION OPERATIONS AND GROUND SYSTEMS

Mission operations and ground systems were reviewed during the Pioneer Venus study to influence the spacecraft design and mission sequence to provide

- 1) A spacecraft design which can operate within the basic framework of Pioneer procedures, equipment, and manpower
- 2) Compatibility with existing Pioneer ground systems and deep space network (DSN)
- 3) Realizable mission sequence of events

Study tasks included preparation of plans for critical mission phases, detailed mission sequences, and ground systems interface specification.

The fundamental elements of a mission operations plan (MOP), (i.e., schedules, organization, and mission description) were organized to influence the spacecraft design and mission sequences. A review of these fundamental elements of the MOP are included herein.

Significant multiprobe and orbiter mission sequences, probe entry timing relationships, and critical parameter (mass properties, sun angle, spin rate) histories are summarized in the following sections. Mission sequences were prepared under Task MS 1 and detailed data is presented in Reference 1.

Mission operations and ground system data presented in this section are based primarily on the Thor/Delta midterm baseline with a multiprobe mission launch in 1977 and an orbiter launch in 1978. The basic approaches described herein are also applicable to the two mission launch in 1978 and Atlas/Centaur launch vehicle. Details of the Atlas/Centaur 1978 dual launch mission are presented in the informal data book provided as a supplement to the final report. Final details will be presented in the Hughes execution phase proposal.

Requirements for ground processing of command and telemetry data were analyzed to provide maximum compatibility with the DSN and other elements of the Pioneer ground system. An interface specification (Task SP-3, Reference 2) was written to identify the interface requirements. Interface

specification data and work to further identify spacecraft interface parameters are summarized in the following paragraphs.

The original Thor/Delta multiprobe mission would have been launched from AFETR during a 10 day launch window from 6 January to 15 January 1977, inclusive. A daily launch period of 10 min existed between 0424 GMT and 0604 GMT, depending upon launch date. Following launch, a thruster calibration was to be performed within 24 h. It was to be followed by the first trajectory correction maneuver (TCM) at 1 to 5 days after launch which corrected for launch injection errors. Subsequent TCMs were to be performed at 20 and 50 days after launch and at 30 days prior to encounter each of which corrected for previous maneuver execution errors. Approximately 5 days prior to the fourth TCM an additional thruster calibration was to be performed. At 23 days prior to encounter the large probe was to be released. The small probes were to be released 20 days prior to encounter. Following small probe release the bus was to be tracked for 2 days to support estimation of small probe trajectories. At 18 days before entry the bus was to be retargeted to its entry point and retarded in velocity to see that its entry would have occurred shortly after all probes impacted the surface of Venus. Ten days before entry a small ΔV maneuver was to correct for execution errors induced in the bus targeting maneuver. Approximately 3 h before entry, probe bus science was to be turned on and operated until spacecraft destruction in the Venusian atmosphere. Entry was to occur at 1430 GMT on 17 May 1977 after a 122 to 131 day Type I transit. Details on the present Atlas/Centaur multiprobe mission are presented in the informal data book.

The original Thor/Delta orbiter mission would have been launched from AFETR during 10 day launch window from 25 May to 3 June 1978, inclusive. A daily launch period of 10 min existed between 1428 and 1707 GMT, depending upon launch date. Following launch, a thruster calibration was to be performed within 24 h. It was to be followed by the first TCM at 1 to 5 days after launch which corrected for launch injection errors. Subsequent TCMs were to be performed at 20 and 50 days after launch and at 20 days prior to encounter. The spacecraft was to be reoriented to its orbit insertion attitude at 1 h prior to encounter. For the Thor/Delta mission, orbit insertion was to be at 1719 GMT on 2 December 1978, after a 183 to 192 day type II transit. It was to occur out of view of the earth and would be followed by an orbit period adjustment maneuver at the first periapsis, and a periapsis altitude adjustment (to 150 km altitude) at the second apoapsis. Details of the present Atlas/Centaur orbiter mission are presented in the information data book.

4.1 MAJOR IMPACT ON SPACECRAFT DESIGN

The mission operations and ground system studies influenced both the spacecraft design and sequence of events. The influence is evident from the descriptions of the design presented in appropriate volumes of the final report. The major impact is reviewed in the following paragraphs.

- 1) Probe Release. The release sequencing of the large and small probes was stretched to a 7 day period to provide adequate time to:
 - a) Change the spin rate three times
 - b) Reorient the spin axis three times
 - c) Perform a velocity change
 - d) Conduct probe tests
 - e) Release the large and three small probes
 - f) Provide more time to obtain more accurate tracking data after this velocity change prior to small probe release
- 2) Small Probe Targeting Trajectory Program. Based on cursory look at software requirements for the Pioneer Venus program and currently available software from other programs, a new trajectory program would be required which would output targeting functions, spin speed, required ΔV , and precession maneuvers for small probe release
- 3) Probe Encounter Data Recovery. A thorough analysis was performed on data recovery from the multiple probes during the encounter and descent sequences. The baseline method of pre-detection recording was selected and filter bandwidth requirements were determined
- 4) Orbit Insertion Thermal Constraint. Solar planetary geometry during the orbit insertion phase causes the sun angle to increase beyond 10 deg for a 2 h period. Sun angles greater than 10 deg create solar interreflections in the spacecraft aft cavity imposing a thermal constraint on the spacecraft. This design constraint was not completely solved for the Thor/Delta orbiter. One approach is to use components capable of operating at elevated temperatures for this transient period. The Atlas/Centaur orbiter design incorporates this approach along with the more louvers available in the Atlas/Centaur orbiter
- 5) Data Storage Configuration. The radar altimeter high sampling rates and the significant number of occulted periapsis passes dictate a data storage capability. To simplify the ground operations the data storage was designed to store all of the radar altimeter data for one periapsis pass. The recommended approach allows telemetry of the altimeter data in a continuous sequence

- 6) DSN Compatibility. Both the probe bus and orbiter spacecraft have been designed for compatibility with the DSN multimission capability (MMC). No changes are required for command, telemetry, or tracking data handling.
- 7) Data Formats. Formats have been developed for each vehicle which simplify ground data processing. Each format consists of relatively short minor frames, each of which is complete unto itself; and each of which contains a unique identification code for triggering the proper processing routine.
- 8) Command Verification. Provision is made so that account can be made of all commands transmitted and accepted by the spacecraft. In addition, a command reject signal is telemetered when commands are rejected so that fault isolation and recovery is simplified.

4.2 SPACECRAFT LAUNCH OPERATIONS

The Thor/Delta launch and injection operations are constrained by the existing ground systems and basic spacecraft constraints imposed by equipment limitations. The sequence of events is compatible with the operational constraints which are summarized as follows:

- 1) Ground station visibility nominally occurs 22 min after separation
- 2) Boom deployment cannot occur at spin rates greater than ≈ 75 rpm
- 3) At least 20 min must be allowed after boom deployment and before the initial precession to allow adequate nutation damping
- 4) For the multiprobe mission, reorientation to an acceptable sun angle (≥ 45 deg) must occur within 54 min after separation to preclude excessive battery discharge

The following paragraphs summarize the launch operations and spacecraft electrical interfaces. Operational constraints are met and correlated with the sequence of events.

Countdown

Countdown activities were to commence several days before the first launch window and only after prelaunch and rehearsal testing indicated sufficient flight readiness of the spacecraft, launch vehicle, launch facility, tracking facility, ground data system, and personnel. During this period, mission readiness of all systems were to be reported regularly along with any anomalous conditions. Activities during the final 4 h before launch were to be primarily concerned with monitoring all system elements to ascertain flight readiness status and maintain that status. To this end, the following operations were to constitute the minimum activity schedule for this period:

- Command transmission and command link interruptions performed hourly using prime and redundant spacecraft units to verify command subsystem operational status
- Switching of operating modes, data rates, formats and redundant units within the data handling subsystem at least once
- Switching in of redundant units in the power, attitude control and rf subsystems at least once
- Switching to internal power for a test period 2 h before launch and finally at 5 min before launch
- Continuous trickle charging of spacecraft batteries except during self-powered periods and immediately following self-powered periods when higher charge rates become necessary
- Verification of command memory contents and attitude control register contents hourly following command transmission interruptions

Boost Phase

Boost phase events were to begin with liftoff and end with the yaw maneuver following spacecraft separation from the third stage. During this period, the spacecraft was to be powered from its own battery and continuously transmit telemetry data using the low power rf mode and 128 bps data rate. An event sequence for this period is presented in Table 4-1.

Post Injection

The spacecraft was to be separated approximately 100 sec after third stage cutoff to allow for tailoff of the third stage motor. At separation the command subsystem was to sense separation switch closure and commence to operate from a sequence which was to have been stored in the command memory before launch. Spin rate at this point was to have been 90 ± 10 rpm and sun angle 18 to 39.5 deg for the multiprobe mission and 77 to 84.3 deg for the orbiter. Two minutes after separation the attitude control electronics was to be turned on, the spacecraft despun to 60 ± 10 rpm and the booms deployed. Early boom deployment was desirable in order to balance the spacecraft and commence damping of wobble and nutation induced by separation and deployment events as soon as possible. Also, on the probe bus a large portion of the aft omni antenna pattern would have been blocked by spacecraft structure until after bicone/omni boom deployment. On the orbiter mission the sun angle at separation would have been satisfactory for several hours. However, on the multiprobe mission the small sun angle, which would have resulted in battery discharges, made necessary a precession maneuver to an improved sun angle. This was to occur before excessive battery discharge (>40 percent) which at the worst sun angle (18 deg) would have occurred 54 min after separation. Nominally, communications with the ground would have been established by this time in which case the maneuver would be controlled from the ground. However,

TABLE 4-1. TYPICAL LAUNCH SEQUENCE

| Event | Time (seconds) |
|--|-------------------|
| <u>Lift-Off</u> | L + 0.00 |
| Begin first Stage I pitch rate | L + 8 |
| End first Stage I pitch rate | L + 13 |
| Begin second Stage I pitch rate | L + 13 |
| End second Stage I pitch rate | L + 15 |
| Begin gravity turn | L + 15 |
| Maximum Dynamic Pressure | L + 37 |
| Six Castor II solid motors burnout | L + 39 |
| Three Castor II solid motors ignition | L + 39 |
| Three Castor II solid motors burnout | L + 78 |
| Jettison nine solid motors | L + 85 |
| End gravity turn | L + 95 |
| Begin last Stage I pitch rate | L + 95 |
| End last Stage I pitch rate | L + 226 |
| Booster cutoff (MECO) | L + 226 |
| Booster tailoff | L + 226 to 227 |
| Vernier solo | L + 227 to 232 |
| Jettison booster | L + 234 |
| <u>Stage II Ignition</u> | L + 238 |
| Begin Stage II pitch rate | L + 239 |
| Jettison fairing | L + 276 |
| End Stage II pitch rate | L + 556 |
| Stage II cutoff (SECO I) | L + 556 |
| Begin coast | L + 556 |
| Begin coast pitch rate | L + 650 |
| End coast pitch rate | L + 800 |
| Stage II restart | L + 1486 = M + 0* |
| Stage II final cutoff (SECO II) | M + 8 |
| <u>Stage III Timer Ignition</u> | M + 10 |
| Fire 15 sec delay squibs on motor safe and arm | M + 10 |
| Fire spin rockets | M + 10 |
| Spin rocket burnout | M + 11 |
| Second stage jettison | M + 12 |
| Stage III motor ignition | M + 25 |
| Stage III motor burnout | M + 69 |
| Spacecraft separation | M + 70 |
| Stage III tumble (yaw released) | M + 72 |

* Time applies to multiprobe mission only; for orbiter mission, M + 0 = L + 5956.

if a command link had not been established the spacecraft would be reoriented by stored command. The post-separation sequence is presented in Table 4-2.

4.3 MULTIPROBE MISSION OPERATIONS

The Thor/Delta multiprobe mission operations are constrained by the existing ground systems, basic spacecraft constraints created by equipment limitations and the need to provide a manageable set of sequences and operations. The recommended multiprobe mission phases and sequences are fundamentally compatible with the DSN, ground personnel functions and spacecraft design. All basic spacecraft and ground system constraints are met with the baseline multiprobe sequence of events.

The review of the multiprobe mission operations resulted in three recommendations:

- 1) Provide a several day lag between large and small probe release to implement targeting, tracking, testing, and probe release
- 2) Develop additional software to implement small probe release
- 3) Use predetection recording to handle the telemetry and doppler data from the four probes

The following paragraphs highlight the constraints imposed by the spacecraft and the ground systems, mission description, sequences, and correlates the sequences with the constraints.

Constraints

Spacecraft

The major operational constraints imposed by spacecraft design are:

- 1) Spacecraft's spin axis must be ≥ 10 deg from the sunline due to the sun sensor look angles
- 2) Period of time the spacecraft spin axis attitude deviates from the nominal 90 deg with respect to the sunline is limited by thermal considerations and battery size
- 3) Maximum data rate is limited by rf power, antenna gain, and communications distance
- 4) Spin rate must lie between 5 and 100 rpm due to dynamic control considerations
- 5) Probe downlink frequency uncertainties exist due to oscillator inaccuracy of one part in 10^6 and doppler shift whose predictability is limited by tracking accuracy and atmosphere modeling

TABLE 4-2. POST-SEPARATION SEQUENCE

| Time | Event |
|------------------------------------|---|
| L + 0 | Launch |
| L + 35.9 ^m | Separation |
| L + 37.9 ^m | ACE-ON |
| | Despin to 60 ± 10 rpm |
| L + 38.5 ^m | Despin complete |
| L + 38.6 ^m | PCU-ON |
| | Deploy booms |
| | PCU-OFF |
| L + 40.6 ^m | Deployment complete |
| L + 57.9 ^m | Canberra visibility |
| L + 59.9 ^m | Begin attitude and spin rate determination |
| L + 70 ^m | Complete cursory attitude and spin rate analysis, load reorientation data |
| L + 77.5 ^m | Execute precession |
| L + 80.8 ^m | Precession complete |
| | Begin attitude and spin rate analysis and touchup |
| L + 3 ^h 20 ^m | Complete attitude and spin rate analysis and touchup |
| | Transmitter to bicone data rate, 2048 bps |

Ground System

Constraints imposed by the DSN are delineated in JPL Document 810-5, DSN Standard Practice - DSN Flight Project Interface Design Handbook.

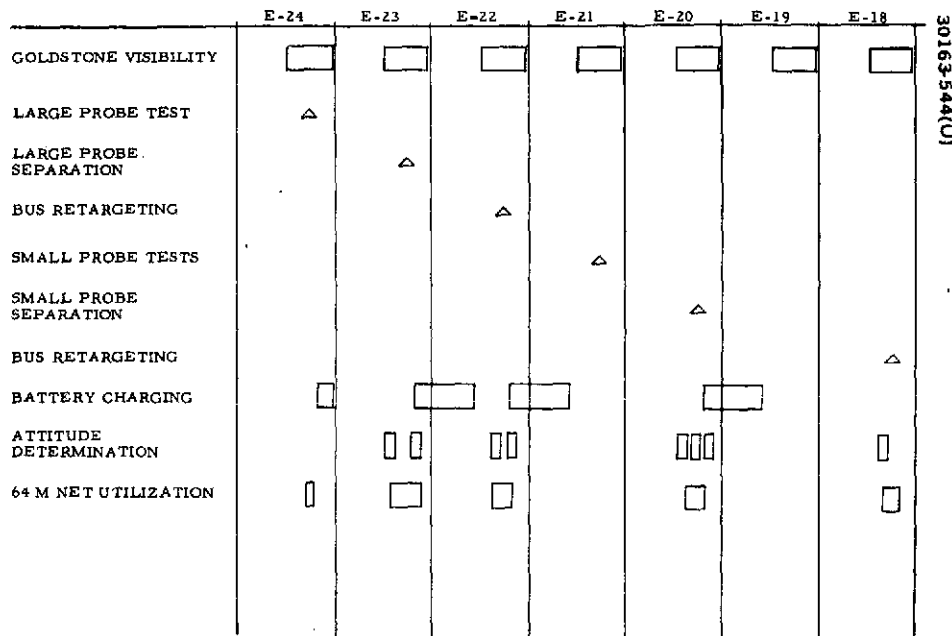
The ground system requires a finite amount of time to process data, generate command sequences, verify, etc. It is also subject to failures which are assumed to disable the ground system no more than 2 percent of the time, and for no more than 0.5 h duration each. All critical maneuvers and probe release events were timed to occur during the Goldstone view period to take advantage of the most reliable ground communications network. In addition, probe and bus entry were timed to occur during the Goldstone/Madrid visibility overlap to maximize the probability of successful entry data reception. The 64 m net would have been employed only during critical mission phases and as required in anomalous situations.

Mission Description

The mission consisted of launch, transit phase, four midcourse maneuvers, release of the four probes, a bus retargeting maneuver, a fifth midcourse, and encounter of the probes and the bus. Launch operations were discussed previously. The first two midcourses would be accomplished by orienting the spacecraft to the attitude that minimized execution errors or fuel consumption. The ΔV thrusting would be performed and then the spacecraft reoriented back to the cruise attitude with spin axis normal to the ecliptic. The third, fourth and fifth midcourses, due to their small magnitudes, would utilize thrust vectoring to eliminate spacecraft reorientation. Thrusting directions and magnitude were to be determined by taking tracking data during the transit phase and analyzing it using iterative trajectory analysis and prediction software on the ground. Firing durations would be determined from maneuver requirements and thruster performance predictions also obtained using ground software. This software would be run almost continuously during the 24 h prior to any maneuver to assure utilization of the latest, most accurate data. Shortly, prior to the anticipated maneuver, the maneuver parameters would be converted to a detailed sequence of events which dictated ground and spacecraft operations necessary to accomplish this maneuver.

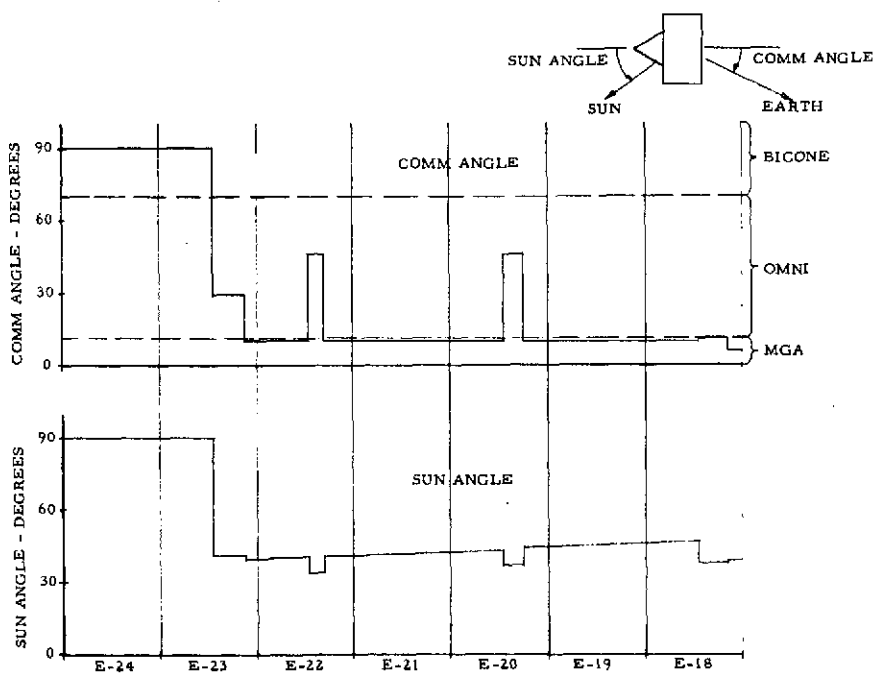
Between maneuvers, (transit or cruise) periods of several days duration existed during which cruise science and engineering data would be received and processed continuously.

The large probe would be released before the small probe in order to isolate the large probe release event from the possibility of failure of one or two small probes to release. Originally the probe release and targeting sequences were planned for a single Goldstone view period. These sequences were expanded over several days to allow for operational flexibility in each targeting or probe release sequence, thus allowing time for additional attempts at events should the first attempt fail. Also, since the probes do not transmit during the period from release to entry, their trajectories would be estimated from bus tracking data after the bus is targeted for release.



30163-544(U)

FIGURE 4-1. PROBE RELEASE SEQUENCE



30163-545(U)

FIGURE 4-2. MULTIPROBE SUN AND COMMUNICATION ANGLE HISTORIES

For this reason, tracking periods of two days would be allowed immediately before and after small probe release during which no maneuvers were to be performed other than the small precessions necessary to orient the bus to and from the release attitude.

Immediately following small probe release, the small probes would all transmit data for 15 min to allow calibration of their magnetometers against the bus magnetometer. This required the DSN to be capable of receiving the four bus and small probe downlinks simultaneously. At entry, five downlinks would be received. Entry operations are discussed under DSN interfaces (ss subsection 4.5).

Detailed Sequences

The operations of targeting and releasing the large and small probes were to be performed during the period from E-24 days to E-18 days (E-0=entry). The necessary sequence of operations is illustrated in Figure 4-1. Figure 4-2 presents sun and communication angles for this sequence.

Large Probe Release. Twenty-three days before encounter large probe release was to occur along with attitude and spin change operations illustrated in Figure 4-3. Initially, the spacecraft would be spinning at 60 rpm with the spin axis oriented normal to the ecliptic and star sensors viewing the southern celestial hemisphere. When Goldstone visibility began at about 1240 GMT, the 64 m antenna would acquire the probe bus downlink and the illustrated sequence would begin. Telemetry rf would be switched to the appropriate omni antenna after the data rate was reduced to 8 bps. After telemetry performance verification the spacecraft would be despun to 30 rpm, precessed ≈ 120 deg to the probe release attitude, and further despun to 15 rpm, the spin rate required for large probe entry. Attitude and spin rate would then be determined and trimmed, and the large probe timer set, verified, and initiated. The large probe would then be released and commence a 15 min rf and subsystem test. After completion of the test the bus would be spun up to ≈ 71 rpm and precessed to an attitude nearly parallel to the ecliptic with a communication angle ≤ 10 deg to allow use of the medium gain horn antenna, and a 40 deg sun angle. Spacecraft power would then be switched to the horn antenna, and the power reduced to 1 W and the data rate increased to 16 bps. The 26 m net can support this mode and the dc power margin is sufficient to allow battery charging. Battery capacity, assuming 40 percent depth of discharge, constrained to 8.2 h the time period between the first precession and the last. The sequence is estimated to require 4.7 h if no anomalous events occurred.

Small Probe Targeting. Twenty-two days before encounter the bus would be targeted to give the desired small probe entry locations using the sequence illustrated in Figure 4-4. Battery capacity constrained to 3.5 h the time period between the first and last precessions. The sequence is estimated to nominally require 3.0 h.

Small Probe Release. Small probe release was chosen to occur at 20 days before entry as a compromise between excessive probe coast time and

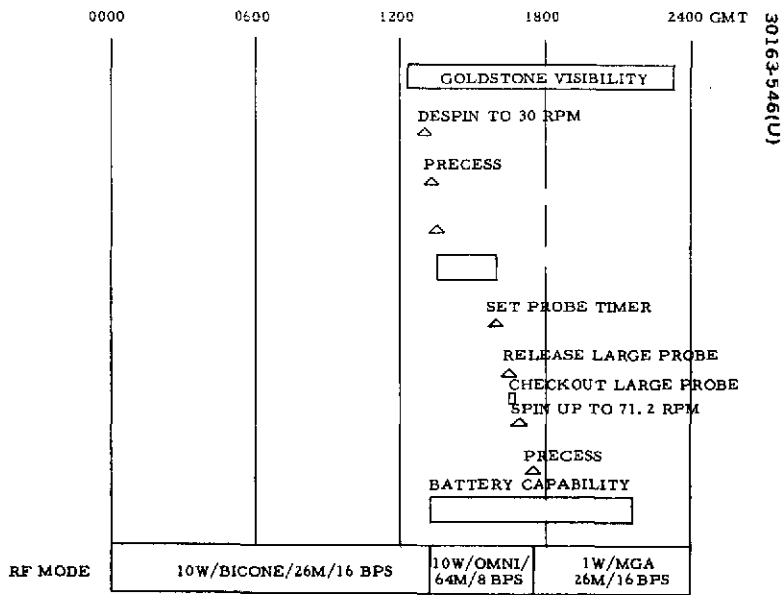


FIGURE 4-3. LARGE PROBE RELEASE SEQUENCE – DATE = E-23 DAYS (24 APRIL 1977)

excessive targeting ΔV and spin rate requirements. The sequence of events is illustrated in Figure 4-5. The probe timers would be set, verified, and initiated following Goldstone acquisition and before the first precession to reduce the time at which the bus must be at the release attitude. The bus would then be precessed, the attitude and spin rate determined and trimmed, and the small probes released. Immediately upon release the small probes would perform a 15 min rf and subsystem checkout after which the bus would be precessed back to the attitude necessary for battery charging. Battery capacity constrained to 4.7 h the time period between precessions. This period is estimated to be nominally 3.0 h. During the small probe checkout period it would be necessary to receive the bus and small probe downlinks simultaneously.

Probe Bus Retargeting. Eighteen days before entry the bus would be targeted to the required entry point and retarded in velocity such that it entered the Venusian atmosphere after the last probe landed. The sequence is illustrated in Figure 4-6. Sun and communication angles were to be such that the battery would be required only for transient loads, so the maneuver was not time constrained by battery capacity.

Probe and Bus Entry. Probe and bus entries were to occur 122 to 131 days after launch. Figure 4-7 presents entry timing relationships. Bus entry was timed to occur after final probe impact in order to simplify data reception activities and also to implement the DLBI experiment. Bus science would be turned on approximately 2.5 h before bus entry to relieve the ground system of any command operations during the critical entry phase. Entry was timed to occur during Goldstone/Madrid overlap to obtain ground station redundancy, and to relieve Goldstone of having to transmit during the entry phase thereby improving the downlink margin by a few dB. Since five downlinks would exist simultaneously during a large portion of the entry period, it would have been necessary to provide either a large number of receivers and operators, or relatively few receivers and necessary predetection recording equipment.

Conclusions

The sequence of events described in the previous paragraphs provides for:

- 1) Spin axis position is greater than 10 deg from the sunline during the mission
- 2) Thermal problems are not created because spin axis is maintained at 90 deg with respect to the sun for most of the mission
- 3) Sequences and data storage have been designed to be compatible with the spacecraft data rate capability
- 4) The spin rate lies between the required 5 and 100 rpm
- 5) Mission operations are compatible with the downlink frequency uncertainties

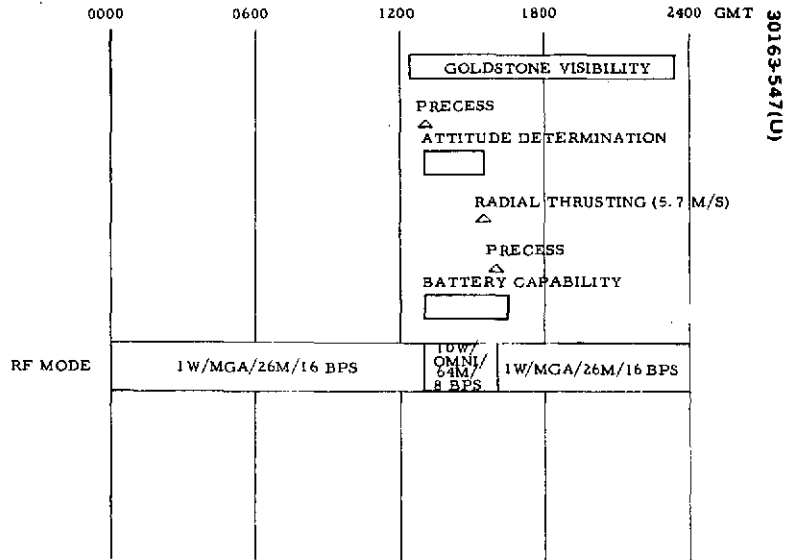


FIGURE 4-4. BUS TARGETING SEQUENCE PRIOR TO SMALL PROBE RELEASE – DATE = E-22 DAYS (23 APRIL 1977)

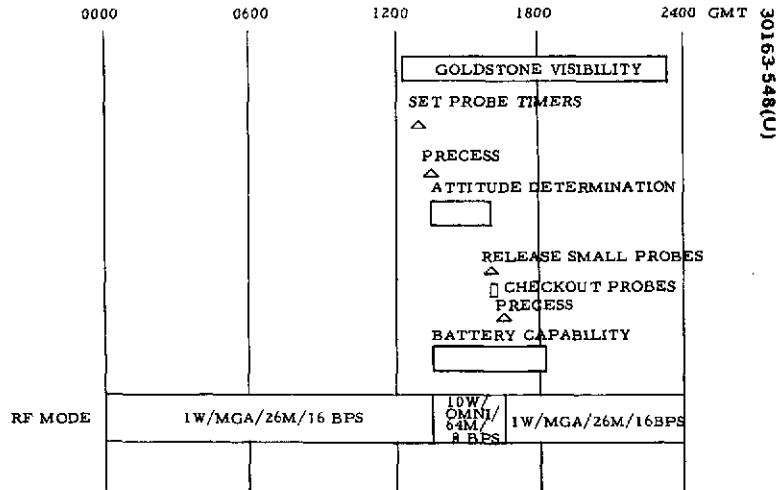


FIGURE 4-5. SMALL PROBE RELEASE SEQUENCE – DATE = E-20 DAYS (21 APRIL 1977)

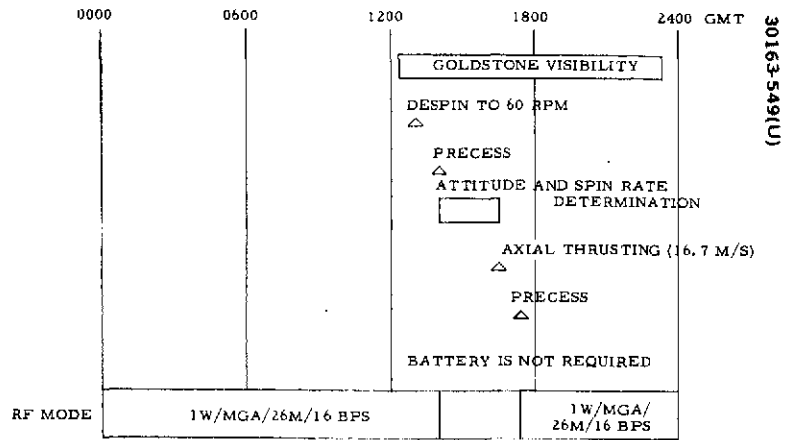


FIGURE 4-6. BUS RETARDATION MANEUVER SEQUENCE - DATE = E-18 DAYS (19 APRIL 1977)

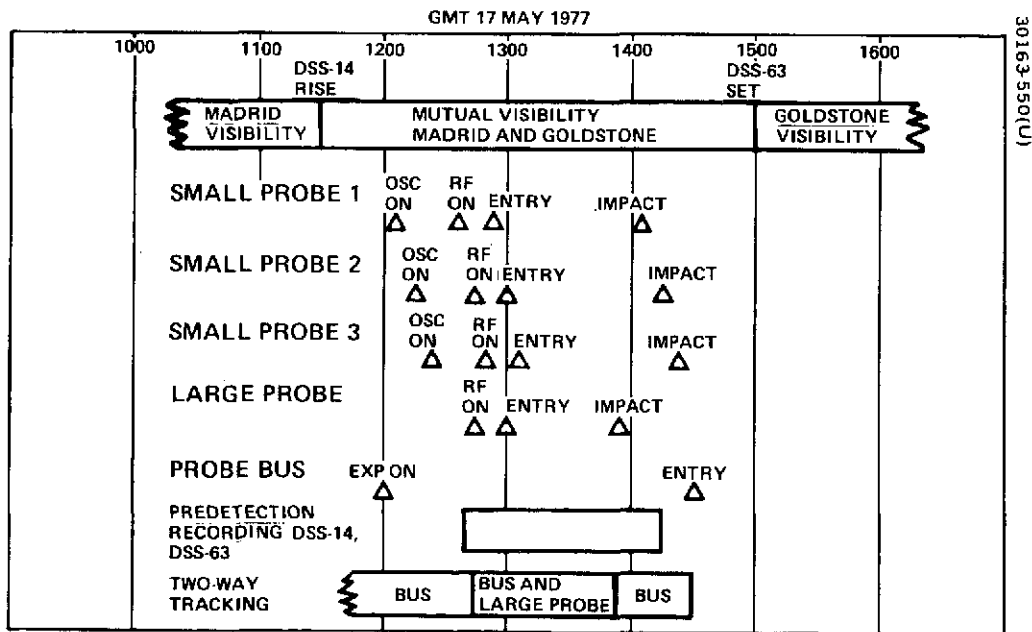


FIGURE 4-7. PROBE AND BUS ENTRY SEQUENCE

6) Compatibility with all ground system constraints

The major recommendations as a result of the multiprobe mission operations analysis are:

- 1) The necessary targeting, tracking, testing and release operations involved in releasing the large and small probes should be spread over a period of several days. Probe release and targeting operations in the midterm baseline were to be accomplished all in one day with in-flight probe tests 1 day before separation and bus targeting 2 days after. It was discovered in the mission operation investigation that insufficient time had been allocated for attitude determinations and trims, or for a contingency plan. In addition, a tracking period immediately before small probe release would improve estimation of small probe trajectories and allow for a targeting trim if it were discovered that the small probe targeting maneuver resulted in a large error. The probe release sequence was therefore expanded over the 7 day period from E-24 to E-18 as illustrated in Figure 4-1. This results in an operationally flexible sequence which allows adequate time for attitude and orbit determinations, and also allows for a contingency plan.
- 2) The technique of spinning the probe bus to impact a lateral ΔV to the small probes is not handled in existing orbit determination software. It will therefore be necessary to supplement existing software with this capability. Other existing software was found to be directly applicable to the Pioneer Venus missions.
- 3) Predetection recording was found to be a viable approach to the task of receiving the four probe downlinks with their associated doppler profiles. It was found that predetection recording was the optimum approach from the standpoint of operational simplicity, safety of reception of short term data, and minimization of DSS impact.

4.4 ORBITER MISSION OPERATIONS

The Thor/Delta orbiter mission operations, like the multiprobe operations, are constrained by the existing ground systems, basic spacecraft constraints created by equipment limitations, and the need to provide a manageable set of sequences and operations. The proposed Thor/Delta mission phases and sequences are compatible with the DSN, ground personnel function and spacecraft design.

The orbiter mission operations studies highlighted two critical points:

- 1) The orbit insertion geometry causes a potential thermal problem.
- 2) Adequate data storage capability should be provided to store all of the radar altimeter data for each pass to simplify data retrieval on the ground during occultations.

The following paragraphs discuss the spacecraft and ground system constraints on mission operations, describe the mission and sequences, and correlates the sequences with the constraints.

Constraints

Spacecraft

The major spacecraft operational constraints are:

- 1) Operational functions must be compatible with a low data rate (8 bps) during the first two TCMs and orbit insertion. Low data rate capability occurs because the spacecraft attitude must be changed during these phases requiring use of the omni antennas rather than the mechanical despun high gain antenna.
- 2) The spacecraft spin axis must be no closer than 10 deg to the sun line because of the sun sensor field of view limit.
- 3) The period of time the spacecraft spin axis attitude deviates from the normal to the ecliptic plane is limited by thermal considerations, and at orbit insertion is 2 h.
- 4) Data storage is required and is sized by the need to store data during occultations. Data storage must be operable at end of life because the downlink data is limited to 64 bps because of the increased communication distance.

Ground System

All mission critical events were to be timed to occur during Goldstone visibility, as the ground communications link through Goldstone is probably the most reliable in the DSN. The entire mission with the exception of the

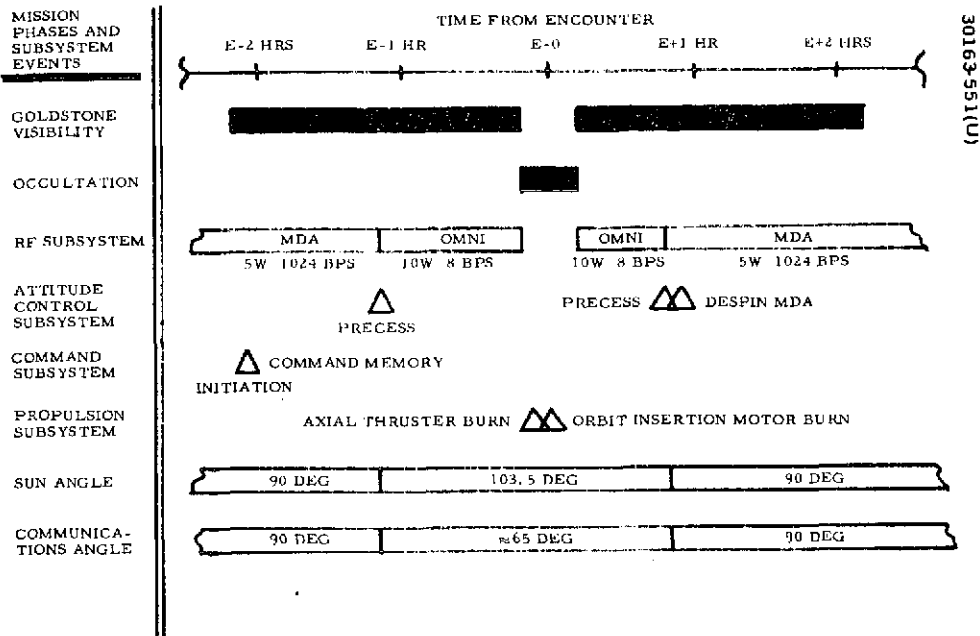


FIGURE 4-8. ORBIT INSERTION EVENT SEQUENCE

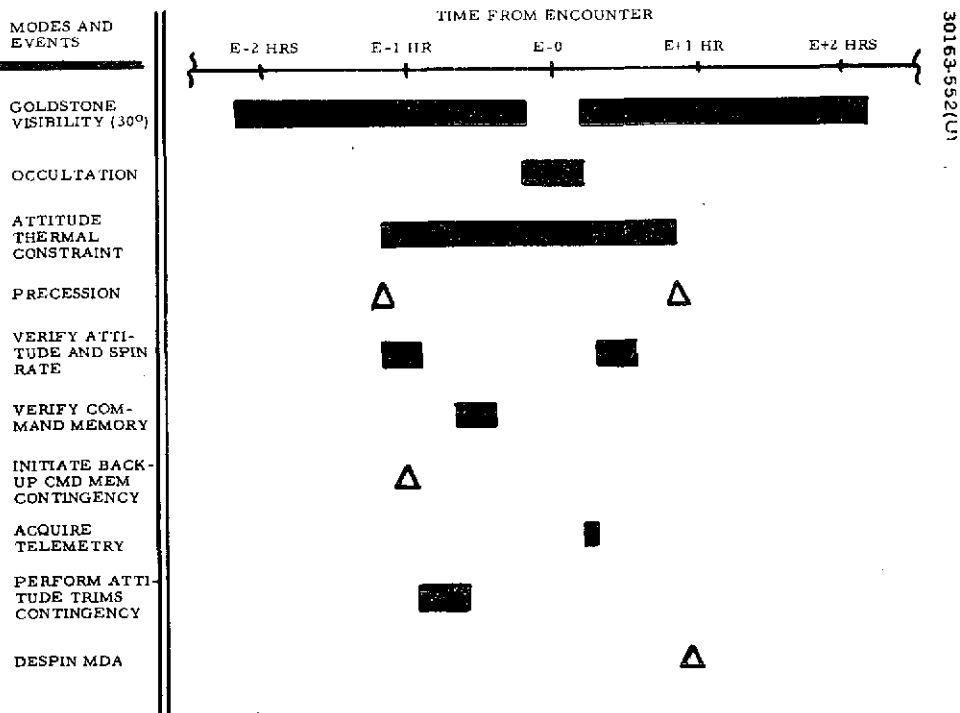


FIGURE 4-9. ORBIT INSERTION OPERATIONS SEQUENCE

four TCMs and orbit insertion phase required only the 26 m net. The aforementioned exceptions required the 64 m net. Mission sequences were designed to accommodate possible DSN outages of 0.5 h. Orbital operations were designed to occur during an 8 h Goldstone view period in order to centralize ground operations. Further constraints imposed by the DSN are stated in JPL Specification 810-5.

Mission Description

The Thor/Delta orbiter mission is comprised of four phases: launch, cruise, orbit insertion, and orbit. Launch operations were discussed previously.

The cruise phase of the mission lasts approximately 185 days. Cruise science required low data rates and consisted of: magnetometer, ultraviolet spectrometer, and solar wind probe data. These instruments would be on continuously, except during the four planned midcourse maneuvers.

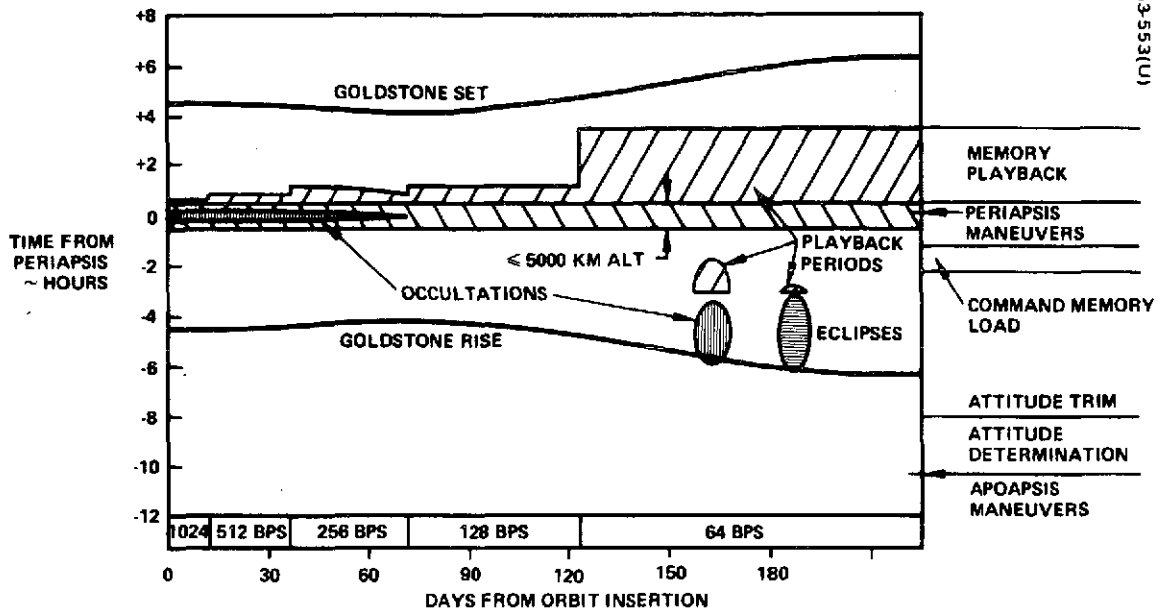
These midcourse maneuvers (TCMs) were to have been scheduled for launch plus 5, 20 and 50 days, with the fourth one scheduled for 20 days before orbit insertion. The first two TCMs were to require spacecraft reorientation for the relatively large ΔV maneuver in order to minimize propellant consumption and execution error. ΔV maneuvers for TCMs 3 and 4 would be accomplished by thrust vectoring. All four TCMs were scheduled to occur within Goldstone visibility. For telemetry data recovery, the 64 m net could be required when the spacecraft attitude required use of the omni antenna. Continuous tracking would be required only for a period of approximately 4 days around each TCM.

The orbit insertion phase included preparation activities before insertion, and the first orbit. Spacecraft tracking and telemetry were to be gathered continuously from 1 week prior to insertion. Due to the interplanetary geometry at the time of insertion, the orbit insertion motor was to be fired while the spacecraft was occulted from earth. The orbit insertion attitude furthermore imposed thermal and communications constraints on the spacecraft which are discussed in a subsequent section. Insertion was planned to occur at the midpoint of the Goldstone view period, in order that the science activities at periapsis may occur over the DSIF with the most reliable ground communications links.

Sequences

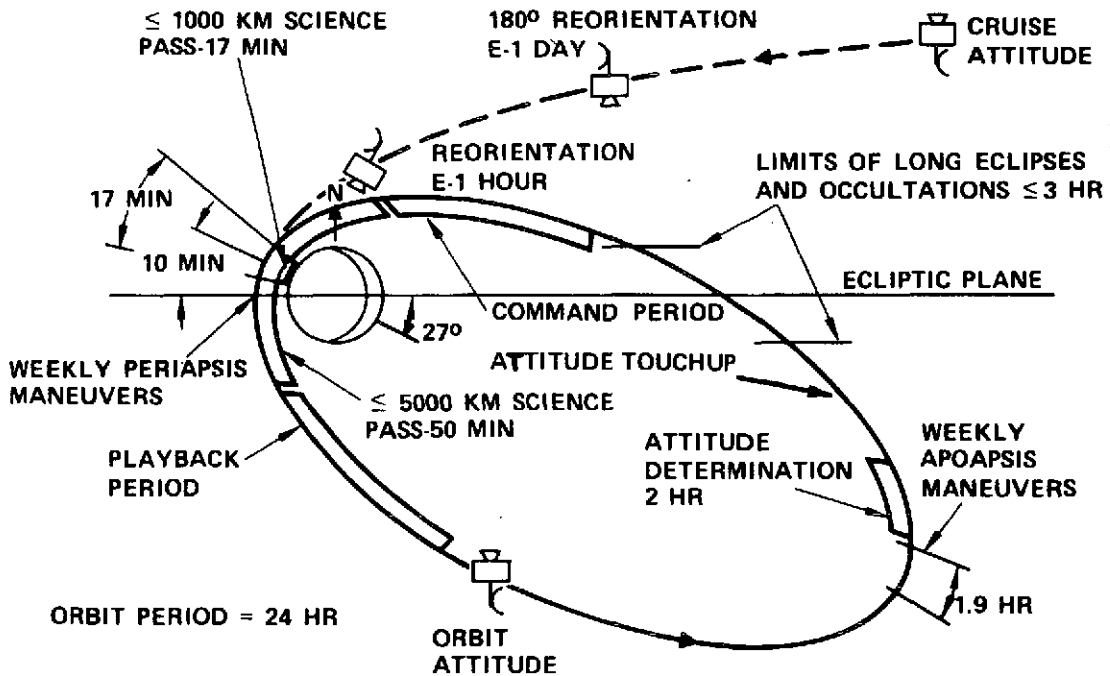
The orbit insertion phase of the mission included the 24 h prior to insertion and the first orbit of Venus. Both command memory modules were to be loaded with the insertion sequence commands during Goldstone visibility 24 h prior to insertion. A complete orbit insertion event sequence is shown in Figure 4-8, where events are broken down by subsystem. A detailed operations sequence for the 2 h before and 2 h past insertion is shown in Figure 4-9. The latter chart shows the impact of the 2 h thermal constraint. The backup command memory can be initiated 10 min before occultation in the event of failure of this prime unit. Time was allotted for generation of a backup reorientation or adjustment maneuver command sequence.

(5W TRANSMITTER/26M NET)



30163-553(U)

FIGURE 4-10. HISTORY OF ORBIT PHASE OPERATIONS



30163-554(U)

FIGURE 4-11. ORBITAL OPERATIONS

The orbit phase has a duration of 225 days to the designed end of life of the spacecraft. Interplanetary geometries again play an important role in the occurrence of occultations and eclipses. These orbit characteristics are further discussed. The Earth-Venus distance increases towards end of life, which decreases the downlink data rate capability to 64 bps. The quantity of science data required at periapsis sets the data storage requirements of the spacecraft.

Attitude determinations are of a "quick-look" type both before and after occultation.

The primary orbit characteristics are as follows:

| | | | |
|-------------|----------|----------------------------|---|
| 2 Dec 1978 | 1719 GMT | E - 0 | Orbit insertion |
| | | E + 1 day | Adjust orbit period to 24 h (1st periapsis) |
| | | E + 1.5 days | Lower periapsis to "safe" altitude (2nd apoapsis) |
| | | E + 0 to E + 66 days | Occultations (22 min maximum) |
| 22 Dec 1978 | | E + 20 days | Periapsis crosses evening terminator |
| | | E + 26 to E + 116 days | Eclipses (24 min maximum) |
| 13 Apr 1979 | | E + 132.5 days | Periapsis crosses morning terminator |
| | | E + 157 to E + 168 days | Occultations (164 min maximum) |
| | | E + 183 to E + 191 days | Eclipses (178 min maximum) |
| 15 Jul 1979 | | E + 225 days | End of mission |

Figure 4-10 depicts the orbit operations for the entire mission, while Figure 4-11 highlights the details of a typical orbit.

The operational periods of the science experiments are centered about periapsis. Figure 4-12 shows the operational periods superimposed over the altitude variation about periapsis.

Due to the heavy concentration of data sampling around periapsis most of the data was to be stored and nominally played back after periapsis. During different phases of the mission different amounts of data required storage. The orbit-life data storage operations history is shown in Figure 4-13. The radar altimeter data would always be stored in its entirety to minimize ground operations generation of data records.

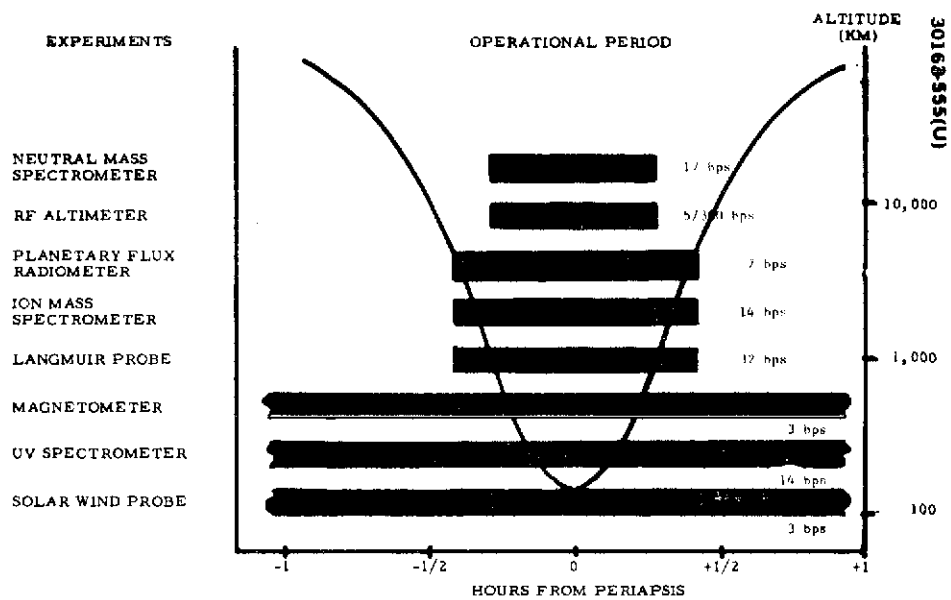


FIGURE 4-12. ORBITER SCIENCE OPERATIONS

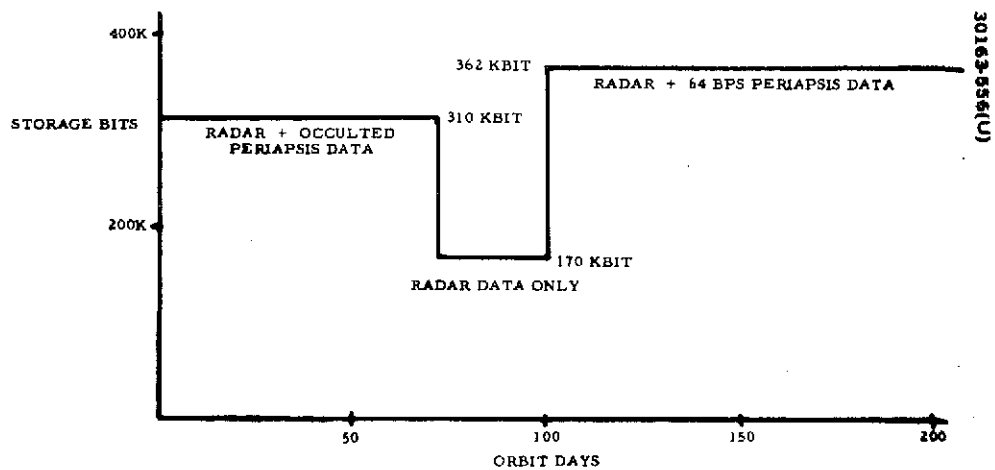


FIGURE 4-13. ORBITER DATA STORAGE OPERATIONS

The orbit phase of the mission can be broken into four typical types of orbits. These are:

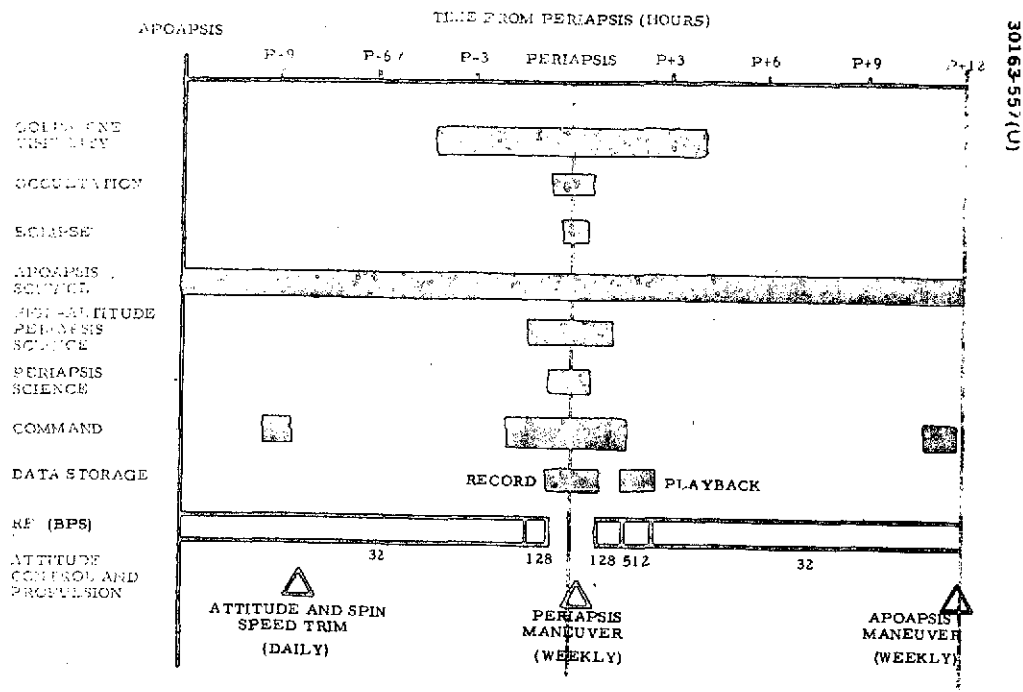
| <u>Typical Orbits</u> | <u>Occurrence in Mission (Days from Insertion)</u> | <u>26 m Net Data Rate, (bps)</u> |
|---|--|--|
| Short occultation and/or short eclipse | 0 to 72 | 1024 |
| | | 512 |
| | | 256 |
| Normal orbit (no occultation, no eclipse) | 72 to 125 | 128 |
| | 125 to 155 | 64 |
| | 167 to 185 195 to 225 | |
| Long occultation | 155 to 167 | 64 |
| Long eclipse | 185 to 193 | 64 |

Figures 4-14 through 4-17 depict orbital operations for short occultation, normal, long occultation, and long eclipse type orbits, respectively.

Conclusion

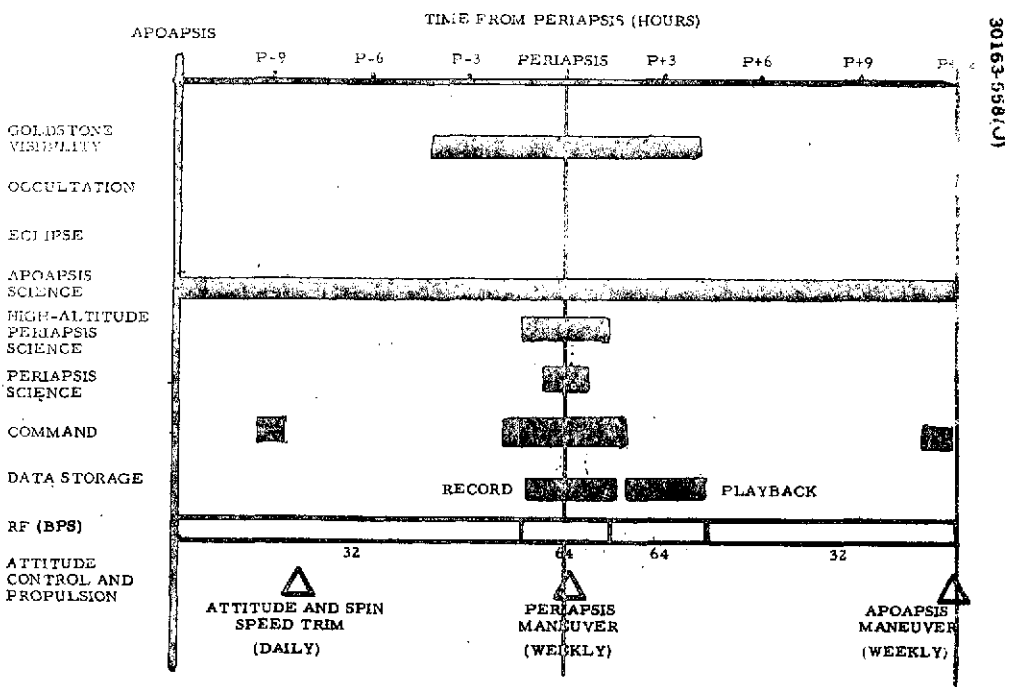
The sequence of events described in the previous paragraphs provides for:

- 1) Compatibility with low data rate during the TCMs and orbit insertion
- 2) Spacecraft spin axis is not less than 10 deg to the sunline
- 3) Thermal design for the Thor/Delta spacecraft did not provide the capability of 2 h with spin axis away from the normal position during orbit insertion. The design problem is solved in the Atlas/Centaur spacecraft by using equipment that can withstand transient elevated temperature and the inherent larger number of louvers. No further work was done on the Thor/Delta spacecraft after the Atlas/Centaur launch vehicle was selected as baseline.
- 4) Data storage capability is provided for storage of altimeter data with capability at end of orbiter life
- 5) The orbit insertion command is loaded into the memory 24 h prior to insertion



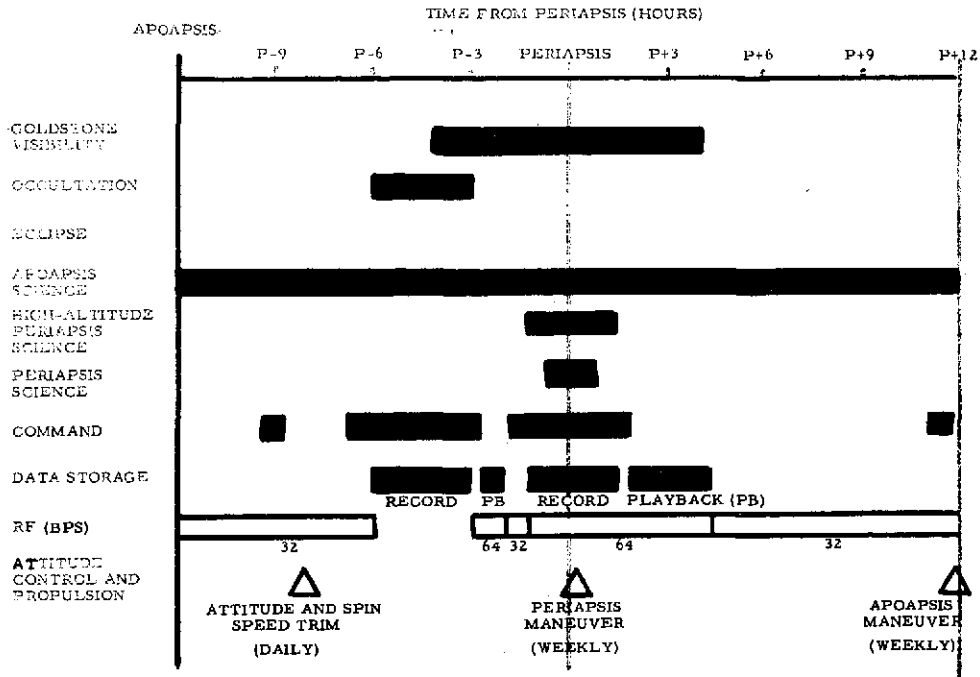
30163-557(U)

FIGURE 4-14. SHORT OCCULTATION AND/OR ECLIPSE ORBIT



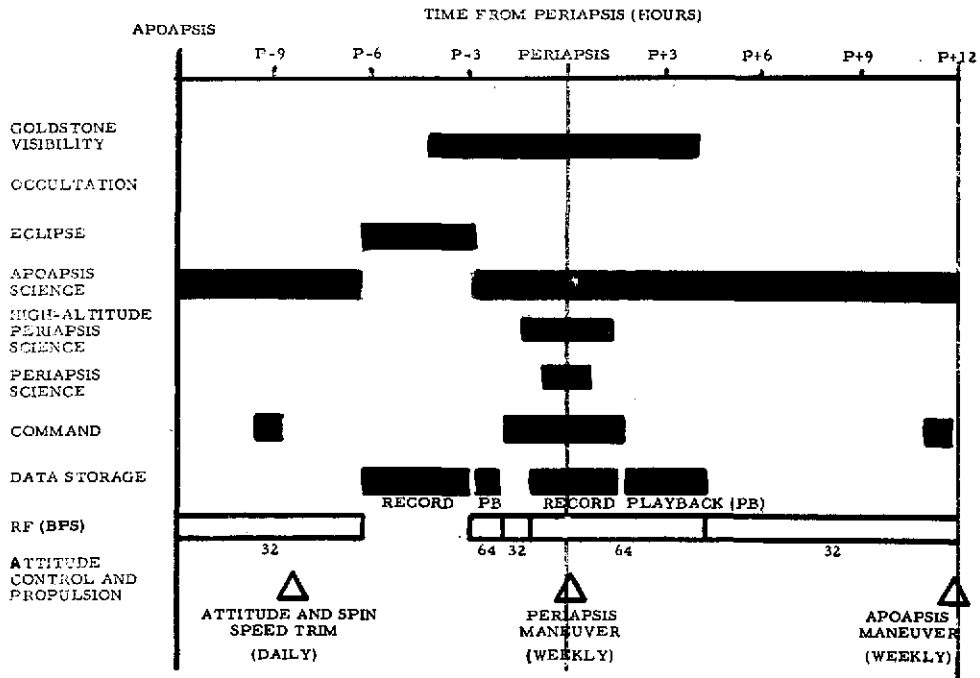
30163-558(U)

FIGURE 4-15. NORMAL ORBIT



30163-559(U)

FIGURE 4-16. LONG OCCULTATION ORBIT



30163-560(U)

FIGURE 4-17. LONG ECLIPSE ORBIT

TABLE 4-3. SPACECRAFT TRANSPONDER CHARACTERISTICS

| | |
|--------------------|------------------|
| Uplink frequency | 2110 to 2120 MHz |
| Turnaround ration | 240/221 |
| Downlink frequency | 2290 to 2300 MHz |
| Tracking range | ±125 kHz |
| Tracking rate | 400 Hz/sec |

TABLE 4-4. DSN SUPPORT REQUIREMENTS - COMMAND

| Function | Requirement | Capability |
|----------------------|-------------------|-------------------|
| Subcarrier frequency | 512 Hz | 100 Hz to 1.0 MHz |
| Type | Biphase PSK | PSK or FSK |
| Rate | 1, 2, 4 and 8 bps | 1 to 8 bps |
| Word length | 36 bits | < 72 bits |

4.5 GROUND DATA SYSTEM INTERFACES

The following subsection details the requirements for interfaces between the DSN and spacecraft. In all cases, the interfaces described are compatible with the multimission capability (MMC) of the DSN.

Tracking, Command and Telemetry

Angle and rf doppler tracking capability would have been required. Turnaround ranging would not be implemented. Spacecraft frequencies, signal levels, tracking ranges and rates, etc., as well as DSN pointing accuracies position readouts, resolution, etc., as quoted in JPL Document 810-5, DSN/Flight Project Interface Design Handbook, are within project requirements. Table 4-3 summarizes pertinent spacecraft characteristics.

Command uplinks will be required to the probe bus and orbiter spacecraft only. An rf carrier only uplink is required to the large probe for two-way doppler tracking. No uplinks are required for the small probes. Command system interfaces are fully compatible with the DSN MMC and are summarized in Table 4-4.

Characteristics of the telemetry interfaces are summarized in Table 4-5.

DSN Predetection Recording Plan

The existence of five simultaneous downlinks at probe and bus entry with their respective doppler profiles has warranted careful examination of the data recovery problem. DSN alternatives that satisfy entry communications requirements are as follows:

1) Downlink reception responsibilities may be split between Goldstone and Madrid using receivers in the closed loop mode with an operator at each receiver. A maximum of nine receivers would be required if one at each station is reserved for backup (three for the small probes, one for the large probe, one for the large probe in two-way lock, one for the large probe in one-way lock, one for the bus in two-way lock, one for the bus in one-way lock and two for backup). Large probe and bus uplinks would be generated by the station receiving the downlink. Simultaneous generation of two uplinks is within the capability of a single 64 m DSN station.

The drawbacks of this scheme are that large numbers of receivers and operators are required and no ground station redundancy exists. An advantage is that real time downlink visibility is possible. To obtain ground station redundancy, each ground station should receive all downlinks, resulting in the prohibitive need for eight receivers at each station.

2) Both stations could employ predetection recording of probe downlinks. This reduces receiver requirements to five per station with backup, but imposes the need for four wide bandwidth tape recorders per station. (This is two more than the present capability.) Predetection recording has

TABLE 4-5. DSN SUPPORT REQUIREMENTS - TELEMETRY

| Function | Requirement | Capability |
|----------------------|-------------|---------------------|
| Subcarrier frequency | | |
| Spacecraft | 32.768 kHz | >20 kHz |
| Large probe | ~20 kHz | >20 kHz |
| Small probe | ~20 kHz | >20 kHz |
| Bit rates (bps) | | |
| Spacecraft | 8 to 2048 | 6 to 2048 |
| Large probe | 184 and 276 | |
| Small probe | 16 | |
| Sequential decoding | | |
| Constraint length | 32 bits | 32 bits (maximum) |
| Rate | 0.5 | 0.5 |
| Tail | ≥20 bits | 8 to 48 bits |
| Frame length | ≤640 bits | 1200 bits (maximum) |

the disadvantage of degrading link performance by ≈ 2 dB and no real time visibility is possible of probe performance, etc., except as is possible using a "roving" receiver to sample probe downlinks individually. Advantages of this scheme are the small DSN impact, the possibility of ground station redundancy, and the possibility of post-entry signal processing which may be required due to the short term nature of the probe descent, and the unpredictability of atmosphere characteristics. This alternative is selected as baseline due to minimal DSN impact and higher probability of data recovery.

Figures 4-18 and 4-19 present functional block diagrams of the multiprobe mission entry phase ground configuration and receiving chain, respectively. The configuration shown employs the frequency plan of Figures 4-20 and 4-21 which accounts for spectral bandwidth, doppler shift (Figure 4-22), and engineering margin. Tape recorder characteristics are presented in Table 4-6.

A detailed description of the predetection recording scheme is included in Table 4-6.

TABLE 4-6. TAPE RECORDER CONSIDERATIONS

| | |
|---|---|
| Ampex 1400 tape recorder characteristics | |
| Frequency response: | 800 Hz to 1.5 MHz at 120 bps 800 Hz to 750 MHz at 60 bps |
| Seven tracks with 0.5 in. tape | |
| 7200 ft standard tape length per reel | |
| Pioneer Venus requirements: | 13 tracks at 500 kHz \pm 100 kHz each |
| Conclusions: | |
| Use two prime recorders/station at 60 bps plus two recorders to implement reel changing with no data loss | |
| Reel changes every 24 minutes/prime recorder | |

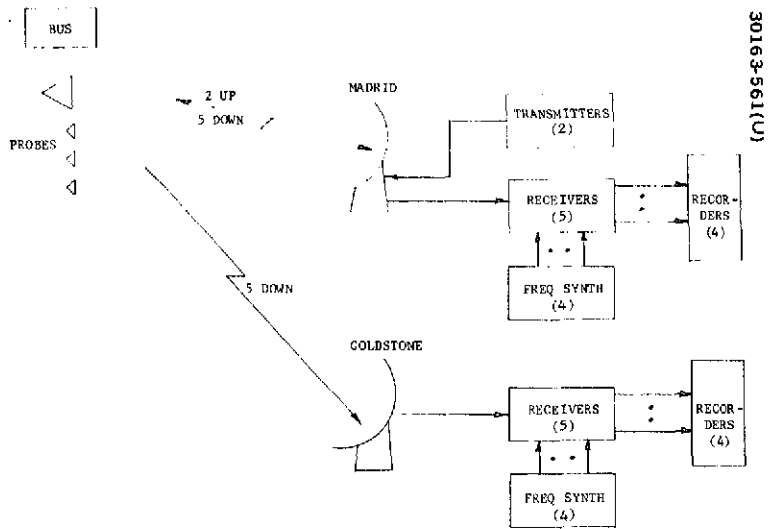


FIGURE 4-18. GROUND CONFIGURATION FOR ENCOUNTER

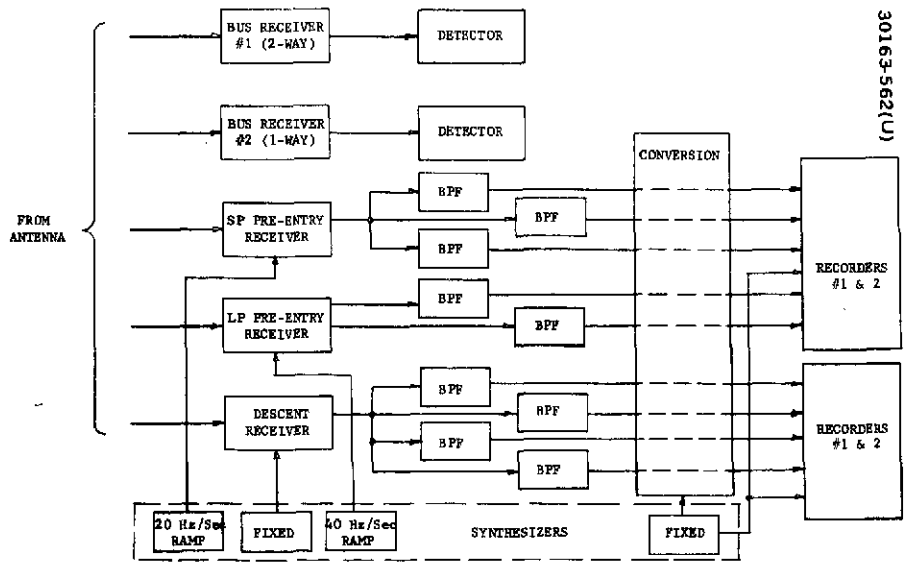
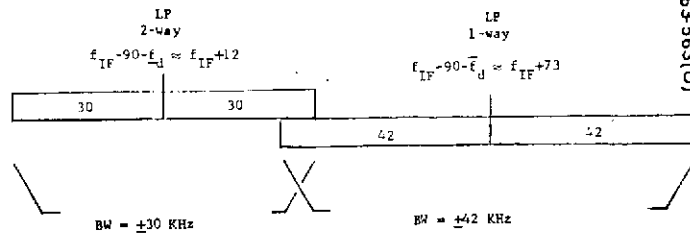


FIGURE 4-19. GROUND CONFIGURATION FOR RECEPTION OF DATA AT ENCOUNTER

• LARGE PROBE RECEIVER:



• SMALL PROBE RECEIVER:

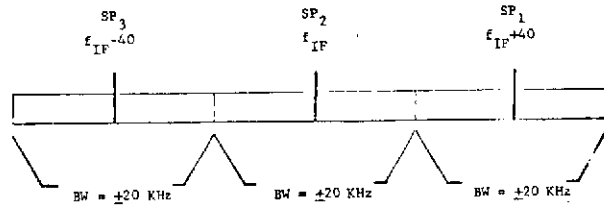


FIGURE 4-20. PROBES PREENTRY FREQUENCY PLAN

• ALL PROBES IN ONE RECEIVER:

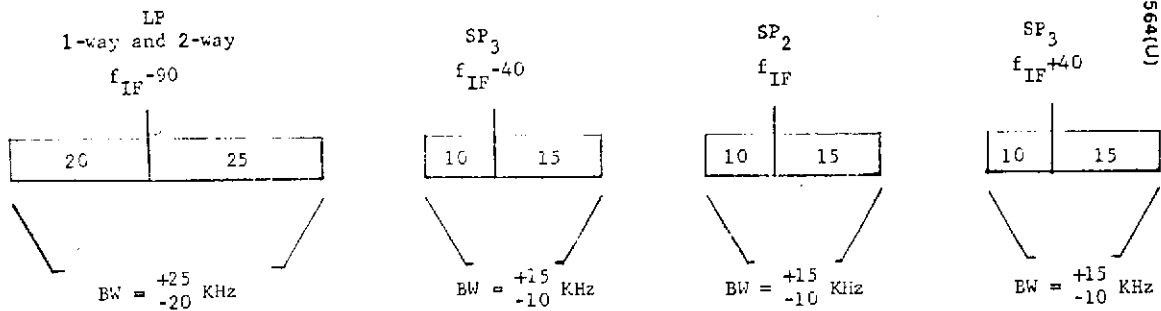


FIGURE 4-21. PROBES DESCENT FREQUENCY PLAN

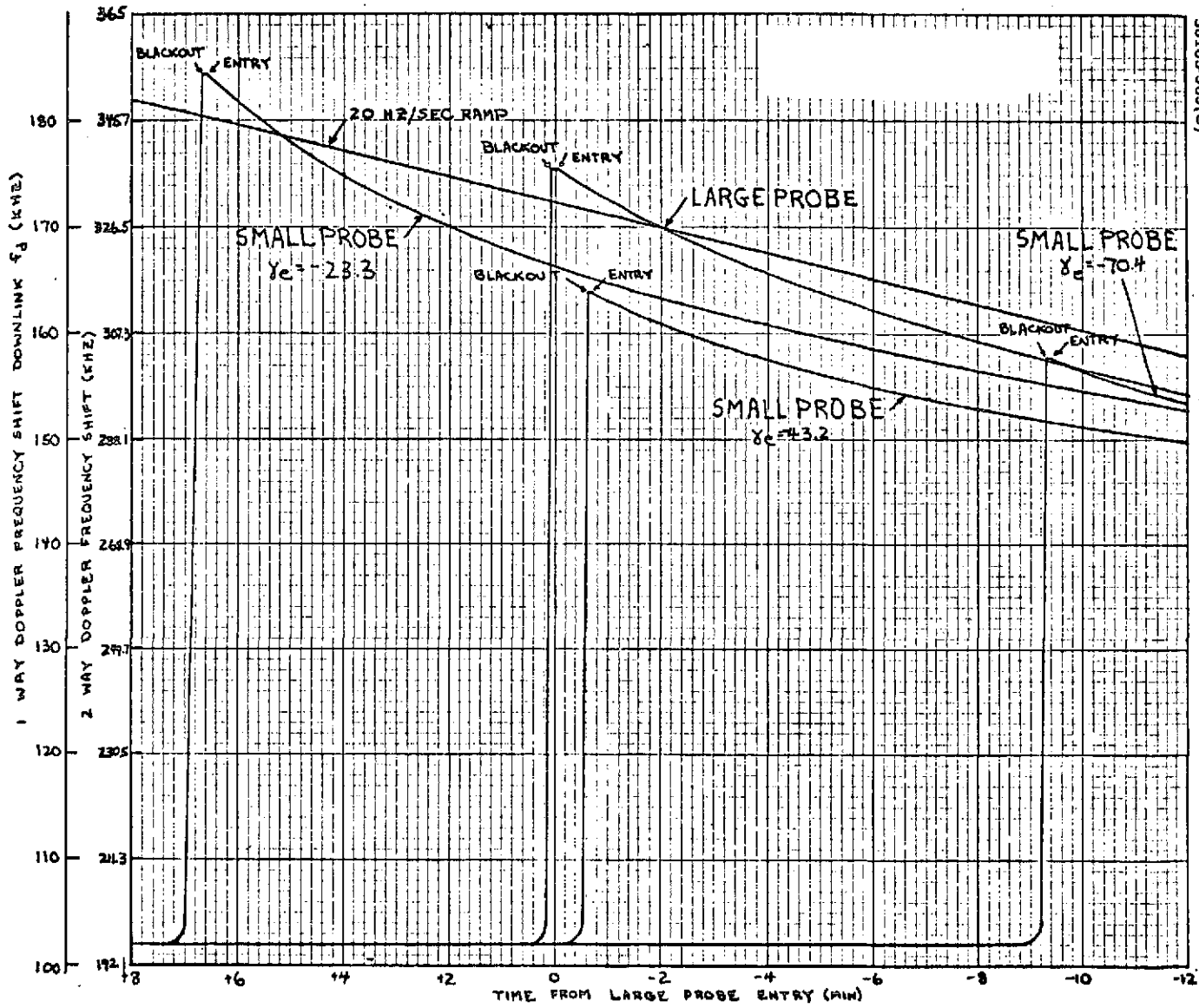


FIGURE 4-22. PROBES DOPPLER TIME HISTORY

Telemetry Data Recovery

Requirements for specialized hardware and software necessary to process the telemetry data to an uncoded PCM data stream have been examined. The spacecraft has been designed so that specialized equipment or software are not required. Equipment and routines presently in use on the Pioneer 10 and 11 programs are satisfactory. The probes, likewise, have been designed so that present Pioneer data processing techniques are applicable. A predetection recording scheme has been recommended for the multiprobe mission to maximize the probability of data capture during probe encounter and descent. It is recognized that the predetection recording and playback equipment is not presently used on the Pioneer program, but it has been used in the past on JPL Mariner programs and is therefore not considered as specialized. The following material describes the factors associated with data recovery, the ground equipment limitations, and the spacecraft and probe designs which maximize use of existing ground hardware and software and which minimize data loss.

Spacecraft and Probe Data Characteristics

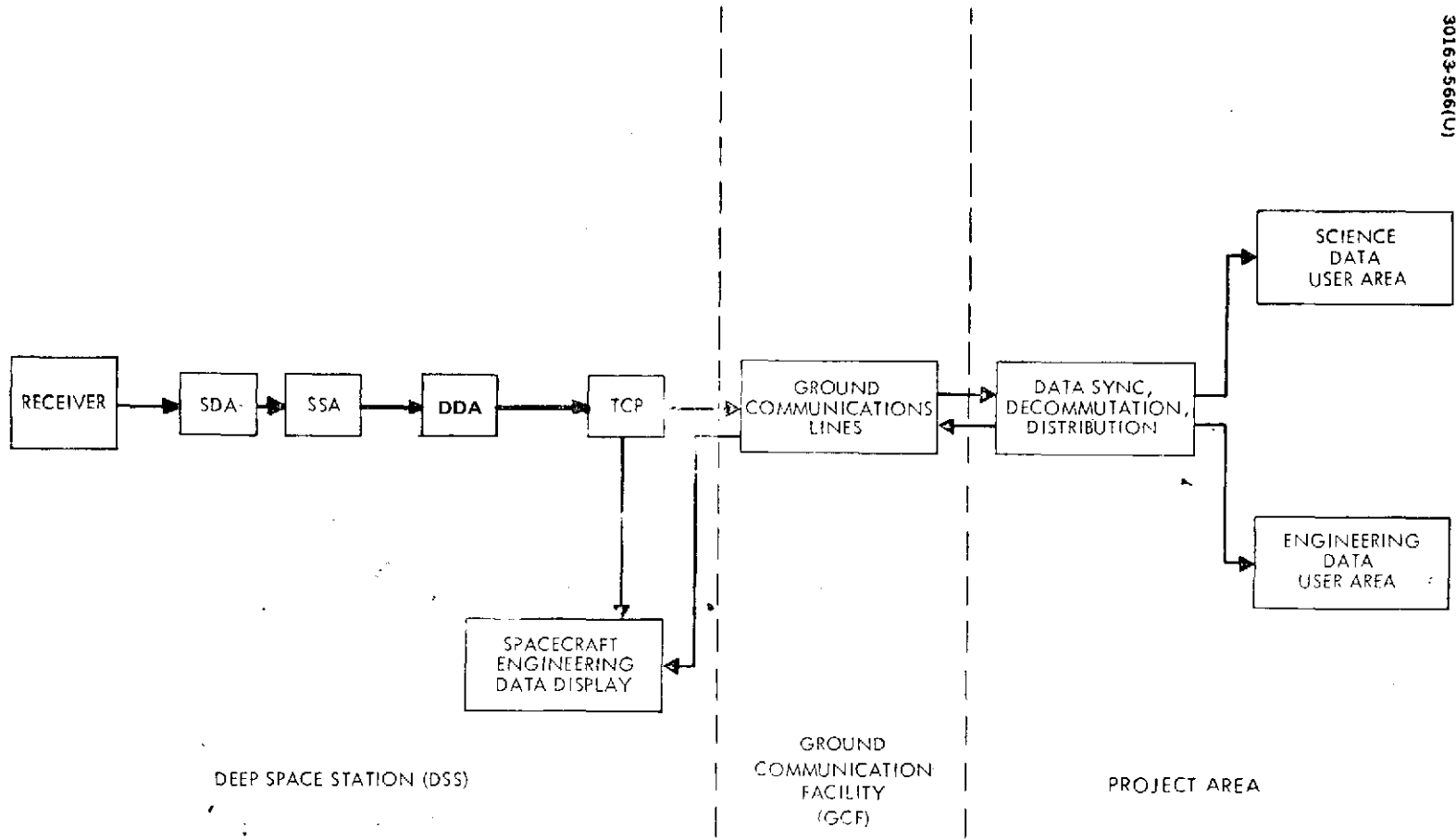
Data is obtained from the subsystems and scientific instruments and processed into a single binary PCM data stream. Analog data is converted into 10-bit digital words. Digital and discrete data are also formulated into 10-bit words.

The spectrum of the telemetry data is kept outside of the tracking loop bandwidth of the DSIF receiver by phase modulating a square-wave subcarrier with the composite PCM data. The data bit stream is modulo 2 added with the subcarrier before phase modulating the rf carrier. Data rates, and subcarrier frequencies are different for each of the Pioneer Venus vehicles and are summarized in Table 4-7. All are compatible with the DSN multiple-mission telemetry applications (MMT), and utilize DSIF channel D, which is described in JPL Document 810-5, DSN/Flight Project Interface Design Handbook.

Prior to subcarrier modulation, the data bit stream is convolutionally encoded. The convolutional encoder replaces each data bit generated with two parity bits which are designated P and \bar{Q} . The value of each parity bit is based upon the values of selected data bits previously generated in a 32-bit shift register. The code utilized is the familiar Pioneer nonsystematic quick-look code. Frame lengths for each of the Pioneer Venus vehicles are summarized in Table 4-7. The DSIF tail sequence requirement is accommodated by jam setting the 32-bit shift register to zero at the end of the last bit of the frame synchronization unit.

Ground Data Processing

Elements of the ground data recovery system are shown in Figure 4-23. The receiver provides a coherent rf reference to demodulate the received carrier while the subcarrier demodulator assembly (SDA) tracks the subcarrier and provides a coherent subcarrier reference to demodulate the



30163-566(U)

FIGURE 4-23. GROUND DATA RECOVERY SYSTEM

TABLE 4-7. DATA RATES AND SUBCARRIER FREQUENCIES

| | Bit Rates, bps | Subcarrier Frequencies, Hz | Frame Length, bits | Modulation |
|----------------|---|----------------------------------|--------------------------|------------|
| Probe bus | $8/111/2N/111/2048$ N an integer 3 N 11 | 32,768 | 256 | PCM/PSK/PM |
| Orbiter | $8/111/2N/111/2048$ N an integer 3 N 11 | 32.768 | 256 | PCM/PSK/PM |
| Large probe | 276/184 | 4416 | 650 | PCM/PSK/PM |
| Small probe | 16 | 512 | 450 | PCM/PSK/PM |

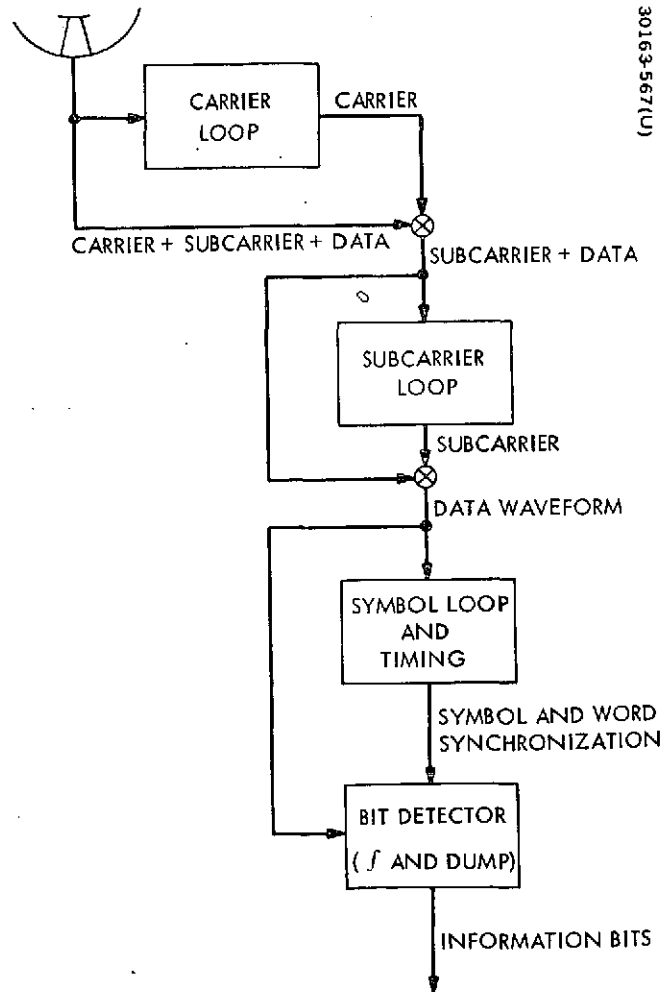


FIGURE 4-24. INFORMATION RECOVERY PROCESS

subcarrier and recover the binary telemetry waveform. The symbol synchronizer assembly (SSA) tracks the transitions in the binary telemetry waveform and provides symbol/bit timing for telemetry detection in the telemetry decoder. The data decoder assembly (DDA) generates branch and block synchronization from the incoming signals and decodes the convolutionally encoded data into a single bit stream. Figure 4-24 presents a schematic representation of the information recovery process.

After the data bits have been decoded, they are formatted and prepared for transmission to the Pioneer Mission Operations Center (PMOC) by the telemetry and command processor (TCP). Data transmission is via the ground communications facility (GCF) high speed data lines (HSDL). The XDS Σ -5 computer in the PMOC provides frame synchronization, data editing, and display.

Telemetry data cannot be output to the high-speed or wideband data lines until all the serial elements in the telemetry chain have acquired lock. The time required to achieve this condition depends upon the configuration used, the data rates, and the SNR of the rf carrier and data.

The total time of acquisition is the sum of the individual acquisition times for each element given in figures that follow.

Telemetry subcarrier acquisition time (theoretical value under strong signal conditions) is shown in Figures 4-25, 4-26, and 4-27, as a function of symbol rate for values of frequency uncertainty (or offset) of 0.5, 1.0, and 2.0 times the SDA two-sided, closed-loop noise bandwidth. Under noisy signal conditions, actual time for automatic acquisition can range from the value shown to 5 or 10 times that value.

The overall time required to acquire symbol synchronization with the SSA, followed by frame synchronization by the DDA plus correlation statistics for confirmation (0.99 probability) for sequential decoding of convolutional coded data is shown in Figure 4-28 as a function of symbol rate for signal-to-noise ratios $\geq +2.5$ dB. Curves are shown for frame lengths of 256 and 512 bits. Performance of the DDA shown in Figure 4-28 assumes that six frames are required for frame synchronization and confirmation.

Operational Considerations

In the preceding paragraphs, data characteristics of each of the vehicles and the ground system were discussed. It was indicated that the vehicle designs provided compatibility with the DSN MMT system. This compatibility provides real time data transmission capability from the DSIF to ARC and minimizes cost of recovery of ground recorded data.

Another data recovery factor has to do with data which is lost due to the ground system being out of lock. The out of lock situation is particularly important to the multiprobe mission where a maximum amount of data is sought in a short time interval between encounter and destruction. The

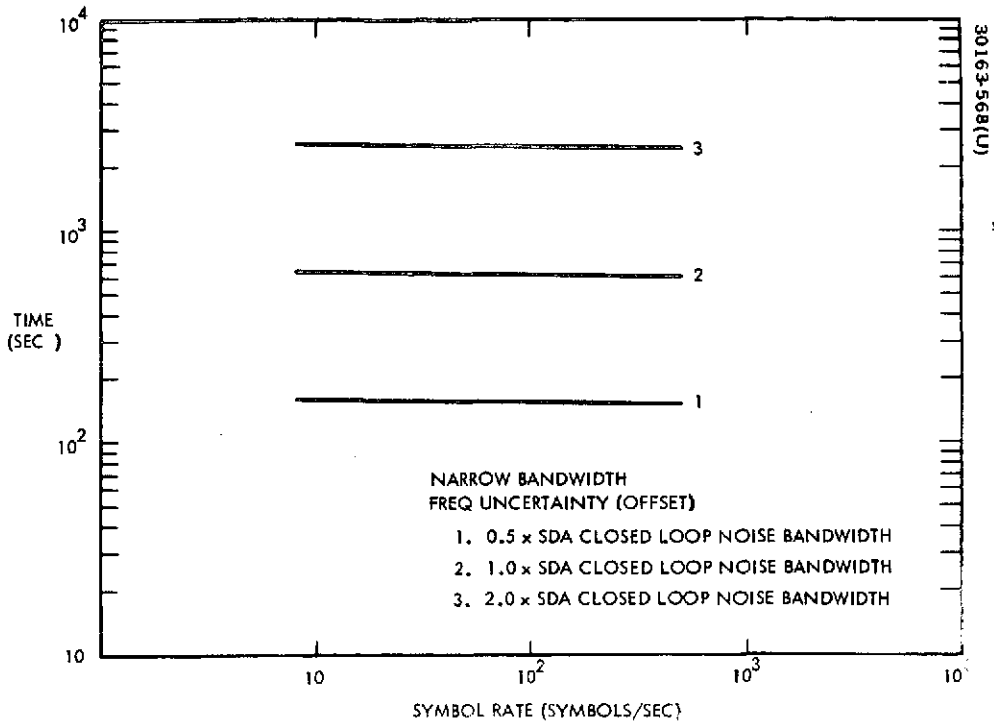


FIGURE 4-25. STRONG SIGNAL ACQUISITION TIME FOR SDA NARROW BANDWIDTH

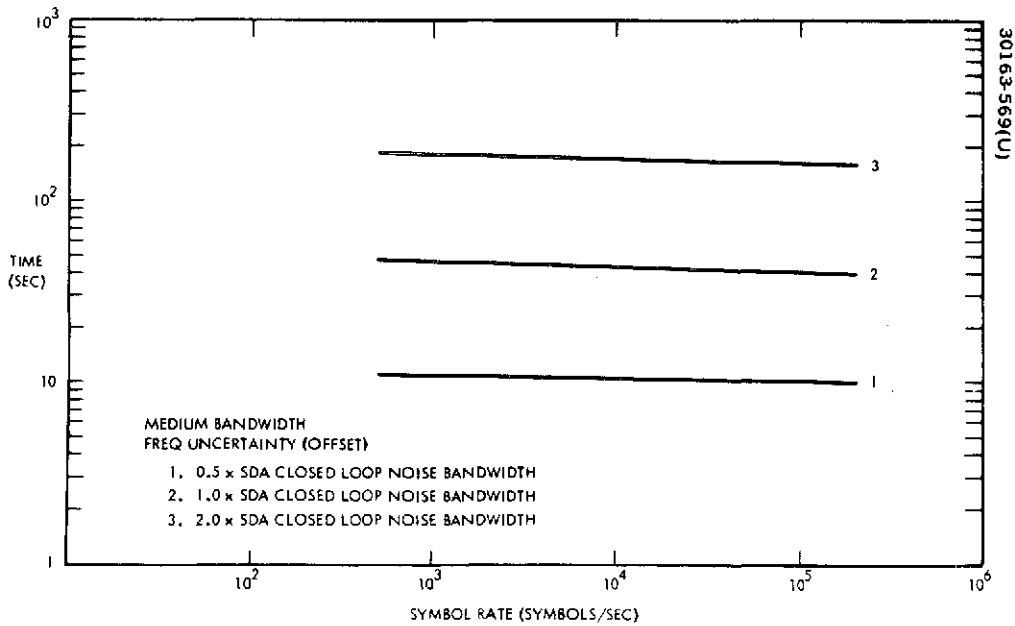


FIGURE 4-26. STRONG SIGNAL ACQUISITION TIME FOR SDA MEDIUM BANDWIDTH

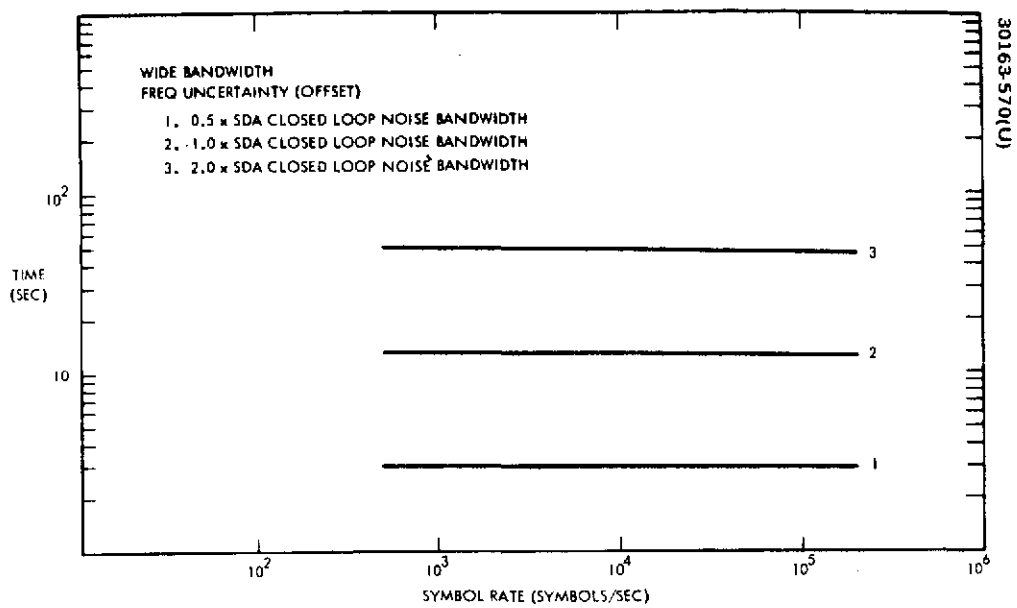


FIGURE 4-27. STRONG SIGNAL ACQUISITION TIME FOR SDA WIDE BANDWIDTH

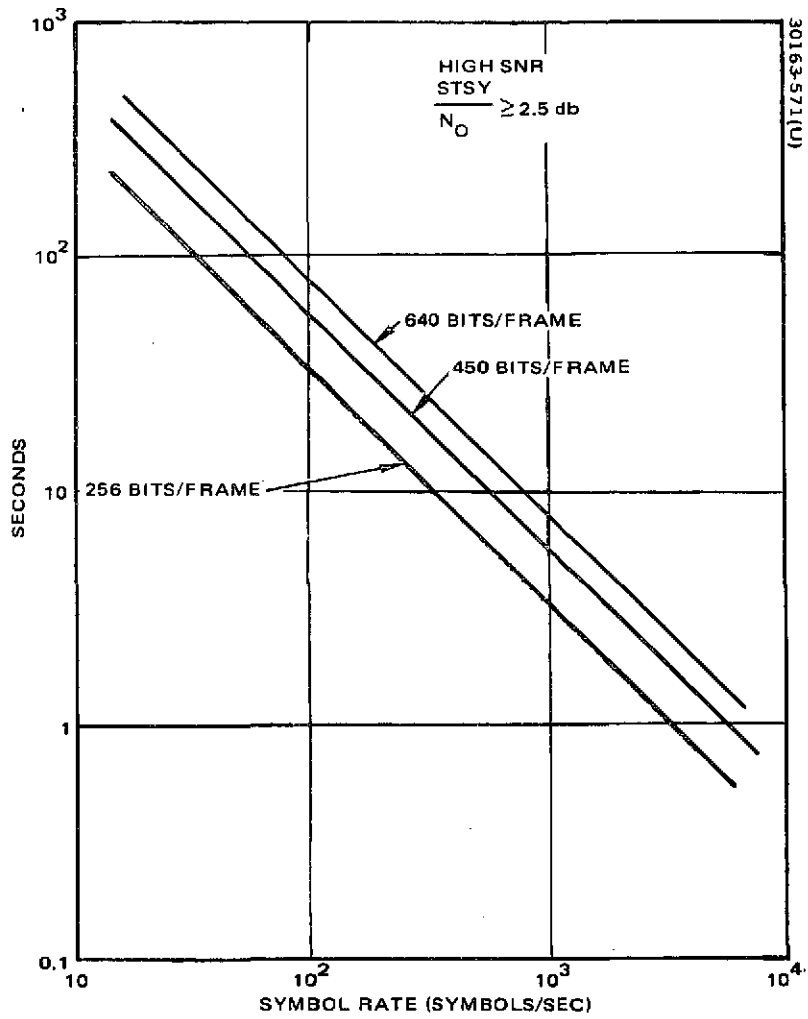


FIGURE 4-28. COMPOSITE SSA AND DDA ACQUISITION AND IN-LOCK CONFIRMATION TIME FOR SEQUENTIAL DECODING OF CONVOLUTIONAL CODED DATA

orbiter mission presents less of a consideration due to the repetitive nature of the daily orbit and the large amount of scientific data which is stored on board the spacecraft and which can be played back repetitively as desired.

Factors which require the ground data processing system to acquire (or reacquire) lock are: 1) initial lockup, 2) channel fades, 3) frame deletions, and 4) changing bit rates and data formats.

Initial lockup is not considered a problem for the probe bus or orbiter spacecrafts. A great deal of current data will be available to allow accurate frequency predictions. Also, signal levels are sufficient to allow ready recognition of the spacecraft signal.

Initial lockup for the large and small probes could require more time due to carrier frequency dispersions at encounter. These dispersions are the result of the combination of long term drift, doppler uncertainty, and thermal effects. For this reason: 1) the JPL scheme for predetection recording has been recommended, and 2) the stored sequences for both the large and small probes provide a 15 min period of unmodulated carrier prior to the black-out phase. Predetection recording eliminates the requirement for receiver lockup. The unmodulated carrier provides a strong signal for a period of time that could be used for a check of the ground equipment setup.

The large and small probe channel fades are caused by turbulence in the Venus atmosphere. An allowance for fades (as derived from the Stanford analysis of the Venus atmosphere stochastic effects) has been included in the telecommunications link performance.

Frame deletions are caused by buffer overflow in the DDA during the sequential decoding process. Discussions of the Fano algorithm and the associated decoding factors are available in the literature. Table 4-8 lists the telemetry characteristics, along with DSIF capability. The buffer overflow problem is reduced by short telemetry frame lengths and low bit rates. In addition, on the multiprobe mission, the buffer overflow problem is further reduced as the predetection recording can be played back at slower than real-time rates, if necessary, thus allowing increased computation time per information bit.

When a probe comes out of blackout, and then again, for the large probe, when the data rate is changed, data would be lost. The loss of data is attributable to loss of SSA and DDA synchronization and is equal to approximately 6 frames in every case. Several schemes have been examined to minimize or eliminate this source of data loss. These are discussed in a separate trade study. The most attractive scheme at present is to provide a separate data buffer which would, in parallel with the real time link, store data during the reacquisition sequence. This stored data would be interleaved in the telemetry format for replay subsequent to reacquisition and at every subsequent bit rate change. The bit rate changes are required to maximize the data which will be returned for a given rf power output level.

TABLE 4-8. CONVOLUTIONAL CODED TELEMETRY CHARACTERISTICS

| | Probe Bus and Orbiter | Large Probe | Small Probe | DSIF Capability |
|-----------------------------|-----------------------------|-----------------------------|-----------------------------|-------------------------------------|
| Constraint length, bits | 32 | 32 | 32 | 32 (maximum) |
| Frame length, bits | 256 | 512 | 512 | 1200 (maximum) |
| Coder connection, vector | Nonsystematic quick-look | Nonsystematic quick-look | Nonsystematic quick-look | Nonsystematic or systematic |
| Code rate | 1/2 | 1/2 | 1/2 | 1/2 |
| Bit rate, bps | $8/111/2^N/111/$ 2048 | 276/184 | 16 | 2048 (maximum) 6 (minimum) |

At probe bus encounter, the telemetry symbol rate is 4096 SPS and the reacquisition process requires less than 1 sec.

Telemetry formats for all vehicles have been designed so that format changes do not result in loss of ground system lock. All frame sync words and tail sequences are identical for all formats.

Software

Software requirements for the multiprobe and orbiter missions were examined. The functions that were developed are summarized in Table 4-9, along with their applicability to system test or mission operations. It is intended that much of the software developed to support system test would be applicable to mission operations due to the opportunity for cost savings and human factors benefits.

Table 4-10 summarizes the software modules required for mission operations. The status and source of these is also indicated. The following material briefly describes the functions of each module.

Telemetry - Real-Time Telemetry Processing Program

Telemetry manages all real time data handling requirements. Tracking, engineering, and science telemetry data are monitored by telemetry with certain limit-checking functions which are relayed to real time displays and consoles. The master data record is produced directly by telemetry. All non-real-time software in navigation, spacecraft, and science is supported by telemetry. All number conversion functions are performed by telemetry.

COMGEN - Command Generation Program

COMGEN is used to generate the command messages which are to be sent to the spacecraft. It also serves as an evaluation tool in designing and checking out command memory programs and activities (i. e., simulation). The memory is programmed to control desired sequences of events using time versus event type inputs from trajectory programs. COMGEN also outputs sequence of events files to be used by the other MOS program. COMGEN interfaces directly with AESOP and SEQGEN in input and output roles, respectively.

SEQGEN - Sequence of Events Generation Program

SEQGEN will produce a time ordered display of planned activities and MOS events. It will provide the following functions; accept inputs of planned events from other programs, compile inputs in a time ordered sequence of events, validate this sequence with respect to predefined restrictions, and display the finalized sequence.

TABLE 4-9. SOFTWARE FUNCTIONAL REQUIREMENTS AND APPLICATION

| Function | Description | Applicability | |
|----------------------------------|---|-------------------------------|--------------------|
| | | System Test | Mission Operations |
| Real time processing | TM frame synchronization, limit testing, suppression testing, engineering unit conversion | Yes | Yes |
| Engineering subsystem displays | Subsystem status and display | Yes | Yes |
| Limited scientific data analysis | Quick look scientific instrument status and data display | Limited | Yes |
| Command processing | DSN CMD MSG formatting, CMD memory verification | Limited (memory verification) | Yes |
| Engineering subsystem analysis | Power management, thermal management, spin rate determination, telecom analysis | Limited | Yes |
| Off-line processing | Midcourse maneuver, science data analysis, celestial reference | No | Yes |

TABLE 4-10. SOFTWARE STATUS

| Name | Description | Status | Source |
|------------------------|---|--------|---------|
| Telemetry | Real-time telemetry data processor | New | HAC |
| Command generation | Command message generation, minemonics translation, memory verification | New | HAC/ARC |
| Sequence generation | Provides time ordered sequence of events | New | ARC |
| ICG | Launch phase injection conditions generator | Exist | JPL |
| DPTRAJ | Double precision trajectory prediction | Exist | JPL |
| ODE | Orbit data editor for the prediction program | Exist | JPL |
| ODP | Orbit determination program | Exist | JPL |
| MOPS | Maneuver operations program system | Exist | JPL |
| Pogasis | Science instrument pointing and geometry | Exist | JPL |
| Probe NAV | Probe targeting requirements | New | HAC/ARC |
| Thermal management | Lumped mass thermal prediction and analysis | New | ? |
| Power management | Power profile analysis and prediction | New | ? |
| Telecom | Telecommunications link performance analysis and prediction | New | ? |
| Attitude and spin rate | Analysis of spacecraft attitude and spin rate | New | ? |
| Jet management | Thruster analysis and maneuver prediction | New | ? |
| Celestial reference | Celestial reference analysis and prediction | New | ? |

ICG – Injection Conditions Generator Program

ICG will generate the nominal earth-fixed spherical injection conditions and launch azimuth angle corresponding to an input launch time. ICG will be used only in the launch phase of the missions and will provide an initial set of injection conditions for DPTRAJ.

DPTRAJ – Double Precision Trajectory Program

DPTRAJ is comprised of four links. Their cumulative function is to take a set of input conditions on spacecraft position, velocity, etc., are then processed with the ephemeris to generate extensive trajectory data. Tracking station prediction data is an additional output of DPTRAJ. ODP, MOPS, and POGASIS use the links of DPTRAJ as integral parts of their respective functions.

ODE – Orbit Data Editor Program

ODE performs, in support of ODP, data editing, data error determination, equipment error removal, and generation of input data for ODP. ODE must always precede ODP in the mission operations software sequences.

ODP – Orbit Determination Program

ODP assimilates tracking data, edited by ODE, and performs trajectory determinations and predictions. Both orbital and transit modes are accommodated in ODP. Orbit determination error statistics and uncertainties are calculated. ODP supplies MOPS and DPTRAJ with input data.

MOPS – Maneuver Operations Program System

MOPS analyzes requirements for midcourse maneuvers, orbit insertion maneuvers, and orbit trim maneuvers. MOPS includes a design and analyses (D. A.) link and a command (CMD) link for each of these maneuvers. ΔV and precessions are predicted and target data is calculated for midcourse maneuvers. The spacecraft thrust vector and ignition time are calculated for the orbit insertion maneuver along with the precession required to align the spacecraft with the nominal thrust vector. ΔV and spacecraft precessions are calculated for the orbit trim maneuvers. DPTRAJ is used in conjunction with MOPS for the orbit insertion and orbit trim maneuvers. MOPS supplies JETMAN with required ΔV data for any given maneuver. ODP provides MOPS with the tracking data necessary in the ΔV calculations.

POGASIS – Planetary Observation Geometry and Scientific Instrument Sequence

POGASIS performs trajectory path and science instrument geometry functions. The trajectory path computations include look angles of earth based tracking and telemetry networks, times of earth occultation, and times of eclipses. The geometry functions will determine the sequences required to obtain desired science observations. The field of view and orientation

with respect to spacecraft spin axis for each science instrument along with spin rate are inputs to POGASIS along with desired science coverage requirements.

PRONAV – Probe Navigation Entry Program

PRONAV provides the small probe targeting functions and maneuvers. In a method of calculation similar to MOPS, the required spin speed and spacecraft attitude are calculated for the desired small probe targeting. ΔV and precession maneuvers are calculated, ASPIN is used to determine the necessary change in spin speed, and these data are then fed to JETMAN. Small probe release time requirement is an input.

THEMAN – Thermal Management Program

THEMAN will predict the equilibrium temperature of each lumped mass (NODE) of the spacecraft. Input data include solar intensity, sun angles to each nodal surface, power dissipation, and heat inputs to each node. An independent option in THEMAN facilitates the large and small probe pre-separation thermal analyses.

PWRMAN – Power Management Program

PWRMAN assimilates spacecraft power subsystem telemetry and converts this data into power and voltage levels for the major spacecraft components. This is then used to determine spacecraft power profiles, energy balance, and power margins. An additional function of PWRMAN is to simulate a proposed sequence of events and predict the power margins and capabilities resulting in the execution of the sequence. PWRMAN provides large and small probe pre-separation power analyses as an option.

TELCOM – Telecommunications Prediction and Analysis

TELCOM is used for telecommunications performance analysis and prediction. TELCOM makes telemetry, command, or ranging performance predictions and then performs the corresponding actual versus predicted performance comparisons. Trajectory data from DPTRAJ or MOPS is required as an input.

ASPIN – Attitude and Spin Rate Determination Program

ASPIN calculates the spacecraft spin rate and attitude on the basis of sun sensor and star sensor telemetry.

JETMAN – Jet Maneuvered and Propulsion Management Program

JETMAN is a group of computer programs whose purpose is to calculate propulsion subsystem analyses and maneuver associated parameters. The independent programs will include means of calculating turn angles, turn angle times, pointing errors, and spin rate changes. In addition, JETMAN will predict attitude control propellant depletion and predict the performance

and capabilities of the propulsion subsystem. Attitude control jet firing durations for orbit inspection and trim maneuvers are generated for given ΔV requirements specified by MOPS.

CELREF - Celestial Reference Program

For given attitude and/or trajectory from DPTRAJ, CELREF predicts the celestial bodies which will fall in the field of view of the star sensor. This is plotted in the form of a star map. The sensor optical characteristics along with a star catalog are additional inputs to CELREF. The positions of celestial objects and predicted star sensor telemetry response are additional outputs of CELREF.

REFERENCES

1. "Missions Sequences," Hughes Aircraft Company, HS 507-0022-85, Task No. MS-1, 6 February 1973.
2. "Spacecraft/Pioneer Ground Data System Interface Definition," Hughes Aircraft Company, HS 507-0300-2-1, Task No. SP-3, 12 December 1972.

5. SYSTEM TRADE STUDIES

5.1 SUMMARY

System trade studies were identified and performed to optimize the system design. In particular, tradeoffs were made of bus spin axis orientation, bus antenna design, communications parameters, and probe descent profile.

Early selection of the spacecraft spin axis orientation (Task EX-12, Ames Statement of Work (SOW) 2.2.1-(9)) was critical because of its direct impact on the system design. The spin axis was selected perpendicular to the ecliptic based on superior science coverage performance and spacecraft mechanization simplicity.

The bus antenna were chosen (Task CM-12) for the lowest system mass. Diverse requirements of the orbiter and probe bus resulted in selecting different antenna configurations for the two missions. Comparing fixed, electronically despun and mechanically despun antenna performance for the nominal missions and spacecraft configurations and particularly for a spin axis perpendicular to the ecliptic, a mechanically despun parabolic reflector (MDA) was selected for the orbiter. A biconic horn was selected for probe bus communication during cruise and a medium gain horn for the much higher data rates required at entry.

The possibility of adding dual frequency occultation to the orbiter nominal payload was shown to strengthen the advantages of the baseline MDA (Task CM-19).

Tradeoffs of doppler tracking (Task CM-2, Ames SOW 2.2.4-(2)), modulation (Task CM-3, Ames SOW 2.2.4-(3), TIC 4091.1/219 in Volume 15), and coding (Task CM-4, Ames SOW 2.2.4-(4)) were performed to optimize the systems communication performance. Although for the large and small probes Viterbi decoding and for the small probes non-coherent signaling (MFSK) were demonstrated to be theoretically superior, practical considerations including DSN capability and availability of spacecraft hardware resulted in selection of coherent signaling (PCM/PSK/PM) and sequential decoding.

The trade of two-way versus one-way doppler tracking for the probes was driven by the science requirement rather than communications performance considerations. Two-way doppler was selected for the large probe and one-way for the small. In addition, orbiter doppler tracking was analyzed to

determine the ability of the spacecraft receiver to track the expected doppler rates on the uplink signal.

A detailed link analysis (Task CM-5, Ames SOW 2.2.4-(5), TIC 4092.1/081 Volume 15) was performed and detailed atmospheric rf propagation model established (Task CM-14). Adequate system performance to support the required data rates for all mission phases was demonstrated. In addition optimum transmitter powers and moreover modulation indices were established.

A study of enhanced navigation (Task CM-1, Ames SOW 2.2.4-(1)) demonstrated the adequacy of doppler tracking and concluded that ranging was not required although it would speed convergence of solutions. Enhanced accuracy, if desired, could be achieved by dual frequency ranging.

The probe descent profile was treated as a system tradeoff involving the interaction of transmitter, battery, structure, thermal insulation, and parachute parameters. By varying these parameters the system mass was minimized (Task PB-14) consistent with the desired science return. It was shown that in general smaller parachute diameters and higher jettison altitudes were favored. The parachute 3.5 m diameter (D) was selected consistent with positive separation from the aeroshell. The 55 km jettison altitude was selected to minimize system mass.

Sensitivity of the descent profile to variation from the nominal atmosphere (Task MS-23) revealed no substantial problems for the selected use of pressure sensing switches for critical event initiation and for the power and thermal margins incorporated into the design.

Because of the mass constraint of the Thor/Delta launch vehicle, a reduced science payload was considered (Task MS-24) as a low cost method of achieving an adequate weight margin. The net reduction in spacecraft mass including structure and battery resulting from the deletion of particular science instruments from the payload had merits compared to alternate costly weight savings techniques but a reduced payload was not recommended.

5.2 BACKGROUND

Mission requirements often lead to alternate system designs. In many cases comparison of these alternates involves multiple subsystems and several selection criteria. The direct and indirect effects on each subsystem must be identified which will significantly affect the system design and tradeoffs made directed to maximize performance while meeting the requirements.

Because of the tight mass constraint imposed by the Thor/Delta launch vehicle compared to the desired science return to the Pioneer Venus mission, minimum mass received primary emphasis in the system tradeoffs. In addition, the somewhat conflicting requirements of low cost and high reliability were also accorded high priority.

This section describes the system tradeoffs that have been performed. The requirements are briefly reviewed, the alternate solutions to these requirements presented, the relative advantages and disadvantages of each established, and finally the solutions are derived. The particular trades considered include selection of the bus spin axis orientation, selection of the bus antennas and communications techniques and finally selection of the large probe descent profile. The complete tradeoffs have been submitted separately and are cited in the text.

5.3 SPIN AXIS ORIENTATION TRADE STUDY

Two spin axis orientations consistent with a simple communications and solar panel power design were chosen for study. One was directly to earth and the other perpendicular to the ecliptic plane. Two criteria were applied in determining the best orientation. First, experiment pointing and coverage was considered for the orbiter mission with a 24 hour polar orbit with a 150 km periapsis altitude at 30°N latitude. Second, spacecraft configurations were established in order to determine the spin axis orientation leading towards the least cost and mass.

There were five classes of orbiter science coverage considered: 1) no preference, 2) velocity oriented, 3) planet oriented, 4) earth oriented and 5) sun oriented. A summary of the nominal payload pointing preferences is given in Table 5-1. Except for the radar altimeter which was estimated to require a ± 1 deg pointing accuracy relative to the instantaneous radius vector at some point during the spin cycle, and for the rf occultation experiment which required the high-gain telemetry antenna pointed directly at earth during occultations by Venus, none of the other experiments required precise pointing. Another important observation was that all of the planet and velocity oriented instruments had measurement altitude regimes near periapsis extending to perhaps 1000 to 2000 km in altitude. This did not mean that some of these instruments stopped making measurements at higher altitudes. Rather, it implied that the more important measurements were made at the lower altitudes. The planet oriented instruments, with the exception of the altimeter, were all of a scanning type. Thus, a figure-of-merit which could be used in this evaluation was the slant range measurement distance from these instruments to a given point on the Venus surface being scanned, this distance being inversely related to the resolution. For the velocity oriented and sun oriented instruments, the minimum angle during each spin cycle that a particular instrument made with the instantaneous velocity vector or the sun vector could be used as a figure-of-merit.

Another consideration was the percentage of the total mission time in orbit that each instrument would be expected to make satisfactory measurements. Although no requirement could be stated, it was expected that satisfactory measurements would be required for all instruments over 100 percent of all orbits or at least at all opportunities during the mission.

Finally, periapsis was located near midlatitude to scan the northern or southern hemisphere at low measurement distances, since measurement

TABLE 5-1. ORBITER EXPERIMENT POINTING PREFERENCES

| Experiment | Instrument Pointing Classification | Pointing Requirement | Measurement Altitude Regime |
|----------------------------|------------------------------------|---|--|
| Magnetometer | (N) No preference | None | Entire orbit |
| Electron temperature Probe | (V) Velocity oriented | Forward hemisphere | Periapsis to 2000 km |
| Neutral mass spectrometer | (V) Velocity oriented | Velocity ± 30 deg | Periapsis to 1000 km |
| Ion mass spectrometer | (V) Velocity oriented | Velocity ± 30 deg | Periapsis to 2000 km |
| UV spectrometer | (P) Planet oriented | Scan Venus limb | Near periapsis (also scans Venus disk and space at higher altitudes) |
| IR radiometer | (P) Planet oriented | Scan Venus disk | Near periapsis |
| Altimeter | (P) Planet oriented | Along instantaneous radius vector 1 deg | Periapsis to 1000 km |
| RF occultation | (E) Toward earth | Antenna toward earth | Arbitrary |

over the entire planet surface at low measurement distances was impossible. Thus, latitude coverage from equator to one of the poles, but not both, was used as another figure-of-merit.

Two orbiter spacecraft configurations are shown in Figure 5-1 for a spin axis oriented perpendicular to the ecliptic and parallel to the ecliptic, respectively. As shown, spacecraft 1 featured solar cells only around the drum and a mechanically despun antenna. The electronically scanned radar altimeter is shown in several possible fixed but adjustable mounting positions. This was the baseline concept. Spacecraft 2 featured a fixed antenna with its boresight slightly offset from the spin axis for conical scanning.

Spin Axis Perpendicular to Ecliptic

As shown in Table 5-2, by proper orientation of the experiment lines of sight, all types of experiments could be operated either ideally or nearly so, in accordance with the measures adopted for figures of merit.

Planet scan patterns were determined for the 24 hour polar orbit with periapsis at 30°N latitude and for the instrument locations shown in Figure 5-2. For a spin axis perpendicular to the ecliptic these patterns were independent of the positions of the earth and sun. This was of great advantage because there would be no degradation in planet coverage over the course of a Venusian year. In addition, the baseline measurement distance over all northern latitudes, as shown in Figure 5-3, differed from the theoretical minimum by less than 10 percent. Thus, from the resolution viewpoint the planet oriented experiment performance was nearly ideal.

Another advantage was that the surface would be scanned in roughly the east-west direction (as opposed to north-south) which meant that if for some reason the taking of this type of data had to be omitted for some restricted number of orbits resumption of these experiments at a later date could still cover the surface area omitted even if the measurement distances had to be somewhat greater. For a north-south type scan required when the spin axis is normal to the orbit plane certain longitude sectors are lost permanently.

As shown in Figure 5-4, for the velocity oriented experiments the sampling angle was less than 15 deg from periapsis to 5000 km altitude. This was within the desired range of 0 to 30 deg.

For the radar altimeter, an assumed +45 deg elevation boresight freedom allowed measurements to be taken along the local vertical sometime during each spin cycle so that all northern latitudes were covered.

Spin Axis Directed to Earth

The alternate design science performance is summarized in Table 5-3. The major deficiency of orienting the spin axis to earth was in the planet oriented science coverage. The spin axis was required to follow the earth and therefore changed its orientation with respect to the orbit plane as shown in Figure 5-5. The scan geometry of the planet therefore changed with time.

30163-178(U)

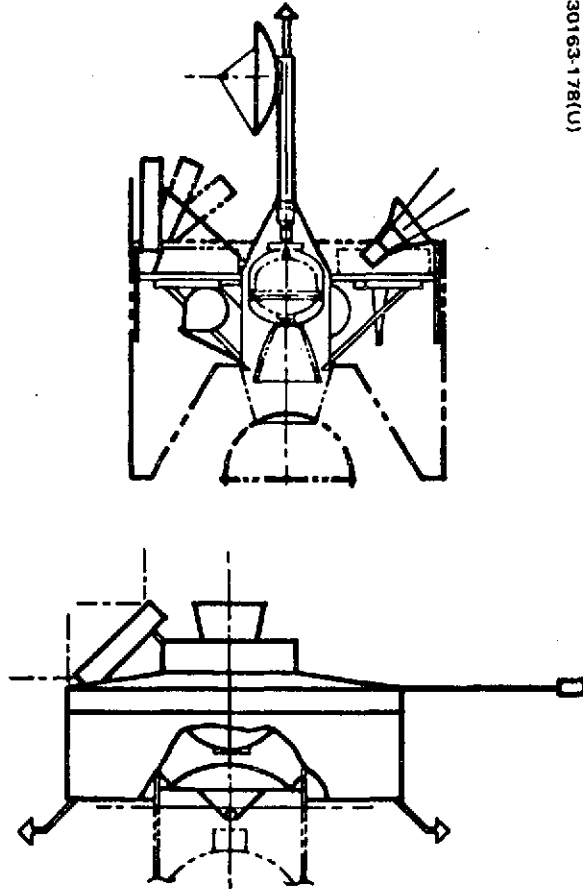


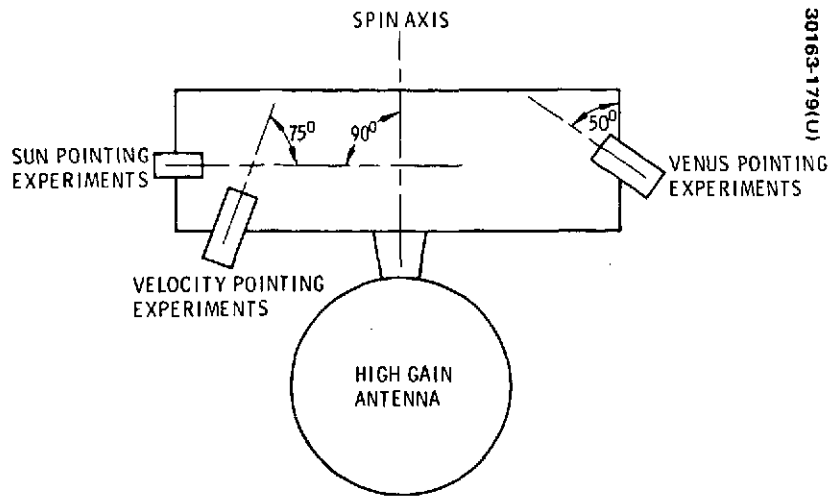
FIGURE 5-1. ORBITER CONFIGURATIONS

TABLE 5-2. BASELINE DESIGN SCIENCE PERFORMANCE SUMMARY

| Experiments | Percent Mission Data Coverage | Performance |
|-------------------|-------------------------------|---|
| Velocity oriented | 100 | Measurement between periapsis and 500 km at less than 15 deg sampling angle |
| Sun oriented | 100 | Ideal; scan is in ecliptic plane |
| Earth pointed | When applicable | Ideal; no need to interrupt downlink |
| Planet oriented | 100 | Measurement of all northern latitudes taken within +10 percent of minimum distance Altimeter coverage of all northern latitudes achievable by ± 45 deg elevation boresight freedom |

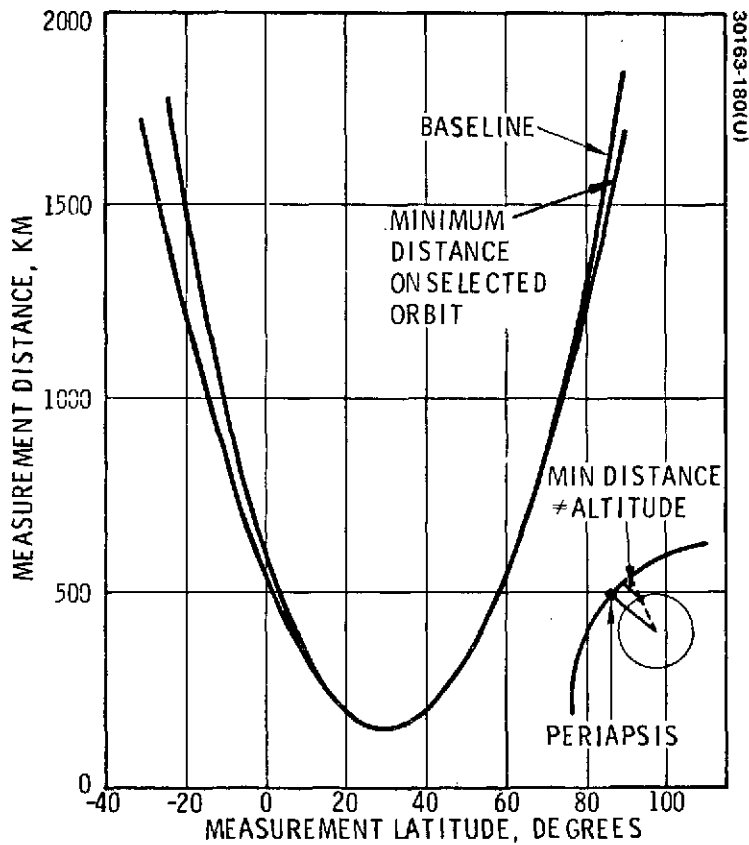
TABLE 5-3. ALTERNATE DESIGN SCIENCE PERFORMANCE SUMMARY (SPIN AXIS DIRECTED TO EARTH)

| Experiments | Percent Mission Data Coverage | Performance |
|-------------------|-------------------------------|---|
| Velocity oriented | 100 | Measurement between periapsis and 500 km at less than 30 deg sampling angle |
| Sun oriented | 100 | Measurement angle to sun may be as high as 80 deg |
| Earth pointed | When applicable | Okay if no maneuver to break downlink |
| Planet oriented | Partial | Measurement of all northern latitudes restricted to certain times in mission. Increased measurement distances at most times. Altimeter coverage of all latitudes effective less than 35 percent of mission with ± 45 deg elevation boresight freedom |



30163-179(U)

FIGURE 5-2. EXPERIMENT DEPLOYMENT (FOR TYPE II TRAJECTORY AND PERIAPSIS SELECTION)



30163-180(U)

FIGURE 5-3. VENUS POINTING EXPERIMENT MEASUREMENT RANGE VERSUS LATITUDE (FOR TYPE II TRAJECTORY AND PERIAPSIS SELECTION)

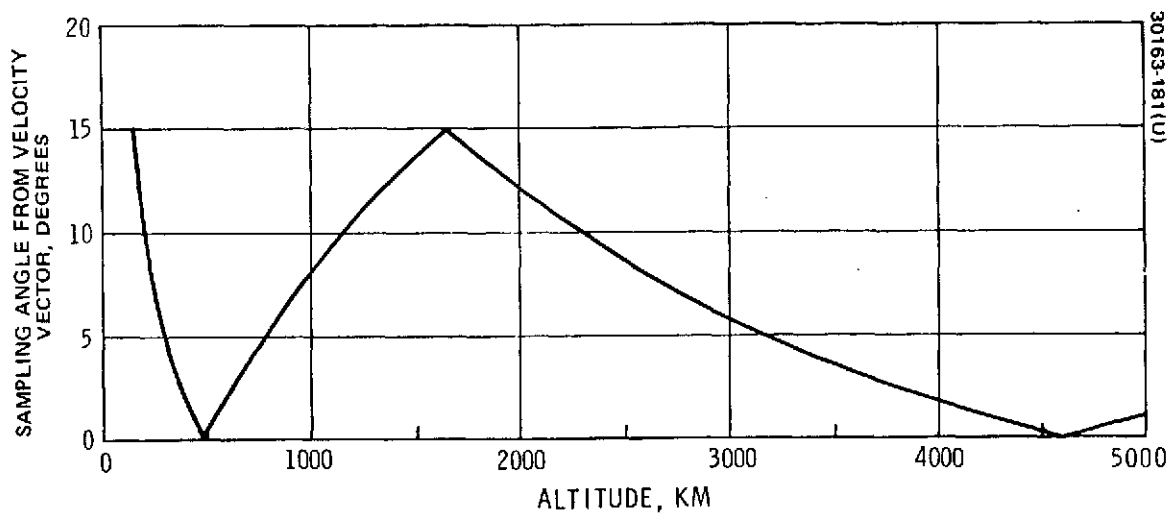


FIGURE 5-4. VELOCITY POINTING EXPERIMENT SAMPLING ANGLE VERSUS ALTITUDE. (FOR TYPE II TRAJECTORY AND PERIAPSIS SELECTION)

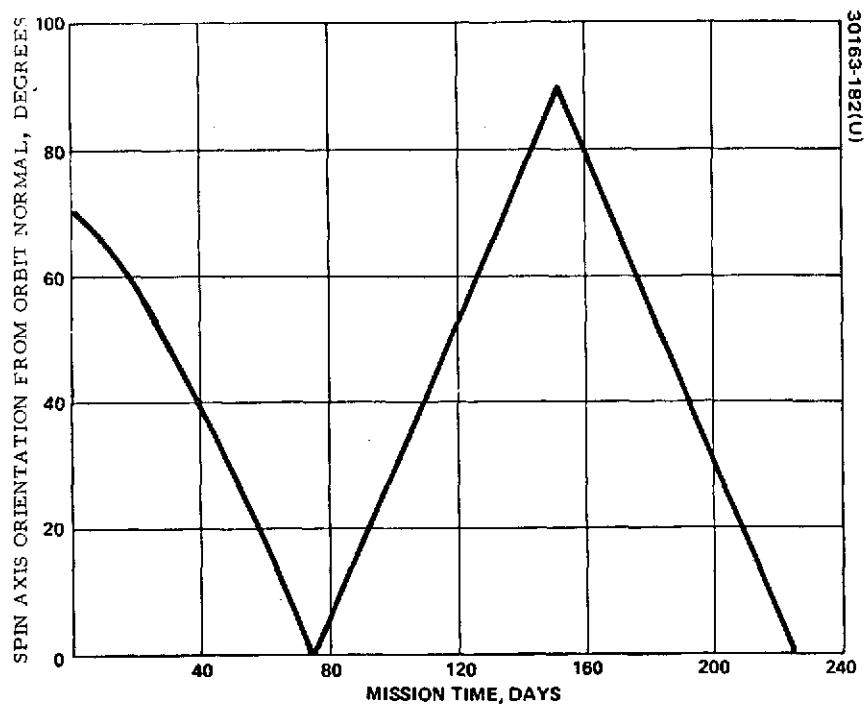


FIGURE 5-5. SPIN AXIS ORIENTATION - SPIN AXIS DIRECTED TO EARTH

For this orientation, the optimum field-of-view direction of all planet oriented, velocity oriented and sun oriented experiments was assumed to be radial; i. e. , perpendicular to the spin axis, this being the best possible direction over the entire Venusian year. The optimum direction of spin axis orientation for the planet and velocity oriented experiment was then along the orbit normal. The deviation of the spin axis from this optimum shown in Figure 5-6 was less than 20 deg for only 20 percent of the mission.

For planet oriented experiments, the measurement attitude shown in Figure 5-7 varied from an ideal situation when the spin axis deviation from orbit normal was zero to something significantly less than ideal when the angle was 90 deg. Measurement distances could be many times the minimum distances. As shown in Figure 5-8, sun pointed coverage varied considerably during the mission with the pointing angle ranging from 0 to 80 deg. It was concluded that the performance over the entire mission was highly inconsistent. Coverage of all the northern hemisphere with good resolution was not possible.

For the radar altimeter, this varying geometry resulted in a large elevation gimbal or boresight angle requirement to cover all northern latitudes at near 100 percent of the mission opportunity. For the selected phased array design, 90 deg was considered an achievable limit. As shown in Figure 5-9, only over 35 percent of the mission could all latitudes be covered. Thus, from the altimetry standpoint, this orientation resulted either in marginal coverage or in severe requirements for gimbal or boresight freedom.

For the velocity oriented experiments, the geometry varied from nearly ideal to something less. As shown in Figure 5-10, a maximum angle of 30 deg could be achieved from periapsis to 5000 km. This was not as good as the baseline performance but was acceptable.

Spacecraft Configuration

A spacecraft design suitable for use with the spin axis in the plane of the ecliptic was studied in some detail to evaluate the problems of spacecraft mechanization. The major problems of this design were the need for additional solar panels at both front and aft ends, a complex thermal control arrangement possibly with heat pipes to accommodate the highly variable solar aspect angle, and the increased mass of the increased thrust tube diameter necessary to accommodate the high gain telemetry antenna. Because of the continuous precession necessary to point the spin axis towards earth, the control system mechanization required more propellant, Figure 5-11, if not some added complexity. The added benefit of the conical scan of the high-gain antenna was merely the addition of another attitude reference, good from the functional redundancy viewpoint. However, the star sensor could not be eliminated because it was found from Venus orbit perturbation studies that ΔV maneuvers would be performed quite frequently, at least once a week, and a satisfactory attitude reference system would be required continuously during the entire Venusian year. If there were no star sensor and the only attitude reference objects were the earth and the sun, then the attitude reference system would be of little value during the portion of the mission life

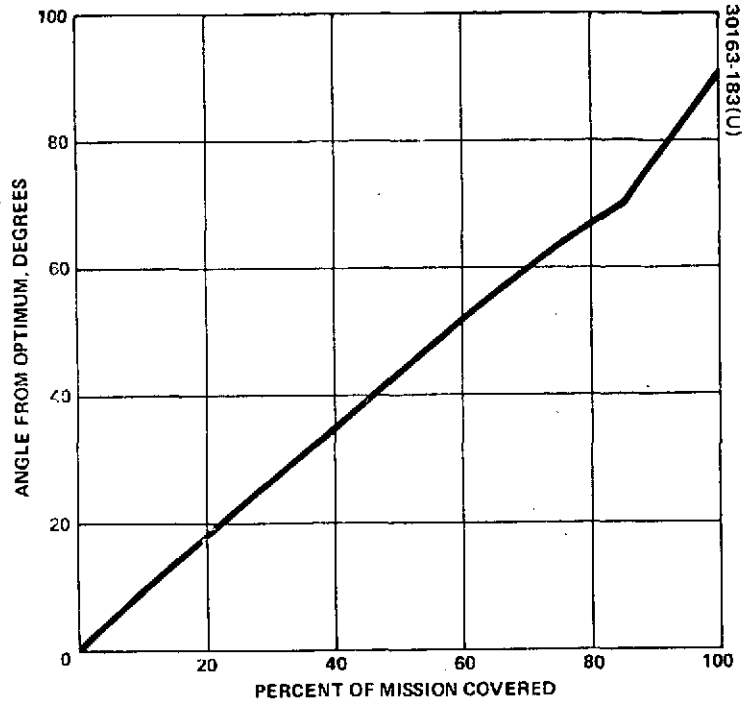


FIGURE 5-6. VENUS POINTED EXPERIMENT COVERAGE - SPIN AXIS DIRECTED TO EARTH

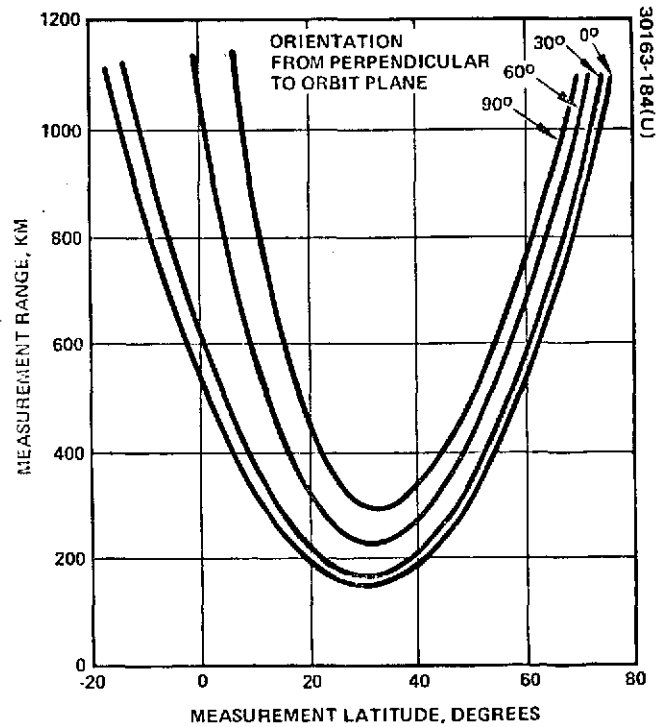


FIGURE 5-7. VENUS POINTED EXPERIMENT MEASUREMENT RANGE-SPIN AXIS DIRECTED TO EARTH

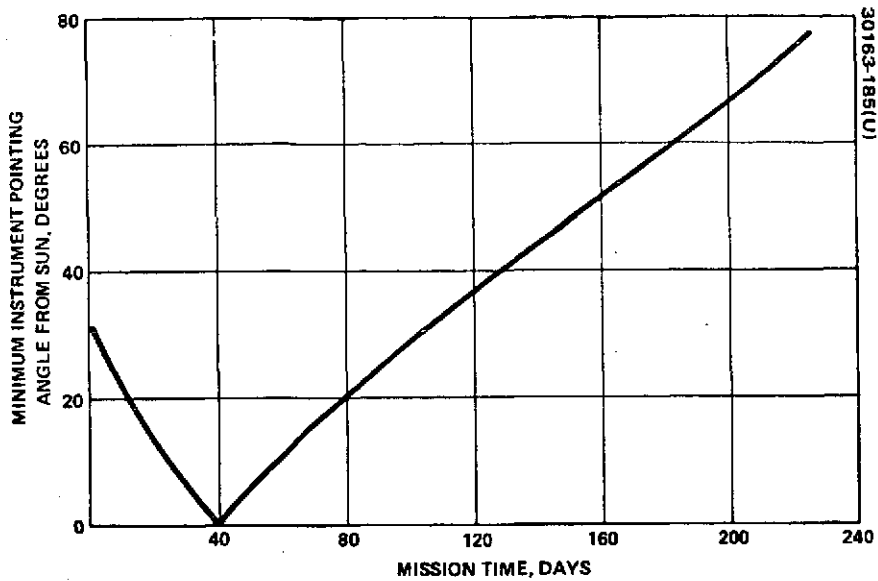


FIGURE 5-8. SUN POINTED EXPERIMENT COVERAGE - SPIN AXIS DIRECTED TO EARTH

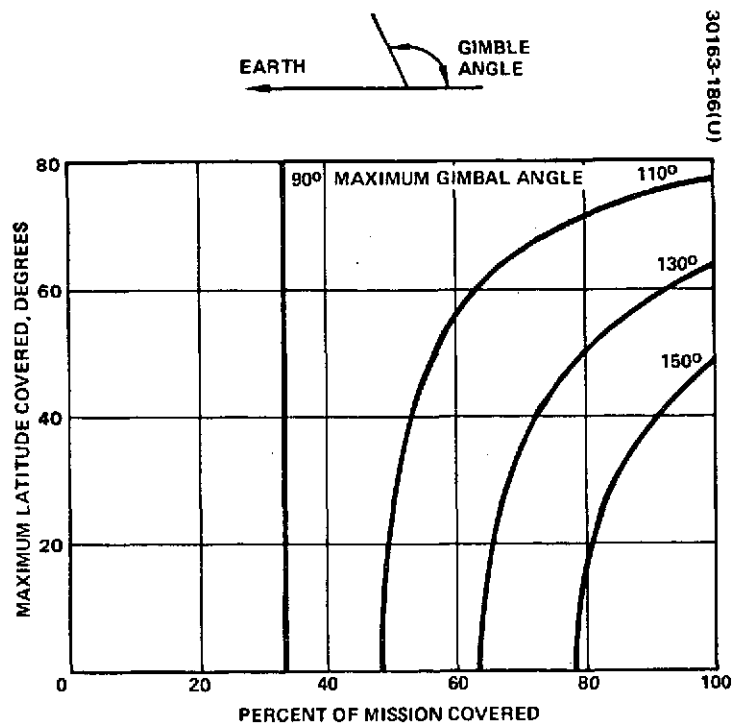


FIGURE 5-9. ALTIMETRY COVERAGE - SPIN AXIS DIRECTED TO EARTH

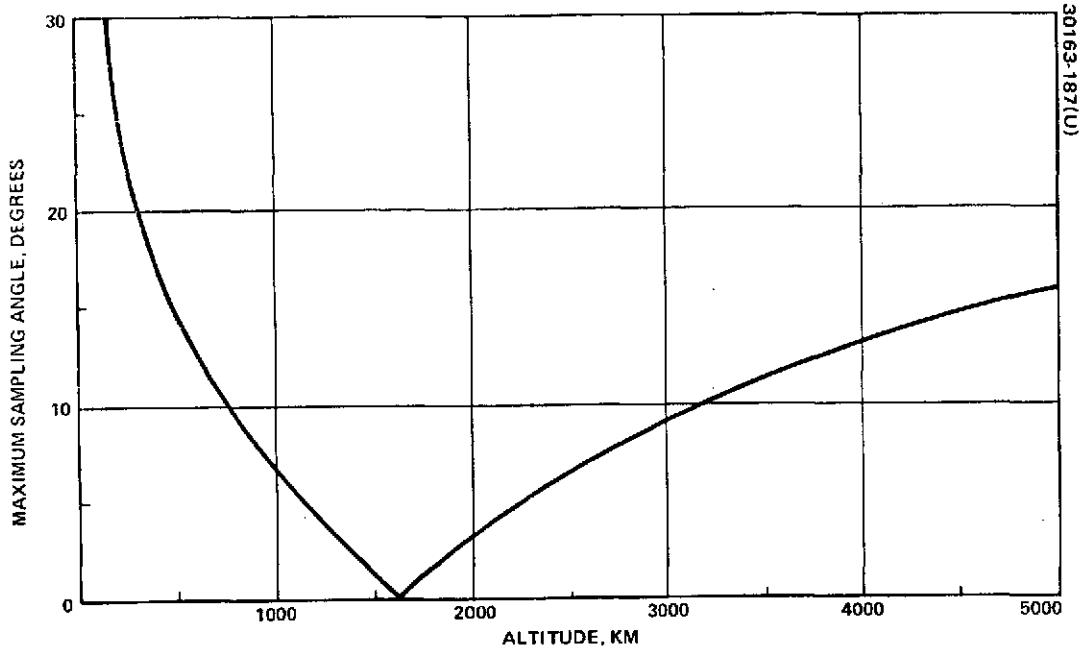


FIGURE 5-10. VELOCITY POINTED EXPERIMENT COVERAGE - SPIN AXIS DIRECTED TO EARTH

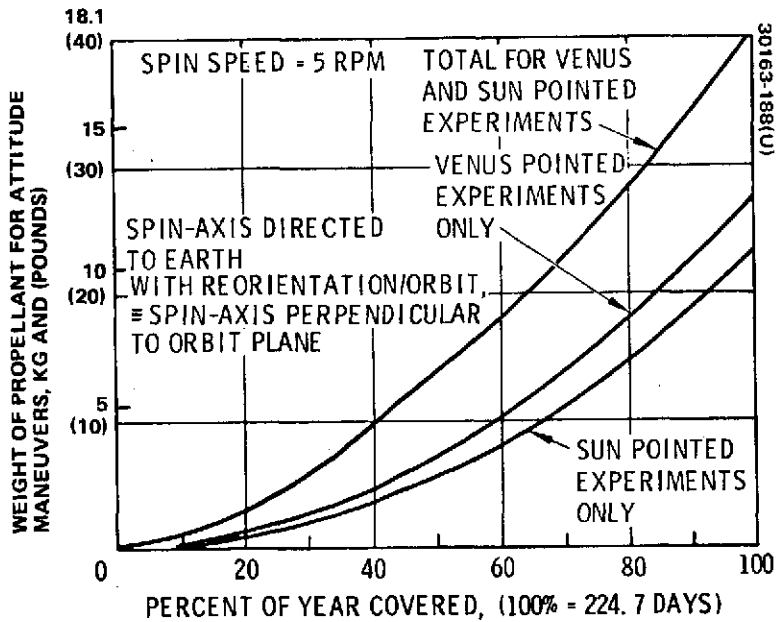


FIGURE 5-11. PROPELLANT REQUIRED FOR EXPERIMENT ORIENTED ATTITUDE MANEUVERS

TABLE 5-4. ORBITER SPACECRAFT MECHANIZATION/SYSTEM DESIGN COMPARISONS

| Affected Area | Change From Baseline to Spin Axis Directed to Earth | |
|--------------------------------|---|--|
| | Pro | Con |
| Power subsystem | | Add solar cells front and back |
| Thermal control subsystem | | Increased louver areas; possible need for heat pipes |
| Attitude control subsystem | Conscan earth reference (additional attitude reference) | Greater propellant requirement 2.6 kg (6 lb) for transit 10.9 kg (25 lb) to 17.4 kg (40 lb) if reorient for science in orbit |
| Spacecraft structure subsystem | | 15.9 kg (35 lb) |
| Adapter | | 11.8 kg (26 lb) |
| Communication subsystem | Delete motor bearing assembly and electronics | |
| Science | | Reduced coverage if not allowed to reorient |
| Mission operations | | Break rf downlink if reorient for science every orbit |
| Overall weight | | 43.1 kg (95 lb) (not including fuel for reorientation) |

5-14

when the earth and the sun were nearly in line with Venus. A second reason for the star sensor was that it could furnish a spin or azimuth reference during eclipses for many of the experiments, particularly the radar altimeter. Loss of this reference would have seriously affected the satisfactory performance of these experiments. The alternate spin axis designs are compared in Table 5-4.

It was apparent that the configuration with the spin axis perpendicular to the ecliptic was superior from the standpoint of weight. It was also felt that it was less complex. The chief advantage of pointing the spin axis towards earth was in the increased reliability and decreased cost of the fixed antenna relative to the despun antenna of the baseline. However, Hughes despun antenna experience on TACSAT, ATS, Intelsat IV and Anik, demonstrated that acceptable levels of cost and reliability could be attained with a mechanically despun antenna. The trade conclusion was thus to select the spin axis perpendicular to the ecliptic.

5.4 BUS ANTENNA TRADES

It was demonstrated (Reference 5-1) that requirements of both orbiter and multiprobe missions could not be satisfied effectively by using the same antenna configurations. Only the low gain omnidirectional antennas were common to both missions. The higher gain antennas were uniquely selected to meet specific mission requirements.

Mission Requirements

The design of the telecommunications subsystem had to satisfy the mission scientific and engineering data return and interplanetary navigation objectives. The selection and placement of the antenna were major facets of this design. The following ground rules were adopted for the telecommunications design.

- 1) Full mission spacecraft command capability in any attitude
- 2) Near-earth telemetry coverage in any attitude (launch, near-earth, early TCMs)
- 3) Full mission coverage in nominal cruise attitude
- 4) Coverage for unique scheduled situations (probe release, probe bus entry, orbit insertion)

Additional ground rules arising from mission requirements and design decisions included the following:

- 1) Compatible with deep space network (DSN) configuration specified for the 1975-1980 period
- 2) Maximum use of the 26 m net; 64 m net used only for mission critical events

- 3) S-band utilized for all telecommunications. X-band limited to possible radio science applications.
- 4) Maximum commonality between the telecommunications subsystems on each of the vehicles

Good spacecraft operability considerations included:

- 1) Separate transmit and receive functions as much as possible
- 2) Circular polarization for all links for operational simplicity
- 3) Beamwidths sized for minimum operational impact

The design philosophy arising from these ground rules was to provide spherical command capability throughout the mission by the use of two switched omni antennas which together would give greater than -6 dBi gain over the sphere. It was estimated that at least 98 percent of the sphere would exhibit greater than -6 dBi gain. The use of switching between the two omni antennas, rather than coupling, was to eliminate interferometric effects which would produce nulls in certain regions of the sphere. For the baseline spin axis orientation, perpendicular to the ecliptic, and for the desired omni antenna locations, on or close to the spin axis at either end of the spacecraft, the region of interferometer fringes would be directed at earth. Only the omni antennas were used for the receive function. As a matter of design and operational simplicity all higher gain antennas were transmit only.

The omni antennas required for the receive function were also designed for the transmit function during times of nonstandard spacecraft attitude such as the launch phase and TCMs. The transmit function during standard or predictable spacecraft attitudes (cruise, bus entry and orbital operations) was provided by antennas selected especially for these purposes.

The orbiter widebeam omni was placed on top of the MDA on the despun platform. The top of the spacecraft provided the best vantage point. Moreover despinning the widebeam omni allowed command reception into a fixed antenna, thus eliminating any spin modulation effects. Since the maximum communication range for the orbiter mission was much greater than for the probe mission, it was also desirable to orient the despun omni such that the maximum receive gain cut was directed along the high gain antenna boresight (nominally toward earth).

Probe Bus Antenna Selection

The mission sequences that sized the probe bus telecommunication subsystems were cruise at maximum range, probe release and bus entry. Cruise required antenna gain perpendicular to the spin axis whereas probe release and bus entry required gain aft, generally along the spin (-z) axis. The first attempt at fulfilling these requirements was to provide a bicone antenna to give the cruise coverage in the ecliptic plane and to utilize a

broadbeam endfire antenna for the probe release sequence and for bus entry. However, the requirements for the endfire antenna to give broadbeam performance for probe release when the earth was 28 deg (large probe) and 46 deg (small probes) off the aft spin axis and to also give maximum gain for bus entry when the earth was only about 2.5 deg off the aft spin axis, were not compatible. Therefore, the probe release sequence coverage was assigned to the aft (widebeam) omni antenna and a medium gain horn was dedicated to bus entry. This allowed an increase in bus entry gain and subsequent science data return of about 10 dB. Probe bus antenna usage is summarized in Table 5-5 and the antenna configuration is shown in Figure 5-12.

Bicone Antenna

To provide higher gain while the spacecraft was in its nominal cruise attitude a bicone antenna (45.7 cm [18 in.] diameter, 22.9 cm [9 in.] height) was selected. This antenna was stowed in the thrust tube during launch and then deployed with the widebeam omni along the aft spin axis after separation from the launch vehicle. The bicone antenna provided a RHCP "pancake" pattern in the plane symmetric with and perpendicular to the spin axis with a peak gain of 3 dBi and an elevation beamwidth of 30 deg. This elevation beamwidth could have been reduced by a factor of two or three (with the attendant increase in gain) without impacting the spin axis erection accuracy criterion if the necessary aperture size had been available. However, the size of the antenna was limited by the stowage space available in the thrust tube and the penalty associated with increasing the antenna size mitigated against any increase in gain since the 3 dBi was sufficient to fulfill the mission requirements.

TABLE 5-5. PROBE BUS ANTENNA USAGE

| Mission Phase | Antenna Usage | Nominal RF Power, W |
|---|-----------------------|---------------------|
| Launch and acquisition | Omnis/26 m (DSS 42) | 1 |
| Near-earth | Omnis/26 m | 1 |
| Early (large) midcourse maneuvers | Omnis/64 m | 5 |
| Cruise | Bicone/26 m | 1/5/10 |
| Later (small) midcourse maneuvers | Bicone/26 or 64 m | 5 |
| Probe checkout (prior to probe release) | Bicone/64 m | 10 |
| Probe release | Widebeam omni/64 m | 10 |
| Probe bus entry | Medium gain horn/64 m | 10 |

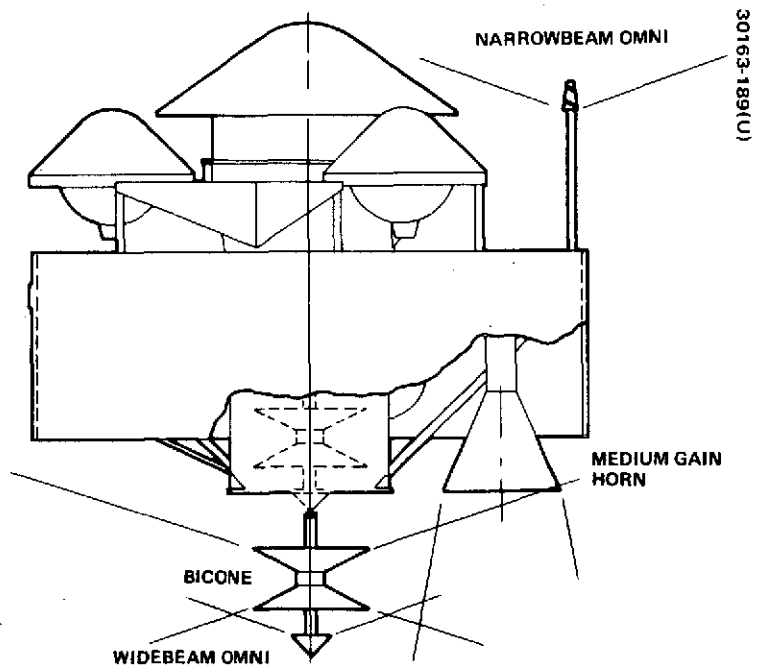


FIGURE 5-12. PROBE BUS ANTENNA CONFIGURATION

Medium Gain Horn

The medium gain horn was a large conical horn antenna directed along the aft spin axis but necessarily mounted off the spin axis. This antenna was dedicated to science data return during the bus entry phase of the mission but was also used for telemetry just prior to that time since the mission geometry was favorable. The antenna had a 45.7 cm (18 in.) aperture and was 66.0 cm (26 in.) long overall. It was a transmit only RHCP antenna with an on-axis gain of 18 dBi and a beamwidth of 20 deg. This antenna was designed to give the maximum possible scientific data return during the brief bus entry phase of the mission. The aperture was sized by spacecraft design considerations, 45.7 cm (18 in.) being the maximum that could be accommodated without creating excessive blockage problems, especially for the thermal control louvers. The resulting beamwidth of 20 deg was considered adequate to accommodate any attitude perturbations which might have occurred prior to final burnup. The bus targeting was such that nominally the earth was 2.5 deg off the aft spin axis at bus entry. Five rf W delivered to this antenna was sufficient to support 2048 bps with the 64 m net during this phase. The mission sequence called for the use of both rf power amplifier modules (10 W rf at the antenna) during bus entry giving an even greater margin for the nominal mission.

Orbiter Antenna Selection

The orbiter antenna subsystem was sized principally by the orbital science telemetry and tracking requirements at maximum range. This required high gain perpendicular to the spin axis which was provided in the baseline system by a mechanically despun high gain antenna. In addition, telemetry and tracking coverage was provided for nonstandard attitudes by use of the omni antennas. The omni antennas also provided the receive function. Orbiter antenna usage is summarized in Table 5-6 and the antenna configuration is shown in Figure 5-13.

The selection of the high gain antenna was difficult because different system requirements tended to different configurations and because of the interaction that existed with other tradeoffs such as the spin axis orientation.

Initially, the trade consisted of a relatively simple weight optimization among several candidate systems. The principal difficulties in making this trade related to the problem of breaking out the weights of the various systems so that an "apples to apples" comparison could be made.

Several important factors such as technological maturity, reliability, magnetics, radio science accommodation and growth potential were not considered except, perhaps, implicitly in selecting the candidate systems.

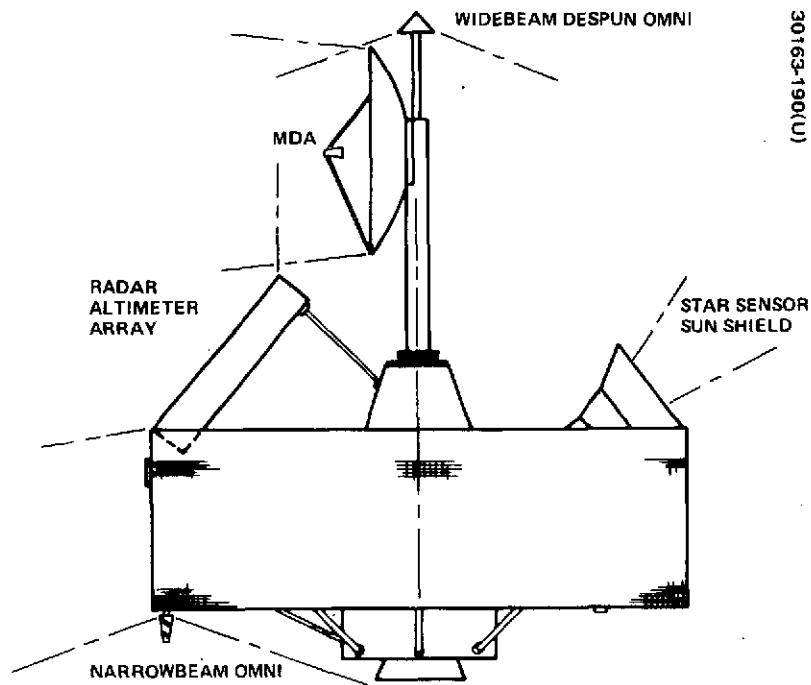


FIGURE 5-13. ORBITER ANTENNA CONFIGURATION

TABLE 5-6. ORBITER ANTENNA USAGE

| Mission Phase | Antenna Usage | Nominal RF Power, W |
|-----------------------------------|--------------------------------|---------------------|
| Launch and acquisition | Omnis/26 m (DSS 51) | 1 |
| Near-earth | Omnis/26 m | 1 |
| Early (large) midcourse maneuvers | Omnis/64 m | 5 |
| Cruise | MDA/26 m | 1/5 |
| Later (small) midcourse maneuvers | MDA/26 or 64 m | 5 |
| Orbit insertion | Widebeam (despun) omni/64 m | 10 |
| Orbital operations | MDA/26 m | 5 |
| RF occultations | MDA/26 or 64 m | 5 |

Table 5-7 summarizes a weight optimization trade. In this comparison, the entire communications system including the omni antennas and their necessary drive was included as well as the high gain antenna. The ERP used as the leveling constant in this trade (60.5 dBm) was that required to support the 64 bps science rate at maximum range with the 26 m net. Unless the 64 m net was considered, any antenna configuration such as the stacked bicone with an omnidirectional pattern in azimuth was not competitive at this level of ERP. This was a direct consequence of the large amount of DC power required to illuminate all 360 deg with sufficient rf power.

Both electronically and mechanical despun antennas were feasible provided the system was sized correctly. For example, the 188 cm (74 in.) diameter mechanically despun antenna (MDA) shown in column 1 of the table would meet the ERP requirements at a competitive weight. However, the narrow beamwidth of this antenna would add to attitude control and operational complexity. Because the omnidirectional approach was not weight-effective and the earth pointed spin axis presented other systems problems, the trade was basically a choice between a MDA and an EDA approach. The principal liens against these two approaches were the single-point failure mode of the MDA and the immature technology of the EDA.

The EDA (HAC) parameters shown in Table 5-7 were for an antenna developed on company funds by Hughes for possible use on METSAT/SMS (Volume 7). The radiating elements for this antenna were cavity-backed slots integrated into the spacecraft solar panel. The despun controller for this antenna was derived from PACE which was the switching and phasing network used for the despun antennas on the Hughes ATS spinning satellites.

TABLE 5-7. ANTENNA MASS OPTIMIZATION TRADE

| | MDA | MDA | Three Stacked Bicones | EDA (HAC) | EDA (TI) | | FDA (SMS) |
|---------------------------------------|-------------|-------------|-------------------------|-------------------------|----------------------------|----------------------------|--------------------------|
| | | | | | Separable | Integrated | |
| Antenna Parameters | | | | | | | |
| Size, cm | 82.55 dia | 59.44 dia | 45.72 dia by 68.58 high | 101.6 dia by 59.69 high | 76.2 dia by 40.64 high | 213.36 dia by 40.64 high | 76.2 dia by 38.1 high |
| Beamwidth - 3 dBm, deg | 11.0 | 15.0 | 360 by 10 | 10 by 12 | 13 by 16 | 6 by 16 | - |
| Gain, dBi | 23.5 | 20.5 | 10.0 | 23.5 ¹ | 21.0 ¹ | 24.5 | 16.15 |
| Transmitter Parameters | | | | | | | |
| RF power, W | 5.0 | 10.0 | 20.0 | 5.0 | 10.0 ⁸ | 5.0 ¹ | 20.0 |
| DC power, W | 25.8 | 51.7 | 105.0 | 25.8 | 31.8 | 15.9 | 103.4 |
| Effective Radiation Power, dBm | | | | | | | |
| Mass Summary, kg (lb) | | | | | | | |
| Antenna | 0.8 (1.7) | 0.5 (1.1) | 4.6 (10.1) | 6.1 (13.5) | 4.0 (8.9) | 3.6 (8.0) ⁹ | 4.6 (10.1) |
| Coax | 0.3 (0.6) | 0.2 (0.5) | 0.7 (1.5) | 1.8 (4.0) | 0.7 (1.6) | 1.9 (4.2) | 1.6 (3.5) |
| Support | 1.0 (2.2) | 0.7 (1.5) | 0.1 (0.2) | 2.5 (5.5) | 2.5 (5.5) | 2.8 (6.1) ¹⁰ | 2.5 (5.5) |
| Feed | 0.2 (0.4) | 0.2 (0.4) | - | - | - | - | - |
| Feed support | 0.2 (0.4) | 0.1 (0.3) | - | - | - | - | - |
| Circulator, switch, filter | 0.7 (1.5) | 0.7 (1.5) | - | - | - | - | - |
| DCE ² | 3.4 (7.4) | 3.4 (7.4) | - | 3.6 (7.9) ³ | 0.9 (2.0) | 0.9 (2.0) | 3.0 (6.6) ¹¹ |
| Logic cabling | - | - | - | - | 0.8 (1.7) | 1.5 (3.4) | 0.7 (1.5) |
| Power amplifier, | 0.5 (1.0) | 1.0 (2.1) | 2.0 (4.3) | 0.5 (1.0) | 1.8 (4.0) (32 by 2 oz) | 2.7 (6.0) (48 by 2 oz) | 2.0 (4.3) |
| Power amplifier, omni ⁴ | 0.5 (1.1) | - | - | 0.5 (1.1) | 1.0 (2.1) | 1.0 (2.1) | - |
| BAPTA ⁵ | 5.1 (11.2) | 5.1 (11.2) | - | - | - | - | - |
| BAPTA support | 0.8 (1.8) | 0.8 (1.8) | - | - | - | - | - |
| Omni antennas ⁶ | 0.6 (1.3) | 0.5 (1.2) | 0.7 (1.6) | 0.7 (1.6) | 1.3 (2.8) | 0.7 (1.5) | 0.7 (1.6) |
| Solar panel (relative) ⁷ | - | 1.7 (3.8) | 5.4 (11.9) | - | 0.4 (0.9) | - 0.7 (-1.5) | 5.4 (11.9) |
| Total relative mass kg (lb) | 13.9 (30.6) | 14.9 (32.8) | 13.9 (29.6) | 15.7 (34.6) | 13.4 (29.5) | 14.4 (31.8) | 20.4 (45.0) |

- NOTES:
- HAC EDA gain is 23.5 dBi rather than 22.5 as per (CM-17) because of different bookkeeping
 - DCE - despun control electronics. All cases use redundant DCE
 - 2.9 kg DCE, 0.7 kg switches
 - Additional power amplifier to provide total of 10 rf W to omnis for nonstandard attitudes
 - BAPTA - bearing and power transfer assembly; includes rotary joint
 - Omni weights include masts
 - 0.068 kg/dc W including substrate
 - Eight modules active, change from TI baseline
 - Structure included in support; include dipoles and manifolds
 - Additional substrate and axial jet support
 - 0.9 kg DCE (optimistic estimate) 2.1 kg switches

Since an antenna quadrant was built as part of the development program, the weights and performance parameters used to obtain the EDA (HAC) entries in Table 5-7 were believed to be representative.

The Philco-Ford SMS EDA antenna design adapted for Pioneer Venus use and a Texas Instruments (TI) EDA design (Reference 5-2) using their AESPA modules were also studied. Two TI configurations were considered. Shown in Figure 5-14, one was a separable antenna similar to the TI baseline design and the other was an antenna integrated into the solar panel. In addition to its obvious integration difficulties the integrated design restricted the sunline to be within 2 deg of normal to prevent cell shadowing. The leveling constant was again an ERP of 60.5 dBm. It was not possible to obtain exactly this ERP. The separable TI EDA parameters were obtained by taking the baseline system of Reference 6-2 but using only eight modules at a time to get the closest possible ERP level to that desired. The integrated version also assumed eight modules at a half-power level to obtain the required 5 rf W. For the Philco-Ford SMS adaptation the level was taken as presented in Reference 5-3. The TI mass estimates resulted in a total system weight about equal to the MDA design. It was felt that the performance parameters and mass tabulations were optimistic.

Other factors considered in deciding between the MDA and TI EDA are summarized in Table 5-8. One important consideration was the technological maturity of the two candidates. Mechanical despinning mechanisms were, especially at Hughes, well within the state of the art, having been used on a number of programs. On the other hand there was very little flight experience with EDAs, the exceptions being one version of the Hughes ATS and the current SMS development.

Another consideration was reliability. With the TI EDA the most likely failure mode (loss of one or more distributed modules) was degraded performance rather than catastrophic failure. However, the MDA was designed with redundant despin motor windings to reduce this possibility. A reliability analysis of the complete MDA success derived from this analysis for the total orbiter mission (10,128 h) was 0.977. The corresponding TI EDA number from Reference 5-3 was 0.975 for a 9000 h mission.

Magnetic cleanliness was more of a problem with the MDA than with the EDA because of the despin motor fields. The fact that it was a variable magnetic field presented a problem area. However, the motor could be magnetically compensated to mitigate this problem somewhat. Magnetic cleanliness analysis performed indicated that the required levels could be obtained with the baseline MDA systems.

Finally, radio science accommodation was considered. For the orbiter radio science capability (S-band occultation only, one dimensional steering) contained in the baseline design, both MDA and EDA had essentially equal capacities. Both provided a signal of about equal ERP and beamwidth.

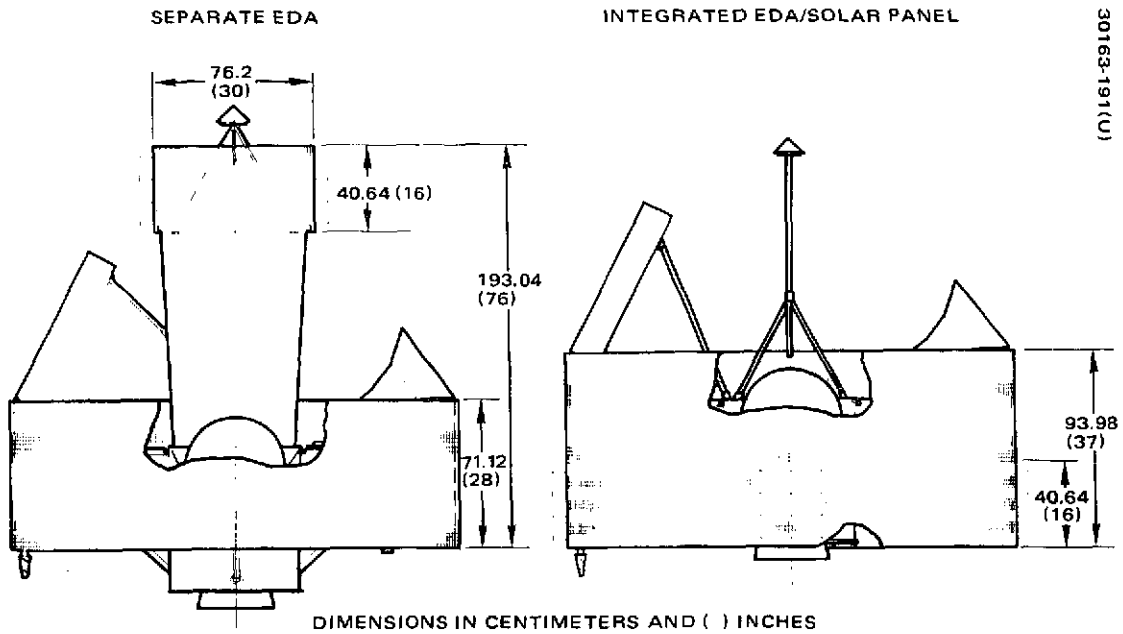


FIGURE 5-14. ELECTRONICALLY DESPUN ANTENNA CONFIGURATIONS

TABLE 5-8. MDA/EDA TRADEOFF

| Consideration | Hughes Baseline MDA | TI EDA |
|-----------------------------|--|---|
| Technological maturity | Flight-proven technology | Predevelopment status |
| Reliability | Good; possible single point failure with BAPTA | Good; graceful degradation with distributed amplifier module failures |
| Magnetic cleanliness | Motor requires compensation | Good |
| Radio science accommodation | Easy dual-frequency and two-dimensional steering modifications | Difficult; beam forming phasing must be compensated |
| Growth capability | Good; lumped amplifier design allows easy growth | Limited without complete system redesign |

Both had one axis steering by virtue of their despun control. However, for any increase in radio science capability such as dual frequency occultation or two dimensional steering, the accommodation impact was considerably reduced in the case of the baseline MDA.

The distributed amplifier scheme used in the TI EDA tended to make growth more difficult. With a lumped amplifier design, additional power was easily coupled into the system by providing an additional power amplifier, switch and summer. Thus, a dual level capability could exist for use when DC power was available. With the TI EDA, power could be added by turning on more modules but this was more and more inefficient as the additional amplifier drive elements were at larger and larger angles to the earthline. Capability could be added to the EDA by using larger modules or more than one module per column of elements but this would negate the simplicity of the TI baseline system. Also, with a distributed amplifier EDA the power for the omnidirectional telemetry coverage for TCMS and other nonstandard attitude maneuvers would require separate additional lumped amplifiers.

The MDA was selected as the baseline orbiter high gain antenna primarily due to the predevelopment status of the TI EDA. If the performance of the EDA was demonstrated and the weight verified, the EDA would be viable depending on the priorities assigned to the varied factors discussed above.

An MDA design without a rotary joint such as the Helios design was considered. However, it was felt that the principal advantage of this approach, the elimination of the rotary joint, was overshadowed by the disadvantages of lower efficiency, higher sidelobes and more difficult radio science integration. In particular, mechanical elevation steering was not possible and adding a second frequency was difficult. Also, the linear polarization of this system, although acceptable, did not meet the ground rules discussed earlier. In Table 5-9 the baseline mechanically despun antenna is compared to this alternate despun reflector concept.

5.5 COMMUNICATION SYSTEM DESIGN TRADES

Small Probe Modulation Selection

A tradeoff was undertaken to determine the optimum modulation and coding scheme for the Pioneer Venus mission. Because of the relatively low efficiency of coherent modulation schemes at low bit rates and low signal to noise ratios, the use of noncoherent MFSK was considered for the small probes. A comparison of coherent versus noncoherent modulation is given in Figure 5-15 for the small probe as a function of altitude. As shown in Table 5-10 (Reference 5-4) for link conditions representative of those of the small probes, MFSK showed a slight, approximately 1.1 dB, advantage over the standard PCM/PSK/PM of the DSN multimission telemetry system. However, principally because no DSN MFSK reception capability existed or was planned, PCM/PSK/PM was selected for the small probes telecommunications links in spite of its small performance disadvantage. The retention of a sensible S-band carrier also allowed the DSN to use standard doppler extraction techniques for the wind drift measurement experiment. Another factor which led to this selection was the availability of DSN compatible coherent modulator/exciter. A MFSK transmitter space-qualified by Hughes could

TABLE 5-9. MECHANICALLY DESPUN ANTENNA (MDA) SELECTION

| | Despun Antenna (Telesat) | Despun Reflector (Helios) | Comment |
|--------------------------|--|--|--|
| Feed | Despun | Spinning | Despun feed is simple antenna design |
| Rotary joint | Yes | No | Rotary joint not considered design problem |
| Backup mode | Medium gain antenna with (despun) switch | Jettison reflector or medium gain antenna with (spinning) switch | |
| Other antenna anchorage | Yes | Yes | Telesat requires slip rings |
| Dual frequency operation | Easy feed addition dual channel joint | Difficult | |
| Elevation scan | Requires gimbal or movable feed | Doubtful | |

have been modified for use in the small probes if a decision were subsequently made to go to a MFSK system, but this would have required extensive redesign. It was estimated that the use of a MFSK system would increase the small probe rf subsystem weight and volume by 1.04 kg (2.3 lb) (62 percent) and 376.9 cm³ (23 in.³) (24 percent), respectively.

Probe Coding Selection

A summary of tradeoff considerations for Viterbi and sequential decoding is given in Table 5-11. For the bit rates and error probabilities specified for the large and small probe telecommunication links, there was little to choose on a theoretical basis between sequential and Viterbi decoding of the probe convolutionally encoded data (References 5-4 and 5-5). However, there were practical and operational reasons favoring Viterbi decoding. For example, sequential decoding would require that data be transmitted in blocks of symbols each with a "tail" to reinitialize the encoder. This tail would contain no data and thus would add to the data processing overhead. More serious, however, would be the complication introduced into the data handling system which could not maintain a constant rate flow of data bits but which would have to provide spaces between data blocks for insertion of the "tails."

Additionally, sequential decoding with many quantization levels would be very sensitive to receiver AGC variation. The probe links could be expected to have much more AGC variations than extra-atmospheric spacecraft since both probe motion (antenna pattern modulation) and atmospheric effects would modify the amplitude of the signal received at the DSS. Thus, sequential decoding would most likely be limited to hard decision capability. Under these conditions and at modest error rates, it was pointed out (Reference 5-6) that a short constraint length code with soft decisions and Viterbi decoding could have the same performance as the hard decision but longer constraint length sequential decoder.

Carrier loop phase error had a double effect. First, since the error versus E_b/N_o curves were steeper for the sequential machine because of longer constraint lengths, the noisy reference (radio) loss would be more severe for the sequential decoder. Second, the assumption that the phase varied so slowly that errors occurred independently would not necessarily have held for the long error bursts which characterize sequential decoding. It was anticipated that symbol interleaving to mitigate the effects of long fades on the channel would be required. The interleaver buffer size would be dependent upon code constraint length and, therefore, would be smaller for the shorter constraint length Viterbi decoded code.

Although for the Venus Pioneer probe bit rates and error rates Viterbi decoding was favored, sequential decoding was selected to comply with the predicted DSN capabilities for the time of the mission. In particular, the Pioneer constraint length 32, rate one-half, quick-look-code was selected to maximize the use of existing software and to be able to draw from the extensive performance data accumulated on this code. If the DSN could obtain a Viterbi decoding capability prior to the time of the Pioneer Venus probe mission it was recommended that Viterbi decoding with interleaving be used.

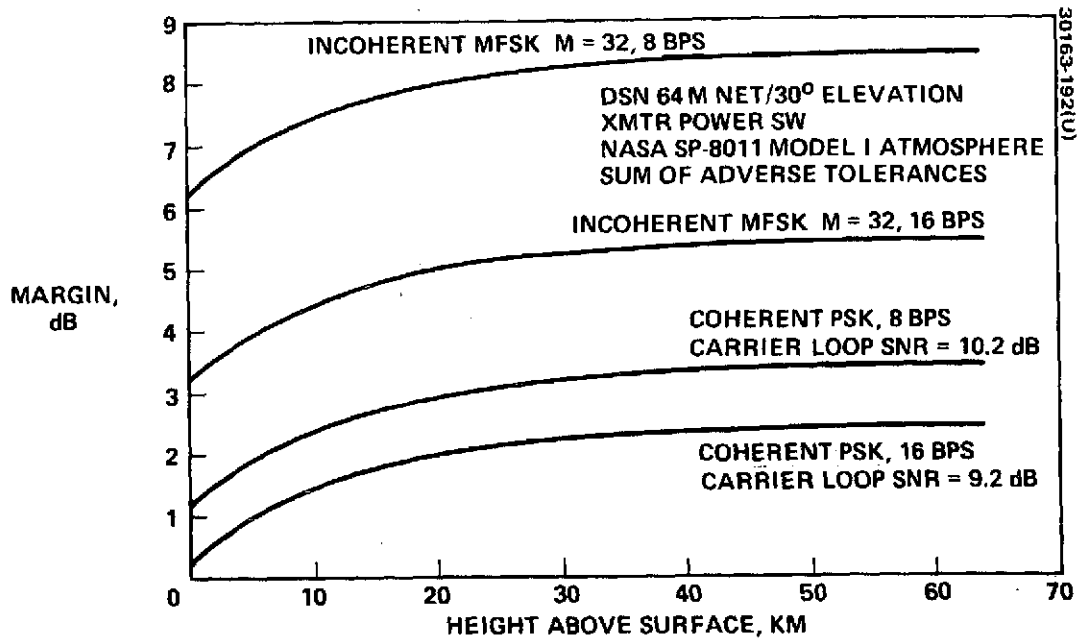


FIGURE 5-15. SMALL PROBE MODULATION TRADEOFF

TABLE 5-10. SMALL PROBE MODULATION COMPARISON

| <u>Coherent</u> | |
|--|--|
| Received $\frac{P_T}{N_o}$ | = 27.10 dB |
| Received $\frac{P_D}{N_o} = \frac{P_D}{P_T} \frac{P_T}{N_o}$ | = 21.11 dB (includes all data losses) |
| Threshold $\frac{P_T}{N_o} = \frac{E_b}{N_o}$ | = <u>15.24 dB</u> |
| | $\left\{ \begin{array}{l} \text{Threshold } \frac{E_b}{N_o} = 3.20 \text{ dB} \\ \text{Data rate } 16 \text{ bps} = \underline{12.04} \\ \left. \frac{P_T}{N_o} \right _t = 15.24 \end{array} \right.$ |
| Margin | = 5.87 dB |
| <u>Noncoherent</u> | |
| Received $\frac{P_T}{N_o}$ | = 27.10 dB |
| Received $\frac{P_D}{N_o} = \frac{P_T}{N_o}$ | = 27.10 dB |
| Demodulator losses | = <u>1.50 dB</u> |
| | 25.60 dB |
| Threshold $\frac{P_T}{N_o} = \frac{E_b}{N_o}$ | = <u>16.86 dB</u> |
| | $\left\{ \begin{array}{l} \text{Threshold } \frac{E_b}{N_o} = 4.82 \\ \text{Data rate } 16 \text{ bps} = \underline{12.04} \\ \left. \frac{P_T}{N_o} \right _t = 16.86 \end{array} \right.$ |
| Margin | = 8.74 dB |
| 8 Hz spectral widening | = <u>-1.76 dB</u> |
| Resultant margin | = 6.98 dB |

TABLE 5-11. TRADEOFF CONSIDERATIONS FOR VITERBI AND SEQUENTIAL DECODING

| System Variables | Viterbi | Sequential |
|---|---|---|
| Bit errors in output | Short bursts of 10 to 20 bit errors | Bit error probability can be made extremely low, but errors come in bursts of up to L bits at a time |
| Decoder delay | Short, less than $100 T_B$ delay | Output may be delayed many thousands of bit times |
| Transmitted data | Continuous | In blocks with tail of no data added |
| Choice of rate and quantization | Decoder completely insensitive to these variables | Storage requirements strongly dependent on Q and R_N |
| Sensitivity to AGC of receiver | Insensitive | Very sensitive for large Q |
| Sensitivity to carrier loop phase error | Sensitive (See Reference 6.6 and Task CM-5) | Much more sensitive due to steeper curve; also, phase varies over long error bursts, implying errors are not independent. |

L - frame length

Q - quantization levels

T_B - bit time

R_N - code rate

Probe Doppler Tracking

A comparison of two-way versus one-way doppler tracking of the probes was undertaken. It was shown that the scheme dictated by science requirements, two-way for the large probe and one-way (stable oscillator) for the small probe was satisfactory from a communications viewpoint (Task CM-5).

Company sponsored analyses (References 5-7 and 5-8) indicated that in general two-way doppler tracking maintained its performance advantage over one-way tracking when doppler frequency variance was the criterion. The penalty paid for the improved two-way tracking was in the additional hardware required to provide the turnaround capability, the downlink losses incurred by adding the uplink channel, and the additional operational complexity for two-way tracking with the possibility of transfer from ground to auxiliary oscillator anytime uplink lock was dropped.

The rf subsystem costs of adding two-way doppler tracking to the large probe were determined. These figures were obtained by taking the baseline one-way small probe rf subsystem and adding the extra power amplifier module, isolator, cable and hybrids required to equal the large probe output power and configuration, thus synthesizing a one-way large probe communications system. The differences between this system and the baseline (two-way) large probe system were the hardware costs of adding the transponder. As shown in Table 5-12, the total (large probe) system weight penalty associated with the transponder including increased power and volume was 2.8 kg (6.1 lb). This number did not include making up the 6.0 dB additional insertion loss.

The hardware costs for adding a transponder to the small probe were slightly different than for the large probe because of the lack of a circulator (magnetic cleanliness) in the small probe. The addition of transponders to the small probes was deemed prohibitive because the resulting science power and weight requirements shown in Table 5-13 would have been an increase of a factor of four. In addition, there was a slight (0.25 dB) penalty due to the increased antenna size needed to account for the antenna bandwidth penalty for two-way operation.

Predetection Recording

A small probe DSN receiver implementation based on the probe doppler profiles was suggested. It imposed requirements on the DSN as to the number of receivers necessary and predetection recording implementation. To account for the increasing doppler rates during the approach without having an excessively wide bandpass filter bandwidth the receiver local oscillator would be programmed with an approximately 20 Hz/sec ramp for the period from first small probe ($\gamma = -70.4$ deg) turnon until last small probe ($\gamma = 23.3$ deg) entry, a period of approximately 32 minutes. As shown in Figure 5-16, this ramp would compensate for an expected one-way doppler

TABLE 5-12. LARGE PROBE HARDWARE COSTS OF TRANSPONDER

| | Power, W | Weight, kg (lb) | Volume, cm ³ (in ³) | Insertion Loss, dB |
|---------------------------------------|-------------|---|---|-----------------------|
| Large probe, one-way | 49.7* | 1.72 (3.8) | 1531.9 (96.5) | 0.4 |
| Large probe, two-way (baseline) | 52.9 | 3.74 (8.25) | 3857.6 (243.0) | 1.0 |
| Hardware cost of transponder | 3.2 | 1.94 (4.45) (Total, inclu- ding battery and pressure vessel increase = 2.7 (6.1)) | 2325.7 (146.5) | 0.6 |

*Plus 2 W during 0.5 h warmup

TABLE 5-13. SMALL PROBE HARDWARE COSTS OF TRANSPONDER

| | Power, W | Weight, kg (lb) | Volume, cm ³ (in ³) | Insertion Loss, dB |
|---------------------------------------|-------------|--------------------|---|-----------------------|
| Small probe, one-way (baseline) | 27.0* | 1.11 (2.45) | 984.3 (62.0) | 0.1 |
| Small probe, two-way | 30.2 | 3.02 (6.65) | 3262.3 (205.5) | 0.5 |
| Hardware cost of transponder | 3.2 | 1.91 (4.2) | 2278.1 (143.5) | 0.4 |

*Plus 2 W during 0.5 h warmup

shift from -144 kHz at the start of the ramp to -182 kHz at the end of the ramp. The second receiver, called the descent receiver, was tuned (no ramping) for the expected one-way descent doppler shift of -101.7 kHz. Each small probe signal would shift from the preblackout receiver to the descent receiver upon entering the Venusian atmosphere.

Large Probe Frequency Selection

To account for its two-way doppler tracking mode the large probe was handled somewhat differently than the small probes. First, since the descent phase was the mission critical period, the large probe frequency selection/predetection recording scheme was optimized for this period. It was not possible to optimize for both preblackout and descent as was done for the small probes because, although the links were designed so that the two-way large probe link was not uplink critical, (Task CM-5) the possibility of switching from two-way to one-way operation and back again had to be accounted for.

During the preentry period two ways were identified to handle predetection recording of the large probe. The first was to compensate for the uplink doppler rate by programming (ramping) the Madrid ground transmitter so that the probe transmitted frequency remained essentially constant. The signal would then be handled by the same preblackout receiver as the small probes with the receiver ramp compensating for the downlink doppler rate. If an uplink ramp was not acceptable, the large probe could have its own preblackout receiver with a ramp sufficient to overcome the two-way doppler rate. Compensating for the large probe would require a ramp approximately 40 Hz/sec (20 Hz/sec one-way) but extended over only the 15 min of large probe transmission prior to blackout. The large probe frequencies associated with these two-way schemes and with one-way operation in addition to the frequencies required for operation of the three small probes are given in Table 5-14.

Although it was judged extremely unlikely there would be a loss of uplink lock during this extra-atmospheric preentry period (assuming that the spacecraft phase-lock loop receiver was designed for the uplink rates or that the uplink rates were compensated by ground transmitter programming), a possible two-way/one-way switchover had to be planned for. In this case without the programmed ground transmitter approach there would be a considerable offset in frequency received at the ground stations when a switchover occurred. This eventuality could be met by having a separate filter (and recorder track) with the filter parameters selected so that the one-way signal would fall within its bandpass regardless of when in the preblackout period loss of uplink lock occurred. Since, the fixed ground transmitter frequency was selected to minimize the downlink frequency shift associated with a two-way/one-way transfer during descent, a fixed doppler compensation of $f_d \approx -102$ kHz was already applied in addition to the $2f_d$ compensating ramp programmed into the large probe dedicated receiver local oscillator. This resulted in an overcompensation in the one-way case and caused the one-way prerecording filter to be approximately 61 kHz above the two-way filter.

5-34

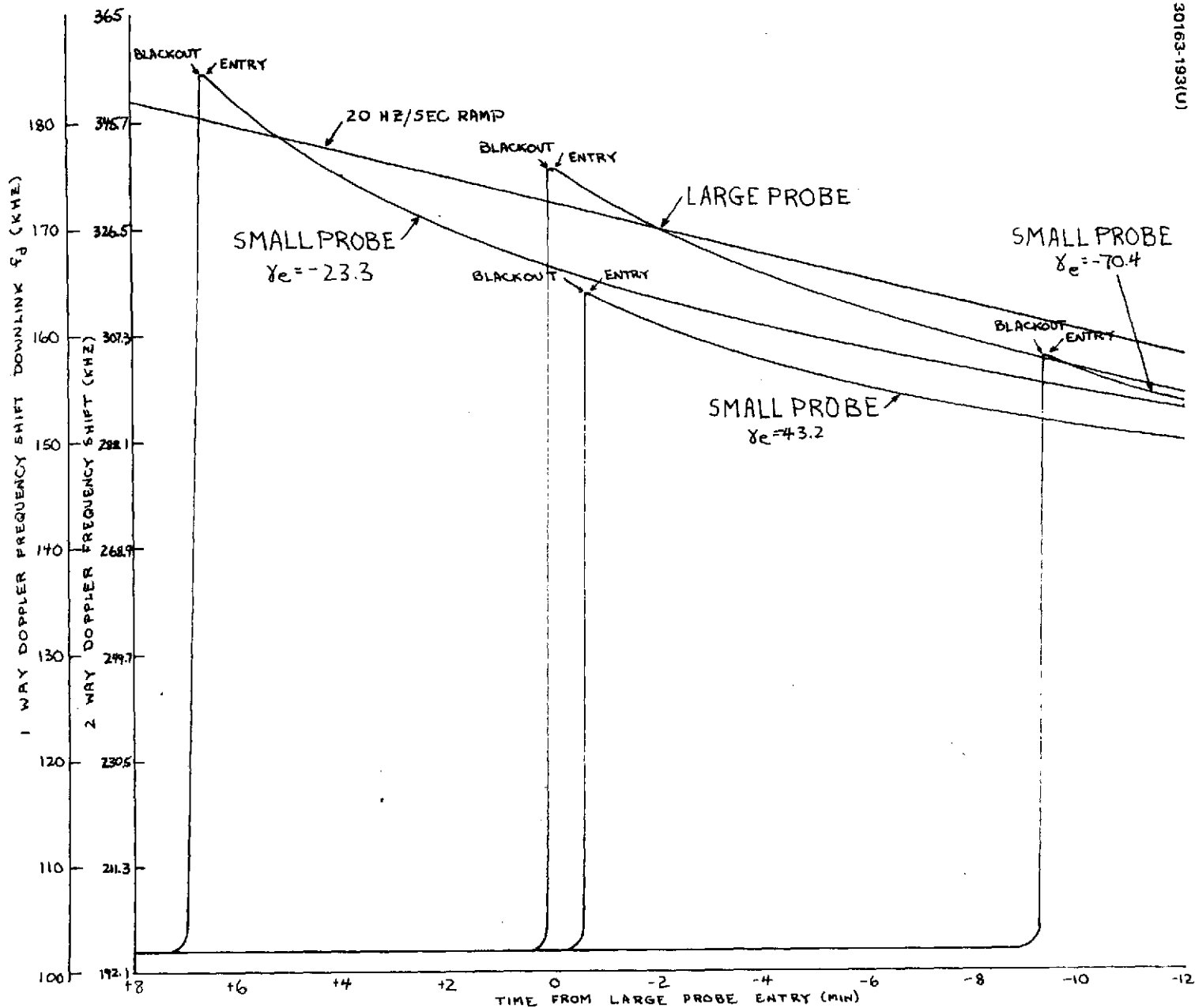


FIGURE 5-16. PROBE PREENTRY DOPPLER HISTORY

TABLE 5-14. PROBE FREQUENCY SELECTION

| | Preentry | | | | Descent | | | |
|--|--|--|--|---|--|--|------------------------------------|------------------------------|
| | Ground Transmitter | Spacecraft Receiver | Spacecraft Transmitter | Ground Receiver | Ground Transmitter | Spacecraft Receiver | Spacecraft Transmitter | Ground Receiver |
| LP two-way fixed ground transmitter | $\frac{221}{240} (f_o - 90 - \underline{f}_d)$ | $\frac{221}{240} (f_o - 90 - \underline{f}_d) + \underline{f}_u$ | $f_o - 90 - \underline{f}_d + \frac{240}{221} \underline{f}_u$ | $f_o - 90 - \underline{f}_d + 2\underline{f}_d$ | $\frac{221}{240} (f_o - 90 - \underline{f}_d)$ | $\frac{221}{240} (f_o - 90 - \underline{f}_d) + \underline{f}_u$ | $f_o - 90$ | $f_o - 90 + \underline{f}_d$ |
| LP two-way programmable ground transmitter | $\frac{221}{240} (f_o - 90) - \underline{f}_u$ | $\frac{221}{240} (f_o - 90)$ | $f_o - 90$ | $f_o - 90 + \underline{f}_d$ | $\frac{221}{240} (f_o - 90 - \underline{f}_d)$ | $\frac{221}{240} (f_o - 90 - \underline{f}_d) + \underline{f}_u$ | $f_o - 90$ | $f_o - 90 + \underline{f}_d$ |
| LP one-way | N/A | N/A | Auxiliary oscillator $f_o - 90$ | $f_o - 90 + \underline{f}_d$ | N/A | N/A | Auxiliary oscillator $f_o - 90$ | $f_o - 90 + \underline{f}_d$ |
| SP ₃ , $\alpha_c = 23.3$ deg | -- | -- | $f_o - 40$ | $f_o - 40 + \underline{f}_d$ | -- | -- | $f_o - 40$ | $f_o - 40 + \underline{f}_d$ |
| SP ₂ , $\alpha_c = 43.2$ deg | -- | -- | f_o | $f_o + \underline{f}_d$ | -- | -- | f_o | $f_o + \underline{f}_d$ |
| SP ₁ , $\alpha_c = 70.4$ deg | -- | -- | $f_o + 40$ | $f_o + 40 + \underline{f}_d$ | -- | -- | $f_o + 40$ | $f_o + 40 + \underline{f}_d$ |

Notes: 1) $\frac{221}{240} \underline{f}_u = \underline{f}_d$

2) All frequencies are kHz

3) Entries not exact but fall within prerecording band-pass filter bandwidths

4) \underline{f}_u and \underline{f}_d should be $\underline{f}_u(t)$ and $\underline{f}_d(t)$

5) \underline{f}_d is ramped out except for the LP fixed ground transmitter case where $2\underline{f}_d$ is ramped out

6) \underline{f}_u and \underline{f}_d are (approximately) constants
 $\underline{f}_u \approx -94$ kHz, $\underline{f}_d \approx -102$ kHz

7) \underline{f}_d is tuned out

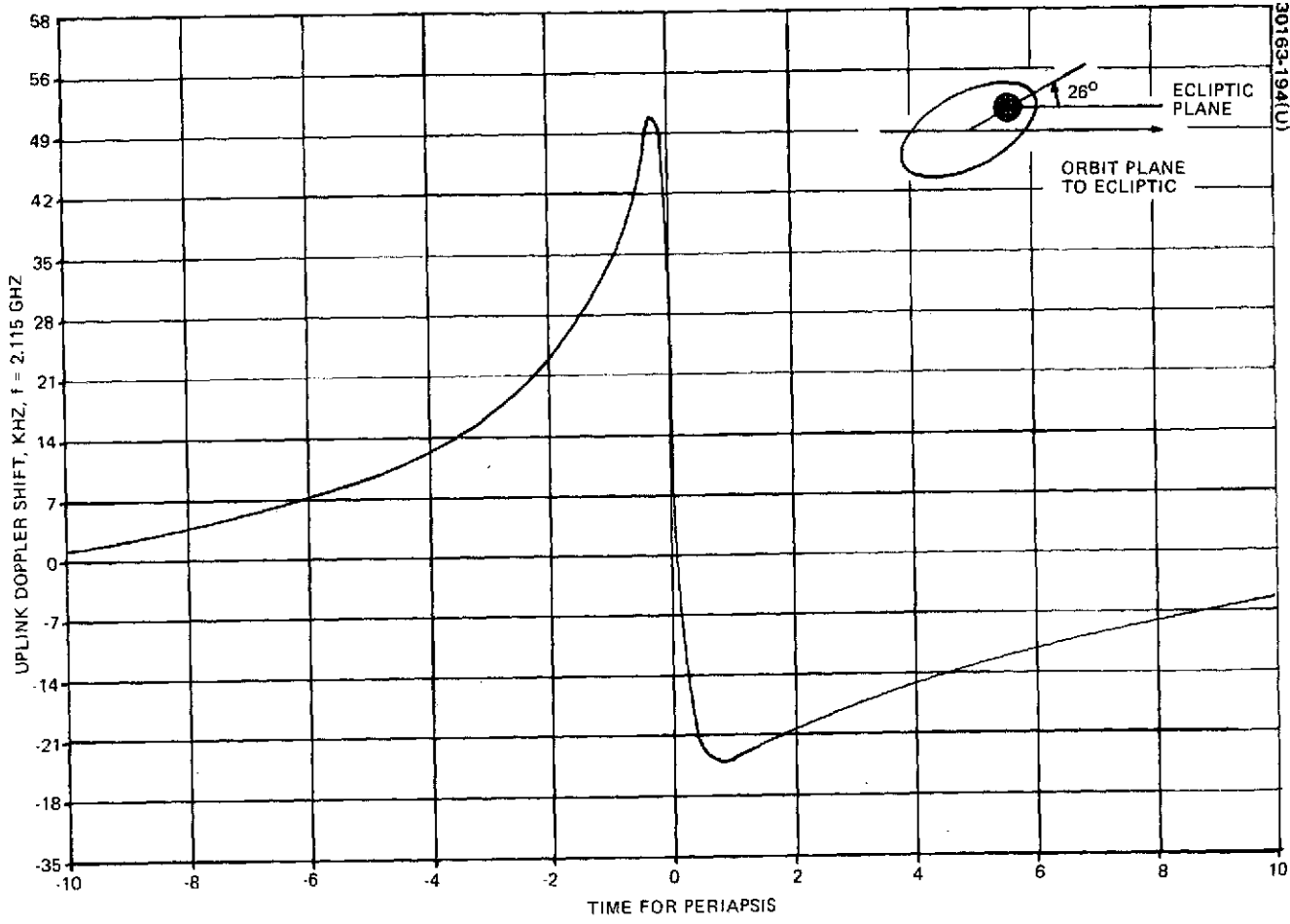


FIGURE 5-17. WORST CASE ORBITER DOPPLER PROFILE

The resulting range of doppler offsets, depending upon when in the preentry period the switchover occurred, required that the one-way filter be 24 kHz wider than the two-way filter for a total bandwidth of ± 42 kHz. It was judged that these complexities in the ground receiver resulting from not having a programmable ground transmitter more than offset the cost of having one. However, because of the potential degradation to differential interferometry (DLBI) that a programmable transmitter might create, a fixed ground transmitter was baselined.

Analysis of the large probe receiver tracking performance indicated that regardless of whether the ground transmitter was programmed or fixed, the spacecraft receiver could track the expected uplink doppler rate during the time immediately prior to blackout with acceptable loop phase errors.

Orbiter Doppler Tracking

Company sponsored analysis (Reference 5-9) indicated that with a minor increase in the orbiter receiver loop bandwidth, satisfactory carrier tracking performance could be maintained until end of mission. The analysis assumed that the worst case doppler profile shown in Figure 5-17 could occur during any part of the orbiter mission. The high doppler rate occurring during passage through periapsis (55 Hz/sec for 0.5 h) introduced unacceptably large phase errors in the carrier tracking loop. The phase error due to doppler rates could be maintained less than 20 deg by either increasing the signal-to-noise ratio in the receiver i. f. bandwidth by approximately 4 dB or by expanding the receiver loop bandwidth. The second approach was adopted since a relatively small bandwidth expansion (from 17.5 Hz to 22.5 Hz) in the two-sided loop bandwidth allowed tracking the worst case doppler rate until end of mission with an increase of only 1.1 dB in the loop threshold.

Link Analysis

A detailed link analysis was performed. Adequate system performance to support the required data rates for all mission phases was demonstrated. In addition, optimum transmitter powers and moreover modulation indices were established. A summary of the critical links is given in Table 5-15. For the required data rate and implemented antenna design, the transmitter was chosen as a multiple of a basic 7 W solid state power amplifier module. The modulation index was chosen to maximize the data rate for a positive carrier margin.

As a basic input into the probe link summaries an atmospheric loss model was developed. Combined atmospheric losses for a landed probe as a function of communications angle is given in Figure 5-18. Combined losses for the nominal communications angles as a function of altitude is given in Figure 5-19.

TABLE 5-15. SUMMARY OF CRITICAL TELECOMMUNICATIONS LINKS

| Mission Phase | Range, 10 ⁶ km | Transmitter Power | Data Rate | Antenna | Communication Angle, deg | Modulation Index |
|----------------------------------|------------------------------|----------------------|--------------|-----------------------|-----------------------------|---------------------|
| Near earth | -- | | 16 | Omni | -- | 36.1 |
| Bus cruise | 0 to 48.7 | 1.4/7/14 | 16 | Bicone | 90 | 36.1 |
| Large probe checkout | 44.3 | 14 | 184/16 | Bicone | 90 | 57.1/36.1 |
| Small probe checkout | 44.3 | 14 | 16/16 | Bicone | 90 | 47.5/36.1 |
| Large and small probe release | 46.5 | 14 | 16 | Omni | 29/46 | 36.1 |
| Bus coast after probe release | 48.7 to 70.3 | 7 | 64 | Medium gain horn | 0 to 4 | 36.1 |
| Large probe release/ entry | 46.5 to 70.3 | 14 | 184 | Equiangular spiral | 28/28 | 57.1 |
| Large probe descent | 70.3 | 14 | 276/184 | Equiangular spiral | 45 | 62.5/57.1 |
| Small probe release/ entry | 46.5 to 70.3 | 7 | 16 | Loop-vee | 46.0/41.7 | 34.7 |
| Small probe release/ entry | 70.3 | 7 | 16 | Loop-vee | 60 | 34.7 |
| Bus entry | 70.3 | 14 | 2048 | Medium gain horn | 2.5 to 4 | 72.0 |
| Orbit insertion | 52.2 | 14 | 16 | Omni | -- | 44.3 |
| Orbiter end of mission | 250.0 | 14 | 64 | HGA | -- | 53.7 |

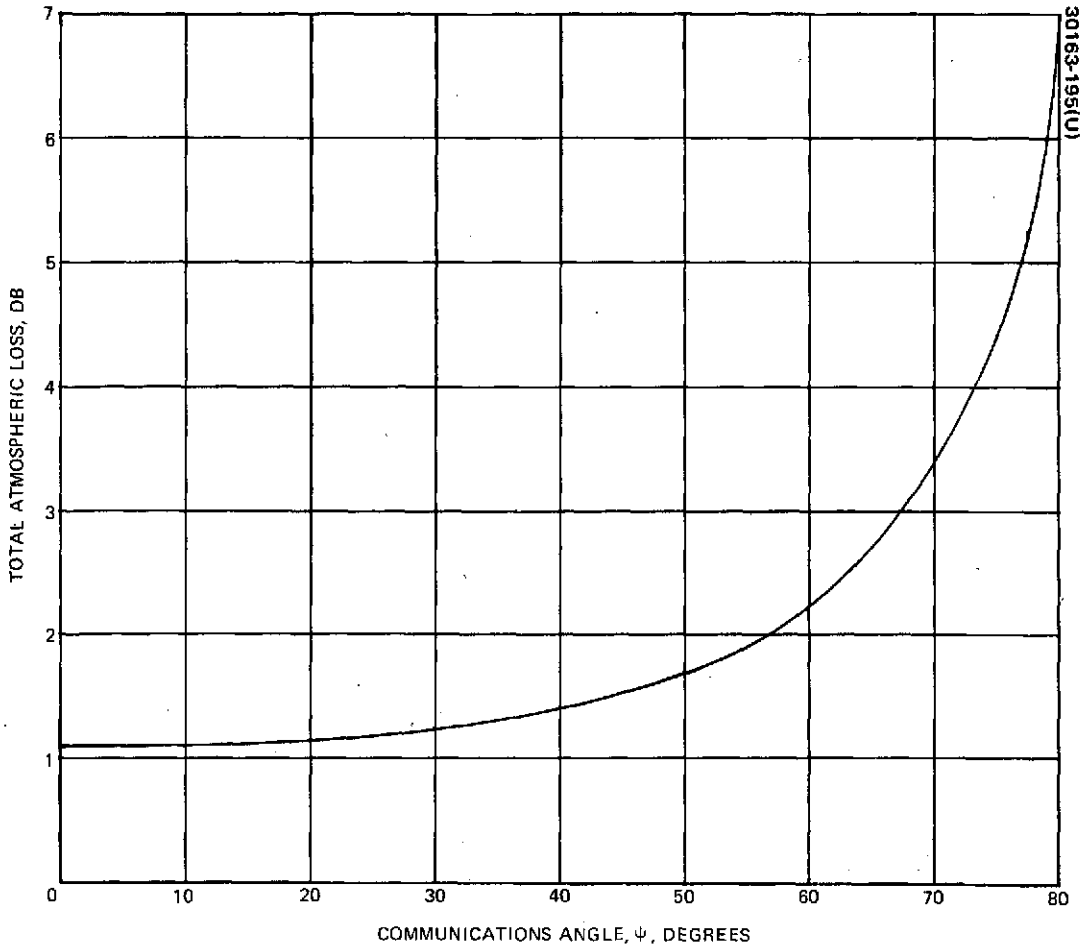


FIGURE 5-18. COMBINED ATMOSPHERIC LOSSES FOR LANDED PROBE

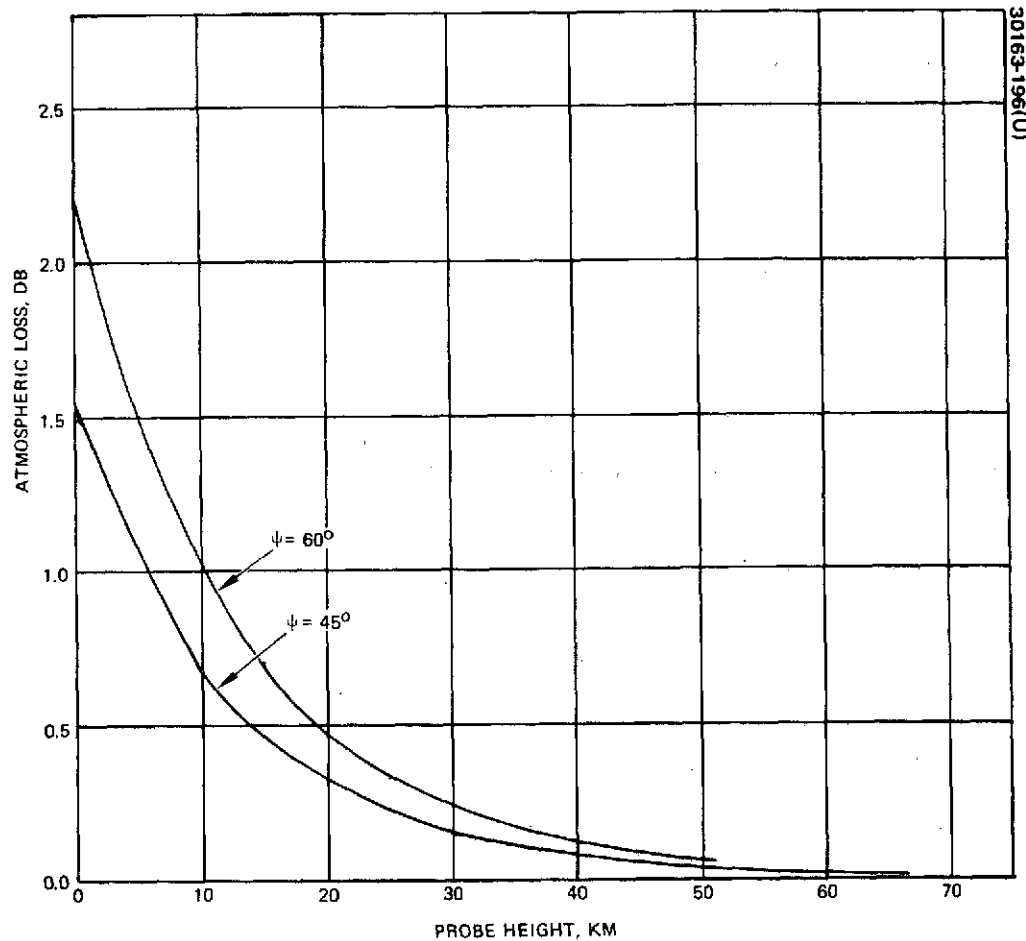


FIGURE 5-19. COMBINED ATMOSPHERIC LOSSES FOR NOMINAL COMMUNICATIONS ANGLES

5.6 PROBE DESCENT TRADES

By varying large probe descent parameters, in particular parachute size and jettison altitude, the system mass was minimized consistent with the science requirements. A system mass model was developed which included transmitter, battery, thermal insulation, parachute, pressure vessel and aeroshell mass. The data rate could most efficiently be transmitted by a continuously variable power amplifier sized to meet the particular requirement. However, to save the cost that would accompany developing a new design, a developed solid state, 7W module was selected and the transmitter incremented in multiples of this basic 7W module. If the required data rate exceeded a transmitter's capability, additional power amplifier modules were added until the data rate could be supported. A data rate reduction at 20 km altitude was included to balance the atmospheric losses near the Venusian surface. Unlike the transmitter, battery capacity was continuously varied to meet the requirement of any particular configuration. Modularization was not necessary for low cost.

Parachute Selection

Decreasing parachute area resulted in decreased parachute subsystem mass and in shorter total descent time. Shorter descent time allowed a reduction in battery and thermal insulation mass which reduced the required pressure vessel and aeroshell mass. The penalty in reducing the parachute diameter was two-fold. First, science altitude sampling required the data rate to increase with velocity. The parachute could only be made so small before the worst case velocity would occur while on the chute requiring the data rate to increase. The diameter below which the data rate requirement would be increased was 2 m. It was judged that the small weight savings that would accrue from further reduction was not worth increasing the data rate requirement. The second constraint was providing positive differential drag between the parachute and aeroshell to provide for separation of the pressure vessel from the aeroshell. A diameter of 3.5 m was required to provide an adequate safety margin for positive separation (Task PB-26). Minimum diameters were thus favored down to this value. A 3.5 m diameter (Do) parachute was selected for minimum mass with adequate margin to guarantee positive separation and impose no increase in the data rate required for the remaining descent.

Jettison Altitude

Because of the weight constraints imposed by the Thor/Delta launch vehicle, the baseline parachute jettison altitude was selected at the relatively high altitude of 55 km in order to minimize mass. Although all quantitative science requirements were met, the major benefit of a lower altitude parachute jettison, increased cloud sampling, was sacrificed.

Varying the parachute jettison altitude affected the system design due to change in descent time and velocity profile. The descent time impacted the system by defining the required battery capacity and thermal insulation thickness. The battery weight varied linearly with descent time. The insulation

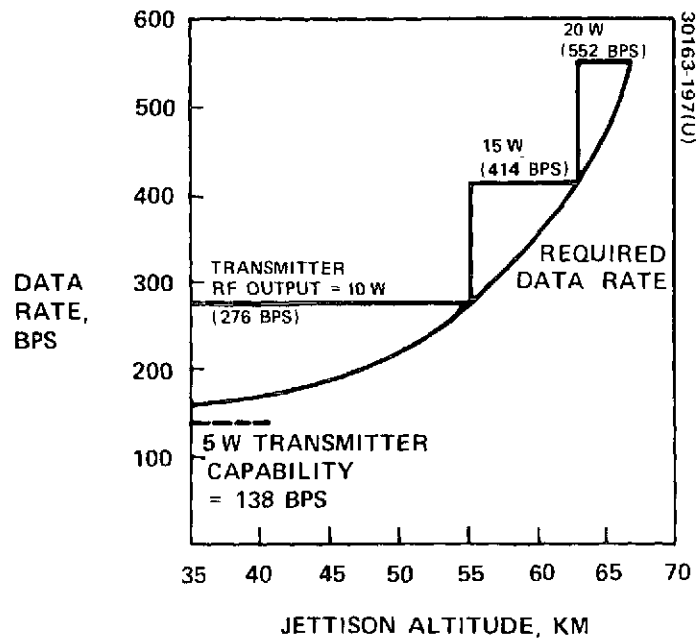


FIGURE 5-20. LARGE PROBE DATA RATE VERSUS PARACHUTE JETTISON ALTITUDE

model was more complicated. The velocity profile impacted the system in defining the required transmitter power. To guarantee a minimum sampling rate for each altitude increment, the required data rate was increased for regions of greater velocity. The worst case velocity defined the transmitter power. Because the sampling rate of several science instruments such as the accelerometer or transponder was time dependent and not velocity dependent, the relationship between required data rate and velocity was not direct.

Because of its velocity dependence, the required data rate shown in Figure 5-20 increased exponentially with jettison altitude. Only certain data rates could be efficiently implemented consistent with the modular transmitter design. For jettison altitudes from 35 km (corresponding to the thermal constraint of the parachute material) to 55 km, a 10 W transmitter was required. The data margin and total science return was maximized for the lower jettison altitudes. However, the weight was minimized (due to decreased descent time) for the higher altitudes. In addition, remaining on the chute through the expected cloud layers (44 to 62 km altitude) increased cloud sampling, although adequate sampling was attained without the chute up to 55 km altitude.

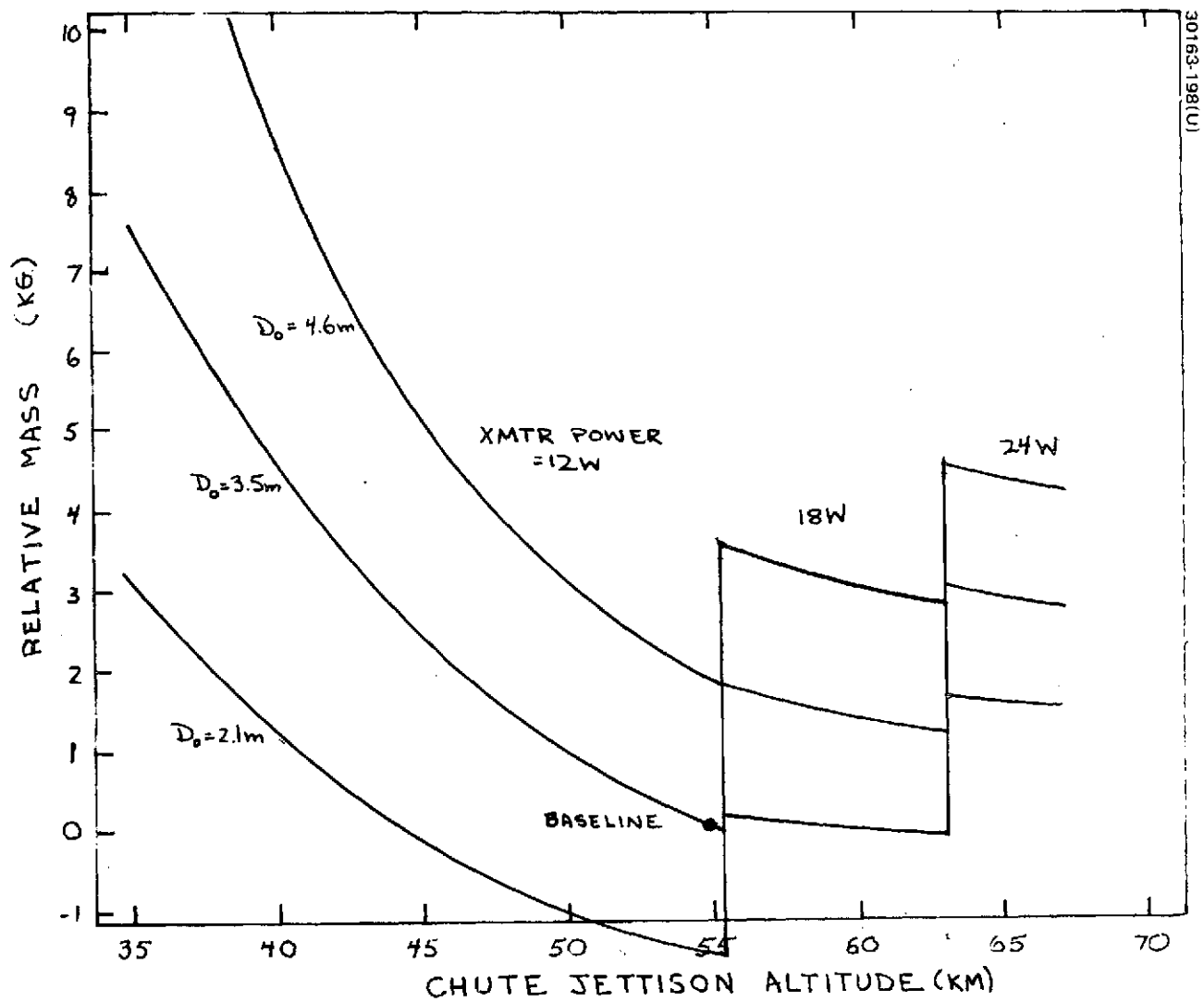
The thermal insulation was a complicated function of jettison altitude, descent time, rf output power, dc input power, structural mass and size and pressure vessel detailed design. A cold wall design was modeled but it was recognized that a hot wall design was also a viable possibility. Although a hot wall design could have reduced the magnitude of the weight advantage of higher jettison altitudes, it was judged that the general trend favoring higher jettison altitudes would have remained the same. The insulation thickness was only accurately determined for the baseline conditions. It was clear that insulation weight especially penalized lower jettison altitudes where the effect was greatest.

In addition to the battery and transmitter mass variations, the attendant variation in pressure vessel and aeroshell mass was added and the total system mass computed as a function of jettison altitude. This system mass plus a representative thermal insulation mass is shown in Figure 5-21.

The possible use of the probe data storage unit to reduce the required data rates for a more efficient design was investigated (Ames SOW 2.2.10-(9)). Such a scheme appeared particularly attractive for the higher jettison altitudes where high data rates were required for only brief periods of time. The data peak could be buffered by recording part of the data and playing it back later when real time requirements were decreased. It was concluded the system weight would not decrease. Basically, it was not possible to reduce the transmitter requirement from two to one module by this technique so there was no advantage in its favor.

Sensitivity to the Atmospheric Model

The uncertainty in large probe performance due to the uncertainty in the atmospheric model was bounded. Descent profiles generated for alternate NASA-SP-8011(72) model atmospheres showed variation in performance



30163-198(U)

FIGURE 5-21. VARIATION IN SYSTEM MASS WITH JETTISON ALTITUDE AND PARACHUTE DIAMETER (REPRESENTATIVE THERMAL INSULATION INCLUDED)

within tolerable limits if events were initiated at the same altitude as planned. The selection of pressure correlated switching reduced this performance variation demonstrated for altitude correlated switching to even narrower limits.

The most significant effect of a change in density profile was the resultant change in descent time. Descent times greater than nominal would cause battery depletion at surface impact beyond the design point of 80 percent. However, the maximum density model resulted in only an 0.5 percent increase in depth of discharge. Increased descent time also would cause the equipment to heat up beyond the design temperature limit. Such heating for the maximum density model was below the qualification level. Descent time less than nominal had no adverse effect except for the corresponding reduction in total science return.

A second significant effect of a change in density profile was the change in velocity after chute jettison and in particular the sampling margin at that altitude. A lower density atmosphere resulted in a higher velocity at chute jettison and a corresponding decrease in altitude sampling margin. Although small, the nominal data margin was sufficient to provide the desired sampling rate for the worst case (least dense) atmosphere.

A comparison of sequencer implementation was undertaken to establish the least sensitive technique. Major requirements included switching the data rate before the atmospheric losses could build up and deploying the parachute low enough such that post-jettison velocity would not exceed that required by altitude sampling. Both of these requirements implied associating events to the local atmospheric density. It was judged that pressure switching could accurately but simply accomplish this. Using a timer to initiate switching would have resulted in a more sensitive design since the system would not have balanced the density variation as well (Reference 5-10).

If the atmosphere was less dense than expected, the parachute would be jettisoned a little lower than planned but the remaining descent would be faster and the descent time about the same. The data rate would be switched lower than expected but the decreased density would reduce the atmospheric losses so that the data rate could be supported to the lower altitude. If the atmosphere was more dense than expected, the parachute would be jettisoned higher than expected but the post-separation velocity would not be significantly increased due to the increased density profile.

For the range of atmospheres presented in NASA SP-8011(72), the variation in altitude at parachute jettison and data rate reduction was less than 1 km and the variation in descent time was less than 1 min. Essentially no effect on system performance resulted in the worst case because of the battery margin associated with designing to 80 percent depth of discharge and the thermal margin associated with doubling the required insulation thickness.

5.7 REDUCED SCIENCE PAYLOAD

A reduced science payload was considered as a low cost approach to increasing the mass margin. The total mass reduction achieved for each probe was determined as a function of the particular instruments deleted from the payload. The payload was defined as everything contained inside the pressure vessel module excluding structural support and cabling. All science and engineering units were included.

The following equations were used to compute pressure vessel mass, M_{PV} , deceleration module mass, M_{DM} , and aeroshell base diameter, D_B , as a function of pressure vessel inside diameter in centimeters, ID, for the large and small probes and beryllium and aluminum aeroshell.

Large Probe

$$M_{PV}(\text{kg}) = 0.001328 (\text{ID}/2.54) + 0.02796 (\text{ID}/2.54) + 0.230 (\text{ID}/2.54) + 1.4$$

$$M_{DM}(\text{kg}) = 0.00077 (D_B/2.54) + 0.222 (D_B/2.54) + 11.9 (\text{beryllium})$$

$$M_{DM}(\text{kg}) = 0.0095 (D_B/2.54) + 0.369 (D_B/2.54) + 14.4 (\text{aluminum})$$

$$D_B(\text{cm}) = \text{ID} + 62.23$$

Small Probe

$$M_{PV}(\text{kg}) = 0.001320 (\text{ID}/2.54) + 0.03960 (\text{ID}/2.54) + 0.1559 (\text{ID}/2.54) + 0.63$$

$$M_{DM}(\text{kg}) = 0.009607 (D_B/2.54) + 0.09961 (D_B/2.54) + 0.68 (\text{beryllium})$$

$$M_{DM}(\text{kg}) = 0.01140 (D_B/2.54) + 0.1651 (D_B/2.54) + 1.0 (\text{titanium})$$

$$D_B(\text{cm}) = 1.472 (\text{ID}) + 13.081$$

The equation relating large probe aeroshell base diameter to pressure vessel inside diameter was based on the criterion that the aeroshell must be sufficiently large to accommodate the parachute and mortar as well as the pressure vessel.

Payload mass and volume versus total probe weight is given for the large and small probe in Figure 5-22. The payload was considered according to priority (Reference 5-11) beginning with the basic engineering mass and volume and adding the appropriate mass and volume for additional units, one at a time. Intersection with the indicated lines of constant total probe mass corresponded to the optimum payload for that mass. Transmitter and battery masses were distributed as required. The transmitter was divided into discrete power amplifiers. Each power amplifier could support a data rate of

about 125 bps. One amplifier was required for engineering telemetry and mass spectrometer data. A second was required for additional science payload. The battery was treated as continuously variable with an appropriate amount added after each unit consistent with the unit's power requirement.

5.8 CONCLUSIONS

The system tradeoffs performed resulted in the following features of the baseline system design.

- 1) The spin axis was oriented perpendicular to the ecliptic plane
- 2) The orbiter high gain antenna was mechanically despun
- 3) The probe bus cruise antenna was a biconic horn and the antenna to be used at entry was a medium gain horn
- 4) Large probe tracking was two-way doppler while small probe tracking was one-way
- 5) Signaling was coherent (PCM/PSK/PM) and coding sequential
- 6) The parachute diameter was 3.5 m
- 7) The jettison altitude was at 55 km

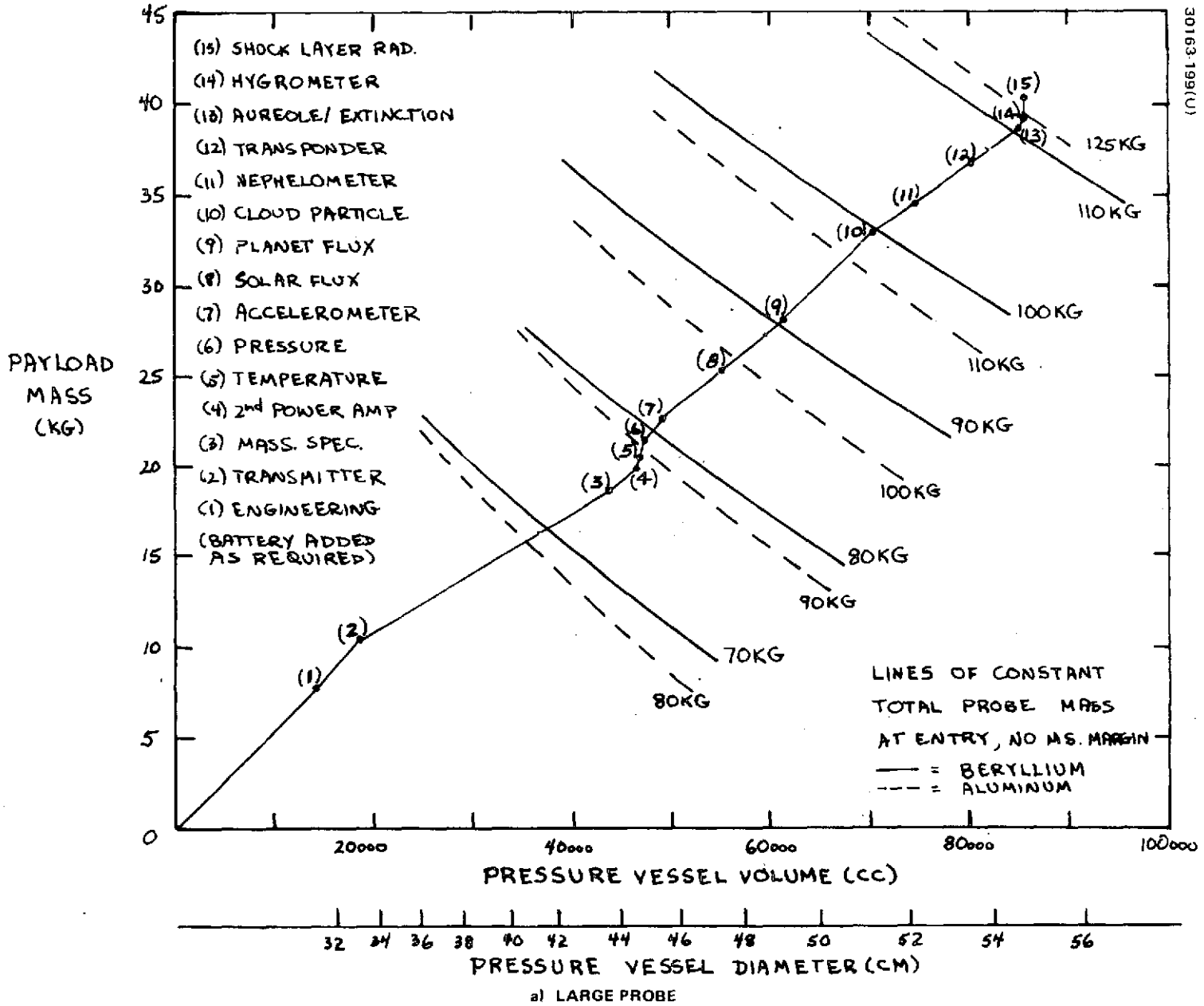
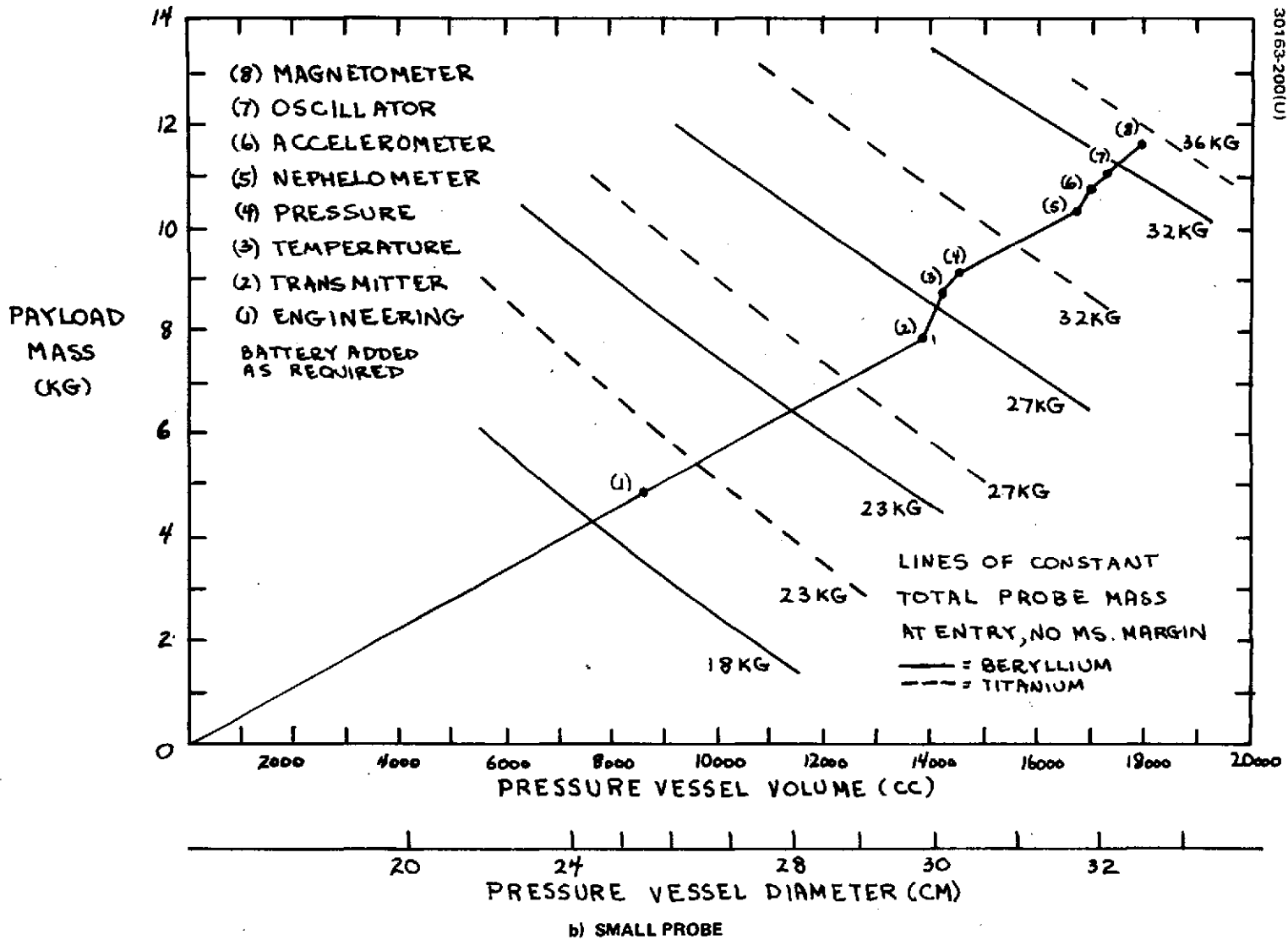


FIGURE 5-22. PAYLOAD MASS AND VOLUME REQUIREMENTS



30163-200(U)

FIGURE 5-22 (continued). PAYLOAD MASS AND VOLUME REQUIREMENTS

REFERENCES

- 5-1 "Proposal for a Systems Design Study of the Venus Pioneer Spacecraft," SCG 20140P, May 1972.
- 5-2 "An Electronically Phase Modular Array Antenna for Pioneer Venus Communications," (Preliminary Draft), Texas Instruments, Inc., Report No. U1-991840-F, 22 November 1972.
- 5-3 "Venus/Pioneer - SMS Comparisons," ARC, 21 January 1972.
- 5-4 J. A. Fink, "Coding and Modulation for Entry Probes in a Planetary Atmosphere," TIC 4092.1/080, 9 February 1973 (contained in Volume 15).
- 5-5 "The Performance of Convolutional Coding with Noncoherent MFSK Modulation in a Gaussian Channel," TIC 4091.1/219, 26 December 1972.
- 5-6 J. A. Heller and I. M. Jacobs, "Viterbi Decoding for Satellite and Space Communications," IEEE Trans. on Communication Tech., Volume COM-19, No. 5, October 1971, pp. 835-848.
- 5-7 R. H. Cager, "Frequency Spacing Considerations for Multiple Probes in a Planetary Atmosphere," TIC 4091.1/224, 10 February 1973 (contained in Volume 15)
- 5-8 R. H. Cager, "Preliminary Survey of One-Way Versus Two-Way Spacecraft Doppler Tracking with Oscillator and Transmission Channel Phase Uncertainties," TIC 4091.1/225, 10 February 1973.
- 5-9 L. G. Rands, "Doppler Tracking by 2nd Order Phase-Lock Loop Receivers," TIC 4091.1/244 (contained in Volume 15).
- 5-10 "1975 Venus Multiprobe Mission Study," Final Study Report, Martin Marietta Corporation, April 1970.
- 5-11 A. M. Lauletta, "Science Payload Priorities," HS507-0353.

6. RELIABILITY

The primary object of this section is to provide a convenient summary of the system reliability of the Pioneer Venus spacecraft.

The complete reliability analysis report is provided in Reference 5-1 and presents subsystem and unit analyses in some detail.

6.1 OVERVIEW

Spacecraft reliability is defined as the probability that spacecraft performance meets or exceeds that specified for some defined period of time. The required performance differs between the orbiter and probe bus missions.

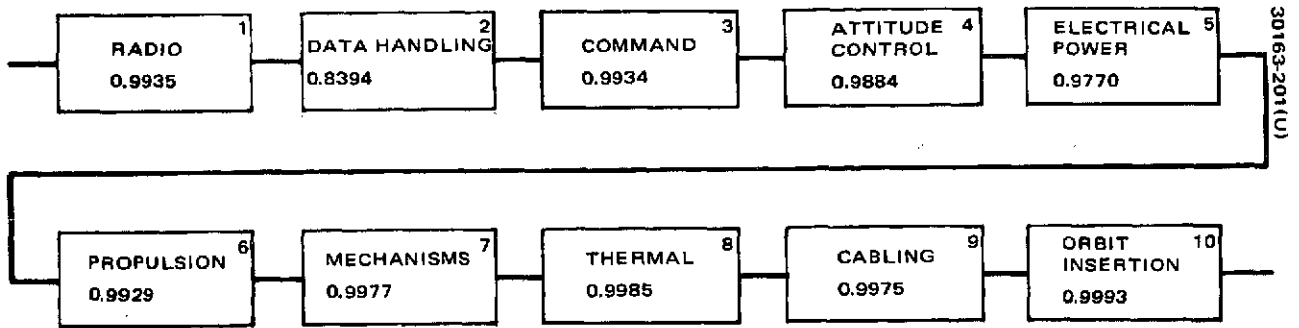
For the orbiter spacecraft the primary mission objective is to carry the complement of experiments to Venus and conduct orbital observations of the planet and the near planet environment for one Venusian year of 225 days.

The probe bus spacecraft mission objective is to carry one large and three small probes to Venus and launch them into the Venusian atmosphere. Thus, the probe bus mission involves not only the probe bus, but the large and small probes. The probability that the orbiter spacecraft will meet its required performance is 0.7904, presented in Figure 6-1. The probability for the probe spacecraft is 0.8718, presented in Figure 6-2 and Table 6-1. Both results exclude the reliability of the science experiments.

General Assumptions

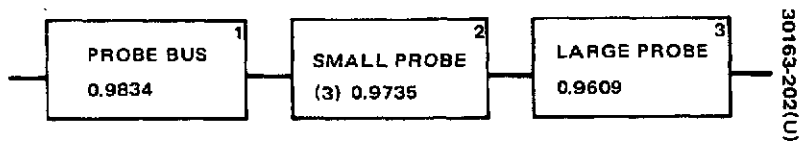
Some of the general assumptions utilized in the generation of the mission reliabilities are listed below:

- 1) All parts exhibit constant failure rates. The assumption is that all parts, both mechanical and electronics, have been properly debugged and have not entered the wearout stage at the end of the mission.
- 2) Failure rates utilized for piece parts are taken from the Hughes Space and Communications Group Product Effectiveness Handbook. These failure rates reflect top quality parts and space environment as defined in this document. The failure rates are specified separately for operating periods and nonoperating or dormant periods of the electronic equipment. In this way the possibility of failures during a nonoperating interval is considered in this analysis.



$$R = \prod_{i=1}^{10} R_i = 0.7904$$

FIGURE 6-1. ORBITER MISSION RELIABILITY LOGIC DIAGRAM



$$R = R_1 R_2 R_3 = 0.8718$$

FIGURE 6-2. PROBABILITY OF MULTIPROBE MISSION SUCCESS

TABLE 6-1. MISSION RELIABILITY SUMMARY

| Probe Bus | Small Probes | Large Probe | Mission Multiprobe |
|-----------|--------------|-------------|--------------------|
| 0.9834 | 0.9225 (1) | 0.9609 | 0.8718 |
| 0.9834 | 0.9978 (2) | 0.9609 | 0.9429 |
| 0.9834 | 0.99985 (3) | 0.9609 | 0.9442 |
| 0.9834 | --- | 0.9609 | 0.9449 |

- (1) Probability of success for all three small probes
- (2) Probability of success for any two small probes
- (3) Probability of success for at least one small probe

3) The failure rates for electronic units, have been modified by the Hughes experience factor of 0.606. The "E" factor is an attempt to reflect the operational experience with all Hughes orbiting satellites, thereby compensating for the basic inaccuracy of most handbook data. It is calculated as the ratio of actual part failures in space to the expected number of failures using the handbook data. This factor is periodically updated to reflect additional orbital experience. The "E" factor is currently 0.606.

4) Various blocks within a reliability logic diagram fail independently of any other block. Where there is a significant interaction of units between subsystems, the attempt has been made to segregate the units by function rather than by package. For example, the valve drivers are physically contained within the attitude control subsystem, but function with the solenoid valves in the propulsion subsystem. Therefore, they have been modeled in the latter subsystem.

5) The configurations analyzed were those of the midterm Thor/Delta baseline and reflect good design practice and judicious use of redundancy to obtain the highest reliability within the constraints of cost and weight.

6) No specific failure mode analysis was performed for this study.

In the succeeding sections, each of the spacecraft missions have been analyzed to determine the reliability.

6.2 ORBITER MISSION

The primary mission objective of the orbiter spacecraft is to carry the complement of the experiments to Venus and conduct orbital observation of the planet and the near planet environment.

The Pioneer Venus orbiter bus is a spin stabilized vehicle using sun and star sensors for attitude references. It is a basic bus providing a platform for science experiments. For the purposes of reliability analysis, the vehicle is assumed to consist of ten subsystems as follows:

- 1) Radio frequency
- 2) Data handling
- 3) Command
- 4) Attitude control
- 5) Power
- 6) Propulsion
- 7) Mechanisms (computed separately, but part of attitude control)
- 8) Thermal
- 9) Cabling
- 10) Orbit insertion propulsion

The orbiter spacecraft will be launched by the Thor/Delta launch vehicle. Figure 6-1 presents the system reliability logic diagram and mathematical model for the orbiter mission.

The mission times for the orbiter are 197 days in transit phase and 225 days in orbit.

6.3 PROBE BUS SPACECRAFT MISSION

The probe bus spacecraft consists of the entire launch vehicle payload and is comprised of the probe bus, science experiments, one large probe, and three small probes.

A summary of the probe bus spacecraft reliability is presented in Table 6-1 and the corresponding reliability logic diagram and mathematical model is shown in Figure 6-2.

Table 6-1 presents the probabilities associated with three different definitions of mission success. All three require probe bus and large probe success over their respective mission times. The differences in reliability lie in the definitions of small probe success:

- 1) All three small probes are successful
- 2) At least two of three small probes are successful
- 3) At least one of three small probes is successful

The analyses of the probe bus, large probe, and small probes are included in succeeding sections.

Probe Bus Mission

The probe bus spacecraft consists of the entire launch vehicle payload and is comprised of the probe bus, science experiments, a large probe, and three small probes. This analysis is concerned solely with the probe bus. Both the large and small probes are covered in the succeeding sections of this report.

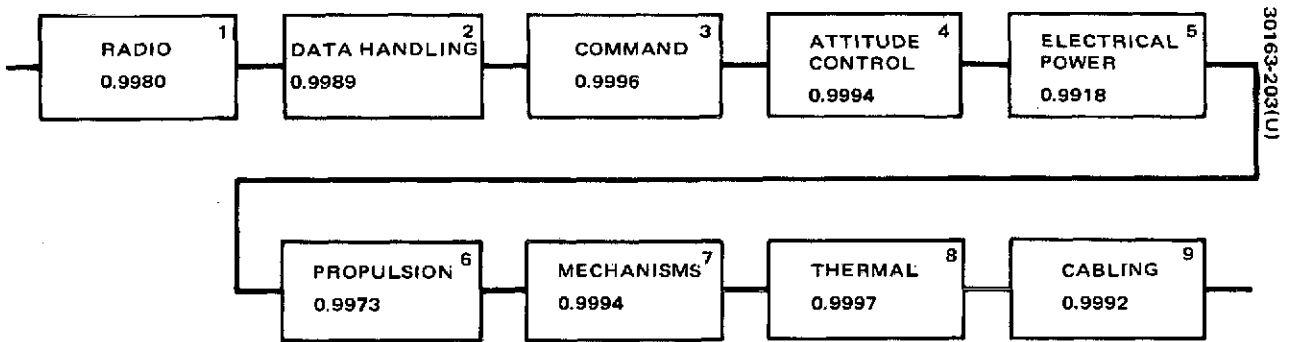
For reliability analysis purposes the probe bus spacecraft is comprised of nine subsystems as follows:

- 1) Radio frequency
- 2) Data handling
- 3) Command
- 4) Attitude control
- 5) Electrical power
- 6) Propulsion
- 7) Mechanisms
- 8) Thermal
- 9) Cabling

The probe bus spacecraft will be launched by the Thor/Delta launch vehicle. The reliability logic diagram and mathematical model for the probe bus is presented in Figure 6-3.

The following sections present reliability logic diagrams, mathematical models, and failure rates used for each of these subsystems.

The mission lifetime for the probe bus is 128 days.



$$R = \prod_{i=1}^9 R_i = 0.9834$$

FIGURE 6-3. PROBE BUS SYSTEM RELIABILITY LOGIC DIAGRAM - THOR/DELTA

Large Probe Mission

For reliability purposes the large probe mission can be divided into seven distinct phases:

- 1) Probe bus operation
- 2) Separation from probe bus
- 3) Coast
- 4) Entry into Venusian atmosphere
- 5) Parachute deployment
- 6) Aeroshell jettison
- 7) Parachute jettison

Each of these phases and the associated reliability model will be discussed briefly in the following paragraphs. Table 6-2 summarizes this information.

Probe Bus Operation

One of the primary mission objectives of the probe bus spacecraft is to carry a large probe to Venus and then launch it into the Venusian atmosphere. The reliability of this probe bus has been discussed in the preceding section.

Additionally, however, the probe peculiar equipment must survive the launch and transit phases of 108 days while in an unpowered state. The reliability of this equipment is $R = 0.9736$.

Separation from Probe Bus

The probe spacecraft will be oriented to target the large probe towards Venus. The large probe will be detached from the bus and a relative velocity imparted to the probe to provide separation at 20 days prior to entry. This is accomplished by a spacecraft-borne separation system involving the completion of two distinct events -- the breaking of the in-flight-disconnect and the separation of the large probe itself. Both of these events are accomplished using pyrotechnic devices. These operations are strictly one-shot in nature and as such a probability of success was assigned to each constituent event. These probabilities were obtained from General Electric who have design responsibility for both the large and the small probe deceleration modules. The product of both these independent probabilities is 0.9986.

TABLE 6-2. LARGE PROBE RELIABILITY BY MISSION PHASE

| Phase | Environment | Duration | Definition of Successful Performance | Large Probe Reliability |
|---------------------------|-----------------------------|----------|---|-------------------------|
| Preseparation | Probe bus transit phase | 108 days | Survival of equipment required in following phases | 0.9756 |
| Separation from probe bus | Pyrotechnic loads | 20 ms | Successful operation of separation system | 0.9986 |
| Coast | Low powered mode | 20 days | Survival of equipment required during descent | 0.9963 |
| Entry | Descent equipment turned on | ~ 15 min | Survival of equipment required during descent | ~1.0 |
| Descent | High power mode | 1.25 h | Experiments data transmitted | 0.99997 |
| Parachute deployment | Pyrotechnic loads | | Parachute deployed | 0.9975 |
| Aeroshell separation | Pyrotechnic loads | | Aeroshell separated from deceleration modules | 0.9987 |
| Parachute separation | Pyrotechnic loads | | Separation of parachute from pressure vessel | 0.9987 |
| Heat shield | | | Thermally protect the large probe deceleration module | 0.995 |
| Large probe mission | | | | 0.9609 |

Coast Phase

The large probe coasts for 20 days after separation with its battery activated. The only other powered element is the timer.

The reliability for this phase is: $R_C = 0.9963$

Preentry and Entry

Entry begins at 150 km altitude and the following events will occur:

- 1) Science instruments are turned on
- 2) Data storage mode turned on to store science and engineering data
- 3) Window heaters are turned on

No specific pyrotechnic events are accomplished during entry. Therefore, the reliability is $R \sim 1.0$.

Parachute Deployment

A parachute system is used to separate the deceleration module structure from the large probe pressure vessel to allow science experiment operation.

The parachute will be deployed removing the deceleration module aft cover. This event also involves operation of pyrotechnic devices.

Aeroshell Jettisoned

Two seconds after parachute deployment, the deceleration module aeroshell will be jettisoned.

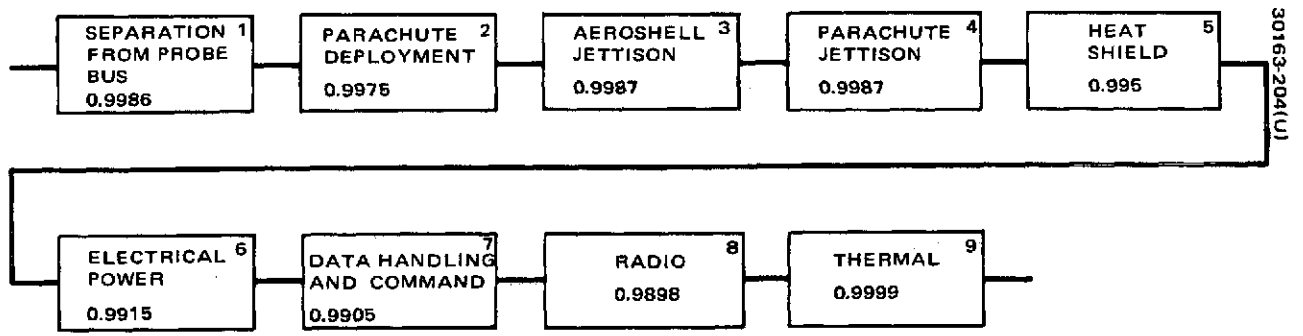
Parachute Jettisoned

Terminal descent begins at 40 km altitude when the parachute is jettisoned from the pressure vessel. The logic diagram and mathematical model for this event is identical to that presented previously for the aeroshell.

A reliability logic diagram and mathematical model for the large probe system is shown in Figure 6-4.

Small Probe Mission

For reliability purposes the small probe mission can be divided into the following five distinct phases:



$$R = (R_1 R_2 R_3 R_4 R_5) (R_6 R_7 R_8 R_9)$$

$$= (0.9885) (0.9720) = 0.9609$$

FIGURE 6-4. LARGE PROBE RELIABILITY LOGIC DIAGRAM AND MATHEMATICAL MODEL

- 1) Probe bus operation
- 2) Separation from probe bus and despin
- 3) Coast
- 4) Entry into Venusian atmosphere
- 5) Descent phase

Each of these phases and the associated reliability mode will be discussed briefly in the following paragraphs. Table 6-3 presents a summary of these reliabilities.

Probe Bus Operation

One of the primary mission objectives of the probe bus spacecraft is to carry three small probes to Venus and then launch them into the Venusian atmosphere. The reliability of the probe bus has been discussed in the preceding section.

Additionally, however, the probe peculiar equipment must survive the launch and transit phases at 108 days while in an unpowered state. The reliability of this equipment is $R = 0.9464$.

Separation from Probe Bus

The separation subsystem will separate the small probes from the probe bus upon command. It will also reduce the spin rate from the launch value to the entry requirement. The separation subsystem consists of:

- 1) In-flight disconnects
- 2) Hinge arm/open latch and bolt thruster
- 3) Yo-yo despin assembly

All of these events are accomplished using pyrotechnic devices.

The product of these independent probabilities is $R = 0.9349$, for all three small probes.

Coast

Each small probe coasts for 20 days after separation with its battery activated. The only other powered element during this time is the timer. The reliability for this phase is: $R_C = 0.9924$.

TABLE 6-3. SMALL PROBE RELIABILITY BY MISSION PHASE

| Phase | Environment | Duration | Successful Performance | Large Probe Reliability |
|-----------------------|-----------------------------|----------|--|-------------------------|
| Preseparation | Probe bus | 108 days | Survival of equipment required in following phases | 0.9464 |
| Separation and despin | Pyrotechnic loads | | Successful operation of separation system | 0.99735 |
| Coast | Low powered mode | 20 days | Survival of equipment required during descent | 0.9924 |
| Entry | Descent equipment turned on | 15 min | Survival of equipment required during descent | 1.0 |
| Descent | High powered mode | 1.25 h | Experiment data transmitted | 0.9997 |
| Heat shield | | | Thermally protect the probes deceleration module | 0.9851 |
| Small probe mission | | | | 0.9225 |

Preentry and Entry

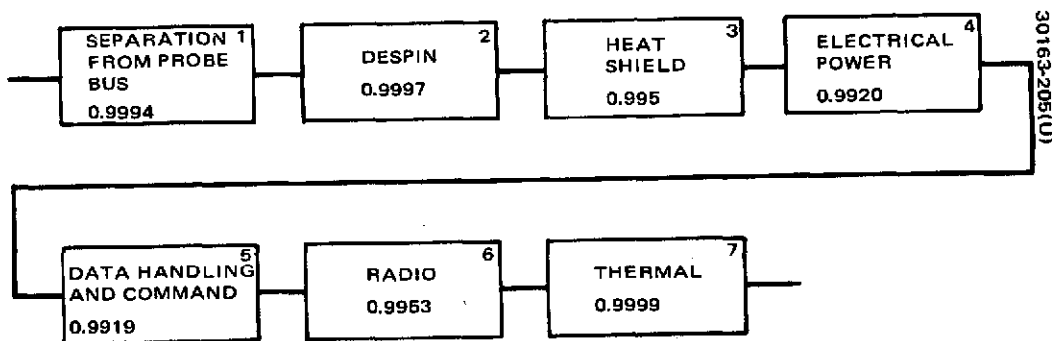
All subsystems and science experiments are turned on and the data handling subsystem is in the record mode. The reliability during this short period of time is approximately $R \approx 1.0$.

Terminal Descent

All science experiments and subsystems are operating and data is being sent at maximum rate.

This period lasts for a maximum of 1.5 hours.

A reliability logic diagram and mathematical model for the small probe mission is presented in Figure 6-5.



$$R_{1sp} = (R_1 R_2 R_3) (R_4 R_5 R_6 R_7) = (0.9994) (0.9793) = 0.97347, \text{ FOR SMALL PROBES,}$$

$$R = (R_{1sp})^3 = 0.9225$$

FIGURE 6-5. SMALL PROBE RELIABILITY LOGIC DIAGRAM AND MATHEMATICAL MODEL

APPENDIX A. SEQUENCING PROBE ENTRY

SUMMARY

Alternate probe entry sequences are evaluated to determine the cost, weight, and reliability impact of relying on real time probe data acquisition if predetection recording is not available.

INTRODUCTION

Simultaneous acquisition of data from four space vehicles relies on predetection recording to provide acquisition of multiple signals at a single ground receiver. In particular, to account for frequency offsets at blackout and to provide ground receiver redundancy, a redundant pair of the four receivers at each 64 m ground station is dedicated to pre-blackout data and the remaining pair to post-blackout data. Each receiver must be capable of receiving four simultaneous signals and this requires predetection recording.

The cost of predetection recording must be traded against the cost of the system complications required to provide nonsimultaneous, sequenced, probe entry. If predetection recording is not available then only one signal can be acquired by a given receiver. To achieve adequate redundancy, two ground stations must be in view during data transmission and two receivers at each ground station must be dedicated to each vehicle. With only four receivers available per ground station, real time data acquisition constrains probe entry to not more than two probes at a time.

Analysis

Ground station overlap for Venus viewing at probe encounter is shown in Figure 1. There are only two periods each day when ground station visibility overlap is long enough to accommodate the nominal 1.5 hours required for probe entry and descent. Because the two periods are adjacent, their total time (4 hours) can be used for three properly phased entry events (as many as six probes), but prime station responsibility must then be switched in the middle of the second event. This complexity can be traded against the fuel required to delay the third entry to the next daily window. Ground station overlap is defined as simultaneous viewing at an elevation angle greater than 30 deg for the prime station and at least 10 deg for the backup station. The 1.45 dB lost at the poorer elevation angle is less than the 2.0 dB saved if predetection recording is not employed.

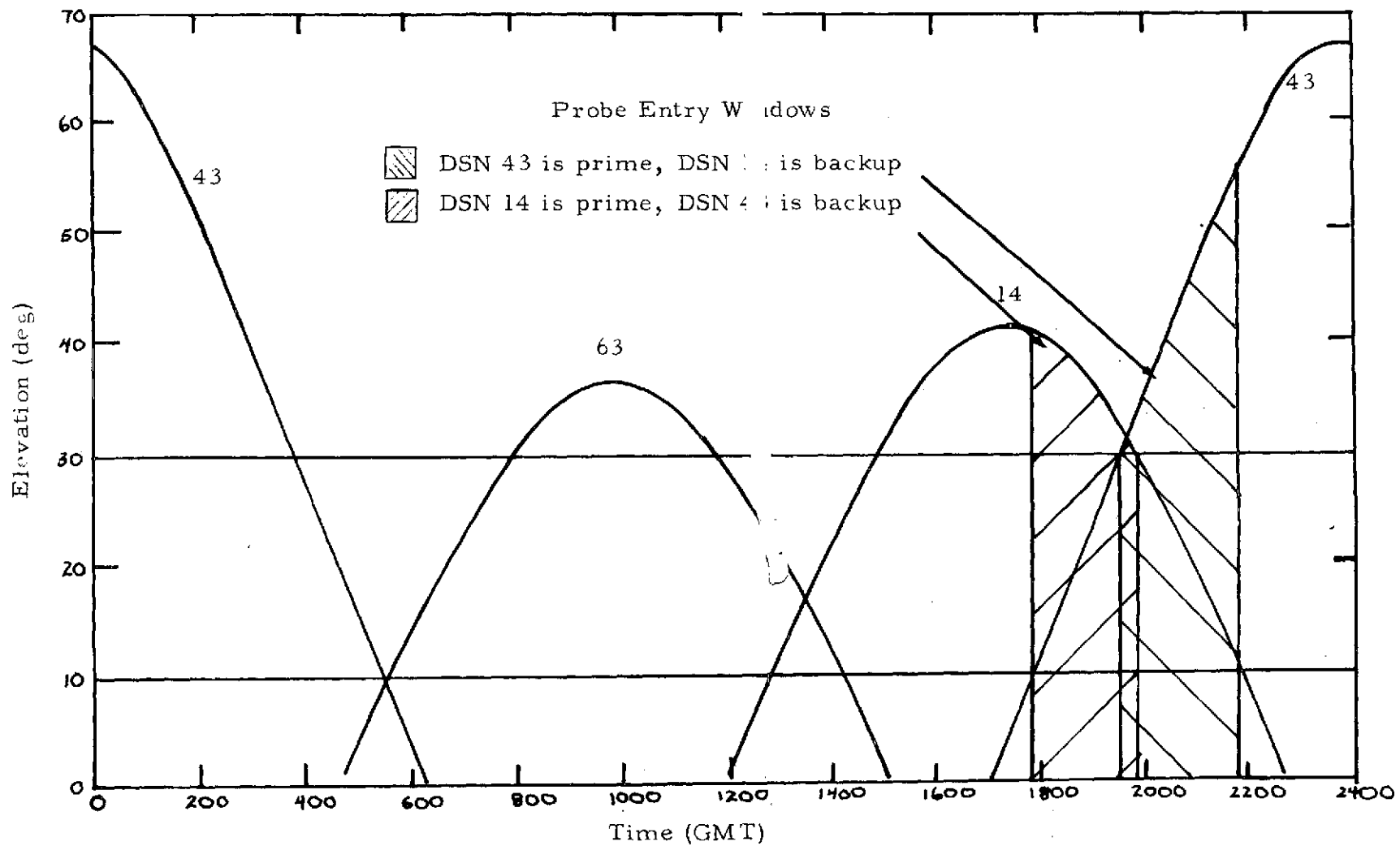


Figure 1. Ground Station Visibility at Probe Entry

For maximum probability of mission success, the large probe must be released from the bus prior to small probe release. If the bus is retarded by about 1-1/2 hours, then one or two small probes can be released and enter during the same ground station overlap view period. The bus must be retarded for 22-1/2 hours till the next ground station overlap period before remaining small probes can be released.

The present entry sequence calls for retarding bus entry by 1-1/2 hours to provide a known reference for differential interferometry of the descending probes. Slowing down the bus occurs after all probes are released independent of the release sequence so the 7.13 pound of fuel required by this 19.1 m/sec maneuver is not a factor in trading release sequences.

Additional retardation maneuvers are, however, a penalty to sequencing probe entry. An additional 17.2 m/sec is required to retard the spacecraft for 1-1/2 hours after large probe separation and before the initial small probe(s) release. The propellant required is 5.0 kg (11 lb) for a four small probe system and 4.5 kg (10 lb) for the baseline three small probe system. A 275 m/sec maneuver is required for a 22-1/2 hour delay between small probe separations. The corresponding propellant weight is 59 kg (130 lb) for two remaining small probes or 51 kg (113 lb) for one.

These propellant weights can be reduced by separating probes from the bus earlier in the mission if resulting decreases in orbit determination accuracy can be tolerated. The increase in probe battery weight due to the increased coast time between separation and entry is insignificant compared to the substantial savings in spacecraft propellant. Additional propellant is saved since the bus need not be spun up as much for small probe separation. Sufficient tracking for O.D. limits separation to about 40 days before encounter. A factor of two weight saving in required propellant can be achieved for separation at 40 days before encounter compared to the numbers described above for separation at 20 days before encounter.

In addition to these propellant penalties, there are hardware penalties associated with accommodating independent small probe separation. Several possible implementation schemes have been identified as follows.

- 1) A complex mechanical bracket can be employed to provide realignment of the small probes such that the spacecraft is balanced with either three or two small probes. A single small probe can then be separated and the bracket actuated to move the remaining two probes to balanced positions until separation. This concept is not pursued in any detail due to its obvious complexity.
- 2) The present scheme can be employed except that one small probe can be given a separate axial ΔV to delay (or advance) its entry with respect to the other two. After large probe separation, the bus can be delayed by 24 hours and then the small probes separated with one being further separated by about 1-1/2 hours. The required 19 m/sec velocity change can be accommodated by a

2) (continued)

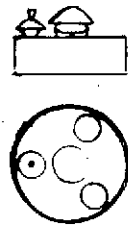
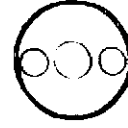
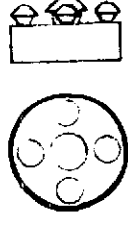
4.5 N (1 lb) solid rocket. If one rocket is employed, it can be mounted over the antenna or at the aeroshell stagnation point. Either mounting requires jettison of the rocket before entry and poses an integration problem. Using two or more rockets mounted at the perimeter interferes with the science instruments. This configuration is rejected due to the integration problems.

- 3) The desired probe entry phasing can be simply achieved if only two small probes are carried. A similar scheme involves selecting the best two of three entering probes as determined by test prior to entry. These cases are not pursued due to the substantial degradation in science return.
- 4) One of the outboard small probes can be relocated to the spacecraft centerline directly beneath the large probe and the remaining two outboard probes diametrically opposed. Stretching the large probe adapter accommodates this configuration but thermal and inertia problems result. The V-band integral to all small probes must be removed on the inboard probe to accommodate a new separation device. This configuration is rejected primarily due to the increased cost of developing a third separation subsystem.
- 5) A bellyband approach can provide flexibility in small probe separation by placing the centers of gravity of the small probes in a plane containing the spacecraft center of gravity after large probe release. Separation of only one or two small probes induces no wobble to the remaining spacecraft system. This approach is viable but requires much more difficult integration and a more complicated solar panel to allow for increased cutouts.
- 6) A jettisonable deployable boom can be used in several ways to solve the sequenced entry problem. The three small probes and the boom can be located at 90 deg spacings around the probe bus and the boom deployed after launch and before spin up to maintain balance in the launch and cruise configurations. After separation of the opposed probe pair and appropriate delay, the boom is then jettisoned with the third probe. Another scheme is to keep the present configuration but add the deployable boom which is then deployed simultaneously with separation of the two adjacent probes and later jettisoned with the final probe. The boom schemes are not desirable due to the significant increase in system complexity and the resulting reduction in reliability. For the second configuration, wobble can become significant (20 deg) between probe separation and boom deployment. Boom deployment is not qualified for such loads.

- 7) A final configuration considered is similar to the previous one except that the complex boom is replaced with a much simpler but much heavier dummy fourth probe. The four probes can be separated in pairs but only three are active and the fourth is the mass model mockup. Impact on cost and reliability are minimal but the weight penalty is a significant 65 kg (143 lb). The present 329 pound weight contingency does, however, accommodate this fourth probe plus the required increase of 64 kg (141 lb) (for separation at E-20 days). The fourth probe can be made active for no additional weight impact but a substantial (\$1.1 M) cost increase. Additional science return is thereby provided.

These configurations are summarized in Table 1, including estimates of effect on spacecraft weight, cost and reliability. All have significant cost and reliability implications except the final one, but it has a significant weight impact of 136 kg (300 lb).

TABLE 1. CANDIDATE SEQUENCED ENTRY IMPLEMENTATION TECHNIQUES

| Configuration Number | 1 | 2 | 3 | 4 | 5 | 6 | 7 |
|---------------------------------------|--|--|--|--|---|---|---|
| Description | Special Mechanical Bracket | Addition of Rocket(s) to One Small Probe | Number of Small Probes Reduced | Piggyback Large and Small Probe | Bellyband Small Probe Orientation | Jettisonable Deployable Boom | 4th Small Probe |
| |  |  |  |  |  |  |  |
| E-18 Day Separation | | | | | | | |
| Increased fuel wt, kg (lb)* | 63 (140) | 71 (156) | 4 (9) | 56 (123) | 56 (123) | 57 (126) | 64 (141) |
| E-36 Day Separation | | | | | | | |
| Increased fuel wt, kg (lb) | 32 (70) | 35 (78) | 2 (5) | 28 (62) | 28 (62) | 29 (63) | 32 (70) |
| Additional battery, kg (lb) | 2.4 (5.4) | 2.4 (5.4) | 1.9 (4.1) | 2.4 (5.4) | 2.4 (5.4) | 2.4 (5.4) | 2.4 (5.4) |
| Bus targeting fuel reduction, kg (lb) | -1.6 (-3.5) | -1.6 (-3.5) | -1.6 (-3.5) | -1.6 (-3.5) | -1.6 (-3.5) | -1.6 (-3.5) | -1.6 (-3.5) |
| Δ Hardware weight, kg (lb) | 11 (25) | 1 (2) | -65 (-143) | 4.5 (10) | 14 (30) | 11 (25) | 65 (143) |
| Δ Hardware cost (\$) | 100K - 300K | 50K | -1.1M | 100K | 100K | 10K | 10K (+1.1M if 4th probe is live) |
| Risk | Significant increase in mechanical complexity; bracket failure would cause loss of bus plus two probes | Complex integration; could interface with science, reduced small probe commonality | Science return significantly reduced | Reduced small probe commonality; large probe separation failure causes loss of third small probe | Sideways small probe deployment complicates solar panel; more difficult integration | Complex deployment device; deployed at launch; a single point failure; deployed at initial small probe separation; a complicated dynamics problem | Minimal impact on reliability |

* NOTE: Fuel weight is reduced to about 20 lbs if three entry events are accommodated during first daily encounter opportunity (10 lbs for configuration 2, 22 lbs for configuration 7).